



HAL
open science

Optimization of DIC assisted hydrolytic conversion of polysaccharides (starch and cellulose)

Harun Sarip

► **To cite this version:**

Harun Sarip. Optimization of DIC assisted hydrolytic conversion of polysaccharides (starch and cellulose). Other. Université de La Rochelle; Université de Kuala Lumpur (Malaisie), 2012. English. NNT : 2012LAROS373 . tel-00986304

HAL Id: tel-00986304

<https://theses.hal.science/tel-00986304>

Submitted on 2 May 2014

HAL is a multi-disciplinary open access archive for the deposit and dissemination of scientific research documents, whether they are published or not. The documents may come from teaching and research institutions in France or abroad, or from public or private research centers.

L'archive ouverte pluridisciplinaire **HAL**, est destinée au dépôt et à la diffusion de documents scientifiques de niveau recherche, publiés ou non, émanant des établissements d'enseignement et de recherche français ou étrangers, des laboratoires publics ou privés.



Universiti Kuala Lumpur
Malaysian Institute of Chemical and
Bioengineering Technology (UniKL MICET)

Doctor of Philosophy (PhD) in Chemical
Engineering Technology



Université de La Rochelle
Pole Sciences et Technologie: Laboratoire des
Sciences de l'Ingénieur pour l'Environnement
LaSIE FRE 3474 CNRS

Doctorat en Génie des Procédés Industriels
Année : 2012

Numéro attribué par la bibliothèque :

--	--	--	--	--	--	--	--	--	--

By

Harun SARIP

Date: 27 April 2012

TITLE:

Optimization of DIC Assisted Hydrolytic Conversion of Polysaccharides (Starch and Cellulose)

Thesis Co-Supervisor:

Professor Karim ALLAF (France)

Professor Mohamad Azemi Mohamad NOOR (Malaysia)

JURY:

Karim	ALLAF	Supervisor	Professor	Université de La Rochelle	France
Mohamad Azemi	NOOR	Supervisor	Professor	Universiti Kuala Lumpur	Malaysia
Eugene	VOROBIEV	Rapport	Professor	Université de Tech de Compiègne	France
Farid	ZERROUQ	Rapport	Professor	Ecole Supérieure de Technologie	Morocco
Vaclav	SOBOLIK	Examiner	Professor	Université de La Rochelle	France
Abdul Manan	DOS	Examiner	Assoc. Professor	Universiti Kuala Lumpur	Malaysia
Omar	BARKAT	Invited	Professor	PetroProTech LLC	USA

CONFIDENTIAL

Acknowledgement

I wish to acknowledge my sincere appreciation to a number of peoples that contributed in many ways to the success of this research work.

My utmost appreciation to my co-supervisors, Professor Karim ALLAF and Professor Mohamad Azemi Mohamad NOOR for their guidance in all aspects of my research works, writing and their willingness to spare their precious time on this piece. Their guidance, encouragement, excitement about results of this work, dedication and trust has put forward my courage to complete this journey and the thesis.

I would like to thank the Examiners; Professor Eugene VOROBIEV and Professor Farid ZERROUQ, and the other invited Panel of Jury; Professor Vaclav SOBOLIK, Professor Omar BARKAT and Assoc. Prof. Abdul Manan DOS Mohamad for taking their time to contribute on various aspects of the thesis.

I would like to thank all my friends in the laboratory in LaSIE (formerly LEPTIAB) of Université de La Rochelle: Sabah, Antony, Armelle, Cuong, Nsreen, Ismail, Alice, Colette, Magdalena, Ibtisam, Negm, Carmen, Maritza and many other names who are not included here.

Staff of LaSIE & ecole doctoral; Sandrine, Brigitte, Isabelle and Jennifer. Dr. Egle Conforto for helping and explaining me with the ESEM/EDX.

There was certain part of this work was done back in my laboratory at UniKL MICET, and I would like to thank Arizam, Suhaida, Farah, Naquib, Mat Hassan (USM) for helping me to perform some part of my research work. Steven Tan for his understanding.

My very sincere appreciation to Vicenta Blasco-Allaf, manager and the staff of Abcar, Ismail Mih and family. Tamara for helping me with DIC machine operation at Abcar and Vicenta, for her support to me and my family.

My friends' families in La Rochelle; Aimon family, Lallement family, Benkimoun family and all their children, and friends of my children for helping me and my family to settle down here.

To Majlis Amanah Rakyat (MARA) for providing me the study fellowship that enabled me to prepare this work and to UniKL for providing me and my family an allowance so that we stay united, in this beautiful city of La Rochelle.

Finally, to all my loving family: Norie, Nazhif, Nazrul, Nabil, Hani & Naquib. My mother and mother in law for their love, support and patience and taking care of my family when I was away. Din, Jelani, Tapa & Fidah for their challenge and love.

I hope with the completion of this journey; I can start with a new chapter and to contribute back to my beloved country, Malaysia. Insyallah.

Harun SARIP

La Rochelle, France

27 April 2012

Nomenclature

A _o	Total polysaccharides (mg/g)
BSED	Backscattered electron detector, in ESEM
CCD	Central composite design
DAH	Dilute acid hydrolysis
DE	Dextrose equivalent
DIC	Détente Instantanée Contrôlée (French for "Instant controlled pressure drop")
DP	Degree of polymerization
E _a	Activation energy (kJ/mol)
(E)SEM	(Environmental) Scanning Electron Microscopy/ micrograph
HMF	Hydroxymethyl furfural
HPLC	High performance liquid chromatography
HWE	Hot water extraction, hot water extracts
k ₁ , k ₂	Rate constant (in s ⁻¹ or min ⁻¹)
LMW	Low molecular weight oligosaccharides
OFAT	One factor at a time
RH	Relative humidity (%)
RSM	Response Surface Methodology
SED	Secondary electron detector, in ESEM
SPW	Sago pith waste
TGA	Thermal gravimetric analysis
X1	Initial moisture content (%)
X2	DIC First vacuum cycle
X3	DIC Second vacuum cycle
X4	Treatment time (min. or sec.)
X5	Acid concentration (molar)
X6	Treatment pressure or temperature (°C)
XRD	X-ray diffraction

CONFIDENTIAL

Table of Content

ACKNOWLEDGEMENT.....	III
NOMENCLATURE.....	IV
TABLE OF CONTENT.....	VI
LIST OF FIGURE	X
LIST OF TABLE	XIV
ABSTRACT.....	XVII
RÉSUMÉ	XVIII
BRIEF OVERVIEW.....	1
THESIS ORGANIZATION.....	2
PROBLEMS REVIEW.....	3
GOALS AND OBJECTIVES OF THE THESIS.....	4
STRATEGY AND PLANNED SOLUTIONS.....	5
PART I. STATE OF ART.....	6
PART I. CHAP 1. REVIEW: GLUCOSE INDUSTRY AND BIOMASS.....	7
I.1.1. Brief overview	7
I.1.2. Conversion of biomass to glucose.....	7
I.1.3. Summary of economic factors in this work.....	8
I.1.4. Carbohydrate and Glucose	9
I.1.4.1. Presentation and main properties.....	9
I.1.4.2. Commercial glucose production from starch.....	10
I.1.4.3. Biorefinery concept and glucose production from biomass.....	11
I.1.5. Lignocellulosic Biomass.....	13
I.1.5.1. Biomass physical and chemical compositions.....	15
I.1.5.1.1. Cellulose	16
I.1.5.1.2. Hemicelluloses.....	18
I.1.5.1.3. Lignin.....	18
I.1.5.1.4. Starch	21
I.1.5.2. Products of Starch and Glucose.....	22
I.1.5.3. Comparison: Starch and Cellulose.....	22
I.1.5.4. Energy value of biomass	23
I.1.6. Water Behavior in Biomass.....	23
I.1.7. Brief Overview on Biomass Waste	24
I.1.7.1. Cassava Starch Industry	24
I.1.7.2. Cassava Processing.....	25
I.1.7.3. Sago Palm.....	26
I.1.7.3.1. Sago Extraction.....	26
I.1.7.3.2. Sago Pith Waste (SPW)	27
I.1.7.3.3. Recent Development in Sago Starch Industry.....	28
I.1.8. Conclusion	29
PART I. CHAP 2. REVIEW: THERMAL PRETREATMENT.....	30
I.2.1. Biomass Pretreatment.....	30
I.2.2. Rationale of Thermal Pretreatments on Biomass.....	30
I.2.2.1. Biomass Pretreatment Summary	32
I.2.2.1.1. Steam Explosion Pretreatment	32
I.2.2.1.2. Modeling of Treatment Severity	33
I.2.2.2. DIC Technology.....	35
I.2.2.2.1. Basis of DIC Process.....	35
PART I. CHAP 3. REVIEW: AUTOHYDROLYSIS, DILUTE ACID HYDROLYSIS AND MODELING OF THE PROCESS.....	37
I.3.1. Introduction.....	37
I.3.2. Biomass Autohydrolysis Phenomenon.....	38
I.3.3. Dilute Acid Hydrolysis Effect on Biomass Morphology.....	39

1.3.4.	<i>Degradation of Glucose and Xylose</i>	40
1.3.4.1.	Methods to Control Glucose Degradation	41
1.3.5.	<i>Enzymatic Hydrolysis</i>	42
1.3.6.	<i>Modeling of Glucose Hydrolysis Kinetics</i>	42
1.3.6.1.	Determination of Activation Energy	46
1.3.7.	<i>Output of glucose hydrolysis kinetic modeling</i>	47
1.3.7.1.	Modeling of non-isothermal process: DIC and dilute acid hydrolysis.....	47
1.3.7.2.	Non-isothermal Model Data	48
1.3.8.	<i>Experimental Design</i>	49
1.3.8.1.	Optimization with Response Surface Methodology (RSM)	50
1.3.8.1.1.	Full Factorial Design.....	50
1.3.8.1.2.	Central composite design (CCD)	51
1.3.8.2.	Statistic for Response Surface Methodology	52
1.3.8.2.1.	Data analysis	53
1.3.8.2.2.	Data Mining for Kinetic Model from Response Surface Model.....	53
1.3.8.3.	Factors Elimination and Optimization of Process	54
PART II.	MATERIALS & METHODS	56
PART II. CHAP 1.	RAW MATERIALS.....	57
II.1.1.	<i>Sago Pith Waste (SPW)</i>	57
II.1.2.	<i>Sampling of treated materials</i>	58
II.1.2.1.	Rapid moisture content determination.....	58
II.1.2.2.	Material characterization.....	58
II.1.3.	<i>Hemicelluloses and Starch</i>	58
II.1.3.1.	Starch Content.....	59
II.1.3.2.	Hemicelluloses.....	59
II.1.3.3.	Total Polysaccharides.....	60
II.1.3.4.	Total Lignin.....	60
II.1.3.4.1.	Acid soluble lignin.....	61
II.1.3.5.	Alkaline extraction.....	61
II.1.4.	<i>Physical Characterizations</i>	61
II.1.4.1.	Particle Size Distribution.....	61
II.1.4.2.	Bulk Density of SPW.....	62
II.1.5.	<i>Instrumentals analysis</i>	62
II.1.5.1.	Carbohydrate and Total Polysaccharides.....	62
II.1.5.2.	Glucose and Glucose Degradation Products with HPLC.....	62
II.1.5.3.	Partial Validation of HPLC Method and Result obtained.....	63
II.1.6.	<i>Thermo gravimetric analysis (TGA)</i>	65
II.1.7.	<i>Environmental Scanning Electron Microscopy (ESEM)</i>	65
PART II. CHAP 2.	DIC PRETREATMENT AND PROCESS PROTOCOLS.....	66
II.2.1.	<i>Material preparation</i>	66
II.2.1.1.	Grinding.....	66
II.2.1.2.	Drying.....	66
II.2.1.3.	Simultaneous Moisture and Acid Concentration Adjustment.....	67
II.2.2.	<i>DIC pretreatment</i>	67
II.2.3.	<i>Hot Water Extraction (HWE)</i>	68
II.2.3.1.	Determination of Hot Water Extractable Glucose.....	68
II.2.4.	<i>Hydrolysis Process and Kinetic Study</i>	69
II.2.4.1.	Dilute Acid Hydrolysis (DAH) Kinetic.....	69
II.2.4.2.	Condition for Dilute Acid Hydrolysis and Hot Water Extraction.....	70
II.2.5.	<i>Glucose Degradation Kinetics</i>	70
PART III.	RESULTS	71
PART III. CHAP 1.	EXPLORATORY STUDY (BACKGROUND STUDY, DEVELOPMENT OF PROCESS AND PROCEDURES)	72
PAPER 1: (I) EXPLORATORY TRIAL TO ESTABLISH DIC PRETREATMENT PARAMETERS FOR AUTOHYDROLYSIS OF CRUDE STARCH BASED ON OFAT. (II) DIC PRETREATMENT WITH EXTENDED TREATMENT PARAMETERS.....		72
<i>Abstract</i>		72
III.1.1.	<i>Introduction</i>	72
III.1.2.	<i>Materials and Methods</i>	73
III.1.2.1.	Chemicals an Materials	73
III.1.2.2.	Trial 1: One Factor at a Time Study	73

III.1.2.3. Trial 2: DIC Treatment at High Temperature with 0, 0.75, and 1.25 Molar Acids.....	74
III.1.2.4. DIC Pretreatment.....	74
III.1.3. Result and Discussion	75
III.1.3.1. Result Trial 1: One factor at a Time (OFAT) Study	76
III.1.3.2. Result Trial 2: DIC Treatment at High Temperature and Acid Concentration (0, 0.75, and 1.25 molar sulfuric acid).....	78
III.1.4. Conclusion	83
PAPER 2: EXPLORATORY TRIAL TO ESTABLISH DIC TREATMENT CYCLES AND MOISTURE CONTENT LEVEL FOR TREATMENT OF CRUDE SAGO STARCH	84
Abstract	84
III.1.5. Introduction.....	84
III.1.6. Experimental design.....	84
III.1.7. Material and method.....	86
III.1.8. Result and Discussion	86
III.1.8.1. Effect of Reaction Factors.....	89
III.1.8.2. Effect of Extended Exposure during DIC Thermal Treatment	92
III.1.8.3. Confirmation Experiment.....	93
III.1.9. Conclusion	96
PART III. CHAP 2. OPTIMIZATION WITH RESPONSE SURFACE METHODOLOGY (RSM) MODEL AND KINETIC MODEL	98
PAPER 3: (i) OPTIMIZATION OF DIC PROCESS AT LOW DIC SEVERITY CONDITION FOR THE CONVERSION OF POLYSACCHARIDES/CRUDE STARCH TO LMW OLIGOSACCHARIDE FRACTION AND GLUCOSE BY RSM (ii) DEVELOPMENT OF KINETIC MODEL OF POLYSACCHARIDES/CRUDE STARCH CONVERSION UNDER LOW DIC SEVERITY PROCESS.....	98
Abstract	98
III.2.1. Objective	98
III.2.2. Introduction.....	98
III.2.3. Material and method.....	100
III.2.3.1. Experimental Design	100
III.2.4. Result and Discussion	101
III.2.4.1. Study of kinetic for Glucose yield.....	106
III.2.4.2. Rate constant and activation energy for the model.....	109
III.2.5. Conclusion	112
PAPER 4: (i) OPTIMIZATION OF DIC PROCESS AT HIGH DIC SEVERITY CONDITION FOR THE CONVERSION OF POLYSACCHARIDES/CRUDE STARCH TO GLUCOSE BY RSM (ii) DEVELOPMENT OF KINETIC MODEL OF POLYSACCHARIDES/CRUDE STARCH CONVERSION UNDER HIGH DIC SEVERITY PROCESS.	113
Abstract	113
III.2.6. Objective	113
III.2.7. Introduction.....	113
III.2.8. Material and method.....	114
III.2.8.1. Material preparation	114
III.2.8.2. Experimental Design	114
III.2.9. Result and Discussion	114
III.2.9.1. Study of kinetic for Glucose yield.....	121
III.2.9.2. Rate Constant and Activation Energy for the Model.....	123
III.2.10. Conclusion	125
PART III. CHAP 3. DILUTE ACID HYDROLYSIS AND GLUCOSE DEGRADATION STUDY.....	126
PAPER 5: DILUTE ACID HYDROLYSIS OF POST DIC TREATED CRUDE STARCH (i) HYDROLYSIS KINETIC STUDY AND ITS MODEL (ii) RSM STUDY ON INTERACTION OF REACTION FACTORS ON THE FORMATION OF GLUCOSE.....	126
Abstract	126
III.3.1. Objectives.....	126
III.3.2. Introduction.....	126
III.3.3. Materials and Methods.....	127
III.3.3.1. Sago pith waste (SPW).....	127
III.3.3.2. Chemicals.....	127
III.3.3.3. Material characterization	127
III.3.3.4. Determination of profile TGA.....	127
III.3.3.5. Glucose determination with HPLC.....	128
III.3.3.6. ESEM and EDX determination	128
III.3.3.7. Experimental procedures	128

III.3.3.7.1. Pretreatment with DIC	128
III.3.3.7.2. Dilute acid hydrolysis kinetic experiments	129
III.3.3.7.3. Response Surface Methodology	129
III.3.4. Result.....	129
III.3.4.1. TGA analysis.....	129
III.3.4.2. Kinetic of dilute acid hydrolysis.....	131
III.3.5. Dilute acid hydrolysis (DAH) discussion	134
III.3.6. RSM Model Study.....	135
III.3.7. Conclusion	138
PAPER 6: GLUCOSE DEGRADATION KINETIC STUDY	140
Abstract	140
III.3.8. Objectives.....	140
III.3.9. Introduction.....	140
III.3.10. Materials and Methods.....	140
III.3.10.1. Chemicals.....	140
III.3.10.2. Experimental procedures.....	141
III.3.10.2.1. Glucose Degradation Kinetic and Glucose Residue Determination with HPLC.....	141
III.3.10.2.2. RSM and factors interaction in glucose degradation.....	141
III.3.11. Result and Discussion	141
III.3.11.1. Kinetic of glucose degradation.....	141
III.3.11.2. RSM Model of Glucose Degradation	143
III.3.12. Conclusion	146
PART III. CHAP 4. HYDROLYTIC BEHAVIOR OF NON-ISOTHERMAL STATE	147
PAPER 7: THE INFLUENCE OF NON-ISOTHERMAL STATE ON THE CONVERSION OF STARCH IN BOTH DIC AND DAH PROCESSES.	147
Abstract	147
III.4.1. Objective	147
III.4.2. Introduction.....	147
III.4.3. Material and method.....	148
III.4.3.1. DIC and Dilute acid hydrolysis system and temperature acquisition	148
III.4.4. Result and Discussion	149
III.4.5. Conclusion	152
PART IV. CONCLUSION AND FUTURE WORKS.....	153
PART IV. CHAP 1. CONCLUSION.....	154
PART IV. CHAP 2. FUTURE WORKS	157
REFERENCE.....	158

List of Figure

Figure I-1:	Glucose exists in the aldehyde ring forms with C1 as centre of asymmetry. Two isomers exist as either α -D-Glucose or β -D-Glucose from open-chain form. β position is when (-OH) on C#1 on same side of cyclic ring of C#6 (on horizontal projection), α position is on different side (on downward position). [34].....	10
Figure I-2:	Processing chart for glucose production from starch obtained from cereals. [Adapted from - http://www.tereos.com/en-gb/activites/filieres/cereales.html].....	11
Figure I-3:	Novel biorefinery concept with biomass as feedstock (adapted from [38]).....	12
Figure I-4:	Stages of conversion of biomass materials into bioethanol (adapted from [41]).....	12
Figure I-5:	Composition of biomass including cellulose, hemicelluloses, lignin, extractive and ash and its respective degradation products. Starch was not included in this figure; normally represent certain percentage with certain percentage in biomass follow similar process steps as cellulose.....	16
Figure I-6:	Plant cell structure. An overview of science (Adapted from Bioenergy Research Center).....	17
Figure I-7:	Cellulose drawing that shows numbering of carbon atoms, non-reducing and reducing ends groups with n-number of glucose repeating units linked by β -1,4-glycosidic link. Cellulose chain with cellobiose unit as its repeating units has a length of 1.03 nm within the cellobiose unit (adapted from [35]).....	17
Figure I-8:	Cellulose chain composed of four β -D-glucopyranose residues (cellotetraose) in three different views. The upper image, viewed perpendicular to the flat surface of the molecule, shows the covalent bonds and electron clouds around the atoms. The dotted lines indicate hydrogen bonds between the O6-H and the O2 atoms and between the O3-H and the O5 atoms. Disregarding the ending hydroxyl hydrogen atoms, the molecule has the twofold helical conformation and hydrogen bonding typical of some proposed structures of crystalline cellulose. The middle image shows a view of the long edge of the molecule, and the bottom image shows the end of the molecule (adapted from [44]).....	17
Figure I-9:	Hemicellulose sugars components.....	19
Figure I-10:	Basic unit of phenylpropane that built lignin [53]......	19
Figure I-11:	Lignin structure still viewed as a contemporary model due to its complexity as presented above.	20
Figure I-12:	Representation of (a) Schematic and (b) detail representation of linkage for lignin and polysaccharides (adapted from [44]).....	21
Figure I-13:	Starch, as (a) amylose with α , (1 \rightarrow 4) linkages, prefers to adopt a helical conformation, whereas (b) cellulose, with β , (1 \rightarrow 4)-glycosidic linkages, adopts a fully extended conformation with alternating 180° flips of the glucose units.....	22
Figure I-14:	Sago starch production processes and source of solid waste known as "sago pith waste" or SPW (adapted from [75]).....	26
Figure I-15:	Schematic of pretreatment goals on lignocellulosic material at a higher severity treatments (adapted from [113]).....	34
Figure I-16:	(a) Schematic diagram of DIC equipments with important service equipments. (b) Four stages of DIC treatment including (1) setting-up an initial vacuum (2) injection of high steam pressure and maintain pressure (3) an instant pressure drop towards vacuum (4) putting back to atmospheric pressure condition.....	36
Figure I-17:	DIC reactor used in this work was MP system (with medium steam pressure).....	36
Figure I-18:	Mechanism of acid hydrolysis of glycosidic bonds in starch, cellulose and hemicelluloses into monosaccharide (\rightarrow shows reaction direction) (adapted from [44])......	38
Figure I-19:	Degradation of glucose and xylose into hydroxymethyl furfural (HMF), levulinic acid, formic acid and furfural. Both process will remove water and produced condensation products (adapted from [44]).....	41
Figure I-20:	General representation for rate kinetic for three conditions, based on relative rate constant (k_1/k_2) with (a) k_1/k_2 : 2 or k_2/k_1 : 0.5 (b) k_1/k_2 : ~1 or k_2/k_1 : ~1 and (c) k_1/k_2 : 0.1 or k_2/k_1 : 10. Time at product or reactant B_{max} was indicated by blue arrow (\downarrow) in plot (a) and (b) (adapted from [140]).....	45

Figure I-21:	Representative plot of (a) Ln concentration of species against time, and (b) Ln concentration of species (A, B or C) against time (t), acid concentration [H ⁺] or moisture content W to determine whether the process is first order or not. First order reaction will give straight line through data point, with R ² value ~1.....	46
Figure I-22:	Arrhenius Plot of ln k ₁ or ln k ₂ (log natural of rate constant) against 1/T (in Kelvin, K ⁻¹) for determination of activation energy of specific process condition.....	47
Figure I-23:	(a) Route of optimization towards the actual optimized parameter combination (adapted from [147]). (b) Perspective response plot for planar, minimum, ridge and saddle for first order and second order response surface equations (adapted from [149]).	50
Figure I-24:	Central composite design with 2 ^k factorial + 2k axial (k: 3). There are two level and three factors in this design. Simulation of two set of data at location of central point (CP), median star point (Star) and median axial point (axial) on axis x ₁ to show data location due to affect of thermal treatment.....	52
Figure II-1:	Research work flow for DIC process and testing method validation during exploratory and optimization study	56
Figure II-2:	General flow of work for DIC and dilute acid process during dilute acid hydrolysis process.....	57
Figure II-3:	Standard chromatogram obtained for glucose, formic acid, acetic acid and levulinic acid for (a) RID and (b) DAD 210 nm, mobile phase 0.5 ml/min.....	63
Figure II-4:	Representative standard curve for glucose.....	64
Figure II-5:	Standardized steps taken prior to DIC pretreatment	66
Figure II-6:	(a) Sample holder and sample container used in this study (b) DIC reactor chamber for thermal pretreatment.....	67
Figure II-7:	Stainless steel tubes in hot oil bath for dilute acid hydrolysis.....	69
Figure III-1:	(a) Schematic diagram of DIC equipments with important service equipments. (b) Four stages of DIC treatment including (1) setting-up an initial vacuum (2) injection of high steam pressure and maintain pressure (3) an instant pressure drop towards vacuum, and (4) putting back to atmospheric pressure condition.....	74
Figure III-2:	Plot (a) shows particle size distribution (SPW raw and SPW DIC) and Plot (b) composition of total polysaccharides for raw SPW. Total polysaccharides (starch, hemicellulose and cellulose) and residues were in percentage of dry material. Composition of total polysaccharides for different DIC severity will be determined separately to represent it as A ₀ for it will be affected by the particle size distribution obtained after each DIC pretreatment.....	75
Figure III-3:	Result Glucose concentration with X abscissa: (a) time, and (b) moisture content.....	76
Figure III-4:	Result Glucose concentration at X abscissa: (a) acid concentration and (b) temperature.....	76
Figure III-5:	Experimental data and model kinetics for extreme DIC treatment conditions.....	79
Figure III-6:	Model autohydrolysis kinetics for DIC treatment with (a) 0, (b) 0.75 and (c) 1.25 molar acid respectively. .	80
Figure III-7:	(a) Typical HPLC chromatogram for SPW with low DIC severity, with the existence of various low degree of polymerization of oligosaccharides, (b) Typical HPLC chromatogram for SPW with high DIC severity (solution was diluted), low degree of polymerization of oligosaccharides has been reduced with an increase in glucose amount, together with noticeable existence of formic acid and several degradation products, mobile phase 0.4 ml/min. was used due to deterioration of molecule separation and to operate below 70 bar pressure specification for HPLC column.	80
Figure III-8:	ESEM micrograph of raw SPW materials.....	82
Figure III-9:	ESEM micrograph of SPW DIC treated materials.....	83
Figure III-10:	Chromatogram for DIC autohydrolysis of SPW polysaccharides into glucose at different moisture content.....	87
Figure III-11:	Plot for glucose concentration (mg/g) against X ₁ for different X ₂ and X ₃ . Two other factors, i.e. treatment time and acid concentration were fixed at 4 minutes and 0.18 molar respectively.....	88
Figure III-12:	(a) Standardized Pareto chart for main effect and interaction effect for glucose response for group represent X ₁ : 150 – 200% together with (b) Main Effect plot that show the magnitude of effect for moisture, vacuum first stage and vacuum second stage.....	90

Figure III-13:	(a) Interaction factor against glucose concentration for moisture level(X1) : X2 at (-1 and +1) and (b) Interaction factor for X1 : X3 at (-1 and +1).....	91
Figure III-14:	Interaction factor for First vacuum, X2 and Second vacuum, X3 at -1 and +1 against glucose response....	91
Figure III-15:	Standardized Pareto chart for confirmation experiment	94
Figure III-16:	Normal probability plot for glucose response.....	94
Figure III-17:	Response surface model moisture content (X1) at low (-1) and high (+1) level.....	95
Figure III-18:	Response surface model for first vacuum (X2) at low (-1) and high (+1) level.....	95
Figure III-19:	Response surface model for second vacuum (X3) at low (-1) and high (+1) level.....	95
Figure III-20:	Central composite design with 2 ^k factorial + 2k axial (k: 3). There are two level and three factors in this design. Simulation of two set of data at location of central point (CP), median star point (Star) and median axial point (axial) on axis x1 to show data location due to affect of thermal treatment. Data set with red color for high DIC severity and blue color for low DIC severity.....	102
Figure III-21:	Pareto chart for effect of treatment factor towards glucose response.	104
Figure III-22:	Main effect and Interaction plots of factor towards glucose response.....	105
Figure III-23:	Estimated response surface, with fix pressure	105
Figure III-24:	Estimated response surface, with fix acid.....	105
Figure III-25:	Estimated response surface, with fix time	106
Figure III-26:	Plot kinetic autohydrolysis for (a) 0.01 and (b) 0.02 molar acid.....	108
Figure III-27:	Plot kinetic autohydrolysis for 0.03 and 0.04 molar acid.....	108
Figure III-28:	Plot kinetic autohydrolysis for 0.05 molar acids.....	109
Figure III-29:	Glucose degradation model for different temperatures at 144°C, 155°C and 165°C. At lower temperature, glucose degradation was bigger than at higher temperature.	110
Figure III-30:	Glucose degradation model for different acid concentration 0.01 molar, 0.03 molar and 0.05 molar at 165°C. At lower acid concentration, glucose degradation was bigger than at higher acid concentration.	111
Figure III-31:	Pareto chart for effect of treatment factor towards glucose response.	118
Figure III-32:	Main effect and Interaction plots of factor towards glucose response.....	118
Figure III-33:	ESEM of (a) crude starch and (b) DIC treated at high severity combination center point combination with X1:150%. Note in (b) for the modification of starch granules surface due to hydrolysis of granules surface with acid in combination with high temperature treatment.....	119
Figure III-34:	Estimated response surface, with fix pressure	119
Figure III-35:	Estimated response surface, with fix time	119
Figure III-36:	Estimated response surface, with fix acid at(a) - α , (b) central point and (c) + α . Acid concentration was the single main effect that significant in this study.....	120
Figure III-37:	Plot kinetic autohydrolysis for 0.17 and 0.20 molar acid (with statistical significant F distribution).....	123
Figure III-38:	TGA and derivative weight (TGD) plot of (a) raw SPW and (b) DIC SPW. Plot (a) show total polysaccharides were about 80% and ash content about 20%. Plot (b) shows that polysaccharides were undergoing changes into different molecular weight materials. Total polysaccharides were between 85 to 90% while ash content was about 15 to 10% of dry weight.....	131
Figure III-39:	Profile of glucose obtained from hydrolysis of DIC treatment in SPW with Low DIC severity (for a, b and c) and High DIC severity (for d, e and f) treatments. Hydrolysis was done with 0.01, 0.04 and 0.08 molar sulfuric acid respectively.	132
Figure III-40:	a) Low DIC, k_1/k_2 : 4.01, t_{Glumax} : 88.04 min; b) Low DIC, k_1/k_2 : 9.27, t_{Glumax} : 31.45 min; c) Low DIC, k_1/k_2 : 4.53, t_{Glumax} : 19.28 min; d) High DIC, k_1/k_2 : 63.96, t_{Glumax} : 20.24 min; e) High DIC, k_1/k_2 : 59.02, t_{Glumax} : 14.68 min; f) High DIC, k_1/k_2 : 17.18, t_{Glumax} : 22.29 min.....	133
Figure III-41:	Pareto chart for standardized effect of glucose at High DIC and Low DIC severities.....	136

Figure III-42:	Main effect plots of glucose yield at High and Low DIC severity	137
Figure III-43:	Response surface model and its contour for dilute acid hydrolysis of DIC treated SPW at (a) High severity and (b) Low severity at temperature 150°C. Acid concentration and treatment time were varied within treatment limit.	138
Figure III-45:	Profile of glucose residue experimental point and respective kinetic model after hydrolysis kinetic for 0.2 molar glucose with (a) 0.01, (b) 0.04 and (c) 0.08 molar sulfuric acid respectively.	142
Figure III-46:	Pareto chart for glucose degradation.....	143
Figure III-47:	Main effect and interaction effect for glucose degradation.	144
Figure III-48:	Response surface model for glucose degradation at acid (a) 0.01 and (b) 0.08 molar.	144
Figure III-49:	(a) Two thermocouple probe with one attached to the product and the other one exposed to reactor environment (b) Stainless steel reactor used for non-isothermal study.....	149
Figure III-50:	Profile of the non-isothermal plot for product temperature during DIC cycles at several saturated steam pressure. Data acquisition was done at several starting temperature.....	150
Figure III-51:	Model plot of heating for (a) DIC and (b) dilute acid hydrolysis process, h value was obtained from experimental data fitting with calculated model data based on Equation 22. Red line indicated time required to pass the non-isothermal temperature.	151

CONFIDENTIAL

List of Table

Table I-1:	Summary of major research areas, progress and challenges for the conversion of biomass into sugars (adapted from [27]).....	8
Table I-2:	Properties of glucose (Merck Index, 13th Ed).....	10
Table I-3:	Chemical composition of some typical cellulose-containing materials (adapted from [46]).....	15
Table I-4:	Properties of amylose and amylopectin in starch (adapted from [54]).....	21
Table I-5:	Energy content of biomass composition, products and its by-products together with several fossil fuels for comparison.....	23
Table I-6:	Composition of several sources of material and waste containing starch.....	27
Table I-7:	Non starch polysaccharides (NSP) and lignin in sago pith materials [79].....	28
Table I-8:	Composition of polysaccharides using acid and enzymatic hydrolysis. (adapted from [10]).....	28
Table I-9:	Biomass pretreatment methods (adapted from [105]).....	32
Table I-10:	Kinetic parameters for acid hydrolysis of various biomass feedstock (adapted from [24]).....	47
Table I-11:	Two level factorial design (2^k) for $k= 2$ and 3 . Other combination can be produced with the same configuration. Present work utilized 2^3 factorial design for vacuum and kinetic studies.....	51
Table I-12:	Actual parameters and its coded form for independent variable of central composite design for low DIC severity study.....	52
Table I-13:	Actual parameters and its coded form for independent variable of central composite design for high DIC severity study.....	52
Table II-1:	Summary and observation of HPLC partial validation. Data was compiled throughout experimental test..	64
Table III-1:	OFAT study factors and level combinations and result of trials.....	73
Table III-2:	DIC treatment at high temperature and acid combination (0, 0.75, and 1.25 molar sulfuric acid) with results.....	74
Table III-3:	Moisture content of SPW after sun drying and oven drying.....	75
Table III-4:	Rate constant k_1 and k_2 together with other data for respective factors at maximum glucose amount.....	77
Table III-5:	Information on mass balance of SPW at maximum amount glucose amount can be obtained from process using model in Figure P3-1-3a), 4b) and Figure P3-1-4a).....	78
Table III-6:	Characteristics of DIC treatment for rate constant (k_1 and k_2), rate constant ratio (k_1/k_2), time for maximum glucose, half life, time for total polysaccharides to depleted and ten half life as indicator for infinity time for the process.....	81
Table III-7:	Present study with 2^3 factorial designs with the following combinations:.....	86
Table III-8:	Summary of 2^3 factorial combinations for First vacuum (X2), steam and Second vacuum (X3). One set of factorial combinations consist of 8 treatments.....	86
Table III-9:	Result for DIC treatment according to respective moisture level and vacuum cycle. X1: 100% and 200% were repeated three and two times respectively with standard deviation.....	88
Table III-10:	Glucose concentration from DIC thermal treatment organized into respective coded factors. Data in grey cells was for (X1:+1) for experimental design X1: 150 (-1) against X1: 200 (+1).....	89
Table III-11:	Main effect for glucose at combination significant 95% X1:150-200% (column 150v200).....	89
Table III-12:	Summary of main effect and interaction effect for glucose response for group represent X1: 150 – 200% (column 150v200).....	89
Table III-13:	Analysis of Variance for glucose response for group represents X1: 150% (-1) and 200% (+1) (i.e. for column 150v200).....	90
Table III-14:	Difference in glucose yield for X1: 100% vs 150% and X1: 150% vs 200%.....	92

Table III-15:	<i>Analysis of variance for glucose yield confirmation</i>	93
Table III-16:	<i>Actual parameters and its coded form for independent variable of central composite design</i>	101
Table III-17:	<i>CCD experimental design in its coded and actual level (not in random order) with its respective glucose response and percentage of total polysaccharide</i>	102
Table III-18:	<i>Analysis of variance for glucose fitted model</i>	103
Table III-19:	<i>Regression coefficients for glucose yield</i>	103
Table III-20:	<i>Estimation Results for Glucose</i>	104
Table III-21:	<i>Data kinetic with acid concentration fix at 0.01 molar</i>	107
Table III-22:	<i>Data kinetic with acid concentration fix at 0.02 molar</i>	107
Table III-23:	<i>Data kinetic with acid concentration fix at 0.03 molar</i>	107
Table III-24:	<i>Data kinetic with acid concentration fix at 0.04 molar</i>	107
Table III-25:	<i>Data kinetic with acid concentration fix at 0.05 molar</i>	108
Table III-26:	<i>Rate constant for glucose generation (k_1) and glucose degradation (k_2) at temperature 149, 155, 161 and 165°C for acid concentration 0.01, 0.02, 0.03, 0.04 and 0.05 molar</i>	109
Table III-27:	<i>Activation energy, E_a (kJ/ mole) for different acid concentration</i>	110
Table III-28:	<i>Statistical data for model based on temperature</i>	111
Table III-29:	<i>Actual parameters and its coded form for independent variable of central composite design</i>	114
Table III-30:	<i>CCD experimental design in its coded and actual level (not in random order) with its respective glucose response and percentage of total polysaccharide</i>	115
Table III-31:	<i>Analysis of Variance for Glucose for fitted model, cell with grey color was with significant value</i>	116
Table III-32:	<i>Regression coefficients for glucose yield</i>	116
Table III-33:	<i>Estimation Results for Glucose</i>	117
Table III-34:	<i>Data kinetic with acid concentration fix at 0.05 molar</i>	121
Table III-35:	<i>Data kinetic with acid concentration fix at 0.08 molar</i>	121
Table III-36:	<i>Data kinetic with acid concentration fix at 0.13 molar</i>	122
Table III-37:	<i>Data kinetic with acid concentration fix at 0.17 molar</i>	122
Table III-38:	<i>Data kinetic with acid concentration fix at 0.20 molar</i>	122
Table III-39:	<i>Rate constant for hydrolysis (k_1) and degradation of glucose (k_2) at temperature 144, 149, 155, 161 and 165°C for acid concentration 0.05, 0.08, 0.13, 0.17 and 0.20 molar</i>	124
Table III-40:	<i>Activation energy E_a, (kJ/ mole) for respective acid concentration range</i>	124
Table III-41:	<i>Statistical data for model based on temperature</i>	124
Table III-42:	<i>DIC treatment combinations for dilute acid hydrolysis studies, initial moisture content X_1: 150%, together with vacuum cycles, X_2:+1 and X_3:+1 at 100 mbar</i>	128
Table III-43:	<i>Summary of TGA result for raw SPW and low DIC severity</i>	131
Table III-44:	<i>Kinetic data (rate constant k_1 and k_2) for dilute acid hydrolysis kinetic for two type of DIC treated materials: low severity and high severity DIC treatments</i>	133
Table III-45:	<i>Activation energy (kJ/mole) for dilute acid hydrolysis for two DIC treatment severities at 0.01, 0.04 and 0.08 molar acid sulfuric</i>	135
Table III-46:	<i>Analysis of Variance for Glucose yield from High DIC severity</i>	136
Table III-47:	<i>Analysis of Variance for Glucose Low DIC severity</i>	136
Table III-48:	<i>Kinetic data (rate constant k_2) for glucose degradation kinetic in dilute acid</i>	142
Table III-49:	<i>Activation energy (kJ/ mole) for degradation of glucose</i>	142

Table III-50: Analysis of Variance for glucose degradation.....	143
Table III-51: Comparison of glucose degradation rate constant ($k_{2\text{SPW}}$) for DIC treated materials normalized against rate constant of pure glucose ($k_{2\text{deg}}$) of respective treatment condition.....	144
Table III-52: Content of acid soluble lignin in hydrolysate of several SPW based materials for reference. All DIC pretreatment was done at center points combination.....	145
Table III-53: DIC treatment rate constant for heating with unit in s^{-1} and min^{-1}	150
Table III-54: Dilute acid hydrolysis rate constant for heating with unit in s^{-1} and min^{-1}	150
Table III-55: Value of h , rate constant for heating at 110, 130 and 150°C as compared to the nearest temperature value. .	151
Table III-56: Value of glucose for DIC and dilute acid hydrolysis system at the end of non-isothermal time. Rate of glucose conversion was calculated to assist in comparison of both system at about 150°C	151



CONFIDENTIAL

Abstract

Present state of art related to biomass conversion technology so far was found to concentrate on an enzymatic process, coupled with thermal pretreatment on biomass rich in cellulose. Biomass that rich in crude starch is also important in terms of strategic and economic point of view. The main objective of this study is to adopt a new strategy for a single step conversion of a crude starch material into oligosaccharide and glucose utilizing DIC technology. In contrast to existing thermal based pretreatment, DIC technology involves two vacuum cycles; first vacuum cycle was to increase steam accessibility on biomass and to reduce generation of steam condensate thus avoid losing of monosaccharide and hemicelluloses, while second vacuum cycle was to reduce potential thermal degradation of glucose. Distributions of products formed were found to be closely associated with severity of treatment on crude starch material. At lower DIC severity, pretreatment favors the formations of high oligosaccharide composition with small fraction of glucose; while at high DIC severity, pretreatment favors formation of high glucose as a major end product. During an exploratory study to establish the relevant reaction factors; vacuum cycle and moisture content were the two main factors influencing the conversion of crude starch into glucose. DIC starch conversion into glucose was found to be moisture dependent. Both factors were combined together to optimize the other three factors: pressure/temperature, treatment times, and acid concentration. High DIC severity treatment alone could convert nearly 50% of crude starch into glucose. During DIC optimization, an experimental design was developed and tested with DIC pretreatment in order to obtain a second order polynomial mathematical model that was then applied for response surface methodology (RSM). The interaction nature of above factors was examined and was found they depend on DIC treatment severity. Two experimental designs with low and high DIC severity were developed; Low DIC severity (acid: 0.01-0.05 molar, time: 0.5-3.0 min) and High DIC severity (acid: 0.05-0.20 molar, time: 3.0-10.0 min) with similar temperature range (144-165°C) were used. Data mining operation was done on RSM model to develop a kinetic model at both treatment severities. Kinetic data, including rate constant and activation energy were calculated from kinetic models of both severities to compare with actual dilute acid hydrolysis kinetic studies on two DIC treated samples. It was found that activation energy (E_a) for glucose generation at High DIC severity (E_a : 59.44 kJ/mol) was lower than at optimum dilute acid hydrolysis (E_a : 91.30 kJ/mol); while for glucose degradation, E_a was higher with High DIC severity (E_a : 144.12 kJ/mol) if compared to dilute acid hydrolysis (E_a : 45.14 kJ/mol). This indicates that glucose generation with DIC requires less energy while its degradation needs high energy. This combination was required to maximize glucose generation and minimize glucose degradation. Further studies with non-isothermal state during DIC and dilute acid hydrolysis support this finding. In normal polysaccharide conversion to low molecular weight (LMW) oligosaccharides and glucose procedures; two process steps were involved, namely the first process involved thermal pretreatment followed by a second process with dilute acid hydrolysis. In the present work, attempt was made to exclude dilute acid hydrolysis stage in order to establish that DIC process alone is sufficient for total polysaccharides conversion into LMW mainly glucose fraction. Information gathered from quantitative and statistical analysis on (i) exploratory studies, (ii) kinetic models from RSM of DIC process and (iii) kinetic data based on experimental works during dilute acid hydrolysis study; support the assumption that DIC treatment alone is sufficient for the total conversion required.

Résumé

L'état actuel de l'art lié à la technologie de conversion de la biomasse a, jusqu'à présent, principalement concerné les méthodes enzymatiques, éventuellement couplées à des prétraitements thermomécaniques ; les biomasses concernées sont généralement riches en cellulose, mais le matériel à haute teneur en amidon brut est également important des deux points stratégique et économique. Notre nouvelle stratégie est une contribution à l'étude de ce dernier type de biomasses riches en amidon, en vue d'une conversion comportant une seule étape de transformation en oligosaccharide et en glucose, à l'aide de la technologie thermo-mécanique de Détente Instantanée Contrôlée DIC. Cette opération a été étudiée, analysée, modélisée et optimisée. Contrairement à un traitement thermique conventionnel, la technologie DIC comporte deux étapes incluant l'instauration d'un vide capable d'accroître l'accessibilité de la vapeur dans la biomasse, puis d'une étape de vide final en vue de réduire la génération de molécules de dégradation thermique du glucose. L'analyse des composés (oligosaccharides, glucose...) a été réalisée ; elle a pu démontrer que le processus était étroitement associée à la sévérité du traitement brut. Le prétraitement DIC de faible sévérité mène à des rendements élevés en fractions oligosaccharidiques avec une petite fraction de glucose. Par contre, le traitement DIC de haute sévérité permet d'accéder au glucose comme principal produit final. Au cours de l'étude exploratoire, le cycle de vide et de haute pression d'humidité a été établi, avec comme facteur de réponse le taux de conversion de l'amidon en glucose brut. Les deux facteurs de pression de vapeur d'eau et de vide ont été combinés ensemble afin d'optimiser trois autres facteurs opératoires : la concentration d'acide, le couple de pression/température et le temps de traitement. Le traitement DIC de haute sévérité a été démontré comme étant capable de convertir près de 50% d'amidon brut en glucose à l'étape du simple et unique traitement thermomécanique. Une autre étape du processus a été impliquée : il s'agit de l'hydrolyse à l'acide dilué, souvent à la suite du prétraitement DIC. Au cours de l'étape d'optimisation du prétraitement DIC, la méthodologie de surface de réponse a été utilisée pour aider au développement de modèles cinétiques auto-hydrolysés DIC. D'autre part, les modèles empiriques de la cinétique ont été développés. Dans le cas de faible sévérité, le modèle aboutit à des réponses étroitement associées aux deux limites inférieures et supérieures de la concentration acide et du temps de traitement. Par contre, ces modèles quand ils sont obtenus à de niveaux de traitement grande sévérité, ont été jugés seulement associés aux valeurs supérieures de ces paramètres opératoires. Cette observation a été déduite de l'équation polynomiale utilisée, tandis que les modèles cinétiques ont été basés sur une série exponentielle. Une série polynomiale de plus grand ordre serait donc nécessaire pour pouvoir explorer avec précision les données de la surface de réponse pour ce genre d'analyse approfondie à tous les niveaux des facteurs. Lors de l'étape d'optimisation de l'hydrolyse dans une solution d'acide dilué, le premier modèle cinétique consécutive a été développé pour étudier les mécanismes de conversion des polysaccharides totale en glucose et en ses produits de dégradation. Le modèle empirique de surface de réponse a été utilisé pour étudier les effets de facteurs pendant le processus opératoire. La teneur en humidité et le cycle de vide ont été des facteurs communs. Plus le temps de traitement est court et plus la température est élevée, et plus la génération du glucose est importante. Cette étude montre que le traitement DIC de haute sévérité est capable de convertir les polysaccharides totaux en glucose avec une faible dégradation du glucose. Les produits solides résiduels pourraient également faire l'objet d'un traitement enzymatique.

Brief overview

Much information has been published in international scientific publications and conference proceedings about the topics related to this work, i.e. thermal processing [1, 2], DIC technologies [3-5], dilute acid hydrolysis [6, 7], enzymatic hydrolysis [8, 9], biomass waste utilizations (specific for reference in present work, including cellulose, starch and sago pith waste [10, 11]). Due to the vast information and subject need to be covered, it is very important to piece together the existing accumulated knowledge and its significant information in order to appreciate the present intention to utilize DIC treatment for biomass physicochemical changes. This will cover some topic on present the challenges and prospects to enhance the potential of biomass waste for industrial application and food uses.

CONFIDENTIAL

Thesis Organization

There are six main topics covered in this thesis: (1) polysaccharides and cellulose materials, sources and applications, (2) present state of the-arts of thermal processes to assist the lignocelluloses/ biomass materials utilization, (3) review of DIC technology and its current applications (4) dilute acid process for polysaccharides-cellulose-sugar conversion with some insight into existing competitive enzymatic processes (5) introduction to the main experimental techniques used in this dissertation and its association for the lignocelluloses properties and (6) application of DIC as a pretreatment process on waste materials for dilute acid hydrolysis of polysaccharides to glucose.

Results obtained from the present work presented in publication's ready style that covers the main aspects of our research works including process optimization, hydrolysis and autohydrolysis of sago waste materials, kinetics of DIC pretreatment and dilute acid hydrolysis.

This thesis is further organized into parts as follows:

Part 1: Literature Review that discusses in depth details of the theoretical background of thermal treatment and state-of-art of thermal processing, polysaccharides autohydrolysis processes, current state of biomass application in polysaccharides to glucose.

Part 2: Materials and Methods. It is divided into small chapter that covers all aspects of material's information, preparation and characterization. Work scopes, including initial work to establish final research plan, laboratory and pilot scale works. Chapters that described test protocol including several background works for validation, experimental design and modeling of the process are included and presented in details with its results.

Part 3: Result and Discussions is divided into several small chapters that cover the specific needs of specific process project being investigated. Each chapter is prepared as part of a journal publication style with respective results and discussion of specific topic.

Part 4: Conclusion and Perspectives. The first chapter covers overall conclusion in this work and summary against existing technology application. The second chapter covers some interesting aspects of concluded work, and some insights related to associated works for future process enhancement, pilot and industrial application.

Problems Review

This work was related to the utilization of DIC technology to produce glucose from agricultural waste. Compared with existing thermal based biomass pretreatment, DIC technology utilizes medium steam pressure technology, between 0.7 and 0.9 MPa and different treatment regime [3-5]. Current technology uses high saturated steam supply such as for Steam Explosion between 1.5 MPa to 3.0 MPa [12, 13], while Ammonia Fiber Expansion (AFEX) was using liquid ammonia at a moderate temperature (100-140°C) for pretreatment [1]. Several systems related to biomass pretreatment will be discussed for comparison purpose and summarized of important points are highlighted.

Generally, there are three factors that correlated to each other in any chemical process industries: good input materials, output products and processing technology being used [1]. For the present work, the specific interest for treatment technology was on thermal based technology, with specific reference on DIC technology and main response for output was glucose. In order to achieve a high composition of glucose at the end of processing stage; a high polysaccharide composition in biomass will eventually ensure a high quantity and quality glucose down the processing line. Factors related to the success of biomass utilizations, including the ability of the process to hydrolyze crystalline parts of materials, the accessibility of chemical or enzyme into biomass internal structures and to overcome lignin that bind together the lignocelluloses materials [2, 14]. Other success factors, including the availability of high surface area to immediately enable chemical and enzyme reaction, combined with substrates are free from toxic composition that may block enzyme accessibility [15]. This was very important if the ultimate usage of the end product were associated with enzymatic reactions.

In general, three thermo-chemical routes can be used to convert biomass materials into low molecular weight (LMW) polysaccharides: (1) gasification to syngas, (2) pyrolysis or liquefaction to bio-oils and (3) through hydrolysis to sugars and lignin [1, 16]. The third route, through dilute acid hydrolysis to sugars and lignin was the main interest in this work.

Due to biomass complexity, the degree of cellulose crystallinity and morphology present before and after pretreatment, the kinetics of the pretreatment reactions and its chemical linkages present were of this work interest. Determination of those parameters will give unprecedented insight into biomass structure and composition. All knowledge obtained from the work will guide modified pretreatment techniques and conversion technologies to increased sugar's yields and also to limit inhibitor's formation. Data obtained also can be used to develop a structured modeling approach to explain the structural and chemical contributions that are most prone to the pretreatment process.

To summarize general solution for high level of product quality and quantity, ultimately; a pretreatment will be required to make biomass polysaccharides available for hydrolysis or even within the same processing step to break down polysaccharides into monosaccharide. Two stage processes will be employed; in first stage, biomass material will be pre-treated to break down ultra cellular components and its cell walls structures. The second step involved with the depolymerization of polysaccharides to monosaccharide, either through acid or enzyme hydrolysis. For this particular work, dilute acid hydrolysis will be employed. In our study, single stage treatments were enough to convert polysaccharides of interest into high sugar concentrate with very low glucose degradation.

Goals and Objectives of the Thesis

This work deals with two-steps conversion of sago pith wastes also known as crude starch into high sugar concentrate through DIC treatment and low acid concentration hydrolysis.

Objectives of the thesis were:

- Development of new process based on DIC thermal processing at lower steam pressure and temperature treatment regime compared to existing biomass thermal pretreatment process.
- Development of a dilute acid hydrolysis kinetic model and test it against experimental data.
- Optimization of DIC pretreatment with response surface methodology (RSM).
- Development of a single high solid autohydrolysis process using DIC technology to produce concentrated glucose syrup from sago waste material (SPW).
- Improvement of steam diffusion into porous materials through vacuum application thus improves the accessibility of materials for the second process of dilute hydrolysis.
- Kinetic study and its application for understanding the kinetics at isothermal and non-isothermal processing stage.

This work will concentrate on the optimization of processes, through experimental design approach and process kinetics that generate minimum glucose degradation. Preliminary investigation was conducted to establish direct DIC and dilute acid hydrolysis parameters and its treatment levels. Thermal processes with nearly complete hydrolysis of polysaccharides content with crude starch or sago pith waste (SPW) were demonstrated. Ultimate objective as described earlier was to develop a process with the ability to control the intermediate stages, improve the generation of glucose (including oligosaccharides and its lower degree of polymerization components), and decrease the amount of total glucose degradation products (such as furfural, levulinic acid). Main responses of the operation studied in this thesis were the amount of glucose to maximize and the glucose degradation products to minimize.

Important aspects of the experimental work in this study were the first DIC vacuum stage, which helps increasing steam diffusion within the porous microstructure of biomass followed by the dilute acid autohydrolysis. Both process stages were used to maximize whole glucose production. Initially, this work established different treatments with vacuum and no vacuum during DIC process to enhance diffusion into micro porous material and to increase glucose amount from the process.

Strategy and Planned Solutions

It was understood that chemical processing usually involved with complex systems, and since this work deals with thermal pretreatment operation, several strategies need to be implemented to ensure good understanding of the system, process reaction and finally to control of the product output quality. A simple but consistent with a high-yield pretreatment process that suitable for a wide range of lignocelluloses feedstock is one of the most critical steps in realizing an efficient and cost-effective biorefinery [17]. Preliminary investigation shows that DIC technology can offer such a simple but efficient operation for biomass pretreatment [18]. DIC as a thermal treatment is greatly different from existing thermal treatment regime currently being used elsewhere. This work is designed with an industrial objective for offering relevant alternative steam pressure pretreatment. The following summarized several important aspects and strategies in this study:

- Selection of materials to match the thermal treatment regime was very important to ensure maximum glucose while minimizing the potential inhibitors' generation.
- In this work, DIC thermal processing was applied to increase the porosity of lignocelluloses materials in order to increase surface area for the hydrolysis.
- Optimization of the process was carried out to ensure complete hydrolysis of starch into glucose while minimize glucose generation. This was done via careful selection of experimental design parameters, and their ranges. Complete autohydrolysis of starch was important for industrialization and total recovery of polysaccharides.
- Identification of the impact of vacuum cycles in DIC to concentrate only one treatment type.
- Modeling of the hydrolysis kinetic for glucose generation and degradation.

Final outputs from this research work, as well as during exploratory and developmental works were outlined as follows:

- Identification of main process parameters that affect directly to the generation of glucose from biomass. This including trial and selection of biomass for actual laboratory work, determined its composition and suitability with research strategy.
- Setting of the minimum and maximum limit of each parameter during DIC and post-DIC treatment to meet material pretreatment requirement, and to ensure homogeneous supply of materials in every step of research work. It is very important to keep the material supply to be very homogenous to achieve good working model for industrial work.

Most of the above trials were conducted based on published methodologies and perfected through several trial runs during establishment of limits for treatment factor and processes. Only final testing methodologies were used throughout research work presented in this thesis. Bulk of this work result was from experimental runs based on optimized process and test methodology and was done according to designed experiments. Results obtained were modeled using response surface methodology or first order kinetic.

PART I. STATE OF ART

This literature review was to cover all basic theoretical and experimental backgrounds necessary to achieve the main objectives outlined in the major work. By providing a review of both relevant current associated research in the literature and certain past work, we could get the basis which were essential to develop key theories of this work. A critical evaluation on important finding will be discussed and summarized to give good insight of previous, present and potential application of this technology.

This review will focus on the product of interest, source of product, present state-of-art of technologies and processes being utilized, optimization process through experimental design, instrumentations for test and on the modeling of the results.

PART I. CHAP 1.

REVIEW: GLUCOSE INDUSTRY AND BIOMASS

I.1.1. Brief overview

Apart of the increasing need in fuels and energy for industrial uses, the requirements to recover, value and use agro-industrial wastes are growing mainly for environmental reasons. Indeed, the presence of large quantities of non-degradable or toxic biomass feedstock waste has led to a large variety of environmental pollution problems, which have stimulated research on different recovering processes such as the utilization of biomass as an alternative source of energy through adequate chemical operations, which should provide a way out of the current fossil fuel sources situation.

Contributing factors besides industrial market forces as suggested more than 10 years ago were the beginning of stricter environmental laws that shift the responsibility of ecological damage to the producer, thereby connecting biocompatibility to the costs of production [19]. This has shifted the operator to look for much more environmental friendly solutions. Majority of industrially utilized cellulose to date finds its application in the industry related to a pulp and paper. Large amounts of cellulose waste however, currently find no application and are treated as waste by-products, being either burned or naturally rotted on the plantation site.

I.1.2. Conversion of biomass to glucose

In principle, biomass containing cellulose, hemicelluloses and starch can be used to produce glucose with some modification of a certain initial process to ensure high quality of final products. Currently, the technologies that utilize cellulose as polysaccharides sources are progressing to be commercially significant [20, 21]. There still a lot of challenges need to be overcome in order to make the technology become commercially available. Wyman and Cutler (2004) [21] has made some cost comparison for the production of ethanol from sugar crops, starch and lignocelluloses material together with energy balance for each process. They concluded that substantially research was needed to advance the technologies and high attention would be focused on overcoming perceived risk and capital investment.

The conversion of biomass into certain valuable chemicals was one of the main research interests in almost every chemical based research laboratories progressing from the first generation of biofuel technologies [22-24]. It was very crucial for the second generation biofuel technologies to utilize lignocelluloses materials and has become a trend now to exploit non-food biomass [1, 25] for some projects related to bio-ethanol/ biodiesel to avoid competition with food demand.

The basic needs of the process are still, however concentrating on finding an effective method to disrupt biomass integrity before it can be optimally utilized. Cumulative challenges comprise of reduction in cost for material collection (logistic), conversion process, (high enzyme cost and high material cost for reactor construction), waste accumulation, as well as in optimizing and process integration.

Present research work was designed to study the interim thermal processing gap with materials containing polysaccharides (cellulose, traces of hemicelluloses, and starch); with as the principal objective to convert them into glucose. Based on above analysis, this work will focus on the area of a specific feedstock (sago pith waste), and thermal pretreatment process carried out at various operating conditions to study the characteristic of material and acid hydrolysis output.

Pretreatment is one of the critical steps in biomass utilization, with high impact on a downstream process. It was suggested to contribute about 18% of total production cost of ethanol production. Pretreatment with dilute sulfuric acid has been the subject of research for more than two decades, particularly for work related to bioenergy research. It was reported that it helps to recover 80% to 90% hemicelluloses in hot water extract after the pretreatment [26].

The integration of DIC pretreatment into biomass utilization process is done to capitalize DIC as a unique process with fast heating (due to saturated steam) and exceptionally fast cooling (due to a pressure drop towards a vacuum). Combinations of both steps were useful for fast starch to glucose hydrolysis and fast stopping the degradation of glucose from occurs.

Major progress and challenges for the conversion of biomass into sugar were reviewed and summarized in the following table.

Table I-1: Summary of major research areas, progress and challenges for the conversion of biomass into sugars (adapted from [27])

Area	Description	Progress	Challenges
Feedstock	Use and modification of biomass sources: agricultural, forestry or municipal waste, or dedicated energy crop	Initial analyses of feedstock yields and collection costs; compositional analyses; research into cell wall biosynthesis and chemistry	Reducing collection/feedstock costs; determination of desired feedstock characteristics; genetic modification of feedstock to maximize value
Pretreatment	Mechanical and chemical treatments to facilitate conversion of lignocelluloses biomass to fermentable sugars	Evaluation of effectiveness of different pretreatment processes on variety of feedstock; characterization of inhibitors of downstream processes	Reducing capital expenses and input costs; reducing energy inputs; recycling/usage of waste streams; process integration
Enzymatic hydrolysis	Enzymatic conversion of cellulose and hemicelluloses polymers to fermentable sugars	Reduction in cost of cellulase enzymes; understanding of <i>T. reesei</i> and <i>A. niger</i> cellulases	High enzyme costs; poor activity/long incubation times; optimized enzyme mixtures for specific feedstock/processes
Fermentation	Conversion of fermentable sugars to ethanol or other fuels and bio-products	Characterization of C5/C6 sugar fermenting organisms; analysis of tolerance to inhibitors in fermentation	Organisms with rapid growth, improved tolerance to inhibitors and fermentation of multiple sugars under industrial conditions
Process engineering	Engineering designs to enable economic biomass processing at commercial scale	Process models constructed, tested and revised	Optimized process integration; incorporating best (sometimes proprietary) data into models

I.1.3. Summary of economic factors in this work

Extensive research work for the conversion of biomass materials into glucose was done by various research groups [28-32] utilizing different model materials such as cotton linters,

biomass waste, filter paper and even pure cellulose, with a majority of them utilized enzyme at the second stage. Two large companies specialized in enzyme technology, Novozyme and Genencor have estimated that the cost of enzyme for cellulose and hemicelluloses conversion to glucose would be 40 to 100 times higher than an enzyme for starch hydrolysis to glucose [33]. At the very beginning, cost of enzyme was reported to be USD 5–10 per gallon of ethanol produced, and reduced to USD 0.50/gallon in 2010 against the current ethanol production cost estimated at USD 2.0/gallon[20]. Genencor further estimated that within next several years, cost of enzyme would be reduced to USD 0.20–0.30/ gallon ethanol.

Based on above information and the stoichiometric reaction of one mole of glucose ($C_6H_{12}O_6$) will produce two moles of ethanol (CH_3CH_2OH) and carbon dioxide (CO_2) respectively; we can deduce that enzyme cost for biomass conversion into glucose was about USD 0.086/ kg glucose. In reality, it may cost more due to impossible to achieve 100% conversion, as small portion will be utilized by the microorganism for their growth.

In another estimate by Wyman & Cutler (2004) [21], ethanol production cost from sugarcane in Brazil was about USD0.006 to 0.007/liter for labor, USD0.004 to 0.006/liter for maintenance, USD0.002/liter for chemicals, USD0.002 to 0.003/liter for energy, USD0.004/liter for other items, and **USD0.127 to 0.134/liter for sugar**. The total cost of ethanol was about USD0.167 to 0.185/liter. The overall capital investment was about USD0.52/annual liter of capacity for a process that operates for 150 days/year making about 240,000 liters of ethanol per day. Allowing another USD0.04 to 0.06/liter for interest on capital, capital recovery, and other fix costs, the total cost including return on capital as applied in Brazil is about USD0.21 to 0.25/liter at the plant gate.

However, the actual problem was lies with the logistic operation and transportation of waste material from waste generation site to the hydrolysis plant. In some report, the cost to transport the material was very expensive due to high water content, as high as 500% on the dry basis of solid material. This was further associated with low bulk density (on dry basis) of material, and availability of material at different location contributed to high logistic cost for the final products [21]. The solution for the burden in logistic was including to re-locate the hydrolysis plant next to its raw material source such as at the plantation specifically produced raw material for fuel such as sugarcane, corncob and cornstalk [27].

I.1.4. Carbohydrate and Glucose

I.1.4.1. Presentation and main properties

Glucose, the main character in this work was part of carbohydrate family. It has been always an ideal substrate and energy source for most microorganism's metabolism as well as the main resource of carbon for variety of products such as biopolymers, antibiotics and bio-ethanol [34]. Selected properties of glucose were presented in Table I-2 as reference.

Carbohydrates are polyhydroxy compounds of nature that exists as small molecules or as macromolecules. Unit of carbohydrate was glucose or sugar, which was formed as a product of photosynthesis of carbon dioxide and water. Sugars act as a source of energy, while certain polysaccharides such as starch fulfill the need as storage or reserved until utilized. Cellulose and hemicelluloses contributing to the strength of the plant cell walls. Carbohydrate can be further classified into three groups: monosaccharide (common plant's

monosaccharides -glucose, mannose, galactose, xylose and arabinose); oligosaccharides (linkage of monosaccharides into di-, tri-, tetra-saccharides, limited to unit of monosaccharide less than ten units); and polysaccharides (complex molecules composed of a large number of monosaccharide units joined by glycosidic linkages) [35].

Table I-2. Properties of glucose (Merck Index, 13th Ed)

Physical properties	Values
Molar mass	180.16 g/mol
Melting point	146°C α -D Glucose, 150°C β -D Glucose
Enthalpy of formation (298°C)	-1,271 kJ/mol
Enthalpy of combustion (298°C)	-2,805 kJ/mol
Optical Rotation	$[\alpha]_D +112.2^\circ \rightarrow +52.7^\circ$
Index of Refraction: n_D^{20} 10% solution	1.3479
Density: $d_{17.5}^{17.5}$ of water solutions	5% (w/v) = 1.019 10% (w/v) = 1.038 20% (w/v) = 1.076 30% (w/v) = 1.113 40% (w/v) = 1.149

Glucose is the most common carbohydrate, aldose monosaccharide also known as hexose sugars, made up of six carbon component. All hexose sugars have five hydroxyl groups (-OH) made them soluble in water [36]. It was synthesized using carbon dioxide by chlorophyll in plants with sunlight as an energy source, and further converted to starch for storage. Glucose can exist in open-chain form and cyclic form with un-branched backbone of six carbon atoms or in cyclic form [34]. Since it contains alcohol and aldehyde or ketone functional groups, the straight-chain form can easily transformed into chair form also known as hemiacetal ring structure. This was done through conversion of C5 -OH group into ether linkage and closing the ring with C1. Scheme of association is presented in Figure I-1.

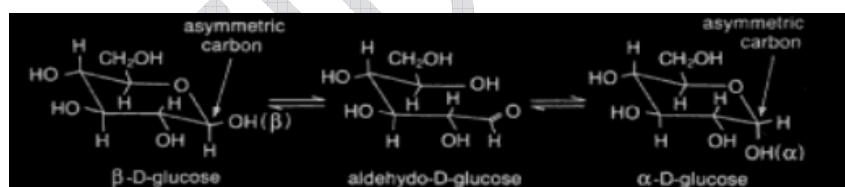


Figure I-1: Glucose exists in the aldehyde ring forms with C1 as centre of asymmetry. Two isomers exist as either α -D-Glucose or β -D-Glucose from open-chain form. β position is when (-OH) on C#1 on same side of cyclic ring of C#6 (on horizontal projection), α position is on different side (on downward position). [34]

I.1.4.2. Commercial glucose production from starch

Presently, the technology for glucose production very much depends on starch with two main hydrolysis processes to obtain glucose, i.e. acid hydrolysis and enzymatic hydrolysis [21]. Enzymatic hydrolysis was the most preferable way currently with starting starch materials from corn, potatoes, wheat, rice, cassava.... etc. The process has been reviewed extensively in publications [21, 34, 37]. Commercial glucose production process was presented in the Figure I-2.

Enzymatic hydrolysis process starts with starch milk emulsion preparation, followed by double injecting process to liquidize emulsion and enzyme saccharification into glucose. Purification steps include removal of remaining solids, discoloring and filtering. Ion exchange process is devoted to recover back the enzyme, followed by a vacuum process to concentrate the solution. At final stage, crystalline glucose is dried, separated and packed.

Starch milk liquefaction is a continuous process, while saccharification was a batch process at pH 4.0 - 4.5 for optimum amylase reaction. Saccharification will cut starch chains into several dextrose equivalents (DE) materials based on requirements. Theoretically, liquefied starch with 8-12 DE can be hydrolyzed completely by the glucoamylase mixture of 100 DE at low solid concentrations. Mixture was purified and concentrated after obtaining a solution with 95-97% glucose, 1-2% maltose and 0.5-2% (w/w) isomaltose, followed by a drying stage.



Figure I-2: Processing chart for glucose production from starch obtained from cereals. [Adapted from - <http://www.tereos.com/en-gb/activites/filieres/cereales.html>]

Acid hydrolysis process follow similar route with modification at saccharification step and acid neutralization. Acid process is used to manufacture intermediate conversion products from 35 to 55 DE. Intermediate and higher conversion products for special purposes can be made by substituting acid with enzymes, in similar two step process as described above. (Note: DE scales refers 100 DE as pure glucose (glucose is also known as dextrose) and a 0 DE as pure starch).

Enzymatic reaction became the preferred choice due to; with enzymes process alone (α -amylase and amyloglucosidase) is possible to produce 28 to 98 DE syrups. Another product, High Fructose Starch-based Syrups (HFSS) can be produced immediately after obtained high DE syrups in a resin fix-bed isomerase enzyme for conversion of glucose to fructose. Simple sugars and series of dextran molecules produced from this process have a range of molecular weight from 180 to 2.4×10^7 and diameter of molecules from 8 to 1600 Å.

I.1.4.3. Biorefinery concept and glucose production from biomass

Present application of glucose from starch was mainly for the food, and considered expensive for other industrial applications. In order to develop a competitive glucose manufacturing process utilizing biomass resource, several strategies were employed. One of the strategies was developed based on a novel biorefinery concept. American National Renewable Energy Laboratory (NREL) explained this concept as "A biorefinery is a facility that integrates biomass conversion processes and equipment to produce fuels, power, and chemicals from biomass. The biorefinery concept was analogous to today's petroleum refineries, which produce multiple fuels and products from petroleum." [38]. NREL's further explain their biorefinery concept is built on two different "platforms" (1) "sugar platform" and (2) "syngas platform", in Figure I-3 which respectively are based on biochemical processes with focus on sugar fermentation and based on thermo-chemical processes with focus on biomass gasification. The concept also has been extensively reviewed [39], since

the very beginning of first generation of biofuel. It was evolved into its current state of development with second generation of biofuel. Detail explanation for each process route was presented in various publications [1, 16] and summarized further in Figure I-4.

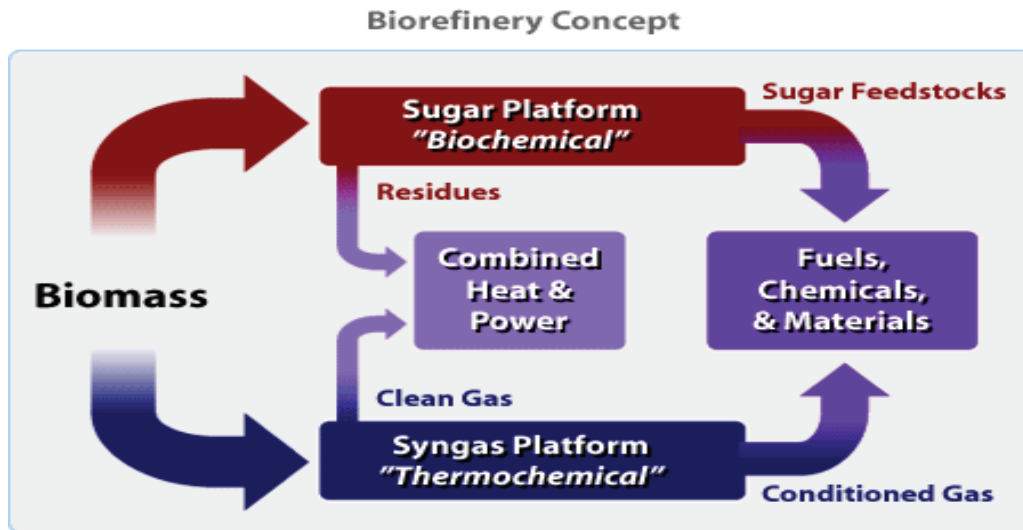
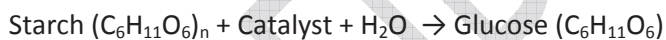
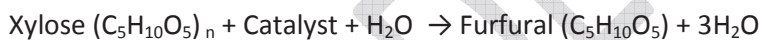
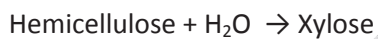
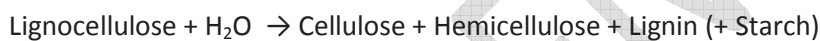


Figure I-3: Novel biorefinery concept with biomass as feedstock (adapted from [38]).

The following general equation of the conversion describe conversion of biomass composition into several chemicals of interest [40].



with n normally > 10,000 unit of glucose or other monosaccharide.

Details of products based on sugar conversion process and its related products can be further explained as in the following diagram.

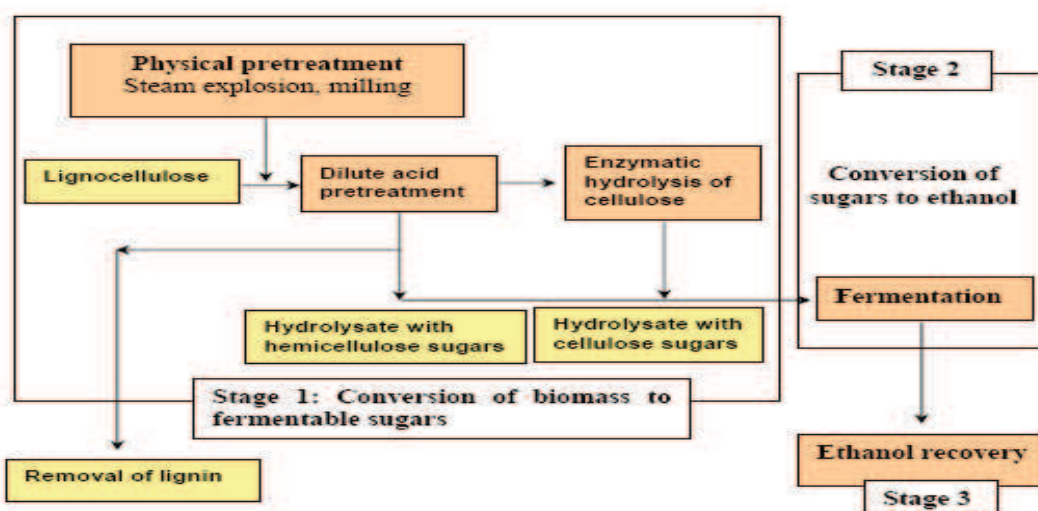
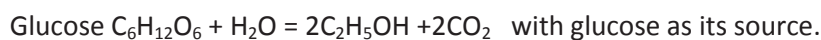
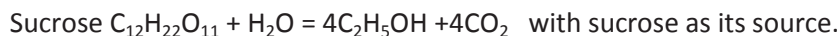


Figure I-4: Stages of conversion of biomass materials into bioethanol (adapted from [41])

The use of biomass for energy, fuel and chemicals as being develop in this work is parallel to the concept of biorefinery as described earlier. Stoichiometry reaction for sugar to ethanol was established as:



More than ethanol, glucose also can be used to produce other important products mainly food, amino acids and organic acids.

Typically, this concept needs the integration of various processes to fractionate biomass into various end products. This review and our work will concentrate on the sugar platform with concentration on the thermal pretreatment and dilute acid hydrolysis process. It initially combined mechanical and thermal fractionation processes followed by chemical, biochemical or thermo-chemical conversion process. Generally, there are three main stages of operation in biorefinery:

- The first step involves the sizing of materials; biomass will need to be cut into suitable size for effective thermal pretreatment. These operations will increase the overall available surface area for next operation due to formation of internal micro porous material. In this stage also, thermal treated material will be extracted and its component such as lignin, hemicelluloses, extractive and cellulose will be transformed into individual components as suggested in above general equations.
- In the second stage, individual component separated earlier will undergo several processes to separate it into its monomers. Several processes need to be employed at this stage such as primary hydrolysis (acid or enzyme), followed by its secondary process such as glucose fermentation into bioethanol.
- The third stage will involve the purification of products of each individual product. If the final product of interest is purified glucose, several steps such as extraction of other intermediate of products such as levulinic acid, furfural and other acid such as formic and acetic acid are taking place at this stage. In the frame of our present work, we will not detail every step of the process necessarily.

I.1.5. Lignocellulosic Biomass

The existence of large supplies of lignocellulosic biomass should offer opportunities to address a significant fraction of fuel and energy needs. Economically, biomass may offer an advantage because it can be produced quickly and at significantly lower cost than food crops [42]. However, most of the processes for converting biomass to fuels are yet fully developed for commercialization [1, 21, 39, 42]. Most recently, it was reported that research was done for fundamental understanding of the physical and chemical transformations at various stages of processing and is yet ready for commercialization [43].

Lignocellulosic biomass materials are the most abundant material in the world. Its sources range mainly from forest and agricultural residues. Lignocelluloses is the collective name for the three main components of plant material, namely cellulose, hemicelluloses and lignin [35, 44]. Another term that is coined for lignocelluloses material was biomass, which can be defined as a renewable material, including those of trees and wood and its residues, agricultural plant and crop residues, energy crops, aquatic plants and wastes generated from

all above [23]. Biomass terms in any case will not included food crops, even though in some cases, biomass was a component of food crops such as the non edible parts or waste generated from the process to extract the edible part. Such non edible parts and wastes sometimes pose a big problem for their disposal and contribute to a major environmental crisis.

In most cases, biomass waste is coming from extraction of edible materials such as in case of sugar canes, palm fruit bunches, wheat and corn stalks, sun flowers and sago barks. In other aspect, biomass waste also can be found from industrial waste such as waste from particle and hardboard operation. Preparation and treatment of these materials are other challenges before their potential to be harvested [30]. Major compositions of biomass include: cellulose, hemicelluloses, lignin, starch and extractives [35, 36, 44]. The first four components contribute to higher mass component and exist as high molecular weight molecules, while extractives usually consist of a number of small molecular weight materials and only available in small quantity. Collectively, cellulose, starch and hemicelluloses can be referred as polysaccharides and can be hydrolyzed into their monosaccharide components through enzymatic or acid hydrolysis.

Cellulose is homopolymer of glucose with β ,1-4 linkage, while starch is a glucose homopolymer build of glucose with α ,1-4 linkage and hemicelluloses is a heteropolymer containing both hexose and pentoses [35, 44]. Lignin on the other hand was highly irregular polymers with three dimensional structures build up from oxygenated phenyl propane units interlinked via β , 0-4 and α , 0-4 aryl ether linkage. Hemicelluloses and lignin behave as a shield to both starch and cellulose in plant cell walls. Extractives which are soluble in neutral organic solvents or water is non-structural wood component comprise of an extraordinarily large number of individual compounds of both lipophilic and hydrophilic types [35, 44]. Main purpose of above cell wall polysaccharides was to behave as structural component and to provide certain function such as transport of water, [45, 46].

There are two types of wood classification: hardwood or softwood. Hardwood refers to wood from broad-leaved (mostly deciduous) or angiosperm trees (plants that produce seeds with some sort of covering). Softwood on the other hand refers to wood from gymnosperm trees (plants having seeds with no covering). In the case of palm trees such as sago and oil palm which comes from the monocotyledon plants, it was covered under the classification of hardwood with some similarity to hardwood such as the existence of high xylose content [35, 44].

Polymers have different reactivity to thermal, chemical and bio processing; and different biomass compounds have different polymer composition making it much more difficult to deal with. Biomass will require a different utilization strategy versus its composition and utilization needed; we always can expect that optimization result in the field of thermal processing will not have the same effect if utilized in the field of chemical process or on another way around. In most cases, different biomass species will require distinctive optimization strategy even in the same thermal processing regime [26, 47].

The degree of elastic or viscoelastic properties in a paper depends largely on environmental conditions of moisture and temperature. There is a well defined transition zone between elastic ("glass-like") and viscoelastic behavior. It is defined by the glass-transition temperature or " T_g ." Below the T_g temperature, dry cellulose will behave as an elastic material, and above its T_g , it will exhibit viscoelastic behavior. For dry biomass materials,

related T_g temperatures are: cellulose at 240°C, hemicelluloses at 190°C, and lignin at 150°C [48]. For the forest products industries, lignin is the major barrier to efficient extraction of cellulose fibers for pulp and paper production. For the bioenergy industries, lignin was a barrier to saccharification for production of liquid biofuel. However, on higher side lignin was with an average of 2.27 kJ/g, i.e. 30% more than the energy of cellulosic carbohydrate could provide [49].

Above information was vital for the development of our theory in this work. In order to have good deconstruction of biomass material, thermal property of lignin need to be overcome first, followed by good extraction and hydrolysis. In this work, thermal treatment in the range of 144 to 175°C was used to exceed minimum T_g of lignin, i.e. to overcome its saccharification barrier on hemicellulose and cellulose.

I.1.5.1. Biomass Physical and Chemical Compositions

Weight percentage of four main lignocelluloses component has been reported in various publications about different raw materials and summarized in Table I-3 and Figure I-5.

Table I-3: Chemical composition of some typical cellulose-containing materials (adapted from [46])

Source	Composition (%)			
	Cellulose	Hemicelluloses	Lignin	Extractive
Hardwood	43-47	25-35	16-24	2-8
Softwood	40-44	25-29	25-31	1-5
Bagasse	40	30	20	10
Coir	32-43	1-20	43-49	4
Corn cobs	45	35	15	5
Corn stalk	35	25	35	5
Cotton	95	2	1	0.4
Flax (retted)	71	21	2	6
Flax (unretted)	63	12	3	2
Hemp	70	22	6	2
Hennequen	78	4-8	13	4
Istle	73	4-8	17	2
Jute	71	14	13	2
Kenaf	36	21	18	2
Ramie	76	17	1	6
Sisal	73	14	11	2
Sunn	80	10	6	3
Wheat straw	30	50	15	5

Due to the nature of this work, it is important to review the potential effect of chemical treatments vis-à-vis cellulose and the creation of new cellulose material with novel properties. In the following paragraphs, we will see how biomass subunits become a barrier towards utilization. Biomass needs to be pre-treated and further hydrolyzed before it can be used. Understanding on internal chemical structure will reveal the importance of pretreatment for the conversion of chemicals in biomass.

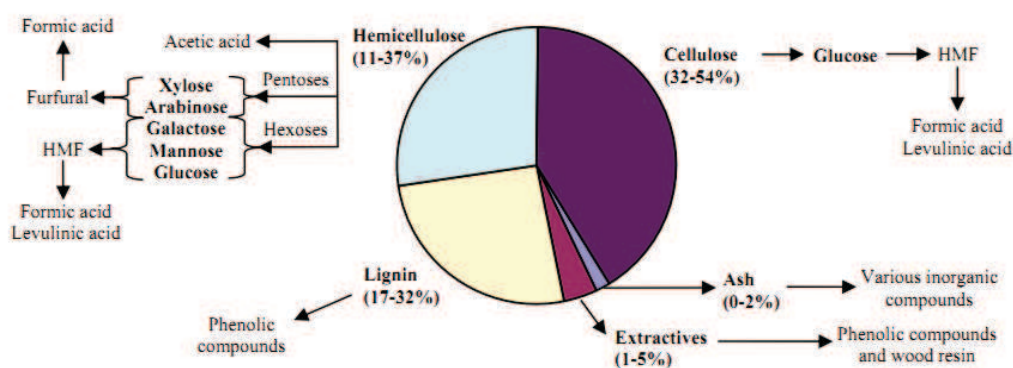


Figure I-5: Composition of biomass including cellulose, hemicelluloses, lignin, extractive and ash and its respective degradation products. Starch was not included in this figure; normally represent certain percentage in biomass that follow similar process steps as cellulose.

There are two types of polysaccharides: structural polysaccharides and storage polysaccharides. Both have very distinct properties due their main function even though the compositions of these two types are similar. Important structural polysaccharide was cellulose, while for storage polysaccharide was starch.

1.1.5.1.1. Cellulose

Cellulose is the major chemical component of fibrous lignocelluloses material followed by hemicelluloses and lignin. Representation of lignocelluloses materials at various levels is presented in Figure I-6. Cellulose microfibrils situated in the plant cell walls were made of linear glucose polymer units, forming chain known as glucan chains. These anhydroglucose units are bound together by β -(1,4)-glycosidic linkages [35, 50]. Due to this linkage, smaller sub-unit, or cellobiose was established as a repeat unit for cellulose chains (Figure I-7). Each unit of D-anhydroglucopyranose in cellulose possesses hydroxyl groups at C2, C3, and C6 positions, are capable of undergoing reactions similar to primary and secondary alcohols.

Chemical and physical properties of cellulose are very much depending on the properties of its monomer and binding properties. To illustrate the stability of cellulose it was proposed that cellulose exists in the form of dense crystals with an extensive van der Waals' attractive forces as well as hydrogen bonds as presented in Figure I-8 [44]. However, cellulose crystals possess flexibility unlike other crystal materials that is rigid due to its polymeric nature in the forms of microfibrils and fibrils of cellulose. The formation of linear cellulose fibrils and microfibrils from combination of several hundred to thousands of cellulose ribbon chains creates the structure of the fiber walls in plant that have a very strong modulus due to bonds described earlier.

Cellulose linkage β -(1, 4) glycosidic was very different from α -(1, 4) glycosidic that present in starch and glycogen. This makes cellulose properties to become different from other carbohydrate, insoluble in water and most organic solvents. Cellulose, like starch is a monomer chain of glucose with nearly 12,000 glucose unit bind together by β -D, (1, 4) glycosidic bond. Glucose in starch (helical amylose and branched amylopectin) bonded together by α -D, (1, 4) glycosidic bond. The difference in α -D, (1, 4) and β -D, (1, 4) glucose linkage of starch and cellulose respectively makes it impossible for the starch digesting enzymes to digest cellulose, that led to an enzymatic process exclusive to each other.

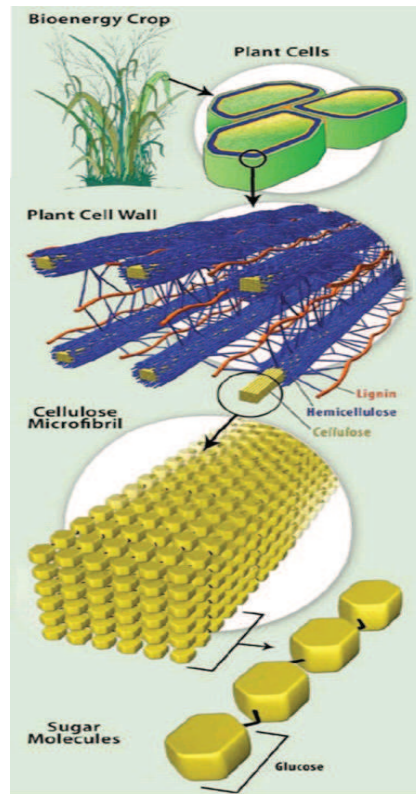


Figure I-6: Plant cell structure. An overview of science (Adapted from Bioenergy Research Center)

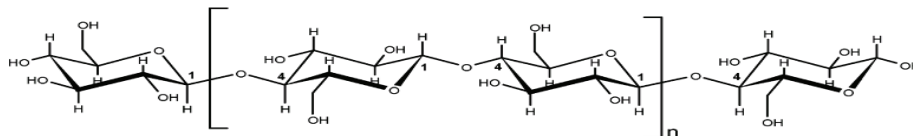


Figure I-7: Cellulose drawing that shows numbering of carbon atoms, non-reducing and reducing ends groups with n -number of glucose repeating units linked by β -1,4-glycosidic link. Cellulose chain with cellobiose unit as its repeating units has a length of 1.03 nm within the cellobiose unit (adapted from [35]).

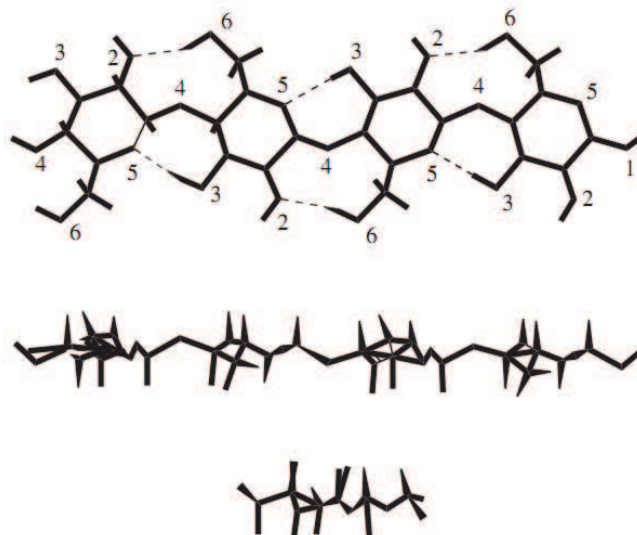


Figure I-8: Cellulose chain composed of four β -D-glucopyranose residues (cellotetraose) in three different views. The upper image, viewed perpendicular to the flat surface of the molecule, shows the covalent bonds and electron clouds around the atoms. The dotted lines indicate hydrogen bonds between the O6-H and the O2 atoms and between the O3-H and the O5 atoms. Disregarding the ending hydroxyl hydrogen atoms, the molecule has the twofold helical conformation and hydrogen bonding typical of some proposed structures of crystalline cellulose. The middle image shows a view of the long edge of the molecule, and the bottom image shows the end of the molecule (adapted from [44])

Several experiments has confirmed that amorphous region between the crystallites was easily accessible to water or heavy water as well as to small molecules, causing it to swell, leading to an exchange of hydrogen between the cellulose hydroxyl groups with deuterium of the heavy water [51, 52]. However, the penetration of small molecules into the crystal lattice is much more difficult and needs more time to open and widen the lattice of cellulosic structure [46].

Above information was very important for our work, due to the nature of DIC thermal treatment combined with autohydrolysis that is required to achieve our objectives. Further information on cellulose hydrolysis into glucose will be discussed in dilute acid hydrolysis mechanisms together with degradation mechanisms involved.

1.1.5.1.2. Hemicelluloses

Hemicelluloses consisting of several heterogeneous groups of polysaccharides and exist in an amorphous form. Hemicelluloses were suggested to be fully integrated into the structure of the cellulose and located within and between the cellulose fibrils and lignins as depicted in Figure I-6. The main feature that differentiates hemicelluloses and cellulose was that it has branches with short lateral chains consisting of different monosaccharide. This monosaccharide includes pentose (five carbon sugar: xylose, rhamnose, and arabinose), hexoses (six carbon sugar: glucose, mannose, and galactose), and uronic acids (e.g., 4-*o*-methyl glucuronic, D-glucuronic, and D-galacturonic acids) [35, 44]. The backbone of hemicelluloses was either a homopolymer or a heteropolymer with short branches linked by β -(1, 4)-glycosidic bonds and occasionally β -(1, 3)-glycosidic bonds. The sugars are highly substituted with acetic acid. The branched nature of hemicelluloses renders it amorphous and relatively easy for hydrolyzed to its constituent sugars compared to cellulose. When hydrolyzed, the hemicelluloses from hardwoods release products high in xylose (a five-carbon sugar). The hemicelluloses contained in softwoods, by contrast, yield more six-carbon sugars.

Due to its composition, hemicelluloses are not chemically homogeneous and exist in different composition percentage. Hardwood hemicelluloses contain mostly xylose or xylans, while softwood hemicelluloses contain mostly glucomannans [42]. Xylans are the most abundant hemicelluloses with backbone of β -D-xylopyranose units. Degree of polymerization of hardwood xylans (150 - 200) is higher than in softwoods.

1.1.5.1.3. Lignin

Lignin, the other important biomass constituents acts as a barrier to water penetration and as "glue" that holds tree components in the form of a matrix that also reinforces the tree by fills spaces in the cell wall between cellulose, hemicelluloses and pectin components. Lignin was made up of 3-dimensional amorphous polymer by a basic structural phenylpropane unit as presented in Figure I-10. Lignin behaves as an amorphous thermoplastic polymer, if heated beyond its glass transition temperature, it becomes rubbery similar to chain motion in polymer to enable some structural movements. Once extracted from wood, lignin loses its thermo-plasticity, due to severe degradation that subjected to its high molecular weight and 3-dimensional structure. Thermal treated lignin will normally appear on a surface of cellular structure of biomass.

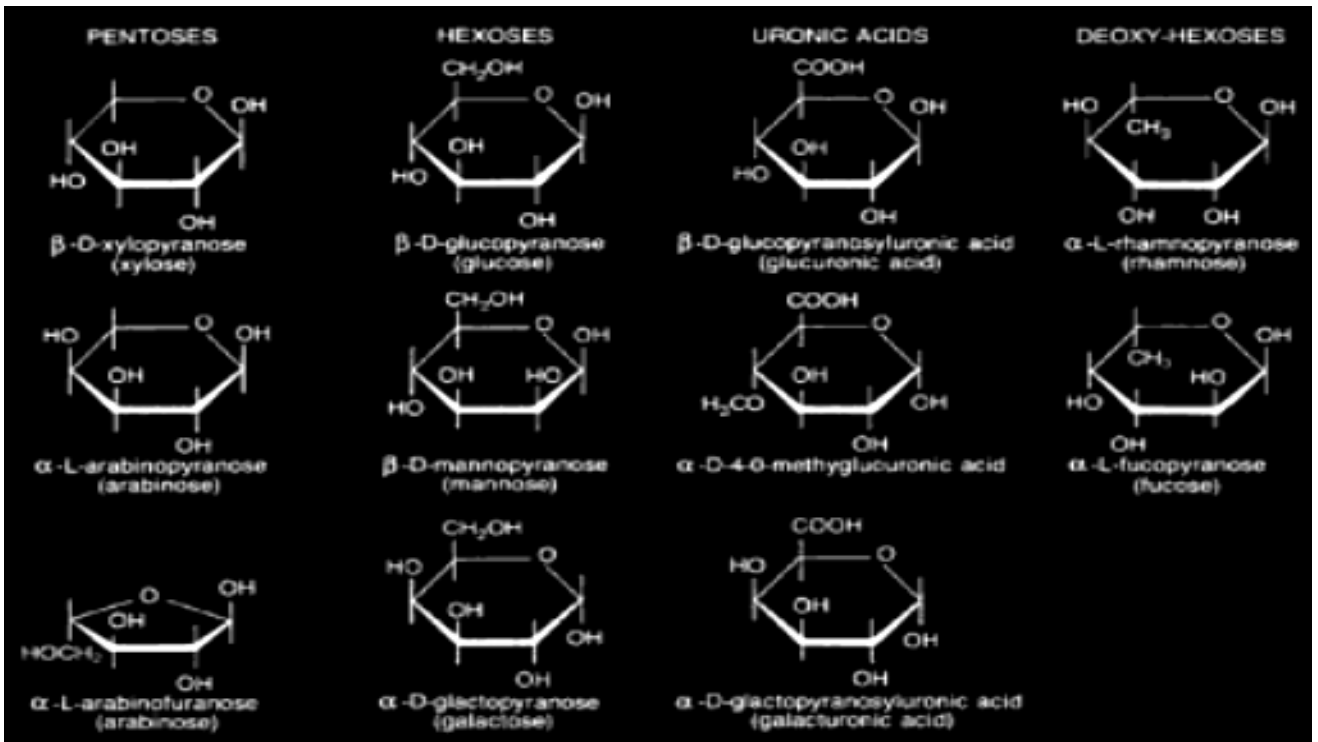


Figure I-9: Hemicellulose sugars components

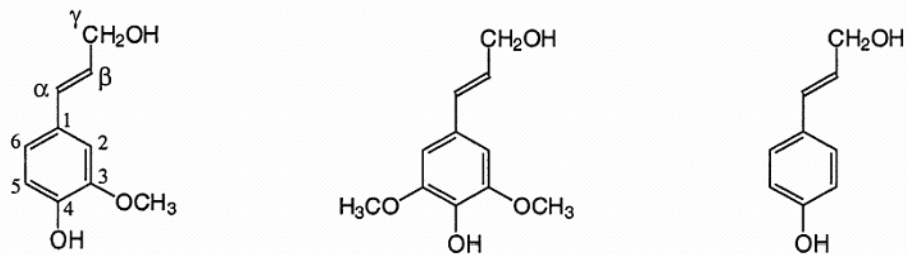
*trans*-Coniferyl alcohol*trans*-Sinapyl alcohol*trans-p*-Coumaryl alcohol

Figure I-10: Basic unit of phenylpropane that built lignin [53].

Lignin also acts as a bulking agent, and with its rigidity and stiffness, lignin imparts strength to the cell wall and its surrounding. Lignin was insoluble and not hygroscopic in nature. It also reduces the dimensional changes that occur with moisture changes in the cell wall. The following chemical structure (Figure I-10) shows the basic building unit of lignin while in next figure (Figure I-11) was the model of very complex lignin structures.

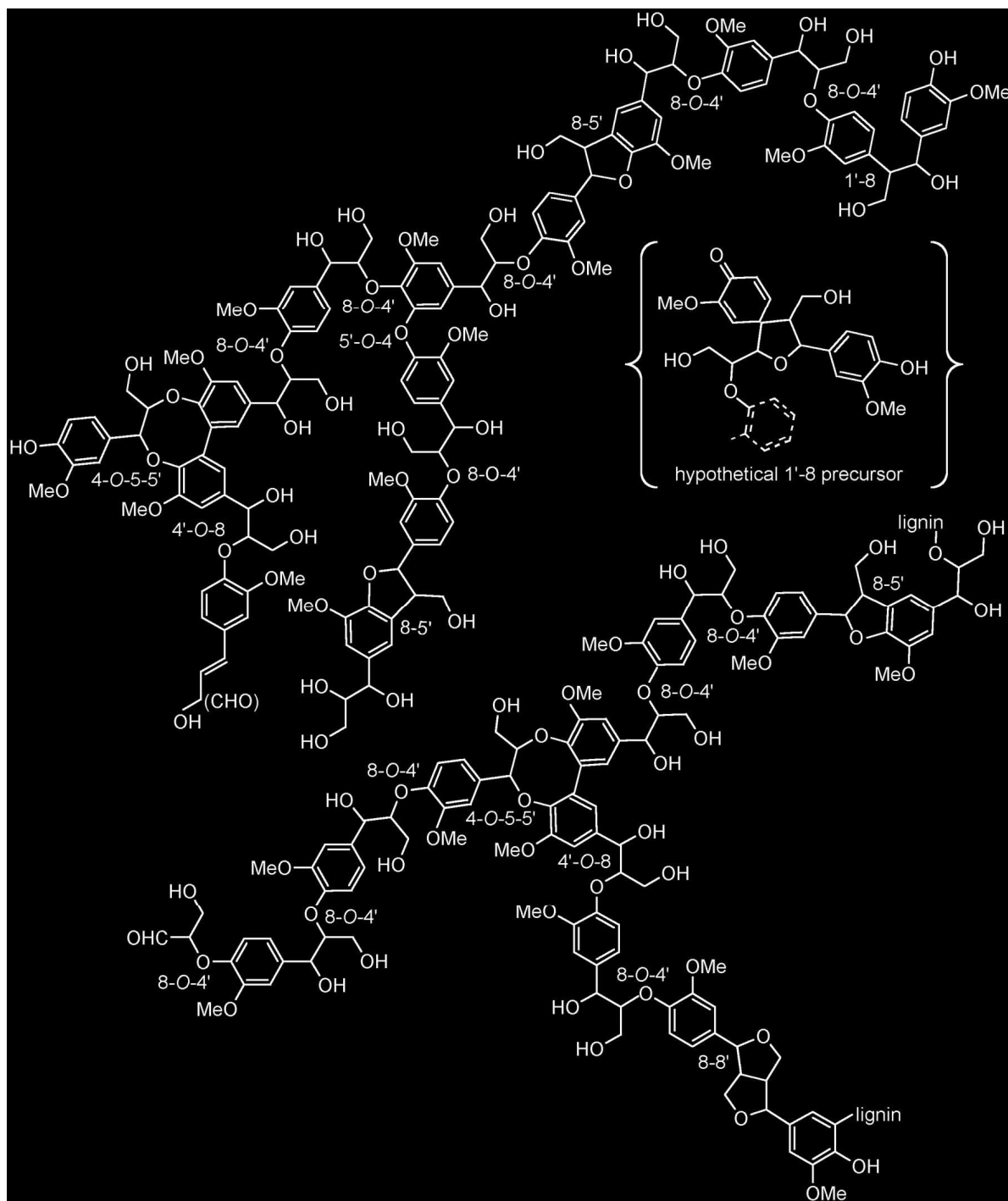


Figure I-11: Lignin structure still viewed as a contemporary model due to its complexity as presented above.

The linkage between polysaccharides and lignin as lignin-polysaccharides complex was proposed as due to the connecting links between lignin to the polyoses side group of arabinose, galactose and 4-O-methylglucuronic acid. This was made possible due to their sterically favored positions [44]. With this composition linkage, it was understood the reason why lignin cannot be totally separated from woody materials.

A set of strategy such as thermal treatment followed by alkaline extraction was normally employed to separate lignin from other cellulosic component.

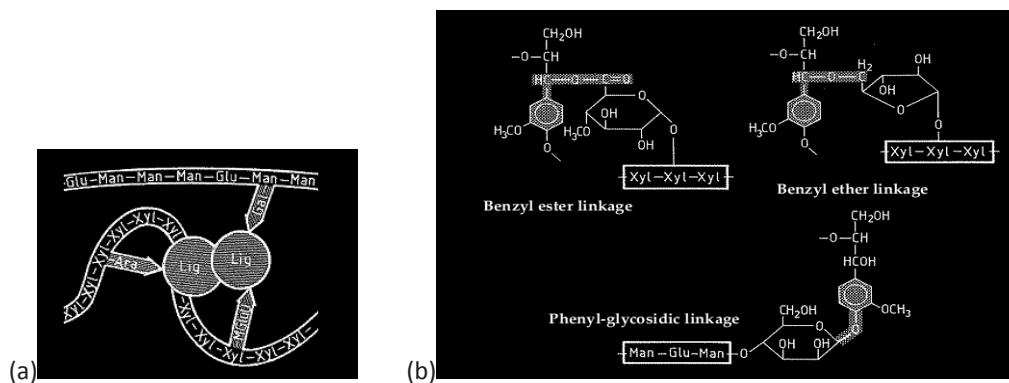


Figure I-12: Representation of (a) Schematic and (b) detail representation of linkage for lignin and polysaccharides (adapted from [44])

Above information is vital for the development of our theory in this work. In order to have good deconstruction of biomass material, the cementous thermal property of lignin needs to be overcome first, followed by good extraction and hydrolysis.

1.1.5.1.4. Starch

Starch or amyllum was a carbohydrate consisting of a large number of glucose units joined together by glycosidic bonds to become the most common storage polysaccharides for plants. Starch was contained in large amounts in such staple foods such as potatoes, wheat, maize (corn), rice, and cassava. Organs and tissues containing starch granules include pollen, leaves, stems, woody tissues, roots, tubers, bulbs, rhizomes, fruits, flowers, and the pericarp, cotyledons, embryo and endosperm of seeds [54]. Starch synthesis takes place during development and maturation of storage organs, such as tubers, fruits and seeds.

There are two types of starch polymers: amylose and amylopectin that exists in nature as composition of 10% to 30% and 70% to 90% respectively. Amylose was a linear homopolymer of glucose with 1, 4 α -glycosidic bond, while amylopectin was a highly branches starch polymer with linear linkage of 1, 4 α -glycosidic bond and its branch was in the formed by 1, 6 α -glycosidic bond. Both types were having reducing and non-reducing ends and having poor solubility in water. Some information about starch was described earlier as a comparison to cellulose. Two types of starch materials were presented in the following table.

Table I-4: Properties of amylose and amylopectin in starch (adapted from [54])

Properties	Amylose	Amylopectin
General structure	Linear	Branched
Color with iodine	Dark blue	Purple
Average chain length (glucosyl units)	100 – 10,000	20 – 30
Degree of polymerization	100 – 10,000	10,000 – 100,000
Solubility in water	Variable	Soluble

Starch in its native form was a versatile product, and the raw material for production of many products, sweeteners and ethanol. Russian chemist G.S.C. Kirchoff has discovered that starch could be transformed into a sweet substance by heating with dilute acid in 1811 when he was trying to develop a substitute for the gum arabic. First starch syrups plant were established twenty years later in 1831, and in 1866, production of D-glucose (dextrose) from starch was realized. This was followed by a number of glucose syrups manufacturing plants establishment in Europe during the 1800s followed by the manufacture of crystalline dextrose in 1882.

I.1.5.2. Products of Starch and Glucose

Starch was not only consumed as a food, but also built its reputations into various other industrial applications. Since 1930s; carbohydrate chemists have developed numerous products that have greatly expanded starch use and utility; including: (1) waxy corn starch with different starch properties and uses; (2) high-amylose starch primarily used by candy manufacturers due to its high-strength gels that give candy shape and integrity; (3) chemical modified starch gives appropriate texture, quality and shelf life for processed foods, such as frozen, instant, dehydrated, encapsulated and heat-and-serve products.

The success in starch technology was due to the advance in enzyme technology during 1940s and 1950s that enable the precise control of its end products through the adjustment in conditions of hydrolysis. At the same time, purification techniques to develop a high purity syrups were successfully developed. That advancement helps to expand the range and utility of glucose syrup products. Isomerizes enzyme coupled with immobilize enzyme technology was successfully convert glucose into sweeter fructose, and led to the introduction of high-fructose syrup (HFS) in 1967. Refinements in production processes further produced liquid sweetener that could replace liquid sucrose on a one-to-one basis. There was a major disruption in the world sugar market at the time also led the major sugar users to seek such an alternative for their product manufacturing. Glucose syrups are easily fermented by yeast to ethanol. According to an estimation, 32 pounds (14.5 kg) of starch in a bushel of corn, will be produced about 2.5 gallons (9.5 liters) of ethanol [54]. Hydrogenation of sugars produces a class of materials known as sugar alcohols or polyols. Major commercial sugar alcohols include mannitol, sorbitol (D-glucitol), malitol, and xylitol and syrups are related to these products.

Another important food and industrial product from starch and glucose was an organic acid, including citric, lactic, malic and gluconic acids have become large-scale food and industrial ingredients. Originally produced from fermentation of sucrose or sugar by-products, they are now mainly produced from fermentation of dextrose. Fermentation technology also has enabled a number of amino acids productions from glucose such as lysine, threonine, tryptophan, methionine and cysteine.

I.1.5.3. Comparison: Starch and Cellulose

In many ways, cellulose and α -amylose share the same linear homopolymer of D-glucose units. However, due to the difference in glycosidic bonds for glucose unit: cellulose with β ,(1,4) and α -amylose with α ,(1,4); both polymers posses different structure and conformation as shown in Figure I-13. The hydrogen bonding that present in such an extended structures of cellulose was responsible for the great strength of tree trunks and other cellulose-based materials. On the other hand, helical conformation of starch amylose makes it suitable as storage materials in plant.

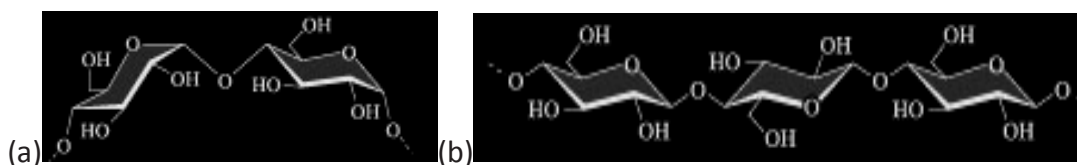


Figure I-13: Starch, as (a) amylose with α , (1 \rightarrow 4) linkages, prefers to adopt a helical conformation, whereas (b) cellulose, with β , (1 \rightarrow 4)-glycosidic linkages, adopts a fully extended conformation with alternating 180° flips of the glucose units.

I.1.5.4. Energy Value of Biomass

Energy value of biomass component from several sources was summarized in Table I-5 in order to appreciate the calorific value of biomass waste. Relatively natural biomass has low calorific value if compared with other sources of energy. Processing it into glucose reduced further its calorific value, but fermentation into ethanol doubled its total energy value. It was important that comprehensive strategies for conversion of biomass were formulated in order to enhance its energy value.

Table I-5: Energy content of biomass composition, products and its by-products together with several fossil fuels for comparison

Biomass composition	Energy (kJ/gram)	Reference
Wood (whole materials)	18.6	[55]
Cellulose	17.6	[56]
Lignin	26.4	[56]
Starch	17.5	[56]
Raw fiber	17.6	[56]
Lignin and Extractive (79.8% and 20.2%)	25.45	[57]
Holocellulose	15.45	[57]
Glucose	15.5	[56]
Ethanol	29.7	[56]
Natural gas	53.5	[39]
Gasoline	46.5	[39]
Crude oil	41.9	[39]
Coal (anthracite)	32.6	[39]
Coal (bituminous)	25.6	[39]

I.1.6. Water Behavior in Biomass

Tree needs water for growth and sustenance of its food. Water transported by the root system throughout the tree. Once the tree is cut down, water uptake stops and moisture content in the wood will start to diminish slowly. Existing water content needs to be dried up before biomass can be utilized. Some species of biomass contain a lot of water making it uneconomical to transport unprocessed biomass due to high amount of water being shipped unnecessarily.

There are three types of water in biomass, particularly in the cell wall levels. Water exists as liquid water in the lumen, water vapor in the lumen, and bound water in the cell wall. This will enable the transportation of important nutrients in the tree. Besides that, because of the existence of water biomass material is defined as hygroscopic, i.e. easily adsorbed moisture after dried to certain extent and exposed back to atmospheric conditions.

Bound water in the cell wall was due to the water being held strongly to the cell walls compared to free water and non-bound water. Hydrogen bonding forms between water and cell walls will release some energy, and to release water from hydrogen bonding will require some energy to overcome that bonding. Bound water will appear first until completely saturated, and the excess water becomes non-bound water and free water after several layers of water are formed. Differential scanning calorimeter (DSC) was a good tool to determine if materials containing water have freezing and non-freezing bound water and has been successfully tested on fibers [52, 58]. Moisture content of biomass normally was reported in percentage, calculated based on weight of water per dry weight of biomass.

Water in the cell wall is bound to the hydroxyl groups through hydrogen bonding (see Figure I-8) that exist in the cellulose polymers and its neighboring molecules. It is primarily associate hydroxyl sites of the cellulose and hemicelluloses. The bound water moisture content is limited by the number of sorption sites available and by the number of molecules that can be held on a sorption site [59]. Certain treatments such as thermal and alkaline treatment was found to increase the percentage of bound water in biomass material together with an increase in sorption sites and amount of lower DP oligosaccharides [60, 61].

The crystalline regions of cellulose do not allow for water to enter. Their sorption sites are not accessible because adjacent cellulose molecules are bound to the sites. The bound water moisture content is dependant on the relative humidity and temperature of the surrounding air. Recent work shows that even after heating cellulose sample up to 170°C, the absolutely dry cellulose still cannot be obtained due to small amount of water is very strongly bounded to cellulose molecules [61].

I.1.7. Brief Overview on Biomass Waste

Currently, a lot of attention has been put on development of a new process for the utilization of agricultural residues such as sago waste, cassava bagasse, sugarcane bagasse, sugarbeet pulp, coffee husk and pulp, apple pomace, potato waste and other materials as feed materials in bioprocesses [62]. Approximately, 3.5 billion tones of agricultural residues are produced per year throughout the world. However, due to its low in protein content and very poor digestibility as food materials, their potential utilization is very poor even though some are rich in carbohydrate content. The conversion of such waste into another form of food base such as glucose is important to answer the needs to increase world food and feed consumption supplies.

Based on several reports, Malaysia produced about 32 Mt annually biomass waste in the form of palm waste, paddy, wood residue and bagasse [63]. Simulated conversion of all resources was estimated to produce about 4.6 Mt gasoline equivalents or about 60% current fuel requirement. Currently, some portion of biomass waste produced is burned for steam and heat supply in palm oil processing plant but in some cases such as paddy stalk, farmers have a problem to dispose it and most of it was burn during dry season in an open field.

In order to appreciate the profitability of glucose generation from the process developed in present work, specific raw material and content of its polysaccharides need to be evaluated. We have decided to concentrate the review on two major sources of polysaccharide's waste available in South East Asia region: solid waste from sago and cassava processing plant.

This literature analysis will digest status on present sago and cassava industries, its source of waste generation (solid and liquid), composition of waste, current methodology of disposal and to associate this work on the potential utilization of waste for higher value added products. Only small part of this review will digest on cassava, in order to gain some insight into the industry for comparison against sago processing industry.

I.1.7.1. Cassava Starch Industry

Small part of this review will concentrate on cassava waste solid or known as cassava bagasse. Cassava (*Manihot esculenta Cranz*) was one of most important crops for food after

rice and corn, especially in tropics. Information collected was to compare with major interest in this work, i.e. waste from sago starch processing plant.

Cassava was a bushy plant producing tubers and made up of aerial and underground parts. The aerial parts can be as high as 2-4 meters. Cassava root or the underground part was made up of two types of roots: the ones responsible for plant nutrition and the other with axial disposition surrounding the trunk or known as tubers that makes the edible part of plant. Each plant can grow 5 to 20 tubers with fresh weight few gram to 5 kg [62].

Cassava starch production per hectare was one of the highest and standing as fourth crops worldwide after rice, wheat and rice. According to FAO estimates, about 600 million peoples depends their lives of cassava starch especially in Africa, Asia and Latin America [62]. Thailand, Indonesia and Vietnam are the countries with highest planted area with cassava in South East Asia. Vietnam very much depend on scattered small scale cassava cultivation with total fresh roots yields of 60,000 to 80,000 tons/year and approximately 100,000 tons of wet starch/year [64]. Thailand, owns 1.043 million hectare of planted area with nearly 17 million tons production (about 17.1 tons cassava root/ hectare) in 2005 [65]. Data for Indonesia, according to FAOSTAT database (FAO) saw an increase of production quantity from 16 million tons in 1990 to 22 million tons with planted area of 1.175 million hectare in 2009 [FAO – through <http://data.mongabay.com/commodities>-Indonesia]. Statistics on Malaysia, shows that there was an increase in plantation area of 39,000 hectare in 1990 to 42,000 hectare in 2009 with production of 440,000 tons in 2009, but at much lower yield of about 10.5 tons cassava root/hectare compared to its neighbourhood region [according to FAO – <http://data.mongabay.com/commodities>- Malaysia].

Up to now, there have been no domestically and internationally recorded documents on waste treatment which can be applied directly to address the pollution in the cassava processing villages in Vietnam. Thailand, the world leader in cassava processing industry, can only use dried root pulp for animal feed [64].

1.1.7.2. Cassava Processing

Processing of tubers, mainly for isolation of its starch flour from other inedible solid, will require a lot of water. Cassava tuber will be cleaned with water in low rotating drum once arrive at the processing plant to remove soil and dirt. Washed tubers will be cut into smaller pieces with cutting blades and feed into rasps [66].

Slurry of root from rasps is pumped through series of extractors in centrifuge system separating fine starch from coarse solids. Pulp from coarse solid will be repeatedly extracted until a minimum amount of starch in coarse solid is left. There are two types of waste generated: liquid and solid waste or cassava bagasse. Processing of 230 to 300 tons of cassava tubers will produce about 280 tons of wet solid bagasse. Cassava bagasse is made of fibrous materials with high starch that cannot be extracted during processing stage. Moisture in solid residue and starch after screw press system is about 70% and 40-50% respectively [66].

The high content of moisture in solid residues together with very low protein content makes the residue was not suitable for other purposes and became some source of an environmental problem for processing plant. In similar way, sago residues in the form of solid residue also share the same outcome with solid residue in cassava industry.

I.1.7.3. Sago Palm

Sago palm of the genus *Metroxylon* belonging to the Palmae family (*Metroxylon sago* Rottb.) grows well in a swampy tropical rain forest of Southeast Asia between 10° of northern and southern latitudes [67, 68]. Some of the important species widely used in sago starch production includes *M. longispinum*, *M. sylvestre*, *M. microcanthum*, and *M. rumphii*. *Metroxylon sago* Rottb. has several advantages as food crops due to (1) economically viable; (2) relatively sustainable; (3) environmentally friendly; (4) uniquely versatile; (5) vigorous and (6) promotes socially stable agro forestry systems [69].

Sago starch reserve accumulates in the pith core of sago palm stem and apparently at their maximum just before flowering, and fruiting depletes these reserves [70]. Sago trunks may reach 7 to 15 m in length and attain an average girth of 120 cm at the base of the palm [71] due to the suitable climate conditions and good supply of nutrients from soil. The vegetative phase of the sago palm lasts between 7 to 15 years before flowering, making its stem saturated with starch from the base of the stem upwards [72].

I.1.7.3.1. Sago Extraction

Small commercial sago palm plantation can grow about 1480 trees with annual harvest of 125 to 140 trees per year for every hectare. A mature sago palm tree produces about 100–550 kg of sago flour. In another report, regional and/or varietal differences in starch yield of sago palms growing in the various regions in Malaysia and Indonesia have been observed, ranging from 34 to 975 kg dry starch/palm, with an average of 375 kg/palm [73]. With an average weight of about 1 ton/ tree, it was estimated that more than 60% of biomass will be generated as waste for every sago tree processed.

Starch-rich flour can be extracted from stem tissue by shredding palm stems with mechanical shredder followed by sedimentation of particles containing starch in water as presented in Figure I-14 [74, 75]. Sago trunks were cut into shorter length of 1.0 to 1.2 m logs and tied into a raft for transportation to the plant via rivers or man-made water system.

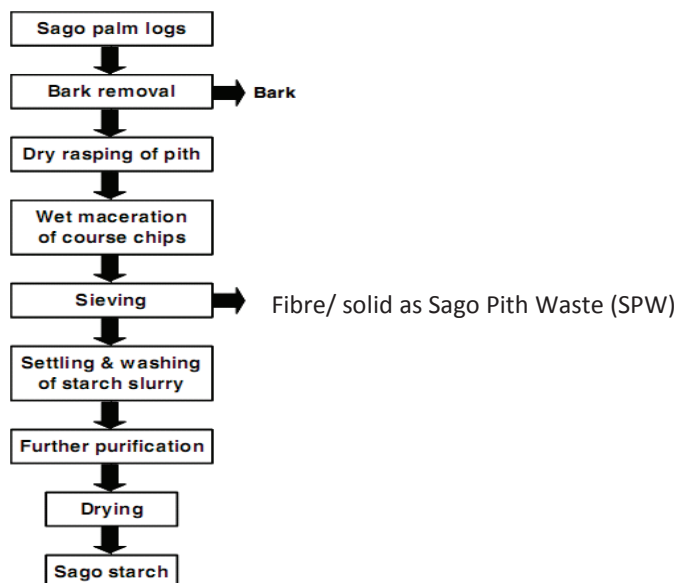


Figure I-14: Sago starch production processes and source of solid waste known as “sago pith waste” or SPW (adapted from [75])

Upon arrival at processing plant, its bark was first removed from sections of the logs. Each of the debarked sections was fed into the mechanical scraper, and scraping was done with scrapers. The scraped piths were transferred into hammer mill and pass through a series of a centrifugal sieve to separate starch from coarse fiber. The starch slurry will further be purified by separation in several sieve bends. Series of cyclone separators also been used to obtain pure starch. Drying will be carried out in a rotary vacuum drum drier followed by hot air drying.

1.1.7.3.2. Sago Pith Waste (SPW)

Route of sago pith waste (SPW) recovery from sago processing plant also was simulated in Figure I-14. SPW was the material in this work also known as **crude starch** due to its content was very high in starch, cellulose, hemicelluloses and lignin. Sago pith waste (SPW) or crude starch was the similar term used throughout this thesis.

A small sago processing plant was capable to produce approximately seven tons sago pith waste daily. Unfortunately it was either dumped into nearby river or deposited in the factory compound for used as boiler feed. Waste water was shown to represent high organic material, chemical oxygen demand and biological oxygen demand which exceed the standard limit discharge of local environmental quality act [11].

The exploitation of solid waste from the discharge point of sago processing plant is a welcoming act to solve part of the environmental problem generated within this industry. Comparison for chemical constituent of corn grains, cassava and sago materials containing cellulose, starch, hemicelluloses and lignin is presented in the following table.

Table I-6: Composition of several sources of material and waste containing starch

	Moisture	Starch	Protein	Fat	Cellulose	Crude fiber	Lignin	Ash
Corn grain ¹	16.7	71.3	9.91	4.45	3.3	2.66	<0.1	1.42
Cassava root ²	63.28	29.73*	1.18	<0.1	nd	0.99	nd	0.85
Sago waste ³	5.91	65.7	1	nd	nd	14.8	nd	4.1
Sago waste ⁴	6.1	70.0	0.98	nd	nd	15.0	nd	4.16
Cassava waste ⁵	12.50-13.00	61.80-63.00	1.50-2.00	nd	nd	12.80-14.50	nd	0.58-0.65
Cassava waste ⁶	78.2 – 82.7	61.8 – 69.9	1.8 – 2.3	0.1-0.2	nd	10.1 – 14.6	nd	1.6-2.4

* reported as carbohydrate, nd: not done

Sources of reference: ¹ [76], ² [66], ³ [11], ⁴ [10], ⁵ [77], ⁶ [78]

In a separate work, content of non-starch polysaccharides and lignin in sago pith waste was further fractionated as summarized in the following table which shows very small amount of potential polysaccharides for economical conversion into glucose.

Based on summary in Table I-6 to Table I-8, it can be conclude that both sago and cassava waste from respective starch extraction plants have very high polysaccharides content in the form of starch and cellulose and very low in protein and lignin content. Total polysaccharides for both wastes, (for both cellulose and starch) dominate nearly 90% of dry content of materials. The following Table I-8 summarized further the composition of polysaccharides for sago pith waste using acid sulphuric and enzymatic hydrolysis. Utilization of acid hydrolysis gives higher glucose value due to hydrolysis of cellulose together with starch.

Table I-7: *Non starch polysaccharides (NSP) and lignin in sago pith materials [79].*

Component	Composition (%)
Cold water soluble NSP	2.6
Hot water soluble NS	0.8
DMSO soluble NSP	0.8
5% NaOH soluble hemicellulose	1.2
5% NaOH soluble lignin	0.6
Sodium chlorite lignin	4.2
24% KOH and 2% boric acid soluble hemicellulose	0.6
Cellulose	5.3
Total	16.1

Table I-8: *Composition of polysaccharides using acid and enzymatic hydrolysis. (adapted from [10])*

Process	Composition (mg/g)
Acid hydrolysis, 1.5 M sulphuric acid, at 90°C for 120 min	623.4 glucose
Enzymatic hydrolysis (glucoamylase) 6 AGU/ml enzyme for 30 min.	564.6 glucose

1.1.7.3.3. Recent Development in Sago Starch Industry

Recent publications on the statistic of sago plantation and production in South East Asia were compiled for this review [68, 80, 81]. In Malaysia, Sarawak state government has developed sago as a plantation crop, providing part of its 1,500,000 ha of peat swamps. The world's first large-scale commercial plantation of 7,700 ha was developed by the Sarawak land development agency, near Mukah district in 1982, and in 1993, a second plantation of 1,600 ha was established near Oya [68]. In 2007, Sarawak was adding another 50,000 ha to its existing 67,957 hectares land under sago cultivation [80].

In Johor, there are about 5,000 ha was semi-developed for sago palm planting. An Indonesian private company runs a 36,000 tons floating extraction plant in Bintuni, Irian Jaya. New plantings place also being started on peat soils for about 3,000-ha planting area, and about 20,000-ha planting will be developed over the next decade. In the province of South Sulawesi there are some scattered 25,000 ha of sago palm area developed for local consumption [68]. There are other areas that actively participate in the development of sago industries such as in Papua New Guinea, South of Thailand and Philippines according to the same source.

Karim et al (2008) suggested that, mechanical process currently employed to extract sago starch is inefficient and often fails to dislodge residual starch embedded in the fibrous portion of the trunks [74]. Observation under SEM micrograph had shown an abundant amount of starch granules still remains in the lumen of materials. This has led us to appreciate the importance of SPW residues in present work. It was further estimated in 2001, that the amount of starch in sago pith residue from East Malaysia alone accounts for nearly 50% of total Malaysian imports of starch about 40,000 tones per year [82]. Sago processing industry in Sarawak shows an increase in its total sago palm plantation hectare by more than 50,000 hectare as described before. Annual sago starch exports was around 25,000 to 50,000 metric tones before 2007 [80] also were increase to 70,000 tones in 2010 [81].

The problem for effective utilization of SPW was due to its high moisture content after final step in sago processing plant (about 400 to 500% of solid material). It was almost impossible to use it in certain process such as fiber-plastic composite application. Moisture content can only be decreased further to about 200 to 300% by adding a screw press step after final washing. Our intention in this work was to manipulate the existence of high moisture

content of SPW and certain autohydrolysis properties of polysaccharides due to the presence of acetyl groups in hemicelluloses using DIC treatment system.

I.1.8. Conclusion

Information on biomass chemical composition, including starch, cellulose, hemicelluloses and lignin has shown a huge potential for utilization. It was suggested that there were still many challenges need to be overcome before full commercial utilization of biomass can be realized.

SPW was selected for this work, mainly due to the availability of a high amount of polysaccharides, combined with high economic viability onsite of sago starch processing plant. Microscopic examination reveals that there are many starch granules is trapped within its lignocelluloses matrix [74, 82]. This was confirmed by several proximate composition analyses done by several research groups [11, 83, 84] as presented in Table I-8. This was further supported by the facts that crude starch waste was available immediately after the processing at size already good for glucose hydrolysis as presented in Figure I-14.

The availability of starch and other polysaccharides composition offer SPW as a good material for this work which allows us to work on a low severity level of thermal treatment compared to other thermal pretreatment exist. This was made SPW material suitable for present state-of-the art DIC technology that was used in this work.

CONFIDENTIEL

PART I. CHAP 2.

REVIEW: THERMAL PRETREATMENT

I.2.1. Biomass Pretreatment

Utilization of biomass for everyday life and industrial applications was a great interest since the beginning of the industrialization. However, due to its stability in its natural forms, making it very difficult for direct utilization; and without pretreatment, biomass cannot be used as feedstock for any industrial processes. Various works and reviews of lignocelluloses materials pretreatment [2, 85-87] were discussed a wide range of pretreatment selection. Biomass pretreatment can be divided into several methods such as physical, mechanical, thermal, chemical and biological. This work will concentrate on the thermal pretreatment only together with dilute acid hydrolysis.

Pulp and paper industries were the first industries that utilized hydrothermal treatment to fractionate biomass such as cellulose and lignin. Most of the present biomass hydrothermal pretreatments were originated from this industry [30], with improvements to suit the need of biomass and its process. In pulp and paper industries, feedstock will be separated into two fractions: an aqueous extract and pulp for making of paper. Aqueous extract composed mainly hemicelluloses, lignin and chemical, which can be further purified. Development of thermal pretreatment on lignocelluloses biomass was aimed for a moderate treatment condition to maximize the hemicelluloses yield which was easily hydrolyzed through steam treatment. It seems that with a simple treatment combining steam and water, the process has become environmentally friendly [88]. With such treatment, hemicelluloses were recovered with good yields, and low byproduct generated.

I.2.2. Rationale of Thermal Pretreatments on Biomass

Factors related to the success of biomass utilization including crystalline index of materials, pore size of internal structure to make it accessible to chemical or enzymatic reaction and content of lignin that bind together the biomass [7, 35]. Other success factors, including high surface area to immediately enable chemical reaction [28] and is free from any toxic composition that may block enzyme accessibility [89, 90].

Most of the biomass the thermal based pretreatment process initially was developed primarily for use with the fermentation process at the second processing stage [16, 42] due to some limitation of biomass immediate utilization with enzymatic hydrolysis. For example, biomass pore size was in range of 51Å, compared to cellulase enzyme in the range of 24Å to 77Å, exist as hydrodynamic spheres in solution [91], while it was known that proton ion, $[H^+]$ size was only 4Å. Without even pretreatment, $[H^+]$ can easily be penetrated into biomass pores for hydrolysis action, but not cellulase enzyme. This was the main reason why pretreatment was required for a successful biomass utilizations. Present interest of this work, however, was to demonstrate the ability of specific thermal pretreatment (with DIC) for direct conversion of polysaccharides into glucose. Treatment with an enzyme was discussed as part of the future strategy for material used in this work.

In most of the present technology, two stage processes were employed; in first stage biomass materials were pre-treated to break down ultra cellular components and its cell

walls structures. The second step usually involved with the depolymerization of polysaccharides to monosaccharide. Most of the present works, during second step, there was a lot of interest to employ an enzymatic process for process related to generation of bioenergy.

On the other hand, hydrolysis through utilization of acid (either dilute or concentrated acid) was found to be a simple process and normally the starting point for most research on the conversion of biomass into glucose [28, 92-95]. The process was found to give moderately high glucose yields in relatively short times compare to enzymatic process. During dilute acid hydrolysis, proton in acid, due to its size, it was almost accessible to the glycosidic bonds of cellulose, starch and hemicelluloses [91]. With its size and due to relatively very reactive during processing in place, it was difficult to limit the extend proton hydrolytic activity on polysaccharides and glucose. Most of the time under extended hydrolysis condition; glucose will undergo further acid catalyzed reaction to form degradation products. The most common degradation products from sugar were furfural (xylose) and hydroxymethylfurfural (HMF) from glucose [96, 97].

Both furfural and HMF was reportedly forms some precipitate with remaining insoluble polymers [98, 99] and became the main cause for reactor problems [17]. The formation of precipitate was linked to the increase in process temperature and became source of yield reduction. Most hydrolysis process for dilute acid was done at more than 100°C, while for concentrated acid were done at temperature below than 90°C. For acid below 0.5 mol/L, the temperature usually >120°C, if temperature about 90°C, concentrated, strong acid >1.0 mol/L is required [100]. The combination of high temperatures and strong mineral acids however leads to faster corrosion of the reactor together with problems related to degradation of sugar and accumulation of non-sugar by-products in reactor.

Biomass materials usually consists of cellulose, hemicelluloses and lignin; and these materials need to be separated by its chemical solubility such as for lignin it is soluble in alkaline solution while for hemicelluloses only need hot water to extract it out. Some of chemical produced during acid catalytic process such as furfural, hydroxymethylfurfural (HMF), and levulinic acid, are desirable chemical intermediates for the liquid alkenes production [16, 17, 24], however it will be an undesirable chemicals for process that depends on enzyme and microorganisms [101, 102]. This makes hydrolysate obtained during high severity treatment usually not suitable for enzymatic and microorganism utilizations. A less severe thermal treatment however does not allow the complete disintegration of cellulosic portion for optimum enzymatic utilization.

Acid catalyzed cellulose hydrolysis was heterogeneous in nature and very much affected by cellulose properties itself (i.e. amorphous or crystalline) and dimension of materials. Saemen (1945) found that hydrolysis reaction rate unaffected when they using particles with dimension 20 to 200 mesh, and suggested the need of uniform material size for optimum hydrolysis condition [28]. However in most cases, to get correct particle size will require high effort in the form of mechanical energy for debarking, cutting and grinding from bulky material to powder-like material. These have made virgin bulky biomass material to be the least choice in the processing or transformation of biomass into sugar and ethanol.

I.2.2.1. Biomass Pretreatment Summary

Biomass treatments can be divided into several methods such as presented in Table I-9. Three main pretreatment methods was physical treatment with no chemicals added, thermochemical and physical with acid or steam; and biological pretreatments. Main objectives of summary were on the economic analysis for establishment and commercialization of the technology [2, 103, 104].

Table I-9: Biomass pretreatment methods (adapted from [105]).

Pretreatment Method	Process and action involved	Output material applications	Cumulative effects/ Objective	Associated problems
Physical - no chemicals involved during pretreatment	Milling and chipping - chipping, ball milling, hammer milling	Sizing of materials Input for other process such as for further thermal pretreatment Use in second step process such as for chemical and enzymatic hydrolysis and saccharification.	reduce in input material size, decrease in cellulose crystallinity, degree of polymerization - decrease in cellulose crystallinity and degree of polymerization	- energy intensive process and not suitable for industrial application. - certain biomass need special tooling due to its properties (fibrous material requires different tool compare to woody material) - lignin is still exist, exhibit some problems to the enzymatic reaction
	Irradiation treatments - gamma ray, microwave, electron beam			
	Other associated treatments - hot water treatment, steaming, gas pressurize, die extrusions			
Thermochemical and, physical process - with steam, chemicals and associated physical treatment involved	Thermal based - steam explosion, ammonia fiber explosion (AFEX, CO ₂ explosion, SO ₂ explosion)	- for enzymatic hydrolysis followed by second hydrolysis Use in second step process such as for chemical and enzymatic hydrolysis and saccharification.	- increase in surface accessibility - partial or nearly complete delignification - increase in amorphous phase - partial or complete hydrolysis of hemicelluloses	- Bulk of research work concentrated in this area, several promising process has been developed in this treatment regime. - process usually rapid and need chemical input - thermal treatment need high severity factors and need some big investment.
	Acidic (process with addition of acid) - sulfuric acid, hydrochloric acid, phosphoric acid			
	Alkaline (process with addition of alkali) - sodium hydroxide, ammonia, ammonium sulfite			
	Gas processes - chlorine dioxide, nitrogen dioxide, sulfur dioxide			
	Oxidizing agents - hydrogen peroxide, wet oxidation, ozone			
	Solvent extraction of lignin - ethanol-water extraction, benzene-water extraction, ethylene glycol extraction, swelling agents			
Biological pretreatments	Treatment with fungi and actinomycetes		- delignification - reduction of degree of polymerization of cellulose - partial hydrolysis of hemicelluloses	- low energy requirement - almost no chemical required - mild environmental process - low in rate of process and require long time to finish. - not viable for commercial application.

I.2.2.1.1. Steam Explosion Pretreatment

One of popular the thermochemical biomass pretreatment was based on the utilization of direct steam injection on biomass materials. Several pretreatment processes were

developed based on this method, such as steam explosion and AFEX technology. Steam explosion technology was developed for hardboard production by WH Mason in 1925. Lately, steam explosion has been extensively studied for pretreatment of lignocellulosic materials due to its ability to hydrolyse glycosidic bonds in hemicellulose, assist in cleavage of lignin-hemicellulose bonds and increase the accessibility crystalline cellulose bonds towards acid and enzymatic hydrolysis. Presently, this kind of pretreatment as proposed for this work already exist at industrial scales, however, its commercial availability was sometimes a trade secret [106]. Steam explosion available with two types of design that tested at laboratory and pilot scale studies, the first type was through a batch process known as the Masonite Gun [12, 87, 107] and the second type was based on the same batch principle but with feeding system run on a continuous basis, called the Stake reactor [8]. Both steam explosion systems have a vertical cylinder to fill with wood chips or other type of biomass. It will be sealed and injected with saturated steam with pressure up to 2.5 MPa. Materials inside of reactor will be steam heated between 180 to 260°C with processing time about 2 to 30 minutes depending on the type of biomass and its final application.

Overend et. al., (1987) [30], in their well-accepted work, has described the Steam Explosion as a thermo-mechano-chemical process, where the breakdowns of lignocelluloses structural components are aided by heat in the form of steam (*thermo*), shear forces due to the expansion of moisture (*mechano*), and hydrolysis of glycosidic bonds (*chemical*). The concepts were evolved into a term known as treatment severity, which combined all factors such as temperature, time and acid concentration involved in steam explosion treatment into single kinetic terms.

1.2.2.1.2. Modeling of Treatment Severity

Steam explosion process has been extensively studied with the aim to overcome 3 main factors for ultimate lignocelluloses material valorization [30]: (1) physical barriers due to the presence of lignin, (2) crystallinity of cellulose, and (3) physical access for acid and enzymatic reaction on lignocelluloses materials. The extraction and fractionation of lignocelluloses materials can be optimized once maximum bulk diffusion is achieved due to high number of individual lignocelluloses fibers. Internal diffusion within the cell walls on the other hand is facilitate by swelling of the structure through introduction of chemical or internally generated chemical due to autohydrolysis [108].

Overend et. al., (1987) [30] has introduced a model based on first order kinetic terms of the combined effect of both temperature and residence time that obey Arrhenius law as presented in the following equation based on per mole reaction. A higher severity treatment will usually involved higher level of parameters.

$$k = Ae^{-Ea/RT}$$

with,

k = rate constant

A = Arrhenius frequency factor

Ea = activation energy (kJ / kg mol)

R = universal gas constant (8.314 kJ / kg mol K)

T = absolute temperature (K)

In a work by Heitz et al (1991), they use Stake II system for steam explosion pretreatment on *Populus tremuloides* to recover hemicelluloses and lignin based on different severity treatment on materials [8]. Cellulose obtained from the processing was subjected to enzymatic hydrolysis. About 65% hemicelluloses and 80% lignin were recovered from the process. Sugar hydrolysate obtained from enzymatic hydrolysis also found suitable for fermentation into ethanol. Various other materials have been subjected to the treatment with both systems such as sugarcane bagasse, corncob [109], corn stalks and almond shell [98]. Various combinations including with addition of acids, alkali, peroxide and gasses was done to find suitable parameters for respective process as well as to suit it with products of interest [2, 88].

Steam explosion process was extensively reviewed, modeled and applied including optimization on several biomass types, acid and enzymatic hydrolysis [9, 95, 102, 107, 110-112]. The basis of process was based on materials in the form of chips will be subjected to direct high steam pressure followed by a sudden decompression through orifice towards atmospheric pressure.

This explosive discharge changes the starting solid cellulose materials into fibrous mulch due to the combination of mechanical and chemical actions towards the materials will cause materials to be defibrillated as depicted in Figure I-15.

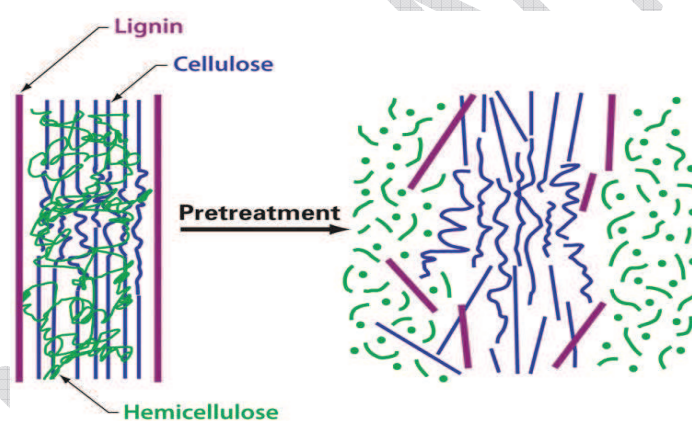


Figure I-15: Schematic of pretreatment goals on lignocellulosic material at a higher severity treatments (adapted from [113])

Steam exploded materials will be then treated with water and chemicals to isolate several interesting chemical components in it. For example, hemicelluloses and lignin are immediate components that can be separated from steam exploded materials by water and alkali extractions. The residue of an extraction process usually exists in the form of insoluble components that was high in cellulose and almost free from hemicelluloses and lignin [113].

There are several setbacks of the steam explosion technology; such as its yield was quite low as reported was due to different treatment severity: i.e. about 78% and 58% at low severity and high severity respectively [114]. This was due to the removal of hemicelluloses and lignin together with condensate produced during heating of treated materials. Formation of pseudo-lignin due to high temperature treatment of the steam explosion also was highlighted to give some problem for direct utilization of the treated material in bioethanol conversion process [12, 95]. This was some of the reason behind the initiative for the utilization of DIC process and technology in our work.

I.2.2.2. DIC Technology

DIC technology was first developed by Allaf et al., [115] at University Technology Compiègne in 1987 when he was trying to solve a problem related to dried vegetable material, which required to be immediately soften back once placed in a water. The process now was called ***Détente Instantanée Contrôlée (DIC)***, or ***Instant Controlled Pressure Drop***. In general, DIC process involves heat treatment of a material inside DIC reactor, then abruptly releasing the pressure towards the vacuum. The sudden pressure drop causes quick cooling of the treated material and massive evaporation of water from it.

Thermal pretreatment regime for biomass material can be divided into three severity treatment class; (1) High severity thermal treatment with steam pressure between 15 to 30 bars; (2) Medium severity thermal treatment with steam pressure between 10 to 15 bars; and (3) Low severity thermal treatment with steam pressure less than 10 bars.

DIC pretreatment was fall under the category of thermal pretreatment according to Table I-9. Eventhough DIC can be considered in a low severity pretreatment regime, it was still expected to contribute some degradation products from glucose and hemicellulose at treatment temperature above 150°C. To avoid this, selection of pretreatment and biomass source was very important, other than parameters used in pretreatment and process to hydrolysis to glucose. DIC pretreatment was also expected to give some chain reactions towards a cleavage of chemical bonding in starch and cellulose superstructure that result to depolymerization into glucose and low degree of oligosaccharides polymer. General outcome based on thermal pretreatment on biomass has been reported by several researchers related to pretreatment and process involved in the thermal operations [12, 87, 98, 107].

The limitation of DIC system currently was due to the supply of steam is limited to a maximum 1.0 MPa only. In order to increase the hydrolysis rate of reaction, very dilute acid is added to the materials. This will enable the use of lower temperature and minimize the residence time. It is also important to ensure that the extended degradation can be controlled by immediately lowering the reaction temperature. Due to the complex nature of lignocelluloses materials used by previous researchers, this work is keen to establish a simple process to study the cellulose autohydrolysis effect with another thermal process known as DIC technology. DIC technology is using a maximum 0.9 MPa steam pressure as compared to steam explosion process that used up to 2.0 MPa steam pressure.

I.2.2.2.1. Basis of DIC Process

The basis of DIC process was established based on a thermomechanical process which requires some moisture level inside material to be treated. The process starts by subjecting process materials inside DIC reactor (in Figure I-16 and Figure I-17) with vacuum followed by pressurized it under steam followed and rapid expansion towards a vacuum (vacuum ~50 – 100 mbar, with rapid valve opening time of approximately ~ 0.2 second). Operating temperature inside DIC reactor usually below than 200°C, while treatment time during high steam pressure was in range from seconds to minutes.

The rapid pressure drop ($\Delta P / \Delta t > 2.5 \times 10^5 \text{ Pa/s}$) during material being heated causes bursting of moisture evaporation inside the bulk of material and this has increased the potential to blows and breaks the cell walls' cavities. The degree of structural damage inside

of materials depends strongly on the nature of the material as well as parameters of the treatment. For processing material with DIC process, it will require a certain level of moisture content in subject material.

Materials subjected towards a vacuum will also undergo an auto-vaporization or also known as adiabatic cooling, which occur instantaneously. The progress of the whole DIC process cycle is shown in Figure I-16(b).

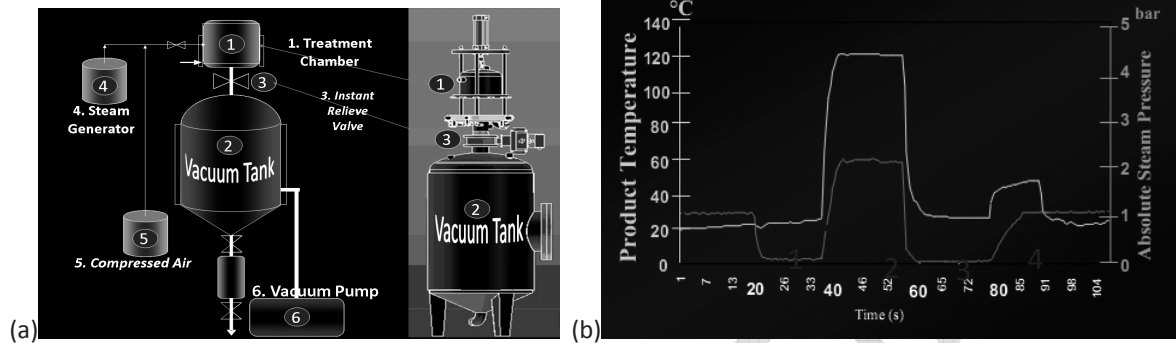


Figure I-16: (a) Schematic diagram of DIC equipments with important service equipments. (b) Four stages of DIC treatment including (1) setting-up an initial vacuum (2) injection of high steam pressure and maintain pressure (3) an instant pressure drop towards vacuum (4) putting back to atmospheric pressure condition.



Figure I-17: DIC reactor used in this work was MP system (with medium steam pressure)

Various research and application based on DIC process was done since the inception of this concept [3-5, 115-122] such as on the structure expansion of fruit and vegetable, drying process assistance, enhancement of extraction of essential oils, sterilization and preservation of food materials.

This work is the first attempt to explore the possibility to use DIC and its unique vacuum stage for the autohydrolysis of biomass with high crude starch into glucose and lower DP oligosaccharides.

PART I. CHAP 3.**REVIEW: AUTOHYDROLYSIS, DILUTE ACID HYDROLYSIS AND MODELING OF THE PROCESS****I.3.1. Introduction**

Over the years, numbers of different methods have been proposed for the conversion of biomass materials into glucose. Initially, source materials need to be either mechanically chipped, milled to decrease its sizes into a suitable size for feeding into pretreatment chambers as described by Saemen (1945) [28]. Once the material was pre-treated with some thermal pretreatment process to increase the accessibility of materials; it is ready for next process, i.e the hydrolysis process through acid or enzymatic hydrolysis to obtain glucose.

This chapter will concentrate on both hydrolysis mechanisms of starch and cellulose to glucose and degradation mechanisms of glucose to several selected fermentation inhibitors such as levulinic acid, acetic acid, furfural and formic acid. Polysaccharide's hydrolysis or glucose generation through hydrolysis of polysaccharides was the main process studied in this work, while degradation of glucose was the main effect for the destruction of glucose that happened simultaneously during hydrolysis step.

It was known that by increasing the severity of pretreatment (combination of several process factors such as time, high temperature and pH) together with the sources of raw materials, the species and concentration of fermentation inhibitors (such as acetic acid, furfural and HMF) can vary greatly [41, 123]. Fermentation inhibitors can be divided into several inhibitor sets depending on its sources, such as acetic acid coming from the breakdown of cellulose and hemicelluloses (due to de-acetylation of hemicelluloses), furfural (due to thermal degradation of 5 carbon sugars), and 5-hydroxymethyl furfural (HMF, i.e. degradation product of 6 carbon sugars) [124, 125]. Other enzymatic inhibitors such as levulinic or formic acid (due to extensive degradation of furfural and HMF) can be formed by increasing the process parameters. Additionally, chemicals with aldehydes groups such as 4-hydroxybenzaldehyde and phenols, including catechol and vanillin can be formed from the available lignin fraction in biomass sources [90].

In specific cases, certain chemicals such as levulinic acid and furfural are the product of interest, for example, are desirable reaction intermediates in the production of liquid alkanes by chemical catalytic processing [16, 24]. For that particular requirement, the process will be developed specifically to obtain an optimum condition of specific products, for example levulinic acid, acetic acid or only glucose. In present work, the process will stop at an optimum processing condition of glucose production.

The mechanism for the formation of glucose from the starch, cellulose and hemicelluloses can be represented by the following reaction mechanisms. Mechanism of glucose degradation into several products such as levulinic acid will be explained in Figure I-19.

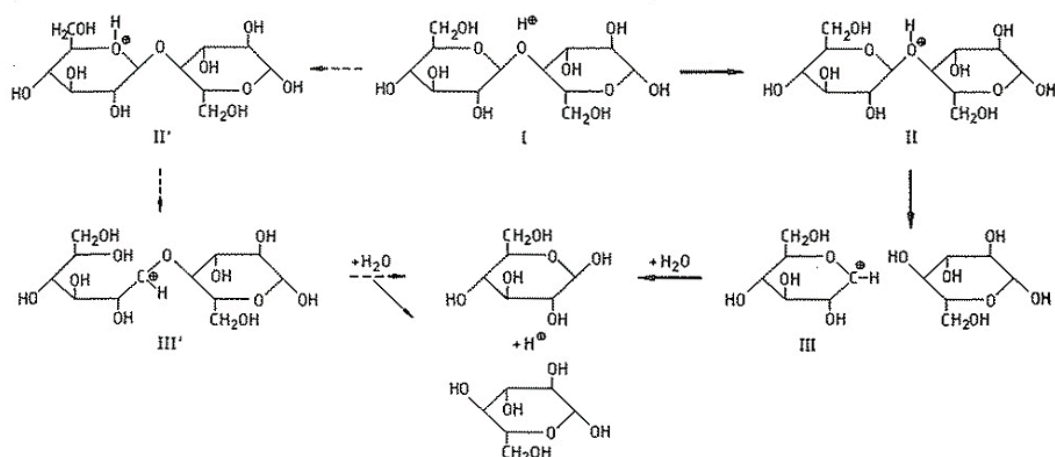


Figure I-18: Mechanism of acid hydrolysis of glycosidic bonds in starch, cellulose and hemicelluloses into monosaccharide (\rightarrow shows reaction direction) (adapted from [44]).

Hydrolysis and degradation of glycosidic bond in starch, cellulose and hemicelluloses, in general can be represented as in Figure I-18 (adapted from [44]). Reactive proton $[H^+]$ presence during reaction will lead to the fission of glycosidic bonds in three steps, with two options. In the potential dominant pathway with Option 1 (route \rightarrow): initially, proton will interact rapidly with the glycosidic oxygen that links two unit glucose (I) to form acid conjugates (II). This was followed by; C-O bonds will slowly cleave to form cyclic carbonium cation (III). For the Option 2: (reaction of the left side) shows that protonation also occurs at the oxygen ring (II') result to the opening of ring and the formation of non-cyclic carbonium cation (III'). It was not clear either cyclic or non-cyclic carbonium cation will occur, due to in the final steps, both cation however will form a stable end product of glucose with the release of the proton [44].

I.3.2. Biomass Autohydrolysis Phenomenon

Autohydrolysis is a hydrolytic process that takes place in the thermal based process which is catalyzed by acids naturally formed from biomass chemical composition (such as acetic acid) or by adding other acids (mineral acid, organic acid) for the reaction to start [23, 98]. Autohydrolysis process normally happened in a thermal process, which was become a basic requirement of present biomass pretreatment technology, which utilizes both physical (high temperature and pressure) and chemical combination to achieve effective pretreatment as presented in Table I-9. Autohydrolysis help to increase surface accessibility for hydrolysis, promotes cellulose decrystallization together with partial starch and hemicelluloses depolymerization and reduces the lignin recalcitrance behaviors in the treated biomass [126].

During hydrothermal pretreatment, a large amount of hemicelluloses will be hydrolyzed and remain in a steam condensate. Lignin will be depolymerized and will release some portion of its phenolic compound into condensate [12]. Lignin will usually remain inside of the biomass system and can be removed with the addition of alkaline solution followed by extraction. Acetic acid that was formed by acetyl group in hemicelluloses (through autohydrolysis) will further help to hydrolyze the beta-glycosidic linkage of hemicelluloses and lignin. Depending on the source of biomass and composition of hemicelluloses; nearly 50% of biomass will be left as a solid residue after hydrothermal treatment consists mainly the cellulose portion [12].

All native lignocelluloses are organized in fibrils, which contain ordered and less ordered region as in Figure I 6 and Figure I 15 (adapted from [113]), and pretreatment was found effectively increase the accessibility of surface availability for enzymatic reaction.

There are certain traits of pretreatments that are preferred such as the ability to increase surface area, size reduction, and removal of certain inhibitor components, swell biomass matrix and increase the amorphous percentage of cellulose. However, certain phenomena usually occur during pretreatment and autohydrolysis of polysaccharides in thermal treatment, including [99, 127]:

- At a higher temperature, the color of treated material becomes dark, suspected due to the degradation of lignin and extractives in the biomass.
- Saturated steam will increase surface temperature and diffuse into a porous structure of biomass. Free acetyl and uronic acid groups from hemicelluloses will be transformed into organic acid such as acetic acid and uronic acids.
- Due to the presence of acids, the hydrolysis of the glycosidic bonds of hemicelluloses chain occurs. Hemicelluloses glycosidic chains are the priority chain due to amorphous structure and available immediately. Depolymerization of hemicelluloses will form intermediate and low molecular weight oligomers, which having active side chains that able to react with water. This makes the oligomers become partially depolymerized and forming monomers.
- Monosaccharide of hemicelluloses usually can be easily dehydrated into furfural and hydroxymethylfurfural (HMF) if exposed to acidic condition and extended temperature [99]. However, the rate of formation for degradation of monosaccharide usually slower than the rate of hemicelluloses depolymerization and its monosaccharide formations.
- Lignin that is available on the surface also being hydrolyzed by acid, plasticization of lignin upon exceed it glass transition temperature will disrupt further lignin and hemicelluloses in the middle cell wall layers. Lignin will form spherical particles due to its polymeric properties.
- Intimate association of lignin and hemicelluloses through bonding between benzyl ester and benzyl ether linkage will depolymerize lignin into soluble component in the aqueous solutions.
- Furfural and other products that were formed by the degradation of hemicelluloses will react with depolymerized lignin and generate products that behave like lignin, or known as pseudo-lignin.
- Cellulose, in particular, at the surface and amorphous region will also be hydrolyzed. Extended hydrolyzed on glycosidic bonds will result to lower the degree of polymerization of cellulose.

I.3.3. Dilute Acid Hydrolysis Effect on Biomass Morphology

Zhao et al (2007) have associated morphology on cellulosic material surface during dilute acid hydrolysis with an amount of glucose obtained from hydrolysis. Cellulose conversion into glucose and its degradation products at 0.1, 0.2 and 0.4 M sulfuric acid was about 5.3%,

11.8% and 25.5% respectively, with an increase in crystallinity (with x-ray diffraction (XRD)) and clean surface morphology (with SEM) due to removal of amorphous portion during hydrolysis [128]. It was observed that there were some changes in length and diameter of microfibrils relative to amount of glucose that was obtained.

The efficient cleavage of targeted chemical links (alpha and beta bond in polysaccharides) was a major goal in the conversion of biomass. Acid hydrolysis of the cellulosic components of biomass was one method to achieve the cleavage of targeted C–O–C bonds for glucose production. Hydrolysis using mineral acid catalysts (e.g., sulfuric acid) has been extensively investigated for sugar production, which was then used to make ethanol [16]. Upon partial acid hydrolysis, cellulose is broken into cellobiose (glucose dimer), cellotriose (glucose trimer), and cellotetrose (glucose tetramer), whereas upon complete acid hydrolysis, it is broken down into glucose [103, 128, 129]. Dilute sulfuric acid treatments were known to hydrolyze hemicelluloses to sugars with high yields, change the structure of the lignin, and increase the cellulosic surface area.

I.3.4. Degradation of Glucose and Xylose

Factors that could influence the degradation of glucose and xylose are similar to factors that enhance the formation of monomer glucose and xylose itself. The only difference will be how to manage each factor in order to maximize the production of polysaccharides monomers and at the same time minimize its degradation.

Factors that heavily influence the rate of glucose generation and its degradations was the concentration of acid and time as limiting factors [44], this together with the characteristic of samples (such as size, chemical composition, phase, physical structure, accessibility in terms of amorphous/ crystalline composition and its moisture content). The hydrolyzing action of acid can be depended on types of acid, concentration, pH and pressure or temperature of a medium.

Degradation of glucose and xylose (part of hemicelluloses) into several degradation products such as hydroxymethyl furfural (HMF), levulinic acid, formic acid and furfural was represented in Figure I-19. Mechanism of acid hydrolysis using acid from polysaccharides into glucose was explained earlier in previous chapter. Glucose will dehydrate three moles of water into HMF, and further dehydrate two moles of water to produce levulinic acid and formic acid. Xylose, will dehydrate three moles of water to form furfural and condensation products.

Under a mild treatment condition, dehydration of water from glucose will lead to the formation of anhydroglucose with intramolecular glycosidic linkages forming sugar with two hydroxyl groups (i.e. 1,6-anhydroglucose)[44]. However, further series of degradation will occur due to lower activation energy was required for the process and due to the instability of the compositions. The final product of degradation will be in the form of cyclic compounds as hydroxymethylfurfural (HMF) (formed from hexose sugars, like glucose). The existence of five carbon sugars such as xylose will give a final product of a cyclic compounds furfural. Condensed products will form solid residues that difficult to be removed from reactors.

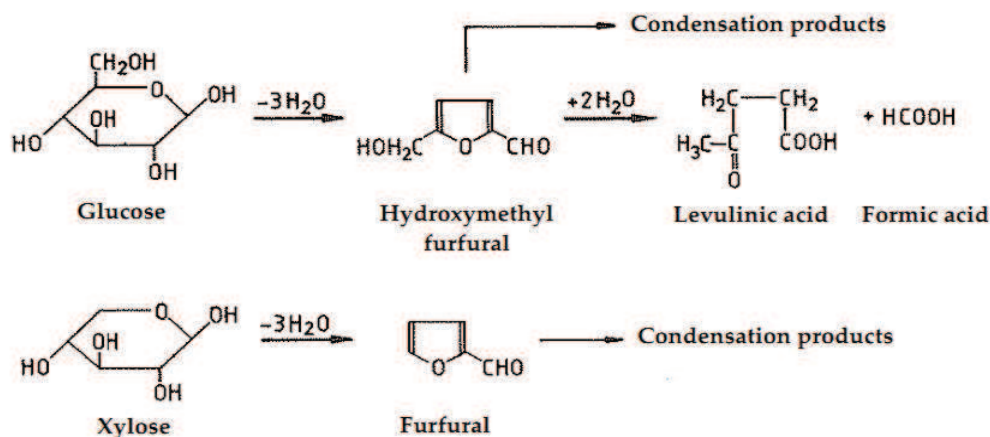


Figure I-19: Degradation of glucose and xylose into hydroxymethyl furfural (HMF), levulinic acid, formic acid and furfural. Both process will remove water and produced condensation products (adapted from [44]).

I.3.4.1. Methods to Control Glucose Degradation

While most publications show that thermal pretreatment helped to increase a rate of enzyme hydrolysis of cellulose to several folds due to biomass polysaccharides was made accessible for enzymatic reaction, at the same time there were very high possibilities that several fermentation inhibitors will be generated as explained in Figure I-18 and Figure I-19. Certain strategies were employed to reduce the generation of fermentation inhibitors such as through the utilization of chemicals [12, 17], hot water extraction, enzymatic reactions and activated carbon.

Huber et al., 2006 believed that undesired by products, including 5-hydroxymethyl furfural (HMF) and levulinic acid are produced by acid-catalyzed degradation of sugars [17] and formation of the fermentation inhibitors can be reduced by adding an oxidizer [12]. Sun et al., (2005) in their work on alkaline peroxide, found that thermal stability of steam exploded residues were increased when alkaline peroxide was added prior to the pretreatment. Increase in thermal stability was believed to be corresponding to an increase in the crystalline portion of cellulose (amorphous portion was hydrolysed, leaving behind the higher crystalline portion)[12]. Alkaline peroxide was an important treatment to lower the requirement for higher energy in hydrothermal treatment. Alkaline peroxide was known functioning as an oxidizer in pulp and paper bleaching process with an oxidation potential of 1.8V (i.e. the loss of electron, Fe^{2+} becomes Fe^{3+}).

Several research groups have proposed methods of inhibitor removals such as through hot water washing followed by enzymatic hydrolysis on solid residues [101], sulfite addition during pretreatment to reduce the inhibitor toxicity [99, 130], filtration through activated carbon and ion exchange [99, 131] to adsorb the inhibitors. These, however have some effects on its own such as loss of glucose within an ion exchange process (up to 26% losses) and during phenolics treatment (up to 35% sugar losses) [99]. Recently, there was a method to reduce fermentation inhibitors through sequential polyelectrolyte (PE) adsorption followed by resin-wafer electro-deionization (RW-EDI). The combination process PE-RW-EDI was found to successfully remove large quantities of inhibitory compounds, increase the rate of cellulose hydrolysis with enzyme and improved overall fermentation to achieve 99% of the theoretical ethanol yield compared with a process without treatment [132].

Based on above reviews, it was important to study factors related to the formation of inhibitors through kinetic's studies and develop treatment with very short exposure time for steam on biomass during thermal treatment. One of the ways to study it was through incorporation of kinetic studies for both treatments with DIC (first stage) and during dilute acid hydrolysis (second stage). In this work, kinetic study was incorporated to find a combination of high rate constant for glucose generation and lower rate constant related to glucose degradation. This strategy will also incorporate the study of hydrolysis factor's effect through response surface methodology.

I.3.5. Enzymatic Hydrolysis

Enzymatic hydrolysis undergoes through different mechanism if compared with dilute acid hydrolysis. The highly organized, crystalline structure of cellulose, added to a close interaction with hemicelluloses and lignin, has often been described as an obstacle to enzymatic hydrolysis [133]. Most often, without pretreatment, enzymatic hydrolysis will only occur on the surface of lignocellulosic material. Hydrolysis with an enzyme, particularly with cellulase was very specific for cellulose and final product was only glucose. Cellulase can be divided into five general types of cellulases (endocellulase, exocellulase, cellobiase, oxidative cellulase and cellulose phosphorylase) based on the type of reaction catalyzed, with the first three was very important in cellulose hydrolysis.

Cellulase was a large enzyme, and very difficult to fit into a porous structure of lignocellulose materials. This was the most reason for a pretreatment requirement prior to enzymatic hydrolysis on the biomass. It was found that there is a linear relationship between the initial reaction rate and the surface area accessibility of biomass due to the size of cellulase molecules of 40Å diameter that restrict its accessibility into a microstructure of cellulose [91].

Hydrolysis condition was normally within mild temperature and pH condition (50°C and pH 4.8 - 5.0). If compared to acid hydrolysis, hydrolysis of lignocellulose with an enzyme produces no degradation products [134].

Cellulases attack the cellulose chain resulting in formation of cellobiose, which is catalyzed by β -glucosidase into glucose [134]. Two enzyme need to be used together to reduce the inhibition of cellobiose on cellulase enzyme. It was found that pretreatment with high acid (3% during a steam explosion) give an increase in crystalline substrate and become a limiting factor for successful enzymatic as shown that there was a rate declining of enzymatic hydrolysis [110]. At the fiber level, accessible regions are often associated with cracks and defects that are encountered along the fiber axis. At a molecular level, they are characterized by a larger pore volume and/or available surface area, higher availability of chain ends and a lower crystallinity index, i.e. amorphous cellulose [133, 135].

I.3.6. Modeling of Glucose Hydrolysis Kinetics

In analyzing thermal and engineering problem, a mathematical model was frequently being set up to describe the system. It may be based on past experience including existing similar cases, or based on a theory of the physical behavior of the system. For this particular work, it is well known that glucose will degrade to several chemicals such as levulinic acid, acetic acid, formic acid and furfural during dilute acid hydrolysis process.

General schematic representation for consecutive reaction of polysaccharides into glucose and its degradation product(s) was discussed in detailed in several kinetic text books. Simplified arrangement for the whole operations can be represented according to several equations in the following paragraphs [136, 137]:



With

A: source of potential glucose or polysaccharides for transformation into glucose

B: glucose

C: degradation product of glucose.

Concentration and rate constant for its respective species represented as follows:

[A]: concentration of total polysaccharides

[B]: concentration for glucose

[C]: concentration for total degradation products from glucose.

k_1 : rate constant for total polysaccharides into glucose

k_2 : rate constant for glucose into total glucose degradation products.

The differential rate expressions for hydrolysis from initial source material into glucose and degradation product of glucose can be solved against the first order irreversible consecutive kinetic reactions as in the following equations:

$$\frac{d[A]}{dt} = -k_1[A] \quad \text{Equation 2}$$

$$\frac{d[B]}{dt} = k_1[A] - k_2[B] \quad \text{Equation 3}$$

$$\frac{d[C]}{dt} = k_2[B] \quad \text{Equation 4}$$

Variables involved in Equation 2 can be integrated between limits at variable time: 0 and t:

$$\int_{[A]_0}^{[A]_t} \frac{d[A]}{[A]} = -k_1 \int_0^t [A] dt \quad \text{Equation 5}$$

$$\ln \frac{[A]_t}{[A]_0} = -k_1 t \quad \text{Equation 6}$$

With final form as following:

$$[A]_t = [A]_0 e^{-k_1 t} \quad \text{Equation 7}$$

Dependence of concentration Glucose, [B] against time ($[B]_t$) from Equation 3 can be written with integration method as:

$$\frac{d[B]}{dt} + k_2[B] = k_1[A]_0 e^{-k_1 t} \quad \text{Equation 8}$$

And multiply both sides with $e^{k_2 t}$ will give:

$$\left(\frac{d[B]}{dt} + k_2[B] \right) e^{k_2 t} = k_1[A]_0 e^{-k_1 t} e^{k_2 t}$$

Equation 9

Also, notice that:

$$\frac{d[B]e^{k_2 t}}{dt} = \left(\frac{d[B]}{dt} + k_2[B] \right) e^{k_2 t}$$

Equation 10

Equation 9 and Equation 10 give:

$$d \frac{[B]e^{k_2 t}}{dt} = k_1[A]_0 e^{(k_2 - k_1)t}$$

Equation 11

Integration Equation 11, yield:

$$[B]_t e^{k_2 t} = \frac{[A]_0 k_1}{k_2 - k_1} e^{(k_2 - k_1)t} + const.$$

At $[B] = 0$ and $t = 0$, constant will be $-\frac{[A]_0 k_1}{k_2 - k_1} e^{(k_2 - k_1)t}$, thus integration will be:

$$[B]_t = \frac{[A]_0 k_1}{k_2 - k_1} e^{(k_2 - k_1)t}$$

Equation 12

And for simple form to use in numerical calculation:

$$[B]_t = [A]_0 \frac{k_1}{k_2 - k_1} [e^{-k_1 t} - e^{-k_2 t}]$$

Equation 13

At initial condition, when $[B]_0 = 0$ and $[C]_0 = 0$, only $[A]_0$ exist as follow:

$$[A]_0 = [A] + [B] + [C]$$

Equation 14

Substitution of Equation 7 and Equation 13 into Equation 14 and simplify it to find $[C]_t$ yields:

$$[C]_t = [A]_0 \left[1 - \frac{k_1}{k_2 - k_1} e^{-k_1 t} + \frac{k_1}{k_2 - k_1} e^{-k_2 t} \right]$$

Equation 15

Notice that Equation 13 and Equation 15 is not applicable if $k_1 = k_2$.

As expected, the knowledge of initial material composition or the glucose potential is very important for understanding the model. Content of total potential glucose was found to be either 600 or 800 to 950 mg/ g SPW depending on condition of treatment and will be used as A_0 through out the calculation of rate constant of the hydrolysis and degradation of glucose.

Time for maximum glucose concentration ($t_{[B]_{max}}$) can be estimated once $d[B]/dt = 0$:

$$t_{[B]_{max}} = \frac{1}{k_2 - k_1} \ln \frac{k_1}{k_2}$$

Equation 16

As we can see, the whole process can be modeled after obtain rate constant k_1 and k_2 after fitting experimental data into the equation. This first order kinetic model equation will be

solved by with actual $[B]$ from experiment ($[B]_{act}$) fitted against $[B]$ calculated ($[B]_{cal}$) and k with lowest sum of $([B]_{act} - [B]_{cal})^2$ will be obtained (using solver in Excel).

Value of A_0 can be determined using total polysaccharides method or based on existing information from known database. Determinations of glucose concentration during hydrolysis kinetic studies were made possible with good chromatographic system and validated test method. Concentration of $[C]$ is the sum of total products degradation, i.e. in the case of glucose including acetic acid, levulinic acid, formic acid and furfural. Existence of any single component of glucose and hemicelluloses degradation product such as levulinic acid and acetic acid can be determined using Equation 7 through monitoring that single species throughout kinetic study. With this information, biomass hydrolysis research and optimization requires generalized kinetic correlation, mechanism of glucose generation and glucose degradation only to describe several important conditions in the process [138, 139].

Numerical based solutions from Equations 7, 13, 14, 15 and 16 were very useful in this work. To simplify its usefulness in this work, the following figures help to summarize each equation into respective numerical solution based on fitting of experimental data.

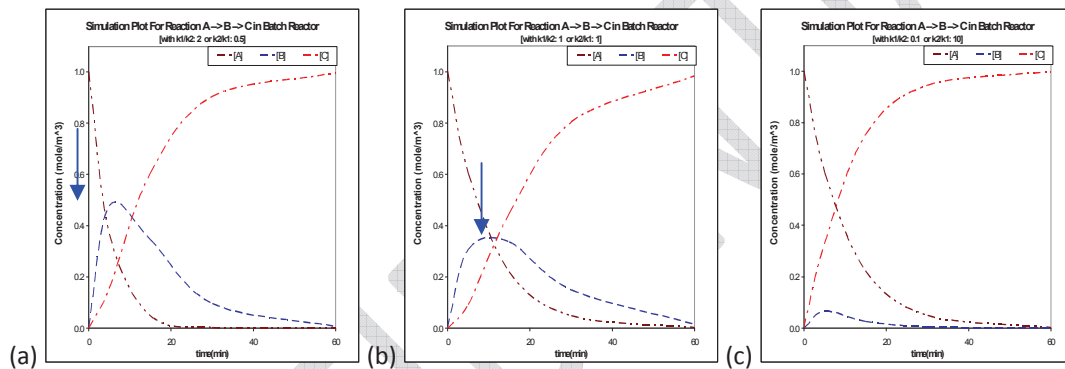


Figure I-20: General representation for rate kinetic for three conditions, based on relative rate constant (k_1/k_2) with (a) $k_1/k_2: 2$ or $k_2/k_1: 0.5$ (b) $k_1/k_2: \sim 1$ or $k_2/k_1: \sim 1$ and (c) $k_1/k_2: 0.1$ or $k_2/k_1: 10$. Time at product or reactant B_{max} was indicated by blue arrow (\downarrow) in plot (a) and (b) (adapted from [140])

Figure I-20, above represent three situations involving different size k_1 and k_2 during reactions in place. When $k_1 \gg k_2$, reaction involving species A to B goes to completion before B gets started. For $k_1 \gg k_2$, concentration of species A, B and C vary as shown in Figure I-20(a). It shows, the disappearance of A into B, and B is slowly converted into C at the same rate. Figure I-20(b) however, shows $k_1 \approx k_2$, i.e. to consider the rate of conversion species A to B and B to C was almost at the same rate. During initial reaction, species A will be converted into B, so that rate constant k_1 can be determined. However, before reaction A to B progress very far, the condition of reaction for B to C was permitted once concentration $[B]$ was enough to starts with conversion into C. In this case, $[B]$ will be drain-off due to the conversion. Concentration $[B]$ will rise to a maximum and fall-off due to availability of species A also has become limited.

Figure I-20(c) was for condition with $k_1 \ll k_2$, i.e. due to very slow formation of species B during reaction but it was immediately converted into C due to permissible reaction conditions. Concentration $[B]$ will never rise very much, while C will appear at similar time of A disappearance.

In all cases presented above, the initial set of species exists at time, $t=0$ was only $A = [A]$, while $[B]$ and $[C]$ were zero, and progressively $[B]$ and $[C]$ will exist due to the reaction condition has permitted their survival.

Relative rate constant (k_1/k_2 or k_2/k_1) was an important term for determination the degradation products based on temperature. For example, if activation energy was substantially difference between generation and degradation process, reaction temperature play important roles in the degradation process. With this, other factors such as acid concentration, treatment time and other potential factors can be manipulated for optimization purpose.

Measurement or monitoring of species can be done as either species A or B or C during the reaction. In this work, only species B or glucose was monitored quantitatively, while C was measured to gain some information of the various species that was available. Actual rate constant for each species needs to be measured quantitatively to calculate a respective rate constant. Since there are many species exist and with the advancement in HPLC method, it was possible to monitor any single species of interest (such as levulonic acid, formic acid, etc.) that exist as [C] in the form of $k_{1(\text{species of interest})}$. Measurement of glucose was made possible with highly sensitive HPLC test method that was developed, that able to isolate its composition from other heterogeneous components exist in liquor [141].

It was found that *Equations 7, 13, 14, 15 and 16* was not only useful for kinetic operation (i.e. [A], [B] and [C] against time, t) but also for studying chemical species (eg. in this work [B]: glucose concentration) against other factors such as moisture and acid concentration levels. Each factor suitability can be decided through data fitting for irreversible consecutive first order kinetic through Log natural (Ln) of response against time, acid concentration or initial moisture level of material. Figure I-21 (a) and (b) summarized the plot of Ln of concentration against factors at X abscissa.

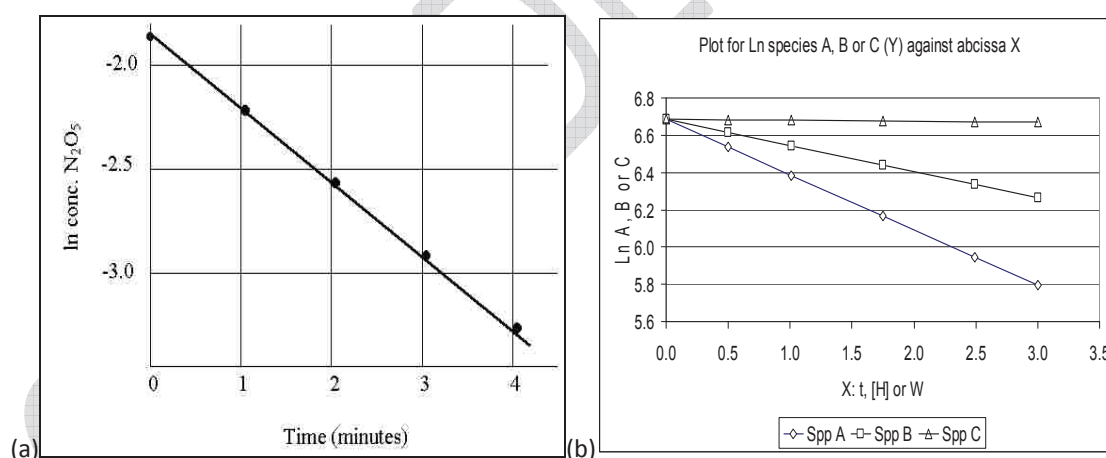


Figure I-21: Representative plot of (a) Ln concentration of species against time, and (b) Ln concentration of species (A, B or C) against time (t), acid concentration $[H^+]$ or moisture content W to determine whether the process is first order or not. First order reaction will give straight line through data point, with R^2 value ~ 1 .

I.3.6.1. Determination of Activation Energy

A minimum three temperature determination was required for determination of the activation energy (E_a) for thermal system. Procedure for determination of activation energy was described in details in several text books [136, 137, 140] and publications [100, 109, 142] and will not be discussed in details here. Figure I-22 show the Arrhenius plot of Ln k (rate constant) against $1/T$ for the determination of activation energy.

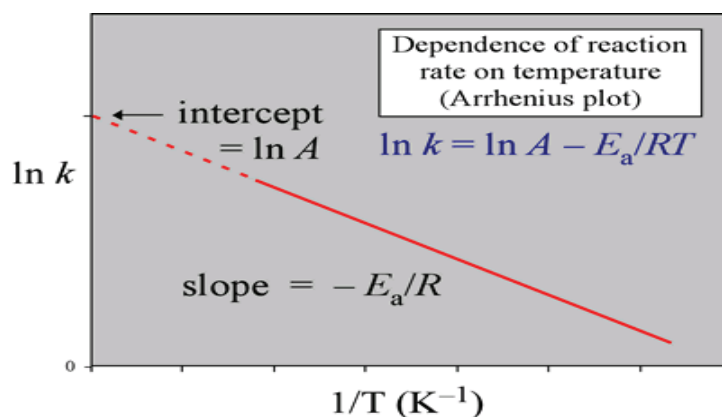


Figure I-22: Arrhenius Plot of $\ln k_1$ or $\ln k_2$ (log natural of rate constant) against $1/T$ (in Kelvin, K^{-1}) for determination of activation energy of specific process condition.

I.3.7. Output of Glucose Hydrolysis Kinetic Model

Several important kinetic data that can be obtained from modeling of the hydrolysis kinetic including rate constant for glucose generation and its degradation; and activation energy of the system. In some work, kinetic expression was divided into fast kinetic and slow kinetic action [143] as identification of wood species and main component exist in that species. These reactions data will reveal the state of reaction that occurs during the process which is important for the optimization purpose.

Table I-10: Kinetic parameters for acid hydrolysis of various biomass feedstock (adapted from [24])

Feed	Temp ($^{\circ}C$)	Acid conc (wt%)	k_1 (min^{-1})	k_2 (min^{-1})	E_1 (kJ/mol)	E_2 (kJ/mol)
glucose	160-260	n/a		1.85×10^{14}		136
cellulose	100-130	5-40 H_2SO_4	1.57×10^{14}		142	
Douglas fir	170-190	0.4-1.0 H_2SO_4	1.71×10^{19}	2.38×10^{14}	180	137
Kraft paper	180-230	0.2-1.0 H_2SO_4	28×10^{19}	4.9×10^{14}	189	137
newsprint	200-240	1.0 H_2SO_4	28×10^{19}	4.8×10^{14}	189	137
Solka-floc	180-240	n/a	1.22×10^{19}	3.79×10^4	178	137
Cane bagasse	100-130	5-40 H_2SO_4	1.15×10^{21}		152	

I.3.7.1. Modeling of Non-isothermal Process: DIC and Dilute Acid Hydrolysis

In this work, two system based on closed thermal system were studied. Non-isothermal situation of the system can be calculated in order to investigate and correlate the system with products than was obtained from respective process. It was known that thermal system was associated with the heat transfer system and it will further affect the hydrolysis of polysaccharides into glucose. In this work we will heat transfer equation to find the relationship of non-isothermal situation of respective system. To model the increase in temperature of product during DIC pretreatment and dilute acid hydrolysis, the following heat transfer equation was use:

$$\text{Heat transfer equation: } mC_p T = UAT \quad \text{Equation 17}$$

With

- m – mass, g
- C_p – heat capacity of water, J/g K or Ws/ g K
- T – temperature, K

- U – overall heat transfer coefficient, $W/m^2 K$
 A – heat transfer area, m^2

For a close thermal system such as DIC reactor or small stainless steel reactor used in dilute acid hydrolysis, the m and C_p are constant over the time, the equation can be arranged to reflex only the changes in temperature T of the reaction mixture (in this work, we use temperature from surface of system) over time, t , in a positive heat transfer from source (steam or hot oil bath) to the reaction mixture inside system. Heat transfer coefficient U , and heat transfer area, A also will became constant in this case.

Overall heat transfer will be reflected by the temperature gradient only as follows:

$$\frac{d(mC_p T)}{dt} = UA(T_{source} - T) \quad \text{Equation 18}$$

$$\frac{dT}{dt} = \frac{UA}{mC_p}(T_{source} - T) \quad \text{Equation 19}$$

for integration and solving the constant with $h = \frac{UA}{mC_p}$ Equation 20

$$\int_{T_0}^{T_f} \frac{dT}{(T_{source} - T)} = h \int_0^t dt \quad \text{Equation 21}$$

Final form of heating equation becomes:

$$T = T_{source} - (T_{source} - T_f) \exp^{-h_h t} \quad \text{Equation 22, and}$$

The final form of cooling equation as follows:

$$T = T_{source} - (T_{source} - T_f)(1 - \exp^{-h_c t}) \quad \text{Equation 23}$$

With

- h_h – rate constant for heating from bath to reaction mixture, min^{-1} or s^{-1}
 h_c – rate constant for cooling from bath to reaction mixture, min^{-1} or s^{-1}
 T_{source} – temperature of steam for DIC or oil bath for dilute acid hydrolysis, K or $^{\circ}C$
 T_f – temperature of mixture, K or $^{\circ}C$
 t – treatment time in minute (min) or second (s)

Equation 22 will be used to determine value for rate constant, h at each experimental temperature by fitting data obtained from experiment into equation to find T calculated. Similar first order kinetic model equation will be used by with actual T from experiment (T_{act}) is fitted against T calculated (T_{cal}) and h with lowest sum of $(T_{act} - T_{cal})^2$ will be obtained (using solver in Excel).

I.3.7.2. Non-isothermal Model Data

Important kinetic data (rate constant for heating) that can be obtained from modeling of the non-isothermal state for both DIC and dilute acid hydrolysis will be presented in Part 3 of the

thesis. Observation of heating cycle against model data, for the first few seconds of heating shows there was great difference between predicted temperature of product and actual temperature being observed due to heat was supplied to heat DIC reactor. Actual product temperature becomes stable after about 5 seconds with difference between product temperature and DIC chamber at about 1°C. Similar observation also found for stainless steel reactor for dilute acid hydrolysis.

Rate constant for heating for DIC and dilute acid hydrolysis system will be used to evaluate both systems in term of the efficiency and the capability of the hydrolysis process.

I.3.8. Experimental Design

Initially, process improvement was established using classical experimental design (one factor at a time - OFAT); however it was changed dramatically with adoption of a quadratic polynomial statistic in 1951 by Box and Wilson and progressively into current statistically designed experiments with response surface. Experimental design or designed experiments were used to study processes and its products. A chemical process, for example, can be defined as any chemical reactions involving substrate, reactants and catalyst, which will yield new products. This process could be governed by certain environmental condition such as reaction temperature and time. The documented examples of sizable quality improvements due to implementations of these methods have been discussed in detail on the optimization of a dyestuff [144] and for effect on silicon wafer production due to different process characteristics (such as deposition temperature, deposition pressure, nitrogen flow, etc.) that affect the variability of the silicon surface thickness [145].

In most cases, a designed study was intended to find out how to set the factors to optimize the product that was required from the process, and to certain extend minimizing other products that were not required. In most experiments, it was not only optimization a concern, but also understands the complex relationship between factors and its product or response. A well designed experiment will be a highly efficient way of learning about this relationship. To achieve that learning curve, generally, involve several steps during optimization such as [146]:

- Selection of factors by its significance on a measured value-response;
- Physical and chemical studies to establish constants, understand properties of materials (chemical compounds and physical)
- Preliminary studies to get the gap for design and develop its processes parameters;
- Optimization of mixture or “composition-properties”;
- Mathematical modeling of a system;
- Estimates and definitions of theoretic model constants, etc.;
- Optimization of process and testing procedures in the lab, pilot-plant and full-scale plant systems.

I.3.8.1. Optimization with Response Surface Methodology (RSM)

The optimization study with response surface methodology need to be done within certain requirement; such as to start with a simple experimental design and towards much complex design at the end in order to minimized number of trials. It was also very important to keep the experimental design to be very simple but able to fulfill the requirement of experimental criteria such as resources (material, steam, process equipment and testing methodology) [147, 148]. Output of designed experiment can be represented as different type of response surface, such as planar surfaces, twisted surfaces or quadratic surface response, depending on initial choice of experimental design as represented in Figure I-23(a) that shows the route of optimization from low yield of response towards high yield response. Most of the time, two optimization study would be required to achieve the required optimum condition.

In some cases, the optimized condition that was generated maybe not suitable to some external factors such as the optimized process works on a lower moisture content of material being processed. In reality, reducing moisture content of material could be much costly than the end product, which was part of present study strategy i.e. to utilize existing material high moisture content for DIC treatment.

This review will discuss about the steps to be taken for a specific condition. The process can be repeated on different conditions to suit with the profitability in mind with a possibility to emulate similar optimization steps in future work. Two type of experimental design will be used: full factorial design and central composite design. Both designs were selected for their qualitative and quantitative aspect, also for the calculation of main and interaction effects capability [147, 148].

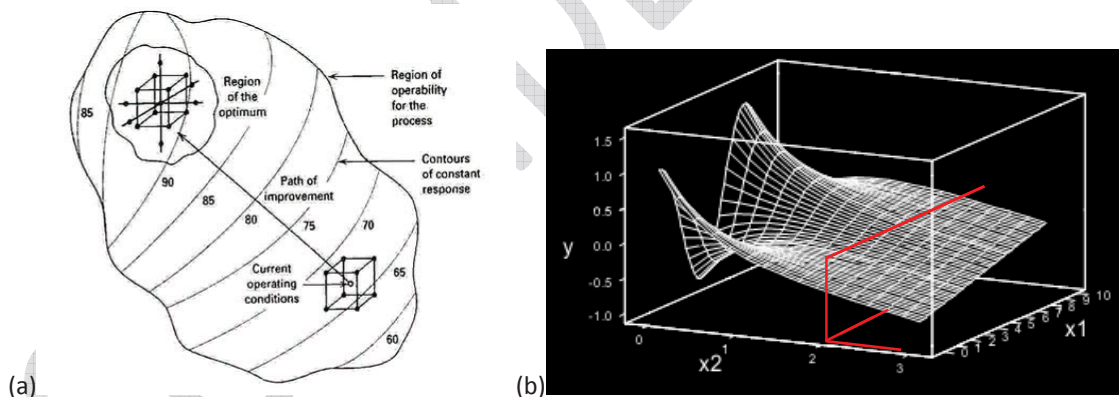


Figure I-23: (a) Route of optimization towards the actual optimized parameter combination (adapted from [146]). (b) Perspective response plot for planar, minimum, ridge and saddle for first order and second order response surface equations (adapted from [148]).

Diagram in Figure I-23(b) depict a perspective plot obtained from optimisation process. Region for x_2 (between 2 and 3 along x_1 across 0 to 10) versus y (along imaginary red line) can be considered as a planar surface represented by a first order polynomial equation. The rest of the plot was represented by a second order polynomial equation.

I.3.8.1.1. Full Factorial Design

One of important experimental design model that was used in this work is based on the factorial design which is represented by 2^k (parameter of experiments or factor is represented by $k = 2, 3, 4, 5, \dots$), with two levels coded as ± 1 . Higher level is coded with $+1$

and its lower level is coded with -1 [147]. Table I-11 below shows possible configuration for factorial design with $k=2$ and 3 for an example.

Table I-11: Two level factorial design (2^k) for $k=2$ and 3. Other combination can be produced with the same configuration. Present work utilized 2^3 factorial design for vacuum and kinetic studies.

Factorial Run	$2^2 = 4$		$2^3 = 8$		
	X_1	X_2	X_1	X_2	X_3
1	-1	-1	-1	-1	-1
2	+1	-1	+1	-1	-1
3	-1	+1	-1	+1	-1
4	+1	+1	+1	+1	-1
5			-1	-1	+1
6			+1	-1	+1
7			-1	+1	+1
8			+1	+1	+1

Polynomial equation that was used to describe factorial design was represented by:

$$Y_{Glu} = a_o + \sum a_i x_i + \sum a_{ii} x_i^2 + \sum a_{ij} x_i x_j \quad \text{- Equation 24}$$

With $x_i = X1, X2$ or $X3$, $x_j = X1, X2$ or $X3$ and $x_i \neq x_j$

Y_{Glu} is the predicted response, a_o is the intercept at 0, a_i is the linear term, a_{ii} is quadratic term and a_{ij} is the interaction term.

1.3.8.1.2. Central composite design (CCD)

One of the most popular second order designs was the central composite design (CCD). It composed of factorial points, axial points and center points. CCD can comprise of any number of factors or study variables ($k=2, 3, 4, \dots$). If the study was with two levels (+1: high, -1: low), its factorial points are represented by points from 2^k ($k=2, 3, 4, 5, \dots$), with a level coded as ± 1 . The axial points ($2k$) are representing by $\pm \alpha$, which was important for the rotatability of the system. Central points of a system are located at 0. Spaces in the design are calculated based on a number of variables in experimental design. For any number of variables, α is computed with $\alpha = \sqrt[4]{2^k}$, and for operating parameters with $k=3$, α value is 1.6818 [149]. Rotatability refers to the uniformity of prediction error. In any rotatable designs, all points will be placed at the same radial distance (r) from center point making it to have the same magnitude of prediction error. For most of rotatable designs the factorial points and axial points lie on different concentric geometric spheres and thus have different magnitudes of prediction error.

Each experimental design in this work will need 22 treatments points, including 8 (2^3) factorial points, 6 (2×3) star points and another 8 center points. Experimental run will be conducted with random sequence to minimize effect of variability in observed response [150]. Twelve degrees of freedoms is associated with this experimental design. Representation of CCD was well described in Figure I-24 below, Table I-12 and Table I-13.

It was called as composite due to it comprise of three separate pieces as described above, for $k=3$, eight corners of cube, six points in the center of each cube face known as axial or star points and any number of centre point can be generated.

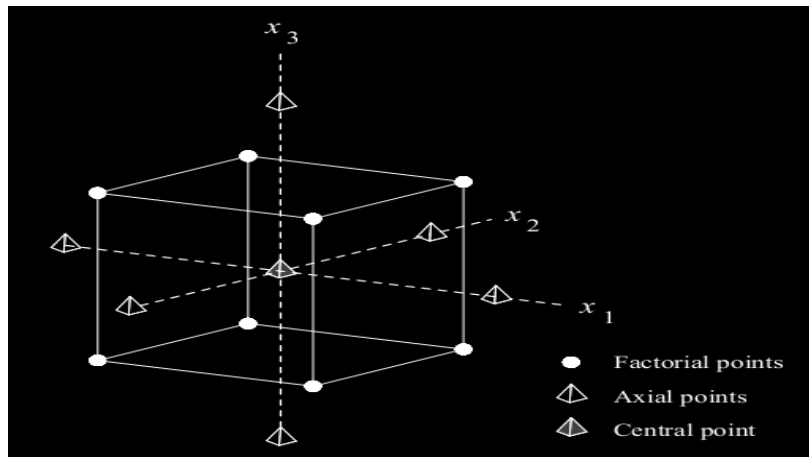


Figure I-24: Central composite design with 2^k factorial + $2k$ axial ($k: 3$). There are two level and three factors in this design. Simulation of two set of data at location of central point (CP), median star point (Star) and median axial point (axial) on axis x_1 to show data location due to affect of thermal treatment.

Polynomial second degree quadratic equation for CCD model was represented by the following equation:

$$Y_{Glu} = b_{k0} + \sum_{i=1}^3 b_{ki} X_i + \sum_{i=1}^3 b_{ii} X_i^2 + \sum_{i \neq j=1}^3 b_{kij} X_i X_j \quad \text{- Equation 25}$$

With b_{k0} as the value of fitted response of central points (0,0,0), b_{ki} , b_{ii} and b_{kij} , were the linear, quadratic and interaction regression terms respectively.

The difference between both equations was that CCD model will include interaction effect from both factorial and axial points while factorial model will only have factorial points.

Table I-12: Actual parameters and its coded form for independent variable of central composite design for low DIC severity study.

Factors	Pressure, bar	[acid], M	Time, min	As
represented by:	X4	X5	X6	Coded form
Point max (+ α)	7.00	0.05	3.00	1.682
Point min (- α)	4.00	0.01	0.50	-1.682
Point central (0)	5.50	0.03	1.75	0
Point (-1):	4.61	0.02	1.01	-1
Point (+1):	6.39	0.04	2.49	+1

Table I-13: Actual parameters and its coded form for independent variable of central composite design for high DIC severity study.

Factors	Pressure, bar	[acid], M	Time, min	As
represented by:	X4	X5	X6	Coded form
Point max (+ α)	7.00	0.20	10.00	1.682
Point min (- α)	4.00	0.05	3.00	-1.682
Point central (0)	5.50	0.13	6.50	0
Point (-1):	0.89	0.04	2.08	-1
Point (+1):	4.61	0.08	4.42	+1

I.3.8.2. Statistic for Response Surface Methodology

Designed experiment need to be based on statistical methodological concepts such as regression and correlation analysis, analysis of variance, randomization, optimal use of factor space, successive experimenting, replication, compactness of information, statistical

estimates, etc. [146, 147]. This will makes the regression analysis statistic was important in the design of experiments. For factorial and central composite design experiment, regression model of second order will be use as described by the equation above.

1.3.8.2.1. Data Analysis

Data obtained from factorial design and CCD experimental trials will be fitted into the equation by numerical technique as described in commercial statistical software Statgraphics Centurion XV, version 15.2.11 (later as Statgraphics). Analysis of variance for glucose yield will be calculated and presented together with Pareto chart, with correlation coefficients R^2 was targeted more than 90%. Statistic for F ratio and statistical probability (P) were calculated from experimental data with total degree of freedom of 21 for CCD and 7 for factorial design. Degree of freedom was high enough to achieve a good statistical model. Value of P less than 5% will be required to decide whether factor or its interaction having significant difference or not against the model based on glucose yield.

Response surface and contour plots for model based on polynomial equation were plotted as a function of any two variables at a time. A total three response surface and contour plots are available for each response surface model.

1.3.8.2.2. Data Mining for Kinetic Model from Response Surface Model

RSM was an advantage over classical experiment methods and offers a large amount of information from a small number of well designed experiments. In addition to analyzing the independent variables, response surface methodology generates a mathematical model that was able to describe chemical or biochemical processes such as determination of reaction kinetics and evaluation of kinetic constant [146, 151]. In addition of optimization, single polynomial equation obtained from experimental design (both factorial and CCD) in this work will be used to estimate an effect of hydrolysis kinetic of the process and to calculate a rate constant of the hydrolysis kinetic.

Several constraints need to be addressed to ensure result or data obtained from data mining operation of a response surface model was adequate to fulfill hydrolysis kinetic model itself. This was due to most of RSM software was based on a second order polynomial equation, while in kinetic operations as described earlier was based on exponential equation. So it was expected that there will be some data points (trends) in the polynomial equation will be very far from trends based on the exponential equations. Actually, it was possible to predict a model equation with a higher degree polynomial equation than the second order only [151]. In addition of this, it was found that kinetic operation was able to describe response surface models very well and also will be used to describe interaction effect of the kinetic model.

To ensure that the operation with data mining from this empirical model produced acceptable result, the following constraints were put in placed:

- Glucose with negative values will not be counted in the model.
- F distribution together with R^2 will be used to check the statistical distribution of data and correlation between model and data.
- Central points will be used to check for the linearity of reaction within the range being studied.

Formula for calculate R^2 and F distribution as following:

$$R^2 = 1 - \frac{\sum_{j=1}^M [(B_s / B_{so})_{\text{exp}} - (B_s / B_{so})_{\text{cal}}]^2}{\sum_{j=1}^M (B_s / B_{so})_{\text{exp}}^2}$$

And

$$F = \frac{\left[\sum_{j=1}^M (B_s / B_{so})_{\text{exp}}^2 - \left[\sum_{j=1}^M [(B_s / B_{so})_{\text{exp}} - (B_s / B_{so})_{\text{cal}}]^2 \right] \right] / M}{\sum_{j=1}^M [(B_s / B_{so})_{\text{exp}} - (B_s / B_{so})_{\text{cal}}]^2 / (M - M_p)}$$

With

B_s : concentration B at specific time [note: similar with B in kinetic previously]

B_{so} : concentration B at time=0

$()_{\text{exp}}$ and $()_{\text{cal}}$ respectively for experimental and calculated value

M : number of experiment

M_p : number of parameters studied

F test was usually used to compare the variances of two populations, and it was use in this study as this statistic often used to compare statistical models that have been fit to a data set. This will identify whether the model will best fits the population from which the data were sampled.

In the case of response surface, F distribution is calculated using Statgraphics, and for kinetic model developed from polynomial equation, above statistical calculation was used. F calculated will be compared with F from Table F distribution (i.e. with 10F) using respective degree of freedom (d.f.).

1.3.8.3. Factors Elimination and Optimization of Process

In most cases, there are [over] four main factors that can affect the optimization of biomass thermal pretreatment such as: size of feed material, choice of catalyst, catalyst concentration $[H^+]$, initial moisture content of material (W), treatment temperature (T) and treatment time (t). In the case of DIC treatment two more factors were added: the use of vacuum (P) during initial and at the end of treatment. Since W and $[H^+]$ was interrelated, material was prepared by adding different acid concentration to the biomass to achieve the desired W and $[H^+]$ value.

As suggested by most work related to DIC treatment, factors such as moisture level of material (W) and the use of vacuum during initial and at the end of treatment are very important parameters [3, 117, 118, 121] and will be maintained during initial work. Investigation on vacuum cycles will be done together with moisture content to obtain optimum combination.

Catalyst concentration $[H^+]$ and treatment time (t) will be evaluated to obtain optimum condition in combination with moisture content, catalyst selected is sulfuric acid due to

relatively easy to obtain and is commonly used in the operation. Size of feed material was not of importance any more based on uniform size of feed material as supplied.

Steps taken for elimination of the process factors, merging of factors and optimization of process will be explained further in respective work in Part 3 of the thesis.

CONFIDENTIAL

PART II.

MATERIALS & METHODS

It was established in the objective of the thesis; SPW will be used as the source of polysaccharides to obtain glucose for this study, to relate it with industrial application of glucose and as well as to solve the current environmental problems due to improper removal of SPW solid waste to the environment. The process involved the optimization of two stages of thermal process (1) pretreatment with DIC system and, (2) dilute acid hydrolysis process.

Both processes will involve autohydrolysis reaction due to the utilization of dilute acid on the treated materials. During the exploratory study, full process was developed followed by actual trials with full experimental design. Response data for both thermal processes was glucose concentration coming from starch and cellulose in material obtained through HPLC determination. Other compositions such as glucose degradation products and hemicelluloses was not counted because the amount was very minimal and of not particular interest for this study. Test methodology and process protocol were developed during first part of research works including its validations. Processes developed including exploratory investigation, optimization and modeling of DIC pretreatment and dilute acid hydrolysis for both processes as represented in Figure II-1 and Figure II-2.

Along the main objective to maximize glucose production, we also developed several process indicators to monitor and understand the underlying fundamentals of the processes, such as effect of DIC treatment on hydration of material, the crystalline structure of materials, surface properties of treated materials etc..

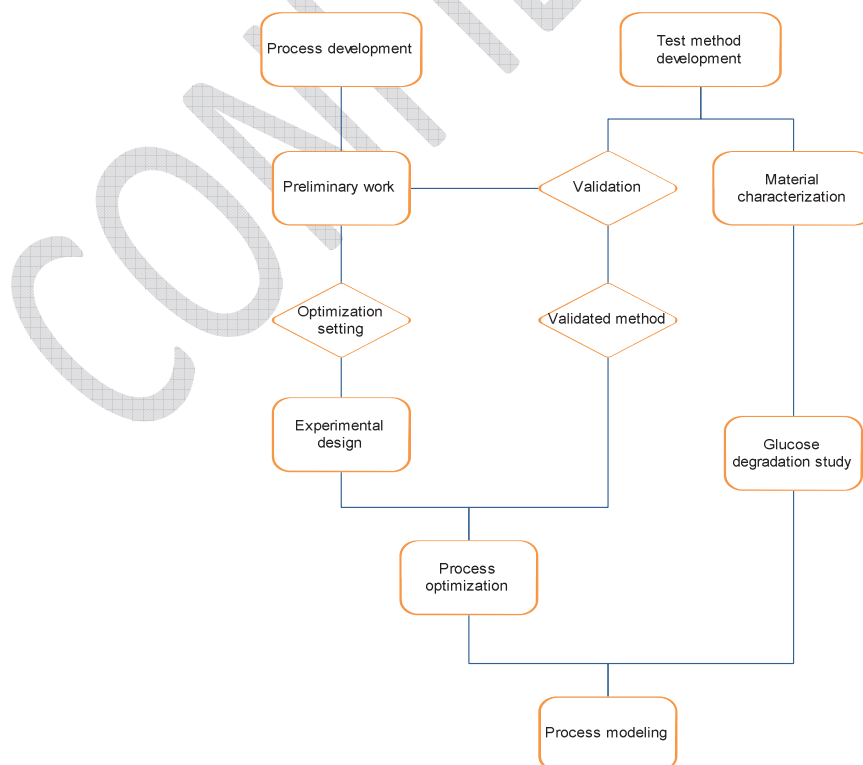


Figure II-1: Research work flow for DIC process and testing method validation during exploratory and optimization study

PART II. CHAP 1.

RAW MATERIALS

II.1.1. Sago Pith Waste (SPW)

Decision to select sago pith waste (after this will be referring as SPW) for this study was based on several criteria posses by the material itself such as (1) the availability of high starch and cellulose content in the materials as presented in literature review (2) lignin content was considerably low, and (3) the material was readily available in the required size and form (i.e. almost completely in the form of small particles) making it suitable for DIC pretreatment immediately after moisture and acid adjustment.

Sago Pith Waste (SPW) was obtained from sago palm processing factory in Batu Pahat, Johor, Malaysia at final washing stage. It contains very high water, in the form of biomass slurry. SPW sample was dried under sun light for 2 days and packed into plastic bags for transportation to France via airplane. Upon receiving, materials were kept frozen until used. It was dried at 45°C for 12 hour in a convection oven and stored in a hermetic plastic container at room conditions. Dried SPW was determined its moisture content, analyzed for its particle size distributions and starch content. Throughout the work, amount of samples that will be used is pre-calculated and an exact amount was taken out from store container. Unused sample was mixed back into container and mixed thoroughly to ensure uniform distribution between each batch of works. Figure II-2 shows several steps of processing and characterization of SPW in this work.

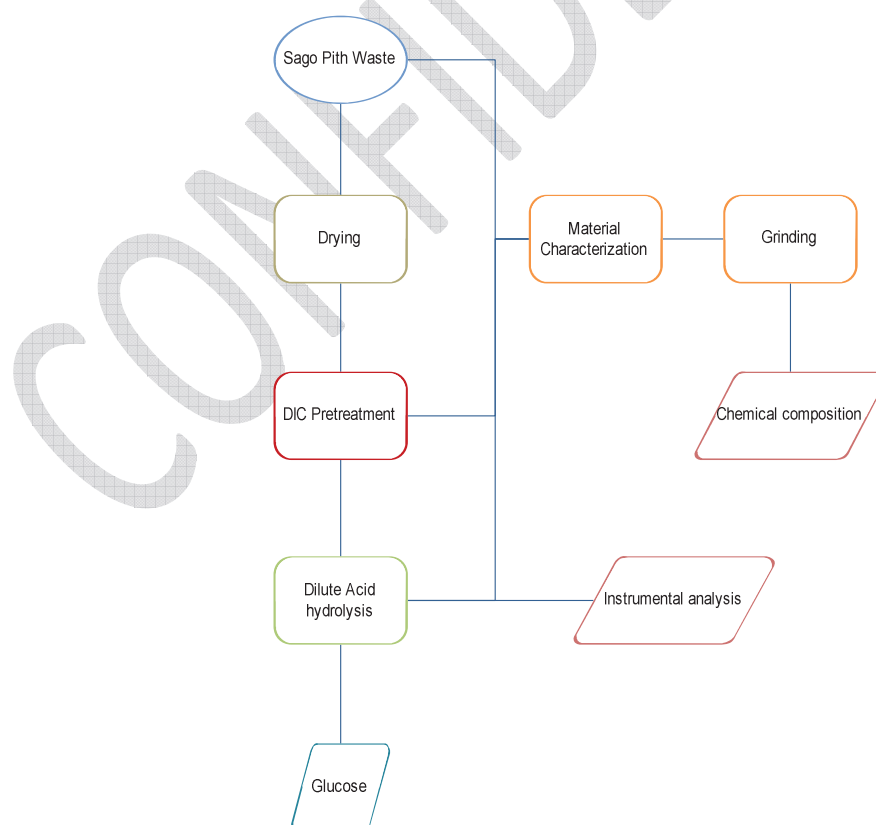


Figure II-2: General flow of work for DIC and dilute acid process during dilute acid hydrolysis process

Dried materials were kept in seal plastic bag to avoid moisture uptake. No drastic moisture uptake was observed for dried materials upon exposure to high humidity room condition, which suggest that material is quite stable even though have high polysaccharides content in the form of crude starch.

Before any further treatment (DIC, hydrolysis), material was further dried for another 12 hour with depth bed of about 2 cm thickness. Balance of material that not used is added back into bulk container and thoroughly mixes to ensure uniform material supply for the next operation. Moisture content adjustment was done with pre-prepared acid solution according to the requirement of the experimental design parameters.

Summary of result for SPW material at several preliminary processing stage and drying is presented in Table III-3 in page 75.

II.1.2. Sampling of DIC Treated Materials

In this work, several steps were planned to ensure a representative sample was taken for relevant testing. SPW materials usually pre-mixed in a small polyethylene bag with zip lock prior to sampling. Sampling was done by taking small amount of sample from random location between top and bottom of sample location after mixes.

II.1.2.1. Rapid Moisture Content Determination

Moisture content determination was done at 105°C for 5 minutes with Sartorius M30. A minimum of 0.5 gram to 1.0 grams materials was placed on an aluminum crucible and put into drying chamber of Sartorius M30 based on modified AOAC method.

This drying procedure was compared with 105°C for 24 hour in an oven, and difference between both procedures was with average difference less than 2% for 10 trials. All determination of moisture content in this work was based on this procedure.

II.1.2.2. Material Characterization

Material characterization for main fraction (cellulose, starch, hemicelluloses and Klason lignin) were done using quantitative acid hydrolysis method under standard condition based on method by Browning (1967) and Moore & Johnson (1967) with detail procedure according to several selected publications [12, 79, 152, 153].

For materials (such as SPW) containing high starch percentage, hot water extraction step was done to isolate starch content followed by characterize all composition of all material. Starch and hemicelluloses were group together during hot water extraction analysis, while cellulose and lignin were grouped together during acid hydrolysis stage.

Data obtained from hot water extraction and hydrolysis was calculated to find total polysaccharides in the material. Result obtained was compared to result obtain by other research groups to check SPW content variation.

II.1.3. Hemicelluloses and Starch

Both hemicelluloses and starch were isolated from SPW using hot water extraction followed by dilute acid hydrolysis as described in several publications [79, 152]. This procedure was

based on capability of starch to gelatinize and highly solubility of hemicelluloses in hot water. The dilute acid hydrolysis on extract obtained from hot water extraction step was done to hydrolyze starch and hemicelluloses into its monomer with HPLC analysis.

Approximately, 10 g materials (SPW) with known moisture content were added into 500 ml conical flask followed by addition of 100 ml water. Materials were mixed with water and heated on a heating plate to a boiling temperature. Observation was made to ensure gelatinization of starch was completed within about 60 minutes with mixing and several addition of water to control water losses as vapors. Conical flask and its content were cooled to room temperature and weighed. Loss in weight was considered as losses due to water vaporization and water was added back to attain original volume based on initial recorded weight.

Sonication was done on material in a conical flask for 15 minutes to ensure all water soluble components that still remain in fibrous material will dissolve into water. Fibrous materials were separated manually from water followed by filtration with nylon cloth to separate cellulosic materials from extract. Final solution after hot water extracts and sonication obtained was high in gelatinized starch and hemicelluloses. Solution was kept below 5°C until determination of its total polysaccharide content. Solid residue obtained was dried in an oven at 40°C for 12 hour. Total polysaccharide for both parts was done concurrently.

II.1.3.1. Starch Content

Water extract obtained from previous hot water extraction was hydrolyzed with sulfuric acid. 1 ml water extract was added with 1.5 ml 72% sulfuric acid and diluted to 56 ml. Hydrolysis was done in autoclave at 120°C for 60 minutes. Extracts obtained was cooled and further diluted with water for HPLC determination. Total glucose obtained in this determination was a mix of a small fraction of glucose from hemicelluloses.

Verification for total conversion of starch into glucose was done with 100 mg sago starch under the same hydrolysis condition. Result obtained shows that 99.99% sago starch was converted into glucose with very minimal degradation occurs. In hot water extract of DIC process, starch is considered as glucose.

II.1.3.2. Hemicelluloses

10 ml hot water extract (HWE) were centrifuged at 5000 rpm with Sigma 6K-15 bench centrifuge in polyethylene container. Solution was separated from solid and homogenized, followed by 3 ml solution obtained was concentrated and dried in oven at 70°C for 12 hours. Drying was done by increased the temperature to 105°C for 4 hours. Remaining solid obtained was weighed. Total hemicelluloses are calculated by difference with glucose amount obtained from starch hydrolysis, with assumption that hemicelluloses was very soluble (main hemicelluloses were sugar that highly soluble in hot water such as xylose, glucose and galactose) and it was not sediment during centrifugation step.

$$\text{Starch} + \text{Hemicellulose} = \frac{(\text{SPW} - \text{Solid})}{\text{SPW}(\text{db}, \text{g})} 100\% = \text{HWE}(\%)$$

$$\text{Hemicelluloses}(\%) = \frac{\text{HWE}(\text{g}) - \text{Starch}(\text{db}, \text{g})}{\text{SPW}(\text{db}, \text{g})} 100\%$$

In most determination, it was found that fraction of hemicelluloses was very negligible.

II.1.3.3. Total Polysaccharides

Total polysaccharides method was based on modified method for Tappi Method T 222 OM88 for hydrolysis of polysaccharides available in biomass with detail procedures described previously (adapted after method in [12, 153]).

Weigh accurately 100 to 200 mg samples into 25 ml glass beaker. Add 1.5 ml cold 72% sulfuric acid into beaker while ensuring all material parts are thoroughly wetted with glass rod. Material was thoroughly mixed for 60 minutes in temperature controlled bath at 30°C. Accurately 10 ml water was then added into beaker while stirring and mixing to ensure all materials were dissolved in water and subsequently transferred into 150 ml glass bottle with tight cap. Rinsed beaker with small volume of water and add into glass bottle. Total volume of water of 56 ml was required to make final acid solution 4%. Hydrolysis was done in an autoclave at 120°C for 60 minutes followed by immersing glass bottle in cold iced water to stop hydrolysis reaction. Final volume of water was recorded to ensure each hydrolysis was done at the same acid concentration within batch and during other hydrolysis batch.

Following the hydrolysis of polysaccharides in materials, hydrolysate containing solid residues was filtered and solution obtained (hydrolysate) was prepared for glucose determination with HPLC as prescribed in the glucose determination procedure with HPLC (refer II.1.5.1 in page 62).

II.1.3.4. Total Lignin

Lignin determination method was based on modified method for Tappi Method T 222 om-88 was used for Klason lignin and Tappi Method UM 250 for acid-soluble lignin (ASL) with detail procedures described previously (adapted after method in [12, 153]).

Weigh accurately 100 to 200 mg samples into 25 ml glass beaker. Add 1.5 ml cold 72% sulfuric acid into beaker while ensuring all material parts are thoroughly wetted with glass rod. Material was thoroughly mixed for 60 minutes in temperature controlled bath at 30°C. Accurately 10 ml water was then added into beaker while stirring and mixing to ensure all materials were dissolved in water and subsequently transferred into 150 ml glass bottle with tight cap. Rinsed beaker with small volume of water and add into glass bottle. Total volume of water of 56 ml was required to make final acid solution 4%. Hydrolysis was done in an autoclave at 120°C for 60 minutes followed by immersing glass bottle in cold iced water to stop hydrolysis reaction. Final volume of water was recorded to ensure each hydrolysis was done at the same acid concentration within batch and during other hydrolysis batch.

Following the hydrolysis of total polysaccharides, residual solid was washed after filtration with distilled water until neutral and dried at 100°C for 24 hour. Klason lignin was the remaining dried acid insoluble residues and reported on a dry basis of materials.

$$Lignin(\%) = \frac{residue(g)}{SPW(db, g)} 100\%$$

Solution obtained (hydrolysate) was prepared for glucose determination with HPLC as prescribed in the glucose determination procedure with HPLC.

II.1.3.4.1. Acid soluble lignin

Acid soluble lignin was determined by using acid hydrolysate obtained from above (refer 60II.1.3.4) based on UV spectrophotometric method at 205 nm according to Tappi Method UM 250 for acid-soluble lignin (ASL) with detail procedures described previously (adapted after method in [12, 153]).

Percentage of acid soluble lignin was determined according to:

$$ASL(\%) = \frac{100BV}{1000w}$$

With

B - average absorption factor of lignin (110 g/1000 mL),

V - total hydrolysate and

w - the dry weight of sample

Acid soluble lignin was reported as dry basis of SPW. Total lignin was reported as:
 $TL(\%) = Lignin + ASL$

II.1.3.5. Alkaline extraction

Hot water extraction was done to remove hemicelluloses and starch from fibers. Remaining solid materials will be cellulose and lignin. Sodium hydroxide, NaOH (5%) solution was used to extract lignin in the sample. The extraction was performed at 70°C for 1 h using a liquor/solid ratio of 20 ml liquor/g dry weight of sample (modified after [79]). Solid fraction was washed twice with distilled water and dried at 90°C for 24h until weight was constant. Composition analysis for total lignin (Klason and acid soluble lignin) and cellulose were determined by difference.

$$AEF(\%) = \frac{fiber(g)}{SPW(db, g)} 100\%$$

Content of cellulose obtained as follow:

$$Cellulose = 100 - (TL\% + Hemicellulose\% + Starch\%)$$

II.1.4. Physical Characterizations

II.1.4.1. Particle Size Distribution

Particle size distribution were done with sieve size less than 200 μm, 200 - 400 μm, 400 - 800 μm, 800 - 1000 μm, 1000 - 2000 μm, 2000 - 4000 μm and more than 4000 μm using vibratory FRITSCH Sieve Shakers.

100 gram of sample was added into sieve and shaken for 10 minutes. Percentage of sample retain on respective sieve size were then weighed and calculated against initial amount.

$$SR\% = \frac{m}{M} 100\%$$

With

m - weight of material retain on respective sieve, and

M - total weight of materials.

Total polysaccharides content retained on each sieves were done according to total polysaccharides procedures as above (refer II.1.3.3) to determine its glucose contribution.

II.1.4.2. Bulk Density of SPW

Bulk density was measured according to ASTM D7481 with Autotap (Quantachrome Instruments, Boynton Beach, FL) using 100 ml or 10 ml cylinder [154].

Density was calculated using the following formula:

$$\text{Density, } \rho = \frac{m(g)}{M_v(ml)}$$

With

m - weight of materials and

M_v - volume of materials.

II.1.5. Instrumentals Analysis

II.1.5.1. Carbohydrate and Total Polysaccharides

HPLC analysis was done for the study of total polysaccharides in biomass material and glucose residue or glucose composition generated from DIC, hydrolysis process, material characterization and during kinetics study for hydrolysis and glucose degradation.

HPLC system use throughout this work was an Agilent 1100 HPLC system consists of G1311A Quaternary Pump, G1315A Diode Array Detector or variable wavelength detector, G1362A RI Detector, G1313A Autosampler, G1322A Vacuum Degasser, Solvent Module and controlled by Chemstation software.

Column used in this work was ICE-COREGEL 87H3 (Transgenomic) at 35°C that separate glucose and certain organic acid in solution.

II.1.5.2. Glucose and Glucose Degradation Products with HPLC

Sample that was ready for glucose determination was either already centrifuges at 5000 rpm for 10 minutes or filtered through minimum 0.25 or 0.45 μm nylon filter size and already placed in respective HPLC vials with label.

Standard (glucose, acetic acid, levulinic acid and formic acid) were prepared from stock solution containing 1000 ppm each component. Standard were diluted to 20, 100, 300 and 500 ppm in respective vials.

Mobile phase was dilute sulfuric acid (5 mM) in deionised water at a flow rate of 0.5 ml/min. 10 μl sample and standards of different concentration are injected separately into HPLC system (as described in II.1.5.1). Representative of standard chromatograms for glucose, formic acid, acetic acid and levulinic acid were presented in Figure II-3.

Selected glucose degradation products as described above are acetic acid (AA), levulinic acid (LA) and formic acid (FA). Standards were prepared by diluting glucose, acetic acid, formic acid and levulinic acid in deionized water [density and purity of each chemical were used to

calculate actual amount of standard in solution]. Concentration of each component was in the range 10 ppm to 1200 ppm.

Hydrolysate from sample will be diluted with mobile phase or deionised water to be in the range of standard if necessary.

Typical standard chromatogram (RID and DAD 210 nm) are represented as follows:

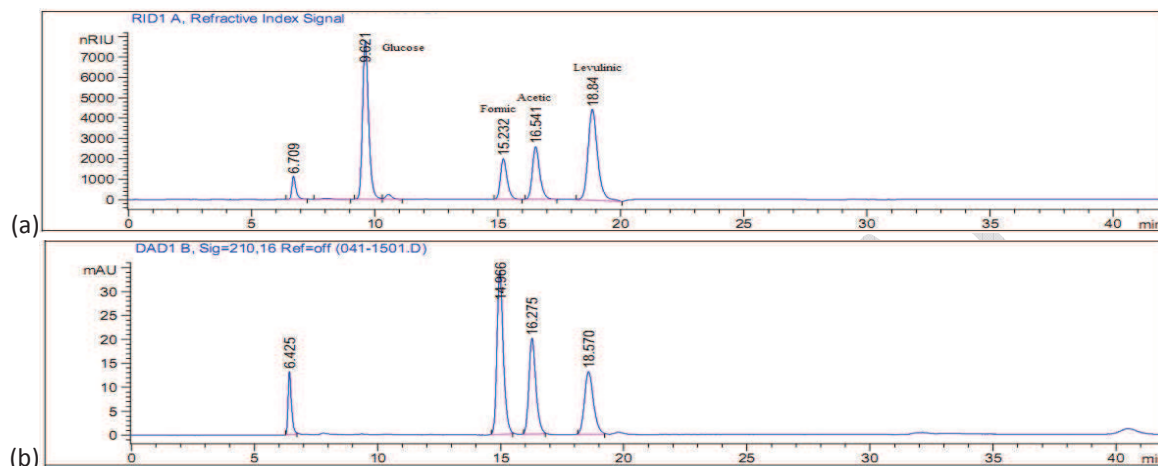


Figure II-3: Standard chromatogram obtained for glucose, formic acid, acetic acid and levulinic acid for (a) RID and (b) DAD 210 nm, mobile phase 0.5 ml/min.

II.1.5.3. Partial Validation of HPLC Method and Result Obtained

In normal glucose determination for sample and potential degradation products, HPLC system will be left to run for 40 minutes to ensure all components has coming out from column. For a full set of trial of 22 experimental points and 4 standard points, HPLC determination will require about 52 hours to complete with triplicate injections. Partial validations were done to address several issues such as stability of standard and samples together with to ensure result obtained from this work is acceptable. Partial HPLC method validation was done to ensure that complex composition of hydrolysate from hydrolysis and hot water extraction was determined within its linear range. Precisions checks were done for retention time, standard area and volume of injection.

Standard injection volume into HPLC system was 10 μ l, however in some sample; there was a need to inject higher volume (about 20 to 50 μ l) especially for very dilute solution that requires high volume injection to meet the limit of detection (LOD) and limit of quantification (LOQ). Very dilute sample injected with volume more than 4 times standard injection will be evaluated for precision of its retention time against value obtained from standard injection. In all case, retention time of sample was found to be within the standard deviation of less than 5%.

Standard and sample stability was done for sample and standard through comparing data obtained at day one against data obtained after exposure to room condition up to thirty days. In normal operation, sample and standard vials were kept in the refrigerator at temperature 0°C after determination is completed. LOD and LOQ are calculated using the formula, $LOD = \frac{3\sigma}{S}$ and $LOQ = \frac{10\sigma}{S}$, with standard deviation, $\sigma = \sqrt{\frac{\sum(Y - Y_i)^2}{n - 2}}$, Y was the area under curve or retention time (in minutes) and S is slope of the calibration curve. Correlation of data is measured using R^2 value and its value was found to above than 0.9999 in all case.

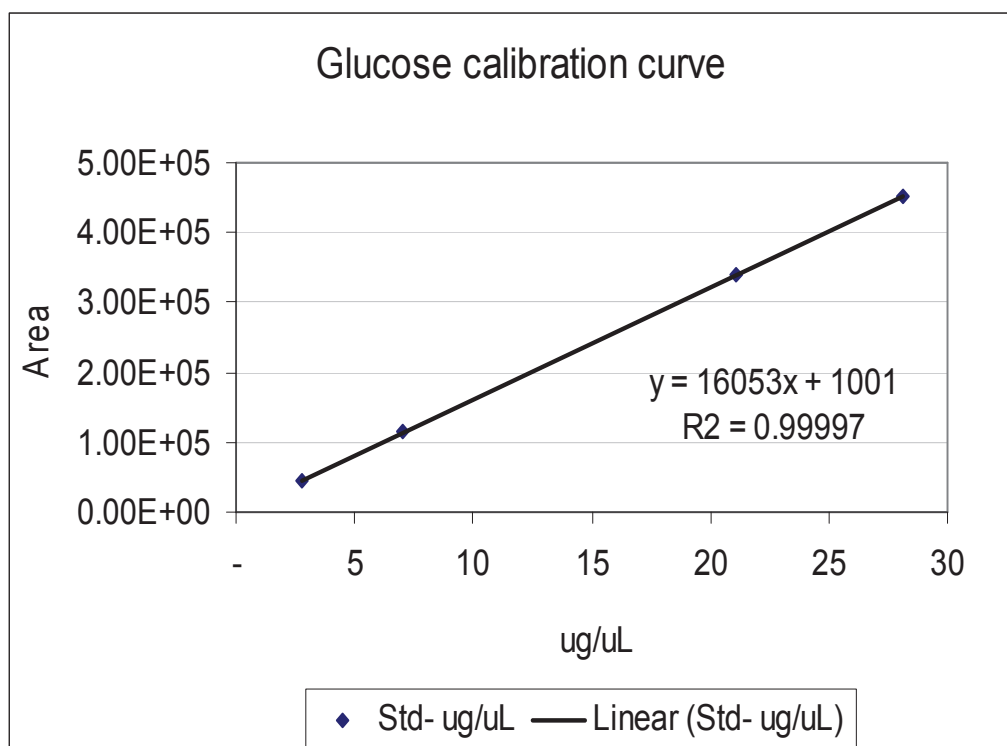


Figure II-4: Representative standard curve for glucose.

Table II-1: Summary and observation of HPLC partial validation. Data was compiled throughout experimental test.

Parameter tested	Data and Note
LOD	0.79 to 0.95 $\mu\text{g}/\mu\text{L}$
LOQ	2.63 to 3.17 $\mu\text{g}/\mu\text{L}$. Experimental data was check to be above these values to be accepted.
Correlation coefficient for standard injection, R^2	> 0.9999
RSD for minimum 2 injections for samples	Less than 5% Samples with more than 5% RSD will be repeated.
Stability of standard	>30 days exposures to room temperature with less than 2% change from initial concentration values.
Stability of samples	Within 72 hour exposure to room temperature – less than 1% changes in area under curve. More than 2 week exposure to room temperature – there was some increase (2-5%) of area under curve. This was due to hydrolysis of oligosaccharides into glucose especially for experimental points from hot water extraction with lower DIC severity. For dilute acid hydrolysis, there was no change in area under curve was observed after longer exposure. Only data from first injection was used in this thesis.
Precision: injection (injector)	2 μL – less than 1% (area) difference between injection 10 μL – less than 1% 50 μL – less than 1%
Precision: retention time (RT)	2 μL – no changes (i.e. less than 5%) 10 μL – no changes 50 μL – no changes

II.1.6. Thermo Gravimetric Analysis (TGA)

TGA was done to check for the pyrolysis of biomass under constant trial condition. Analysis was done by recording the weight of sample in dynamic conditions between 30°C to 600°C at a constant heating rate 10°C/min under inert atmosphere of nitrogen gas. About 10 mg to 20 mg sample were analyzed. The experimental results were achieved using a thermogravimetric equipment Mettler-Toledo (model TG/SDTA 851e). Data was recorded with STAR^e software, and for offline analysis, data was converted into text and imported for analyzed with Universal Analysis software version 4.5A (built 4.5.0.5).

Sample was placed in a little cup made of aluminum hanging from a microbalance. Data obtained from determination in the form of variation of the mass of the sample was plotted to obtain the TG (variation of the mass in function of the temperature) and TGD (derivative of loss of mass versus the time) thermograms. The combination of these two thermograms gives a clear indication of number of stages of the thermal degradation.

II.1.7. Environmental Scanning Electron Microscopy (ESEM)

Environmental scanning electron microscopy (ESEM) was a technique to collect electron micrograph of sample without any preparation. ESEM was done with FEI Quanta 200 FEG system that equipped with an Oxford Inca Energy Dispersive X-ray (EDX) system for elemental analysis. Very minimum sample preparation was done to increase analytical capabilities to inspect actual elemental percentage (i.e. without interference from coating element), type of material porosities and effect of thermal process on biomass without any interference of conventional SEM sample preparation requirement.

ESEM detection was done using configuration under low vacuum of 1.30 mbar with two detectors; secondary electrons detector, (SED, for solid state or morphology detector) and backscattered electrons detector, (BSED, for chemical/elemental composition) with maximum resolution of 2.5nm at 20kV.

In this thesis BSED micrograph was presented because it gives better contrast if compared to SED micrograph.

PART II. CHAP 2.**DIC PRETREATMENT AND PROCESS PROTOCOLS****II.2.1. Material Preparation**

Material preparation steps were done to ensure homogeneous starting materials for all trials as described previously, to meet strict requirement for response surface methodology that need identical starting material for all treatment in block. Treatment steps were done according to the following:

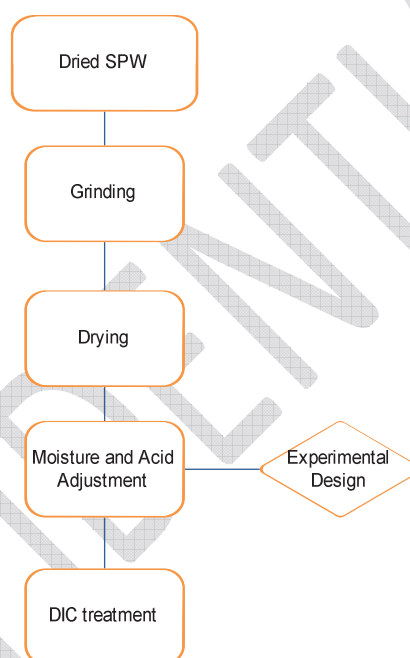
DIC Pretreatment Steps

Figure II-5: Standardized steps taken prior to DIC pretreatment

II.2.1.1. Grinding

Grinding was done only for sample characterization, DIC pretreatment and hydrolysis. SPW is grind to have homogeneous particle size. Grinding operation was done in Retsch Grindomix at 4000 rpm for 30 seconds after first drying operation. Ground materials are kept in airtight plastic bags until used.

II.2.1.2. Drying

SPW materials were dried at 40°C in convection oven for 12 hours and will be used as starting material for all process and trials. In order to ensure that material was having the same moisture level, about 300 grams of material was dried with bed thickness of 2 cm in 40°C in convection oven for another 12 hours.

Moisture content for materials after drying was found to be about 7-8% on dry basis.

II.2.1.3. Simultaneous Moisture and Acid Concentration Adjustment

Moisture adjustment, as part of treatment was done on each material according to the requirement as specified in respective experimental design. The adjustment was done with pre-prepared and carefully calculated sulfuric acid concentration. Moisture and acidity of each material was adjusted with specific sulfuric acid concentration to achieve initial moisture and acid required for the process.

For example, with sample of moisture content 10% db, in each 5 gram sample there were about 0.5 g water, in order to get initial moisture content of 50% db for DIC treatment, final weight of sample will be 6.75 g obtained through adjustment with 0.195 M sulfuric acid to the final weight as calculated. Final acid concentration in the sample will be 0.152 M after taking into consideration initial moisture in the sample.

Adjustment of moisture was done within one to two hour prior to DIC treatment by adding known acid solution and hand mixing for about five minutes. The homogeneity of mixing was checked during process validation stages and was found to be within $\pm 1-2\%$ of required moisture content.

II.2.2. DIC Pretreatment

Material with adjusted moisture content and acid concentrations will be immediately treated within an hour or two after adjustment to avoid any superficial hydrolysis during extended exposure time. Material was placed in an aluminium container in stainless steel holder (Figure II-6(a)) and put into DIC treatment chamber holder (Figure II-6(b)). Sequence of DIC treatment run is based on experimental design presented in respective trials. Stages of DIC pretreatment were presented in Figure I-16 (b) in page 36, previously that also shows changes in steam pressure and temperature inside of DIC reactor during treatment.



Figure II-6: (a) Sample holder and sample container used in this study (b) DIC reactor chamber for thermal pretreatment

Experimental study with DIC system was done for the followings treatments. Detail experimental factors will be presented in respective treatment experimental Paper. Generalized experimental designs for DIC treatment were presented in Paper related to experimental design and response surface. DIC treatments were done for the following study:

- One factor at a time (OFAT) experimental studies

- Vacuum cycle and Initial moisture content experimental studies
- High severity treatment with acid and pressure/ temperature of steam
- Low severity experimental design experimental studies
- High severity experimental design experimental studies
- Preparation of DIC treated materials for dilute acid hydrolysis kinetics with central points from Low severity and High severity experimental design.
- Data logging for temperature cycles.

Data for temperature cycle within DIC treatment was logged with Omega HH147U (Omega, UK) data logger to calculate its heating rate for each combination. Data was plotted and evaluated based on first order heating rate kinetic. Detail of procedure and its study will be presented in Part 3 (refer page 147).

II.2.3. Hot Water Extraction (HWE)

About 500 mg samples are loaded into a glass tube with cap and rubber insert. 10 ml water was added into each tube and tightly capped. All glass tubes were transferred into a hot oil bath previously set at 110°C. Time from addition of water to transfer into the oil bath was less than 5 minutes. Based on initial trial, it takes about 8 minutes (non-isothermal phase) for temperature inside of the glass tube to achieve bath temperature as specified. After 60 minutes (excluding non-isothermal phase) glass tube will be taken out of oil bath and immediately cooled under running water. 2 ml hot water extracts were withdrawn with micropipette into a centrifuge vial, closed and centrifuged at 5000 rpm for 10 minutes. 1 ml of a clear supernatant was carefully transferred into a glass vial for glucose content determination with HPLC. Area corresponding to glucose was obtained, and its concentration in the extracts was calculated with the standard curve. All final concentrations for glucose were reported in milligrams glucose in gram of dry material (*mg Glu/g SPW or mg/g only*) for respective sample.

II.2.3.1. Determination of Hot Water Extractable Glucose

The objective of this study was to determine maximum amount and to estimate minimum time required to extract all glucose in DIC treated materials which form a basis of above method (refer II.2.3 above).

About 500 mg samples are loaded into a glass tube with cap and rubber insert and 10 ml water is added into each tube and loosely capped. All glass tubes are transferred into a hot oil bath previously set at 50, 75 or 110°C. Time from addition of water to transfer into the oil bath was less than 5 minutes. Based on initial trial, it takes about 2, 5 and 8 minutes for temperature inside of a glass tube to achieve respective test bath temperature. Glass tube will be taken out of oil bath and immediately cools under running water at a specific time of 2, 5, 10, 15, 30, 45, 60, 90 and 120 minutes after taking into consideration time for water in the glass tube to achieve bath temperature. 2 ml hot water extracts were withdrawn with micropipette into a centrifuge vial, closed and centrifuged at 5000 rpm for 10 minutes. 1 ml of a clear supernatant was carefully transferred into a glass vial for glucose content determination with HPLC. All final calculation for glucose was reported in milligram glucose

in gram of dry material (*mg Glucose/g*) for respective sample and plotted against time (minutes) to find time when the level-off for glucose concentration and its maximum amount can be obtained.

Based on above hot water extraction study, combination of temperature and time that gives maximum glucose in hot water extract (110°C, 60 minutes) was selected as a standard method for hot water extraction during DIC kinetics study and to identify glucose in all post DIC treatment.

II.2.4. Hydrolysis Process and Kinetic Study

Standard dilute acid hydrolysis kinetic process was employed based on a batch system. Details of system used are discussed in detail in each sub-chapter.

II.2.4.1. Dilute Acid Hydrolysis (DAH) Kinetic

The same methodology was applied for all DIC treated materials for dilute acid hydrolysis (DAH). About 200 mg samples are loaded into a stainless steel tube (as in Figure II-7) with cap and Teflon insert and 10 ml acid solution was added into each tube and tightly capped. All stainless steel tubes were transferred into a hot oil bath previously set at 110, 130 or 150°C. Three acid concentrations were used, 0.01, 0.04 and 0.08 molar.

Based on initial trial, it takes about 6 minutes for temperature inside of a stainless steel tube to achieve respective test bath temperature (non-isothermal phase). Stainless steel tube will be taken out of oil bath and immediately cools under running water at a specific time of 5, 15, 30, 60, 120 and 240 minutes after considering time for water in a stainless steel tube to achieve bath temperature (non-isothermal phase). 2 ml acid hydrolysate were withdrawn with micropipette into a centrifuge vial, closed and centrifuged at 5000 rpm for 10 minutes. 1 ml of a clear supernatant was carefully transferred into a glass vial for glucose content determination with HPLC.



Figure II-7: Stainless steel tubes in hot oil bath for dilute acid hydrolysis

II.2.4.2. Condition for Dilute Acid Hydrolysis and Hot Water Extraction

Sample composition together with homogenous mixing and hydrolysis process were given high attention in DAH and HWE, due to the limitation of the DAH and HWE kinetic reactors (maximum content for DAH and HWE was limited to 0.2 to 0.5 gram per treatment (2% to 5%). This was due to low bulk density of material, i.e. about 0.28 g/cm^3 . SPW DIC was found to be highly water absorbing, and material cubic volume becomes increase in water. Due to that we decided to kept DAH and HWE with solid to water ratio at 2% only. Initial trial shows that if we exceed 5% solid to water ratio, the mixture does not uniformly mix during HWE and settle on top of reactor. Furthermore, with 2% solid ratio, glucose obtained from both hot water extraction and hydrolysis process was ready for injection into HPLC system without any further dilution.

II.2.5. Glucose Degradation Kinetics

Glucose degradation kinetic was used to determine the behavior of glucose degradation under condition used in dilute acid hydrolysis, i.e. acid concentration, temperature and stainless steel tube reactor used in dilute acid hydrolysis process.

Accurately, 10 ml 0.2 molar glucose solution was prepared and placed into each similar stainless steel tube as in hydrolysis reaction. All stainless steel tubes were tightly capped and transferred into hot a oil bath previously set at 110, 130 or 150°C . Three acid concentrations were used, 0.01, 0.04 and 0.08 molar. Stainless steel tube will be taken out of oil bath and immediately cools under running water at a specific time of 5, 15, 30, 60, 120 and 240 minutes after considering non-isothermal time.

2 ml acid hydrolysate were withdrawn with micropipette into a centrifuge vial, closed and centrifuged at 5000 rpm for 10 minutes. 1 ml of a clear supernatant was carefully transferred into a glass vial for glucose content determination with HPLC system as described previously.

PART III. RESULTS

Result obtained from experiments was divided into four chapters with summary title and its content as follows:

Chapter 1: Exploratory Study (Background Study, Development of Process and Procedures)

- Paper 1: (i) One Factor At a Time and (ii) High Severity DIC Treatment
- Paper 2: DIC Vacuum Cycle Study

Chapter 2: DIC Process Optimization by RSM and Kinetic Modeling

- Paper 3: Low DIC Severity Process
- Paper 4: High DIC Severity Process

Chapter 3: Dilute Acid Hydrolysis Kinetic Model and RSM Studies

- Paper 5: Dilute Acid Hydrolysis Kinetics Study
- Paper 6: Glucose Degradation Study

Chapter 4: Hydrolytic Behavior of Non-isothermal State in DIC and DAH Process

- Paper 7: The influence of non-isothermal state on the conversion of starch in both DIC and DAH processes.

PART III. CHAP 1.**EXPLORATORY STUDY (BACKGROUND STUDY, DEVELOPMENT OF PROCESS AND PROCEDURES)**

Paper 1: (i) Exploratory trial to establish DIC pretreatment parameters for autohydrolysis of crude starch based on OFAT.

(ii) DIC pretreatment with extended treatment parameters.

Abstract

Two exploratory trials were conducted to establish the level of experimental factors prior to the full experimental design for crude starch materials. Five experimental factors were identified: treatment time, initial moisture content of materials, acid concentration in materials, pressure/ temperature of treatment and cycle of vacuum during DIC treatment. In this work, four experimental factors excluding cycle of vacuum were combined in one factor at a time (OFAT) and in the kinetic study to find the limit of associated factors towards yield of glucose. OFAT studies give a treatment combination of 325% moisture, 19 minutes treatment time and 1.18 molar acid concentrations. Consecutive confirmation with suggested combination shows very high glucose degradation occurs during DIC treatment. In an extended DIC pretreatment factors level study using autohydrolysis conversion based on kinetic studies, only 3.5 minutes was required to fully hydrolyzed polysaccharides in crude starch materials. Further evaluation of results suggested that 150% initial moisture level was suitable for further evaluation using full experimental design studies.

III.1.1. Introduction

Optimization of a process usually starts with screening of the treatment parameters, testing of models and setting of level of parameters. In initial work using pure cellulose materials [18, 155], we have made process optimization study for pure cellulose material conversion using a two stage process. However, due to huge difference in material composition as well as properties; similar optimization condition was not applicable for biomass with high crude starch content such as SPW. Another exploratory trial was conducted to study all factors related to DIC treatment parameters such as steam pressure, treatment time, initial moisture content in materials, and acid concentration level in material.

As suggested by most work related to DIC treatment, factors such as moisture level of material and the use of vacuum during initial and at the end of treatment are very important parameters [3, 118, 119] and were maintained in present work. Further work to investigate the importance of initial moisture content and vacuum cycle in DIC treatment will be presented in the following chapter. This exploratory study combines two studies:

- Initially, one set of OFAT study was done with single factor variable (Table III-1).
- The next trial was to study the treatment kinetics at extreme pressure, treatment time and between low acid against extreme acid condition (Table III-2).

OFAT study was very important in order to understand the possible effect of single treatment factors even though it may not give much information as in fully experimental

design studies. Information from the extreme condition is important to understand the overall effect of thermal treatment on yield of glucose and its degradations.

III.1.2. Materials and Methods

III.1.2.1. Chemicals and Materials

All chemicals used in this study were of analytical grades and was used as it is. Sulphuric acid 98%, glucose, levulinic acid, acetic acid and formic acid were obtained from Sigma Aldrich. Deionised water was prepared by the laboratory water system [Purelab Option-Q, ELGA]. Materials of known polysaccharide's content were use in this work was analyzed, and its results were reported below. SPW which contains high polysaccharides in terms of starch, and cellulose was selected for this study. Particle size and composition of material were represented in the following bar chart (Figure III-2). A similar composition result was reported much earlier [83, 156] as in Table I-6, Table I-7 and Table I-8 in page 27 and 28.

III.1.2.2. Trial 1: One Factor at a Time Study

Fourteen experimental treatments were conducted based on one factor at a time (OFAT) study. Each treatment was done on 5 grams material based on the parameter combination in Table III-1. Adjustment of acid concentration and moisture content were done simultaneously with known sulfuric acid solution according to procedure in page 67. Final moisture and acid concentration level in material were according to the OFAT design in Table III-1. Final accounts for all treatments and calculations are based on the dry basis of materials. Immediately, after treatment, sample was carefully collected and dried at 40°C for 12 hours followed by grind for 30 seconds at 4000 rpm. Ground materials were kept in a zip lock polyethylene bag and stored at room temperature until analyzed. Moisture content was determined according to the previously stated procedure in section II.1.2.1 in page 58.

Hot water extractions (HWE) were done on 500 milligrams of ground materials from each sample in a glass tube with 10 ml distilled water and heated in oil bath at 100°C for 60 minutes with shaking. Hot water extract was diluted and injected into HPLC system together with glucose standard determination. Solid residues of hot water extraction were collected for total glucose determination according to total polysaccharide's procedure in page 60.

Table III-1: OFAT study factors and level combinations and result of trials

Moisture	Temperature	Acid	time	Glucose mg/g
50	143.63	0.2	10	67.69
100				108.45
150				166.91
200				165.83
148	133.54	0.2	10	92.63
	143.63			166.91
	151.85			258.29
	161.99			298.01
148	143.63	0.1	10	17.00
		0.2		166.91
		0.3		196.66
148	143.63	0.2	5	83.92
			10	166.91
			15	163.23

III.1.2.3. Trial 2: DIC Treatment at High Temperature with 0, 0.75, and 1.25 Molar Acids

Upon analysis of OFAT data, DIC treatment based on experimental kinetic based on time was developed to find a favorable treatment condition for all treatment factors: acid concentration, treatment time and temperature. Initial moisture content of 150% was selected based on initial trials of vacuum cycle and moisture content effect on glucose yield (in page 84). Materials were prepared in similar ways as in OFAT study.

Table III-2: DIC treatment at high temperature and acid combination (0, 0.75, and 1.25 molar sulfuric acid) with results.

DIC treatment time (min)	Acid (molar)		
	Result – Glucose in mg/ g		
	0.0 molar	0.75 molar	1.25 molar
0.5	94.52	342.34	257.24
3	13.49	669.64	744.44
5	10.75	763.83	845.89
20	13.82	443.19	96.13
40	12.50	50.76	34.92

Fifteen DIC treatments with 10 grams samples were done in a round aluminum sample container with a dimension of 7 cm x 5 cm. Initial moisture content for sample was set at 150%. Moisture and acid concentration were achieved through adjustment at different acid concentration until desired treatment combinations were obtained. Sample were placed in a loosen form to ensure good contact with saturated steam during DIC pretreatment.

DIC pretreatments were done according to condition as stated in Table III-2. Treated samples were dried and prepared for HPLC analysis in similar hot water extraction procedure as stated in OFAT study.

III.1.2.4. DIC Pretreatment

Material that was adjusted its moisture content and acid concentrations will be treated within one to two hour of acid-moisture adjustment to avoid any superficial hydrolysis not related to DIC treatment during extended exposure time. Material was placed in respective container and put into the DIC treatment chamber (Figure III-1(a)). Sequences of DIC treatment runs were randomly based on experimental design presented in Table III-1 and Table III-2. Stages of DIC pretreatments were presented in Figure III 2(b), that also shows changes in steam pressure and temperature inside of treatment reactor.

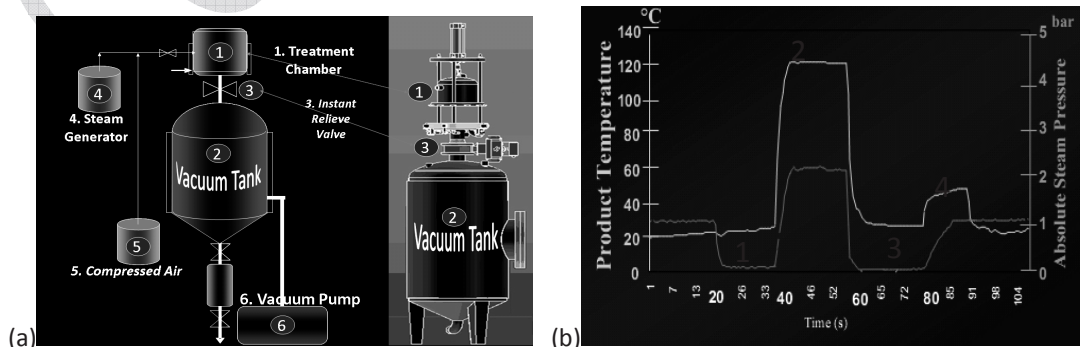


Figure III-1: (a) Schematic diagram of DIC equipments with important service equipments. (b) Four stages of DIC treatment including (1) setting-up an initial vacuum (2) injection of high steam pressure and maintain pressure (3) an instant pressure drop towards vacuum, and (4) putting back to atmospheric pressure condition.

III.1.3.Result and Discussion

In general, Figure III-2(a) shows the distribution and composition of materials under study. Particle size distribution of materials was almost homogenously distributed within 600 μm to 4,000 μm range, while the composition of total polysaccharides (including starch, hemicelluloses and cellulose) was approximately 70 to 75% as in Figure III-2(b). Glucose yield obtained in the hot water extracts of DIC treated SPW for Trial 1 and Trial 2 were presented in Table III-1 and Table III-2 respectively. Moisture content of raw materials at different treatment condition is presented in Table III-3.

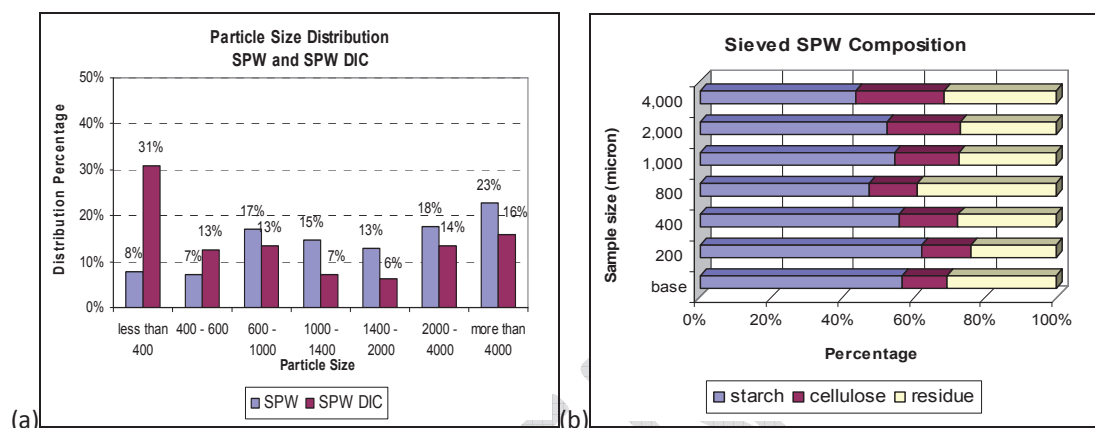


Figure III-2: Plot (a) particle size distribution (SPW raw and SPW DIC) and Plot (b) composition of total polysaccharides for raw SPW. Total polysaccharides (starch, hemicellulose and cellulose) and residues were in percentage of dry material. Composition of total polysaccharides for different DIC severity will be determined separately to represent it as A_0 for it will be affected by the particle size distribution obtained after each DIC pretreatment.

Table III-3: Moisture content of SPW after sun drying and oven drying.

Moisture content stage	Moisture value in % (db)	Notes
Final washing stage, after screw press.	> 500%	Maximum and minimum values obtained from 5 determinations with MA 30 at 105°C until constant weight (approximate for 30 minutes).
After 2 days (18 hours) drying under sun, % db	183% - 200% Average: 192.0 \pm 0.6%	Maximum and minimum values obtained from 10 determinations with MA 30 at 105°C until constant weight (approximate for 30 minutes).
After 12 hours drying, convection oven at 40°C, % db	9.0% - 10.0% Average: 9.5 \pm 0.2%	Maximum and minimum values obtained from 10 determinations with MA 30 at 105°C for 5 minutes.

Figure III-2(a) shows the particle size distribution of raw SPW and DIC treated SPW (condition of treatment was using high DIC severity central points, i.e. pressure: 0.55 MPa, acid: 0.13 molar and time: 6.5 minutes). DIC treatment was found to increase the percentage of low particle size materials. Raw SPW containing 60% particle size of 2000 microns and below with almost similar distribution; however, after DIC treatment, percentage of particle size below than 400 microns was increased by more than 20% to a total 31%, and particle size of 2000 micron and below was increased to 70%. This was due to the decrease in size for the other particle. The decrease in size of DIC treated material was expected due to thermal effect contributed by DIC as well as due to subtraction of material surface as affected by acidic condition; and has resulted to lower overall size of particles. Material was not ground for this measurement.

Result presented in Figure III-2(b) was almost similar to result as presented by earlier researchers [83, 156]; with some percentage difference undoubtedly was due to the different extraction efficiency during sago extraction stage. Total potential polysaccharide

for SPW was almost similar as presented in previous article [83, 156]. Term of total polysaccharides for both materials refers to summation of starch, cellulose and hemicelluloses found in SPW material. Content of starch was about 60 to 70% of total SPW, while cellulose was about 15 to 20% and lignin was about 10 to 15%.

Hemicelluloses fraction was very small and only detected with existence of five carbon xylose component in a chromatogram for raw and DIC treated SPW. Other important observations of the existence of hemicelluloses were the presence of acetic acid in hot water extract after thermal treatment. This was due to the hydrolysis on the acetyl group presence in hemicelluloses. Quantitative determination of the overall hemicelluloses amount was not done due to very small amount and for potentially merging of six carbon sugars of hemicelluloses (such as glucose and galactose) into peak area of glucose.

Result from other research groups supports above finding, such as in Table I-7 reported amount of total hemicelluloses was about 1.2% [79], which was considerably very small to affect overall total polysaccharides coming from starch and cellulose source. In the rest of article, term total polysaccharides will include hemicelluloses due to no separate quantitative study was done here.

III.1.3.1. Result Trial 1: One factor at a Time (OFAT) Study

Four plots based on result in Table III-1 were created with glucose concentration against: time, moisture content, acid concentration and temperature. Kinetic model was developed to describe the result obtained based on consecutive first order kinetic except for the study of temperature. Based on Table III-1 and plots from Figure III-3(a) and (b) together with Figure III-4(a), yield of glucose were analyzed and transformed into plot log natural against respective X abscissa for fitting into suitable kinetic model. Data was found to fit the first order kinetic plot for each abscissa, X: time, moisture and acid concentration. Correlation coefficient, R^2 obtained from log natural glucose concentration (Y) against ordinate X give straight line with value close to 1, which shows highly correlation of experimental data and respective models (time, moisture and acid concentration) for the first order kinetic.

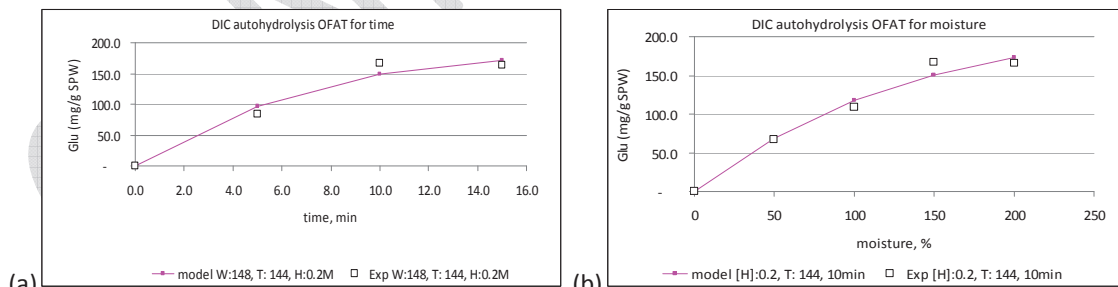


Figure III-3: Result Glucose concentration with X abscissa: (a) time, and (b) moisture content.

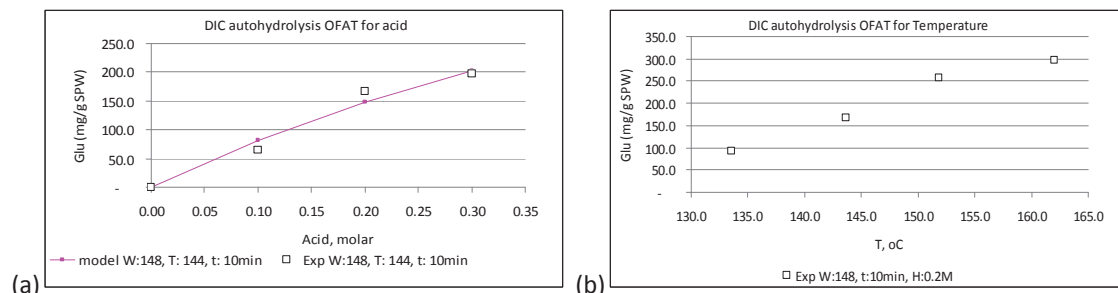


Figure III-4: Result Glucose concentration at X abscissa: (a) acid concentration and (b) temperature.

Data for temperature was not fitted to the first order kinetic model due to very limited data point for glucose yield at temperature below than 100°C. However, it was known that for treatment below 100°C will only produce starch colloid due to incomplete gelatinization in water and without tangible conversion of starch into glucose at temperature below 100°C.

Based on above information, rate constant for first order kinetic for glucose generation and glucose degradation was calculated and presented in Table III-4. Initial moisture content (as a reaction factor, was produced relatively lowest value of rate constant for both k_1 and k_2 if compared to treatment time and acid concentration. Value of relative rate constant (k_1/k_2) of glucose generation (k_1) and glucose degradation (k_2) as affected by the reaction factor of initial moisture content and treatment time was lower than 1 ($k_1/k_2 < 1$) while for acid concentration was more than 1 ($k_1/k_2 > 1$). Detail explanation on representative for different value of k_1/k_2 was presented in literature review for value < 1 , 1 and 2 (refer to Figure I-20, page 45). Based on this finding, as presented in Table III-4, with $k_1/k_2 < 1$ for reaction factors of moisture and time, it is expected that glucose degradation is higher than glucose generation. So with longer treatment time or higher moisture content or combination of both it is expected to have higher glucose degradation as well.

Table III-4: Rate constant k_1 and k_2 together with other data for respective factors at maximum glucose amount

Kinetic Data	moisture	time	acid
A_0	600	600	600
k_1	2.6699×10^{-3}	42.5424×10^{-3}	1497.8134×10^{-3}
k_2	3.5103×10^{-3}	65.4861×10^{-3}	415.9418×10^{-3}
k_1/k_2	0.76	0.65	3.60
Glucose maximum at:	325.6 %	18.8 min	1.18 molar
Unit k_1 and k_2	percent ⁻¹	min ⁻¹	molar ⁻¹

Based on the above result in Table III-4, and the possibility for complete hydrolysis of polysaccharides with DIC system, the possible combination for good treatment was recalculated using the same model that was obtained. This estimation was done by adjustment of acid concentration, moisture and time to get value of residue (as lignin) as close to value 40.0% (equivalent to 400 mg/g) for respective model. Numerical solution for this calculation was based on kinetic model review (in page 42) and presented in Table III-5.

Kinetic model based on numerical solutions from *Equations 7, 13, 14, 15 and 16* were used to make estimate respective moisture, time and acid. From OFAT experiments, level of factors that contribute for maximum yield of glucose were identified and estimated.

As shown in Table III-4, the maximum yield of glucose is estimated to occur at moisture content of 325.6%, whereby for duration of treatment it was estimated at treatment time of about 18.8 minutes. For acid concentration, the maximum glucose yield is estimated to require 1.18 molar concentration of sulfuric acid.

These combinations of level of factors were further tested on DIC pretreatment process in order to verify whether this combination is sufficient enough to produce a maximum glucose. From our observation, using this level of factors tend to produce less than 100 mg/g glucose and apart from that significant amount of glucose degradation products were also detected by HPLC.

Mass balance for respective treatment based on three kinetic models were summarized and used to estimate the value of glucose generated, glucose degraded and remaining polysaccharides available during optimum glucose value. Using the similar way after

obtaining glucose maximum value, it was possible to estimate the residual of remaining polysaccharides in materials. Since value of A_0 can be used to estimate the severity of treatment required, the potential of using the same material for another DIC treatment cycle is possible with treatment at much lower severity combination. Data for mass balance based on the kinetic model for moisture, treatment time and acid were summarized in Table III-5.

Table III-5: Information on mass balance of SPW at maximum amount glucose amount can be obtained from process using model in Figure P3-1-3a), 4b) and Figure P3-1-4a).

	Moisture, W	Time, t	Acid, [H+]
	mg/ g SPW	mg/ g SPW	mg/ g SPW
A_0 (=1+2+3), as total polysaccharides	600	600	600
Estimated Glucose when W, t or [H+] at Glucose max ^[note 1]	191	175	367
Estimated total Glucose degradation when W, t or [H+] at Glucose max ^[note 1]	157	155	131
Non hydrolyzed total polysaccharides at Glucose max ^[note 1]	252	270	103
Lignin and non polysaccharides residues	400	400	400

[note 1] – refer to Equation 16 in kinetic expression in page 44.

Information as obtained from OFAT experiments without subjected to kinetic model, however, shows some important information for the direction of a crude starch optimization process. Glucose in hot water extracts for initial moisture content and treatment time were observed to level-off at moisture content of 150% in Figure III-3(a) and 10 minute treatment time Figure III-3(b) respectively. Higher acid and treatment temperature however were observed to give higher glucose yield as Figure III-4(a) and (b).

Based on that information and verification study as above (time about 18.8 min, acid 1.18 and moisture 325%), another set of trial at higher level of treatment factors were chosen, acid concentration was fixed at 0, 0.75 and 1.25 molar to study the potential of glucose degradation that occurs at a higher temperatures as described in the previous study [155]. Initial moisture content 150% and treatment time to a maximum 40 minutes was chosen for another combination factors.

III.1.3.2. Result Trial 2: DIC Treatment at High Temperature and Acid Concentration (0, 0.75, and 1.25 molar sulfuric acid)

Another consecutive first order kinetic model was developed from an experimental result in Table III-2 in order to understand the relationship between autohydrolysis action for all three factors involved. In the earlier model kinetics based on treatment time, acid concentration and moisture content, it was clearly understood that an increase in each factor will increase yield of glucose. However when all OFAT factors at the maximum glucose was combined together into single DIC pretreatment combination, glucose yield was very low with very high glucose degradation. That study does not show the direction on how to minimize glucose degradation and to maximize glucose yield.

The main interest to continue the study at the extreme level of treatment was to investigate the range of potential optimum condition for all three treatment factors (time, steam pressure/temperature, initial moisture level and acid concentration) and to maximize starch conversion to glucose in single step of DIC treatment.

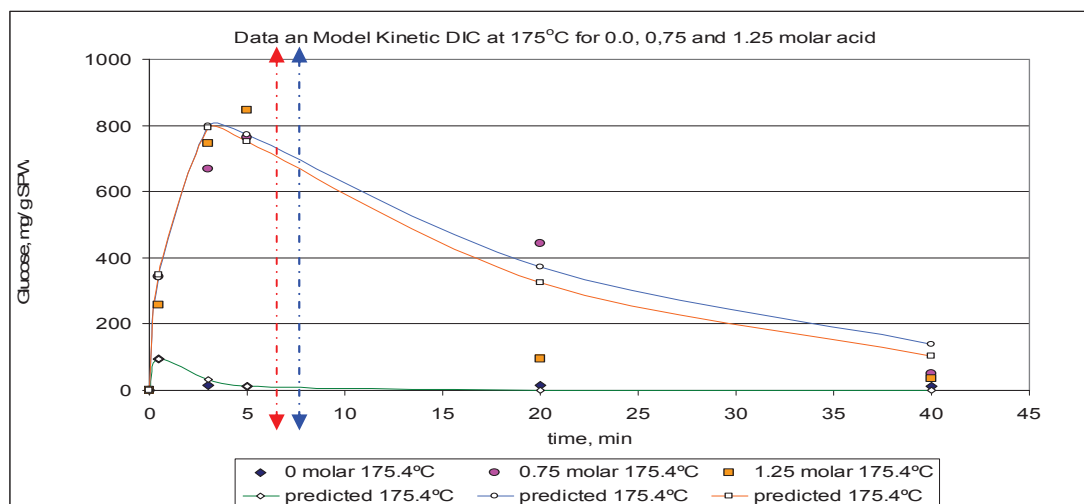


Figure III-5: Experimental data and model kinetics for extreme DIC treatment conditions.

Under DIC pretreatment, the total conversions of polysaccharides into glucose are time dependent as shown in Figure III-5. Within the first two minutes, a significant amount of glucose formed was from the hydrolysis of starch and hemicelluloses components, as indicates by the red line in Figure III-5. About 600 mg/g polysaccharides from starch and hemicelluloses was fully hydrolyzed within 2 minutes of DIC treatment with acid concentration 0.75 and 1.25 molar respectively. Hemicelluloses were included due to treatment condition was favorable to solubilise hemicelluloses at 175°C.

Prolonged hydrolysis to more than three minutes increased further the accumulation of glucose, which may suggest that it is due to the hydrolysis of cellulosic component in SPW. Cellulose composition (about 200 mg/g) was the only polysaccharides portion available for further autohydrolysis reactions. It was also shown the maximum possible glucose amount of about 800 mg/g were obtained at 3.41 minutes and 3.18 minutes for acid concentration 0.75 and 1.25 molar respectively (as represented by blue line in Figure III-5).

Further analysis with Total Polysaccharides procedure (refer to II.1.3.3 in page 60) shows solid residues after HWE for DIC treated sample at 3 and 5 minutes shows only traces of glucose was still available. This indicates that solid residues from both conditions were undergone almost complete hydrolytic conversion to glucose during DIC treatment.

Degradation from DIC treatment after glucose reach maximum concentration was enormous, with rate constant (k_2) of 0.0496 and 0.0569 min^{-1} for 0.75 and 1.25 molar acids respectively in Table III-6. This indicates that degradation rate was increasing with the increase in acid concentration. The increase in acid concentration was reported to decrease the yield of glucose due to degradation. Several studies show that degradation of glucose was following first order kinetic with regards to acid concentration [128, 157]. An increase in acid concentration will increase its rate constant for degradation. Mechanism for glucose degradation into several products was presented in Figure I-19 in page 41.

Figure III-5 also indicates that for DIC treated sample with no acid added but at a much higher pressure could produce nearly 95 mg glucose within short treatment time. In another work of the previous researcher also shows that at lower treatment severity restricts the autohydrolysis of starch to glucose [10]. Prolonged DIC treatment time, however, does not increase the amount further due to glucose degradation. Based on our earlier study on glucose degradation (reaction condition: $[\text{H}^+]$: 0.01 molar, T: 150°C) (refer to Figure III-44(a)),

we found that less than 1% glucose was degraded within 5 minutes and increased to about 3% in 30 minutes. Prolonged treatment between 30 to 60 minutes, about 6% glucose was degraded (refer to Figure III-44 page 142). This information is vital for the development of optimize DIC autohydrolysis and dilute acid hydrolysis. Based on this information, it can be deduced that short treatment time was critical to minimize glucose degradation.

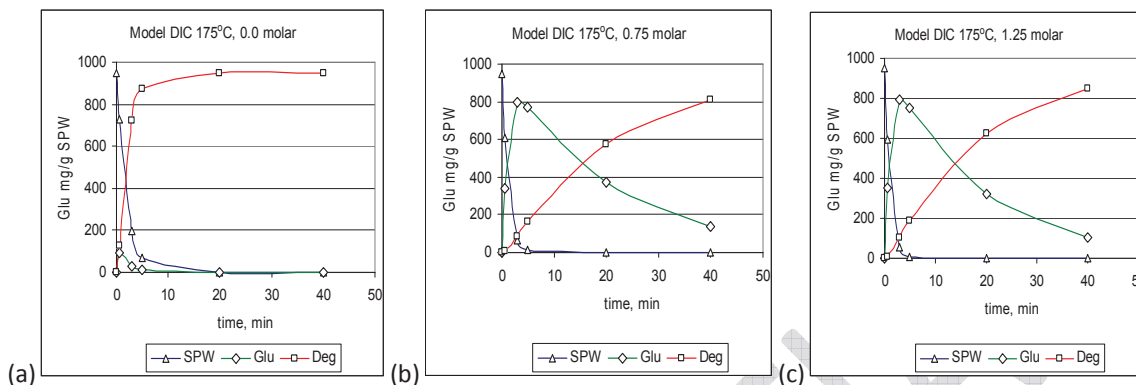


Figure III-6: Model autohydrolysis kinetics for DIC treatment with (a) 0, (b) 0.75 and (c) 1.25 molar acid respectively.

However, in this DIC treated sample (reaction condition: $[H^+]$: 0 molar, 175°C), the rate of degradation was very high as shown in Table III-6 (with k_2 : 3.833 min^{-1}) and its model in Figure III-6(a). In actual observation, evidently an intact starch and cellulosic fibers component still remain in the treatment reactor. This can be attributed to the existence of a fraction of resistance starch in crude starch that able to withstand high temperature and pressure difference due to DIC. Representative of ESEM micrographs for resistance starch remaining after DIC treatments were presented in Figure III-33 in page 119.

The HPLC chromatogram for that particular treatment combination ($[H^+]$: 0 molar, 175°C) shows the existence of oligosaccharides with a very small amount of glucose.

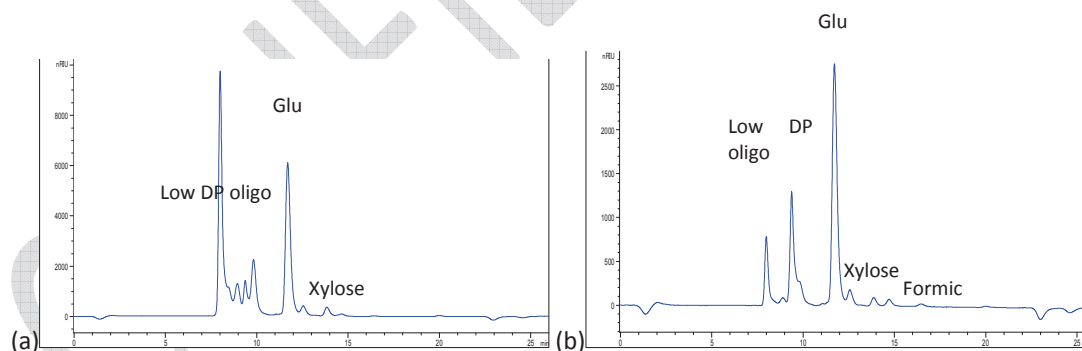


Figure III-7: (a) Typical HPLC chromatogram for SPW with low DIC severity, with the existence of various low degree of polymerization of oligosaccharides, (b) Typical HPLC chromatogram for SPW with high DIC severity (solution was diluted), low degree of polymerization of oligosaccharides has been reduced with an increase in glucose amount, together with noticeable existence of formic acid and several degradation products, mobile phase 0.4 ml/min. was used due to deterioration of molecule separation and to operate below 70 bar pressure specification for HPLC column.

In Figure III-7 shows, the existence of formic acid as one of the glucose degradation products as explained in Figure I-19 earlier. Formic acid exists as a by-product of consecutive degradation of glucose into HMF and levulinic acid. Levulinic was observed as a dominant degradation product at high acid and temperature reaction, similar to finding of previous workers [98, 125, 158]. Xylose was found to exist as a dominant hemicelluloses component in all reactions [98, 159].

An important process indicator between starch hydrolysis and glucose degradation was the relative rate constant or rate constant ratio (k_1/k_2) need to be very high possible (refer to Table III-4 and Table III-6) as explained before in review about kinetic model. High value of rate constant ratio shows the rate of starch hydrolysis was bigger than rate of glucose degradation due to large formation of glucose. Relatively, k_1/k_2 for treatment at 0.75 molar and 1.25 molar was found to be very close to each other (for 0.75 molar: 18.08, and 1.25 molar: 16.47). This was further supported that the time to achieve maximum glucose ($t_{\text{Glu}_{\text{max}}}$) was about 3.41 minute and 3.18 minute respectively as presented in Figure III-6(b) and (c). Another important indicator was that half-life of glucose generation must be shorter than half-life of glucose degradation (i.e. value of $t_{1/2k_1} < t_{1/2k_2}$) in order to ensure glucose generation is much faster than its degradation. For a treatment that was conducted in a certain range of temperature, its activation energy can be calculated. Determination of activation energy (E_a) will also show energy required to initiate a process. Preferable condition for activation energy of glucose generation was the lowest possible against the highest possible activation energy for glucose degradation.

Maximum glucose amount for both conditions (0.75 molar and 1.25 molar acids) was about 800 mg/g. This finding suggests that lower acid concentration was sufficient enough to almost deplete total polysaccharides available in SPW. However further investigations were required for optimization of glucose yield in the form of complete experimental design that combined all treatment factors: time, acid, moisture and steam pressure/ temperature.

Table III-6: Characteristics of DIC treatment for rate constant (k_1 and k_2), rate constant ratio (k_1/k_2), time for maximum glucose, half life, time for total polysaccharides to depleted and ten half life as indicator for infinity time for the process.

Kinetic data	175.4 °C	175.4 °C	175.4 °C
	0 molar	0.75 molar	1.25 molar
A_0 (mg/ g SPW)	900	900	900
k_1 (min^{-1})	529.9795×10^{-3}	897.7688×10^{-3}	937.4874×10^{-3}
k_2 (min^{-1})	3833.4399×10^{-3}	49.6524×10^{-3}	56.9048×10^{-3}
k_1/k_2	0.14	18.08	16.47
$t_{\text{Glu}_{\text{max}}}$ (min)	0.60	3.41	3.18
half life data			
k_1 half life (min)	1.31	0.77	0.74
k_2 half life (min)	0.18	13.96	12.18
Will deplete in cycle	$0.46^{\text{note 1}}$	$4.42^{\text{note 2}}$	$4.30^{\text{note 3}}$
10 half life ^{note 4}			
k_1 (10 half life) (hr)	0.22	0.13	0.12
k_2 (10 half life) (hr)	0.03	2.33	2.03

- Note: ^{note 1} – less than one cycle
- For ^{note 2} and ^{note 3} – all polysaccharides will be depleted in 4.42 and 4.3 cycles respectively
- For ^{note 4} – ten (10) half life is taken as maximum time for kinetic operation, when reaction can be considered complete, i.e. after a ten half-lives, a first-order reaction is normally $(1 - 0.5^{10})$ or 99.9% complete.

Heat transfer for this operation was very fast as presentment in page 147, due to the initial vacuum stage that removes thin air film from the surface of material to enable immediate heating of moisture on the surface of material towards steam temperature and increase the energy of proton ion $[H^+]$ to initiate the autohydrolysis process of starch, cellulose and

hemicelluloses. It was observed that the existence of acetic acid (coming from acetyl group in hemicelluloses) in its chromatogram, similar to most DIC treated samples. The existence of acetic acid was also contributing to the autohydrolysis of polysaccharides into glucose [158].

The hydrolysis of glycosidic bonds in starch and cellulose usually follows first order reaction. Mechanisms for hydrolysis into glucose and its degradation were presented in Figure I-18 and Figure I-19 respectively. Identification of kinetic order was to show that substrate will play the role for the determination of rate, i.e. substrate is the rate determining factor. Upon obtaining that information, it was very important to analyze total polysaccharide's composition (reference as A_0 with unit of mg/ g) for a representative of overall kinetic study.

Different A_0 values were used in this study to reflect the severity of the respective process. In OFAT study at low DIC severity factors, A_0 value of 600 mg/g was used to suggest the potential glucose was from starch portion only. In a higher DIC severity, A_0 value of 900 mg/g was used to include cellulose in total polysaccharides available for the autohydrolysis reaction as presented in Figure III-6.

Grinding of dried SPW DIC treated materials for 30 seconds at 4000 rpm was relatively much easier than to the similar amount of raw SPW materials. Majority of particle of ground DIC SPW treated material was found to be less than 600 microns as presented earlier in Figure III-2(a) (i.e. nearly 45%), which will offer very high surface area for hot water extraction process as an added advantage. With high surface area and moisture absorbing behavior, DIC treated SPW ground materials were found to become like sticky-dough after short exposure to room condition (room RH was about 70%). Moisture content of dough-like material upon prolonged exposure was nearly 70-80% compared to the untreated dried materials of about 7 to 10%. This suggests the treatment was able to convert SPW materials to become a highly hygroscopic material due to reaction towards the surface of materials and promotes the ability of DIC treated materials to hold a high amount of water.

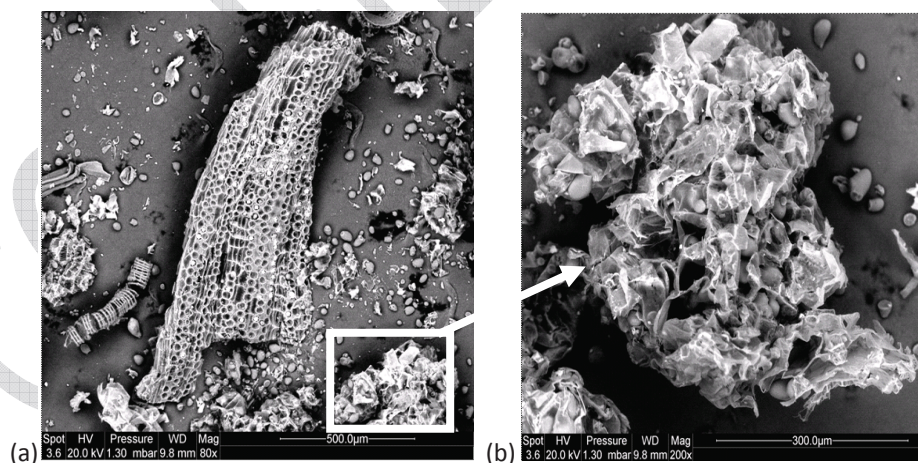


Figure III-8: ESEM micrograph of raw SPW materials.

Further inspection through ESEM micrograph, it was found that surface of DIC treated materials was very rich in disoriented micro structure of biomass material. This observation was supported by previous work that DIC treatment could create porous and expanded material within short treatment time [3, 118]. Several researchers in biomass materials also suggested that surface of thermal treated biomass material was very rich in hydroxyl (-OH) functional groups and very reactive to absorb moisture from its surroundings [160]. This was further evidenced by the wettability of DIC treated materials. High water and moisture

absorption of the cellulose fiber causes swelling and plasticizing effects, resulting in dimensional instability and poor mechanical properties, which were a character of biomass after thermal treatment [60].

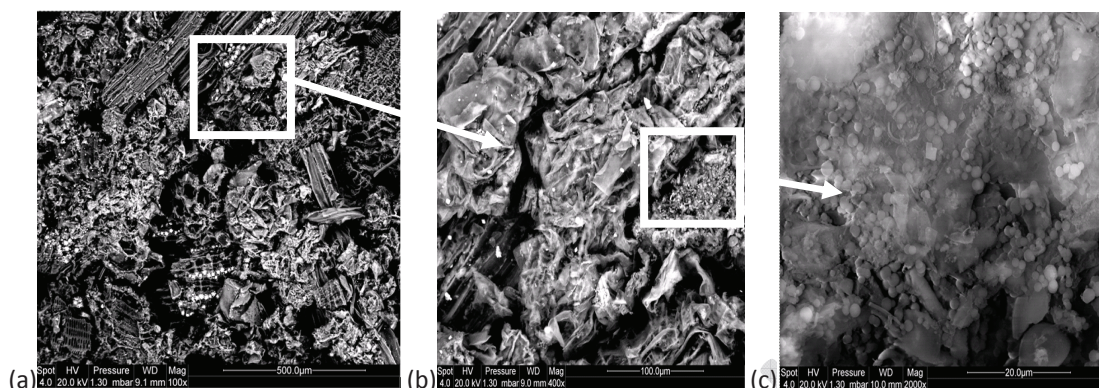


Figure III-9: ESEM micrograph of SPW DIC treated materials.

In Figure III-8 and Figure III-9 show the difference in material composition of raw SPW and SPW DIC materials. Figure III-8 (a) and (b) shows the availability of starch granules within the parenchymatic tissue. In Figure III-9 (a-c) shows the existence of new granular materials, presumably as lignin being deposited on surface of cellular materials upon exposure of SPW to high temperature.

III.1.4. Conclusion

Based on results from these exploratory trials, it can be concluded that hydrolysis of the total polysaccharides in crude starch materials follow consecutive first order kinetic reactions against treatment time, initial moisture content and acid concentrations. A_0 value for autohydrolysis process determines the rate of reaction for the process. High severity process will be represented by a high A_0 value and high rate constant k_1 . With the information on A_0 value, the severity of DIC treatment can be adjusted according to the ultimate requirement of the process: i.e. to minimize glucose degradation while optimize glucose yield.

It was possible, by using DIC pretreatment alone to do nearly a full conversion of polysaccharide in SPW into glucose within 3.5 minutes treatment time. The prolonged DIC treatment either with time, acid concentration or moisture content was found to increase the conversion of available glucose into its degradation products, as evidence by the chromatogram of HPLC.

Paper 2: Exploratory trial to establish DIC treatment cycles and moisture content level for treatment of Crude Sago Starch

Abstract

In this exploratory trial, two DIC treatment factors were studied: initial moisture content of material (as X1) and vacuum cycles in DIC treatment. Vacuum cycles were further separated into two separate cycles of first cycle vacuum (as X2) and second vacuum cycle vacuum (as X3). Moisture content was adjusted to be in the range of 25% to 200% on a dry basis. Data obtained was analyzed using full factorial design for two levels with three factors. A total of eight factorial design combinations were tested in this study and only one was found to have statistical significance on selected response. Yield of glucose was an important response in this study, materials with initial moisture content of $\leq 100\%$ was found to give yield less than 100 mg/g, whereas material with moisture content of $\geq 150\%$ was found to give glucose yield of more than 200 mg/g. During DIC treatment, application of no vacuum at second vacuum cycle (X3:-1) enhance glucose degradation if compared to with the presence of a second vacuum cycle (X3:+1). Based on response surface result, optimization study for crude starch materials favors the treatment with moisture content of 150%. Both vacuum cycles (i.e with: X2:+1 and X3:+1) during DIC treatment will be used throughout the other research work as it was found to give the highest yield in this study.

III.1.5.Introduction

Another set of exploratory study for DIC vacuum cycle and moisture effect were decided upon results from OFAT (III.1.3.1 in page 76) and result of extreme DIC treatment combination kinetic was obtained (III.1.3.2 in page 78). In this exploratory trial, experimental design based on 2^3 full factorial designs were used to eliminate three DIC treatment combinations. In DIC treatment, there are four treatment combination was possible: vacuum-steam-vacuum (V-S-V), no vacuum-steam-vacuum (NV-S-V), vacuum-steam-no vacuum (V-S-NV) and no vacuum-steam-no vacuum (NV-S-NV). It was important to eliminate three possible vacuum combinations and only concentrate on one combination only in this exploratory study in order to intensify our research objective during actual optimization work. Acid concentration was fixed at 0.2 molar for all treatments based on from previous exploratory experiments and our work on pure cellulosic materials [18, 155] and from results in extreme DIC treatment combination kinetic (section III.1.3.2 in page 78). Known amount of SPW was premixed with sulfuric acid solution to obtain final acid concentration of 0.2 molar in materials with respect to required moisture level (X1) as presented in Table III-7.

Final moisture content was adjusted after considering the existing moisture content of material as detailed in procedure for simultaneous acid and moisture adjustment in section II.2.1.3 in page 67.

III.1.6.Experimental Design

In order to understand the effect of moisture level and different vacuum configuration utilize in this study, response surface models were developed. Effects of 1st and 2nd vacuum

on glucose yield were presented. DIC cycle generally consist of several steps as presented in Figure I-16 and detailed as follows: (i) input of material into reactor, (ii) treatment with first vacuum cycle, (iii) injection of steam for specified treatment time, (iv) followed by second vacuum cycle treatment and (v) relief to atmospheric pressure for collecting the material. The isolation and study of effect for both first vacuum and second vacuum at high and low factor level for was the interest of this exploratory study.

Eight full factorial 2^3 design combinations were developed to study interaction effect contributed by both vacuum and moisture level. The design will analyze a stepwise increase of 25%, 50% and 100% in moisture content against DIC treatment for glucose concentration.

This work also was very important to differentiate DIC thermal pretreatment from existing thermal pretreatment, such as steam explosion that released biomass under high steam pressure towards atmospheric pressure to disintegrate biomass into fibers. Two levels, three factor (2^3) full factorial design with eight runs for each factorial design was employed for this screening study. Factor level for vacuum was set at high or low, with high level was with vacuum at 100 millibars and low level was with atmospheric pressure. DIC treatment factors were coded as X1: moisture content, as X2: vacuum cycle 1 and as X3: for vacuum cycle 2.

The quadratic model for predicting the optimal treatment condition was expressed as in Equation 24:

$$Glu = a_o + \sum a_i x_i + \sum a_{ii} x_i^2 + \sum a_{ij} x_i x_j \quad - \text{Equation 24}$$

With $x_i = X1, X2$ or $X3$, $x_j = X1, X2$ or $X3$ and $x_i \neq x_j$

Glu is the predicted response, a_o is the intercept at 0, a_i is the linear term, a_{ii} is quadratic term and a_{ij} is the interaction term.

In present work, X2 and X3 were considered as non continuous factor for this work to simplify our experimental design. In previous work of Kristiawan et al (2008) [5, 121] pressure drop rate was adjusted with different diaphragm size connecting to vacuum tank, and this makes vacuum to behave as a continuous experimental factor in their optimization work. Another way to study vacuum as a continuous factor was by adjusting the vacuum level inside the vacuum tank to appropriate level required. The present work interest; however was aimed to maximize the removal of thin film of air surrounding material to be treated in order to increase heat transfer efficiency from steam to material and to lower time for treatment. Removal of excess moisture will decrease the formation of steam condensate. For this work, maximum level of vacuum 100 mbar was used to justify the need of the experiments.

Moisture level (X1) was considered as continuous factor, and since vacuum was not a continuous factor in this treatment combination; it is impossible to include central points to study overall treatment linearity effect in this particular design due to the presence of a non-continuous factor. The elimination of a non-continuous factor at the early stage was also part of strategy to ensure more flexible experimental design can be employed at later stages, such as central composite design (CCD) especially for the identification and optimization of non-linear effect of glucose response in thermal treatment.

Only moderate pressure regimes were tested in this DIC pretreatment system compared to other thermal pretreatment regimes due to the present limitation of the steam supply.

III.1.7. Material and Method

Material was prepared according to material pretreatment procedure described earlier and according to requirement set out in Table III-7. DIC treatment was done for 4 minutes at 0.6 MPa saturated steam pressure (temperature: 158.8°C, rounded to 159°C) with the following treatment combinations. Vacuum was set to 100 millibar (mbar) for X2:+1 and X3:+1 operation and at atmospheric pressure for X2:-1 and X3:-1 operation. About 3.5 minutes gap were required to generate vacuum level to 100 mbar in vacuum Tank (for condition with X2:+1), and about 30 to 40 seconds was required to reach atmospheric pressure (for condition with X3:-1) in vacuum tank without giving any stress to DIC valve especially during the presence of high pressure differences between DIC reactor and vacuum tank (at condition X3:-1). Four minutes treatment time for all treatment combination was selected to ensure stable vacuum level for all treatment that requires vacuum (X3:+1).

DIC treated materials were dried and known amount was subjected to hot water extraction at 110°C for 60 minutes with solid : liquid ratio of 1: 10. Hot water extraction was done to solubilize all water soluble components due to the thermal autohydrolysis that occurs during DIC treatment. Extracts obtained from process was filtered through 0.20 µm nylon filter, diluted if necessary and injected into HPLC system as previously described. Area in HPLC chromatogram related to glucose response in each sample was quantified with standard curve of known glucose concentration.

Table III-7: Present study with 2³ factorial designs with the following combinations:

Moisture level, X1	Vacuum initial, X2	Vacuum final, X3
25, 50, 75, 100% at 25% step increase	High: +1 Low: -1	High: +1 Low: -1
100, 150, 200 : at 50% step increase	High: +1 Low: -1	High: +1 Low: -1
100, 200: at 100% step increase	High: +1 Low: -1	High: +1 Low: -1

Table III-8: Summary of 2³ factorial combinations for First vacuum (X2), steam and Second vacuum (X3). One set of factorial combinations consist of 8 treatments.

	Combination			
as V and NV	V-S-V	V-S-NV	NV-S-V	NV-S-NV
as X2 : X3	X2 : X3	X2 : X3	X2 : X3	X2 : X3
W:-1	+1 :+1	+1 :-1	-1 :+1	-1 :-1
W:+1	+1 :+1	+1 :-1	-1 :+1	-1 :-1

III.1.8. Result and Discussion

Typical HPLC chromatographic profile of hot-water extracts obtained from autohydrolysis of polysaccharides is shown below (Figure III-10) as represented by different level of moisture content. The lower DP oligosaccharides consist of DP2, DP3 and DP>4 were eluted in the first few minutes of the chromatogram

Based on several HPLC chromatograms in Figure III-10, it was observed that the first few peaks on each chromatogram were identified as low DP oligosaccharides. According to the specification of the HPLC column, high DP polymers will elute first followed by its monomer and much lower molecular weight materials towards the end of the chromatogram. For chromatogram of X1: 150% and 200% (i.e. moisture content), a minimum of three peaks

before the glucose peak were detected which were corresponds to a low DP oligosaccharides peaks. Towards the end of the chromatogram, there was an existence of small peak related to acetic acid, formic acid and levulinic acid. In order to verify the glucose composition of respective dilute acid hydrolysis, hydrolysate obtained was further hydrolyzed according to procedure in Part 2: II.1.3.3 in page 60 and injected into HPLC.

Results show that oligosaccharides peaks were not observed any more (data was not included here), while there was an increase in a glucose amount against the respective sample. This observation, confirms the existence of hydrolysable low DP oligosaccharides in hot water extract for DIC treated materials.

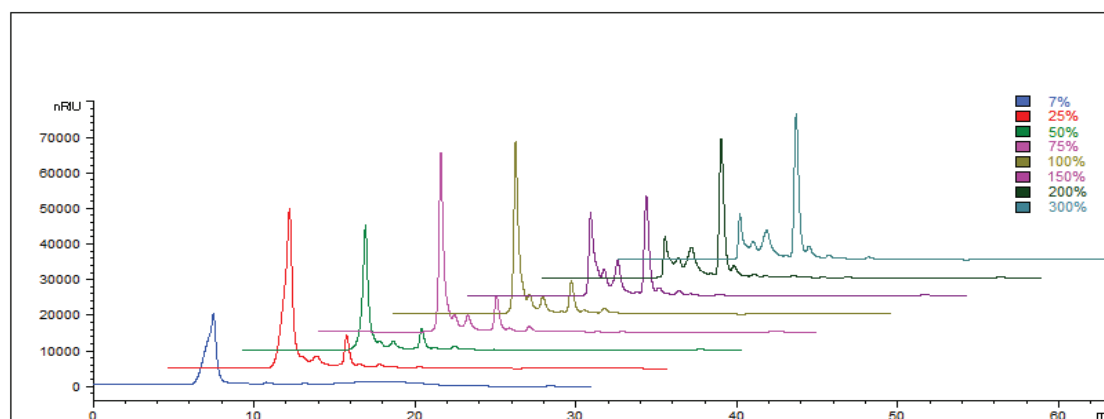


Figure III-10: Chromatogram for DIC autohydrolysis of SPW polysaccharides into glucose at different moisture content.

The existence of oligosaccharides in DIC treated materials was due to incomplete hydrolysis of starch and non starch polysaccharides into glucose. This observation suggests another potential utilization of DIC system, i.e. for rapid liquefaction of starch or other non starch polysaccharides components at high solid loading into short-chain oligomers; namely, oligosaccharides. The partially hydrolyzed starch can be use for enzymatic saccharification to glucose syrup of varying level of dextrose equivalent.

In general, Figure III-11 shows that glucose yield from SPW material with X1: less than 100% moisture content was less than 100 mg/g. Drastic change in glucose yield was observed once moisture content, X1: $\geq 150\%$ for all treatment combinations. This indicates that moisture content (X1) gave very significant effects on the autohydrolysis of polysaccharides into glucose during DIC pretreatment. This phenomenon was due to, as soon as dry steam enters the DIC chamber, the available moisture on the surface of materials will be heated and immediately proton $[H^+]$ on the surface will become reactive for hydrolysis reaction. High moisture content materials were found to enhance the conversion of polysaccharides (starch) to glucose, due to the ability for water movement due to fluidity on the surface as well as in the internal porous structure of SPW.

Low moisture level, however, does not allow the proton $[H^+]$ movement to other polysaccharide's reaction site to initiate other hydrolysis actions. The withholding of $[H^+]$ at the same point increases potential degradation of glucose present at that location. In comparison, movement of $[H^+]$ due to fluidity at high moisture level enables new site for $[H^+]$ reaction to start and contribute to a higher glucose yield.

Autohydrolysis of starch to glucose will start with the partial degradation of the starch polymeric chain from a longer chain into much shorter chain, and this process can never be reversed. When the moisture content was increased from 100% to 150%, this will enhance

the movement of a shorter chain thus further increase the rate of the partial degradation of starch and other polysaccharide's low molecular weight oligomers such as glucose and xylose. In a similar manner, the rate for the degradation of glucose due to an extended exposure to high temperature was unavoidable for treatment without second vacuum cycle. This has decreased the yield of overall glucose for two treatments without vacuum as observed in Table III-9 and in Figure III-11.

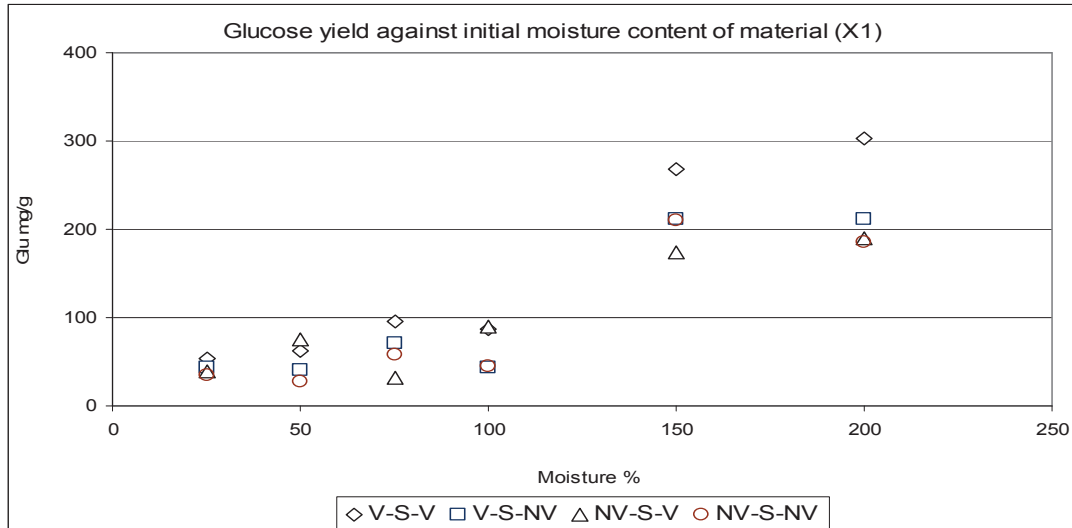


Figure III-11: Plot for glucose concentration (mg/g) against X_1 for different X_2 and X_3 . Two other factors, i.e. treatment time and acid concentration were fixed at 4 minutes and 0.18 molar respectively.

Table III-9: Result for DIC treatment according to respective moisture level and vacuum cycle. X_1 : 100% and 200% were repeated three and two times respectively with standard deviation.

MC % db	V-S-V	V-S-NV	NV-S-V	NV-S-NV
X_1	$X_2:+1 X_3:+1$	$X_2:+1 X_3:-1$	$X_2:-1 X_3:+1$	$X_2:-1 X_3:-1$
25	53.87	43.87	38.74	34.86
50	62.12	41.05	75.12	28.09
75	96.17	70.67	32.09	58.30
100	86.38 ± 0.35	43.04 ± 3.45	90.11 ± 2.55	45.45 ± 1.55
150	267.46	212.10	173.47	209.81
200	303.19 ± 2.53	210.96 ± 3.85	189.49 ± 3.65	185.33 ± 2.13

Note for the rest of article: V-S-V is $X_2:+1 - X_3:+1$, V-S-NV is $X_2:+1 - X_3:-1$, NV-S-V is $X_2:-1 - X_3:+1$ and NV-S-NV is $X_2:-1 - X_3:-1$.

One fixed saturated steam pressure was used i.e. 0.6 MPa (159°C) in this study. This was based on OFAT result described earlier. At a much higher pressure, there was a leak in DIC valve due to stress during vacuum removal from the vacuum tank to prepare for $X_3:-1$ (i.e. no vacuum) cycle. Treatment time of four minutes was decided based on emptying and filling of the vacuum tank to 100 mbar vacuum.

There are eight treatment combinations obtained from these trials as presented in Table III-8. Each treatment combination was subjected to response surface analysis to analyze the effect of parameters and its variance analysis (ANOVA) for statistical significance of combination. Based on ANOVA result, only one combination was found to have significant effect for all X_1 , X_2 and X_3 , i.e. from the combination of $X_1:-1$ (150%) against $X_1:+1$ (200%). Result and analysis of data onward will be based on data from this combination only; i.e. configurations of $X_1:-1$ (150%), $X_1:+1$ (200%) at both X_2 : (+1 or -1) and X_3 : (+1 or -1).

III.1.8.1. Effect of Reaction Factors

In order to calculate factors effects, selected data that was obtained from experiments were organized into respective combination factor of high (+1) and low (-1) according to experimental design as described earlier in Table III-7. Effect of interaction for factor at fix acid concentration can be calculated from above result as $X1*X2$, $X1*X3$ and $X2*X3$. To simulate the calculation of statistical effect, the following Table III-10 was organized according to the coded factors for two levels and three factors factorial design (2^3).

Table III-10: Glucose concentration from DIC thermal treatment organized into respective coded factors. Data in grey cells was for ($X1:+1$) for experimental design $X1: 150 (-1)$ against $X1: 200 (+1)$.

X1	X2	X3	25v50	50v75	75v100	100v150	150v200	100v200	75v150	50v150
-1	-1	-1	34.86	28.09	58.3	45.45	209.81	45.45	58.3	28.09
+1	-1	-1	28.09	58.3	45.45	209.81	185.33	185.33	209.81	209.81
-1	+1	-1	43.87	41.05	70.67	43.04	212.1	43.04	70.67	41.05
+1	+1	-1	41.05	70.67	43.04	212.1	210.96	210.96	210.96	212.1
-1	-1	+1	38.74	75.12	32.09	90.11	173.47	90.11	32.09	75.12
+1	-1	+1	75.12	32.09	90.11	173.47	189.49	189.49	189.49	173.47
-1	+1	+1	53.87	62.12	96.17	86.38	267.46	86.38	96.17	62.12
+1	+1	+1	62.12	96.17	86.38	267.46	303.19	303.19	303.19	267.46

Main effect was calculated by averaging all response related to the factor, such as for $X1$ average (+1) as in Table III-10 (result in grey cell). Data obtained from grey cell (column $X1:+1$) were average as follow. Effect of factor was a residual of average from ($X1:+1$) minus ($X1:-1$).

$$\text{For example; for } X1:+1 = \frac{185.33+210.96+189.49+303.19}{4} = 222.24$$

Table III-11: Main effect for glucose at combination significant 95% $X1:150-200\%$ (column 150v200)

Control parameter	Average :+1	Average :-1	Effect (high-low)
X1	222.24	215.71	6.53
X2	248.43	189.53	58.90
X3	233.40	204.55	28.85

Data for similar calculation was done for other main effect (X , $X2$ and $X3$) and its interaction effect ($X1*X2$, $X1*X3$ and $X2*X3$) using Statgraphics software and are presented in Table III-11 (for main effect) and shown in Table III-12 (main effect and interaction effect) in order to estimate effect for main effect and interaction effect.

Table III-12: Summary of main effect and interaction effect for glucose response for group represent $X1: 150 - 200\%$ (column 150v200).

Effect	Estimate	Std. Error	V.I.F.
Average	218.976	0.45375	
X1: Initial moisture	6.5325	0.9075	1.0
X2: First vacuum	58.9025	0.9075	1.0
X3: Second vacuum	28.8525	0.9075	1.0
AB = $X1*X2$	10.7625	0.9075	1.0
AC = $X1*X3$	19.3425	0.9075	1.0
BC = $X2*X3$	44.9425	0.9075	1.0

Note: the largest variance inflation factor (V.I.F.) was found equals 1.0, and for perfectly orthogonal design, all V.I.F factors would equal 1.0.

In terms of statistical significance, the model presented above need to be improve further with repeat experimental due to very small degree of freedom (df: 1) in this statistical model. An improved model will be presented at the end of this article.

Pareto chart and Main Effect plot for glucose concentration for group represent high and low level, X1: 150 (-1) and X1: 200 (+1) for result from main effect and interaction effect were presented in Figure III-12.

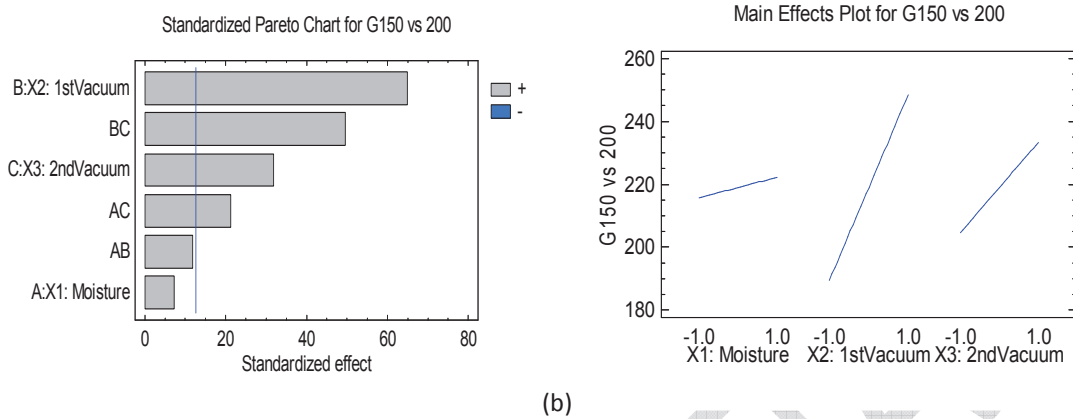


Figure III-12: (a) Standardized Pareto chart for main effect and interaction effect for glucose response for group represent X1: 150 – 200% together with (b) Main Effect plot that show the magnitude of effect for moisture, vacuum first stage and vacuum second stage.

In general, X2 and X3 together with interaction of X1, X2 and X3 in the form X2*X3 and X1*X3 give positive effect for the hydrolysis of starch into glucose. Magnitude of X2 was the greatest to contribute the glucose availability as in above figure. This was suggested due to closely related to the act for the removal of thin moisture layer on the surface of materials that enhance further the autohydrolysis process.

The ANOVA table (in Table III-13) partitions the variability in of the result between 150% against 200% into separate pieces for each of the effects. Its statistical significance was tested for each factor by comparing the mean square against an estimate of the experimental error. In this case, four factors (single reaction factor and its combination factors) have P-values less than 0.05, indicating that they are significantly different from zero at the 95.0% confidence level.

Table III-13: Analysis of Variance for glucose response for group represents X1: 150% (-1) and 200% (+1) (i.e. for column 150v200 in Table III-10).

Source	Sum of Squares	Df	Mean Square	F-Ratio	P-Value
X1: Initial moisture	85.35	1	85.35	51.82	0.0879
X2: First vacuum	6939.01	1	6939.01	4212.83	0.0098
X3: Second vacuum	1664.93	1	1664.93	1010.82	0.0200
AB = X1 X2	231.67	1	231.66	140.65	0.0536
AC = X1 X3	748.27	1	748.27	454.29	0.0298
BC = X2 X3	4039.66	1	4039.66	2452.57	0.0129
Total error	1.65	1	1.65		
Total (corr.)	13710.5	7			

R-squared = 99.99 percent, R-squared (adjusted for d.f.) = 99.92 percent

Standard Error of Est. = 1.28,

Note: Grey areas represent the statistic of significant factors.

The R^2 statistic indicates that the model as fitted explains 99.988% of the variability in column 150v200. The adjusted R-squared statistic, which is more suitable for comparing models with different numbers of independent variables, is 99.916%. The standard error of the estimate shows the standard deviation of the residuals to be 1.283.

Based on a result in Table III-13, it can be concluded that there was a very significant effect on glucose formed due to first vacuum and second vacuum combination for this process, which defines the DIC process itself. The statistical effect was studied further and presented in a graphical form to describe main factors (X1, X2 and X3) and their interaction factors as depicted below.

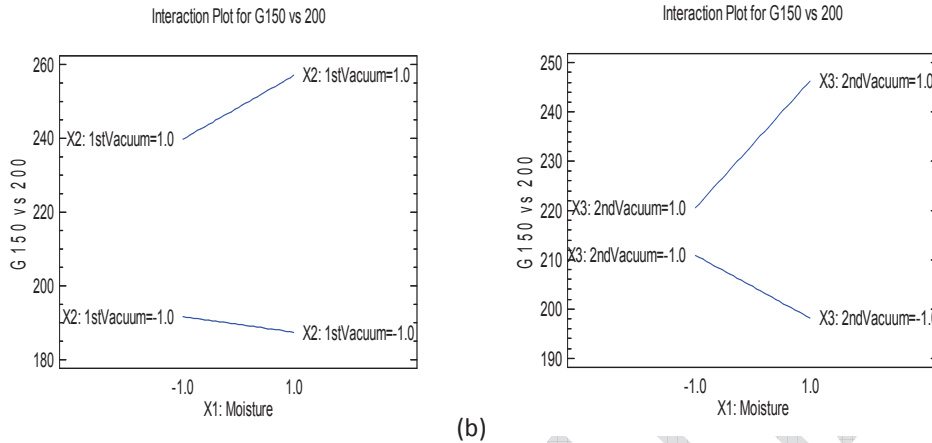


Figure III-13: (a) Interaction factor against glucose concentration for moisture level (X1) : X2 at (-1 and +1) and (b) Interaction factor for X1 : X3 at (-1 and +1).

Interaction factor between X1 and X2 in Figure III-13(a) shows that no effect if no vacuum (X2:-1) and there is an immediate increase in response nearly 50 mg/g if a vacuum was used (X2:+1). Similar response was found for X3:-1, Figure III-13(b) with a possibility that the yield of glucose may decrease nearly 10 mg/g if moisture content were increased. Putting X3:+1 for a similar increase in the moisture level may significantly increase glucose yield by nearly 30 mg/g.

In Figure III-13(a), the difference in glucose at X1: -1 for X2: -1 (no vacuum) against X2:+1 (with vacuum) was due to higher heat transfer for immediate hydrolysis after removal of thin layer of moisture by vacuum treatment. It was also expected that steam was able to penetrate further into a porous structure of material to initiate the hydrolysis of starch and other polysaccharides into glucose. The removal of thin layer of moisture from the surface of material will cause steam to immediately raise the acid temperature and thus increase the activation energy level and subsequently activate proton to start the reaction. It has to be noted that hydrolysis action proceeds very fast, however, only starts if the favorable condition was achieved, such as exceed certain minimum level of the activation energy.

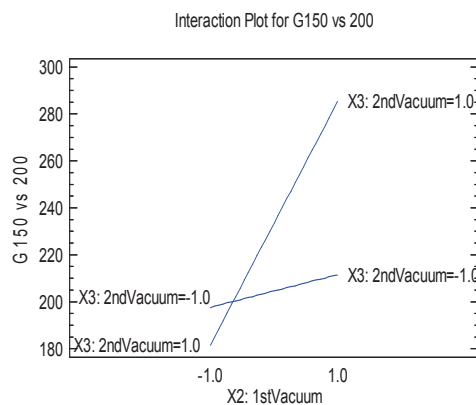


Figure III-14: Interaction factor for First vacuum, X2 and Second vacuum, X3 at -1 and +1 against glucose response.

In Figure III-14 shows interaction for the application of X2 and X3 it was observed that treatment with a combination X2:-1 and X3:-1, (i.e. no vacuum for both vacuum stage) during SPW treatment, the maximum amount of glucose was about 180 to 200 mg/ g. With X2:+1 and X3:-1, it does not help to increase the glucose yield, however, there was a dramatic increase in glucose yield of nearly 100 mg/ g if both X2 and X3: +1.

This can be explained by the association of an extra amount of time and heat to increase the temperature of water vapor at the surface of materials. Introduction of vacuum, X2:+1 will remove a small layer of water vapor and increase the accessibility of steam onto materials. During the cycle with X3:+1, the fast cooling action will immediately stop the potential degradation of glucose due to exposure to high temperature. Immediate cooling action will deactivate the reactivity of proton [H+] that was available for glucose degradation. These explanations were confirmed by result in Table III-14 below that shows the high potential of degradation for X3:-1 at 150% vs 200% data.

Table III-14: Difference in glucose yield for X1: 100% vs 150% and X1: 150% vs 200% (from Table III-9)

MC % db	V-S-V	V-S-NV	NV-S-V	NV-S-NV
100 vs 150	267-86: 181	22-43: 169	173-90: 83	209-45: 164
150 vs 200	303-267: 36	210-212: -1	189-173: 16	185-209: -25

III.1.8.2. Effect of Extended Exposure during DIC Thermal Treatment

There was an immediate increase in glucose yield for all material with high initial moisture content, i.e. for X1: 150% to 200% for treatment with V-S-V, V-S-NV, NV-S-V and NV-S-NV if compared to X1: 100% (refer to Table III-9 and Table III-14). If X1: 100% was taken as a baseline for comparison, it was found that at X1: 150%, for group with X2:+1 and X3:-1 (i.e. group V-S-NV), there were nearly 181 mg glucose/ g SPW or 18% increase in the glucose amount against the selected baseline. This was expected due to; during first vacuum stage (X2:+1), air and water vapor were removed from the surface of materials thus removing a thin air barrier from the material surface for immediate contact with steam. Data in Table III-9 and Table III-14 shows the relationship between first vacuum effects for X1:25% to 150% for all four treatment combinations, with higher glucose yield between 4 mg/g to about 60 mg/g SPW for V-S-V against other treatment groups: V-S-NV, NV-S-V and NV-S-NV.

For group V-S-V, at X1: 200%, glucose yield was the highest of all treatments at 303.2 mg/g. In normal DIC treatment with X3:+1, we can expect there is an immediate material surface cooling from 150°C to nearly 30°C within less than a second, due to very immediate decompression of pressure to vacuum level. The immediate cooling with decompression will immediately stop all autohydrolysis reactions that occur inside of the material. Upon further exposure to surrounding high temperature from the reactor body, treated material may increase back its temperature towards 70 to 90°C within 20 to 30 seconds, however autohydrolysis reaction usually not in favor to restart. In the case of group V-S-NV and NV-S-NV, steam pressure was released towards the atmospheric pressure, i.e. temperature will drop from 150°C to about 100°C, and with extended exposure to heat from reactor body material temperature could return to nearly 110°C to 120°C, and due to such exposure glucose degradation was observed and decrease the glucose yield. Table III-14 shows the potential glucose degradation is higher than glucose generation for V-S-NV and NV-S-NV. This finding was a good basis to decide the importance of a vacuum cycle in the thermal treatment, especially for treatment that produced products that can be easily degraded upon extended exposure to a higher temperature.

The other treatment group was also found to experience a similar increase in glucose response for treatment at a higher initial moisture level in material (refer Table III-9). This finding is parallel to objective for utilization of SPW without any other treatment, except for reducing a certain percentage of water, while mixing it with acid to get back the moisture content of about 150 to 200% on a solid basis.

III.1.8.3. Confirmation Experiment

Based on the statistical result obtained from above work, the same 2^3 full factorial design block was developed and treated with DIC for all treatment combinations with X1: 100, 150 and 200%. Trial was done with two replicate to obtain a new set of data. Data from previous experiment was included in the statistical analysis to increase error degree of freedom (previous d.f: 1) of experimental block to 15. Good experimental design needs to meet criteria that the number of experimental trials required must be greater than the number degrees of freedom associated with the main and interaction effects studied in the experiment. In this case, d.f: 15 was a good choice because there are 6 total effect and combination being studied. Range of experimental block was kept at the same for confirmation purpose.

In this case, 6 effects have P-values less than 0.05, indicating that they are significantly different from zero at the 95.06% confidence level. As shown in ANOVA result in Table III-15, the F value for respective effect X1, X2 and X3; and interaction effect X1 X2, X1 X3 and X2 X3 are 22.67, 791.98, 180.45, 67.69, 110.20 and 403.29 respectively. This implied that the effects were significant and there was only a 0.05% chance that main effect and interaction effect of that amount could occur due to the noise.

Table III-15: Analysis of variance for glucose yield confirmation

Source	Sum of Squares	Df	Mean Square	F-Ratio	P-Value
X1: Initial moisture	532,984	1	532,984	22,67	0,0003
X2: First vacuum	18620,5	1	18620,5	791,98	0,0000
X3: Second vacuum	4242,7	1	4242,7	180,45	0,0000
X1 X2	1591,53	1	1591,53	67,69	0,0000
X1 X3	2590,85	1	2590,85	110,20	0,0000
X2 X3	9481,97	1	9481,97	403,29	0,0000
blocks	4,78742	2	2,39371	0,10	0,9038
Total error	352,669	15	23,5113		
Total (corr.)	37418,0	23			

R-squared = 99.06 percent

R-squared (adjusted for d.f.) = 98.73 percent

Standard Error of Est. = 4.85

The R^2 statistic indicates that the model was fitted that explains 99.06% of the variability in Glucose yield, and this shows that there was a very high correlation between X1, X2 and X3 in this processing regime. The adjusted R^2 for comparing models with different number of independent variables was 98.73%, also shows satisfactory to confirm the significance of the correlation model. This statistical data confirms previous model with some improvement estimation at much higher statistical degree of freedom (df: 15) compared to only d.f:1 during initial screening work.

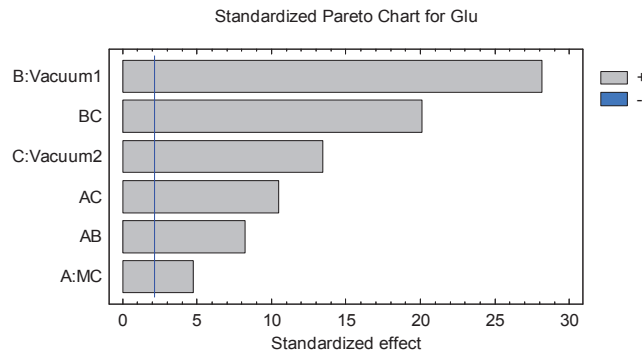


Figure III-15: Standardized Pareto chart for confirmation experiment

Pareto chart in Figure III-15 shows that all factors being studied in this work are significant at 95% significant level, due to an improved result obtained from trial and an increase in number of degree of freedom compared to initial work. The quadratic equation of the fitted model based on second order polynomial model represent all factor and interaction associated to all factors being studied was developed as in the following equation for quadratic response:

$$Glu = 219.53 + 4.712X1 + 27.854X2 + 13.296X3 + 8.143X1*X2 + 10.39X1*X3 + 19.877X2*X3 \quad \text{-- Equation 24-1}$$

Main plot for X1, X2 and X3, and Interaction Plots of X1X2, X1X3 and X2X3 were similar to result obtained previously (refer to Figure III-12, Figure III-13 and Figure III-14). Confirmation for statistically significant main effects and interaction plots were done by studying the normal probability plots of the experiment. In normal probability plots, the main and interaction effects of factors were standardize and plotted against cumulative percentage probability. The less significant main and interaction effects will fall roughly along the straight line whereas active effects which are judged to be statistically significant tend to appear at far points either at the right or the left of the straight line.

In Figure III-16 shows a normal probability plot of effects (main and interaction) of control parameters at 99% confidence level (or 1% significance level). Based on the normal probability plot, we can say that First vacuum (X2) and interaction of X2 and X3 are very highly significant for thermal treatment in this regime. Second vacuum (X3) is quite significant as it does not fall on the normal probability line. The other factors: X1X3, X1X2 and X1 was not statistically significant even though appear in the Pareto chart.

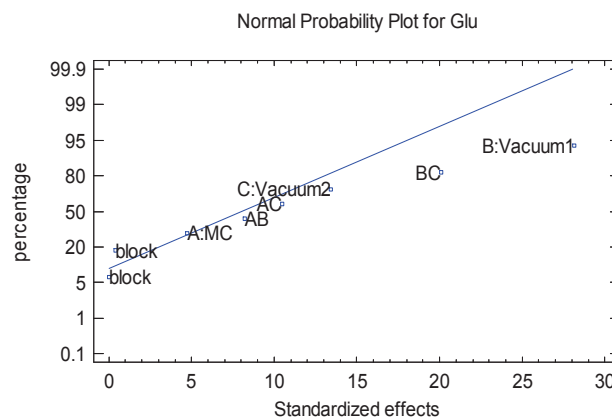


Figure III-16: Normal probability plot for glucose response.

Equation 24-1 was used to develop the following response surface plots to represent effect of X1, X2 and X3 towards glucose response obtained from the process, and to simulate different condition of at low (-1) and high (+1) level while keeping another 2 factors as variable as presented in Figure III-17, Figure III-18 and Figure III-19 for response based on moisture content, 1st vacuum and 2nd vacuum respectively.

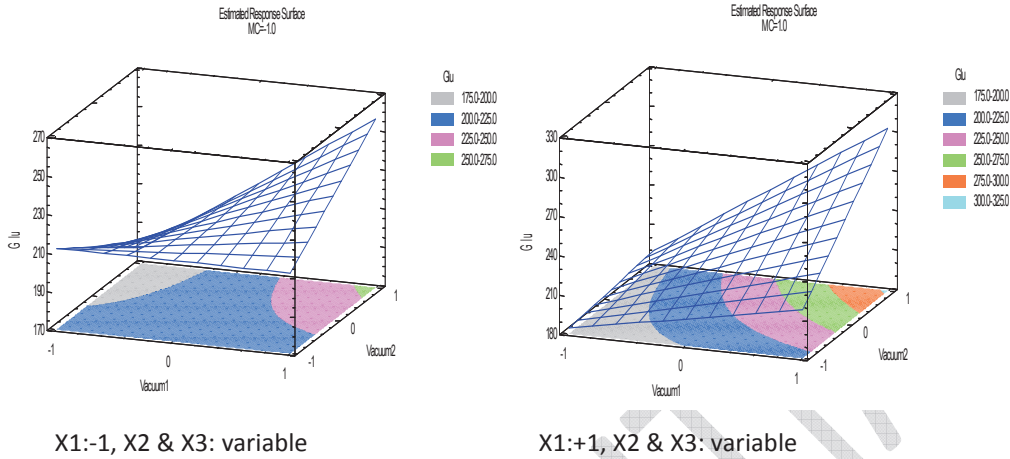


Figure III-17: Response surface model moisture content (X1) at low (-1) and high (+1) level

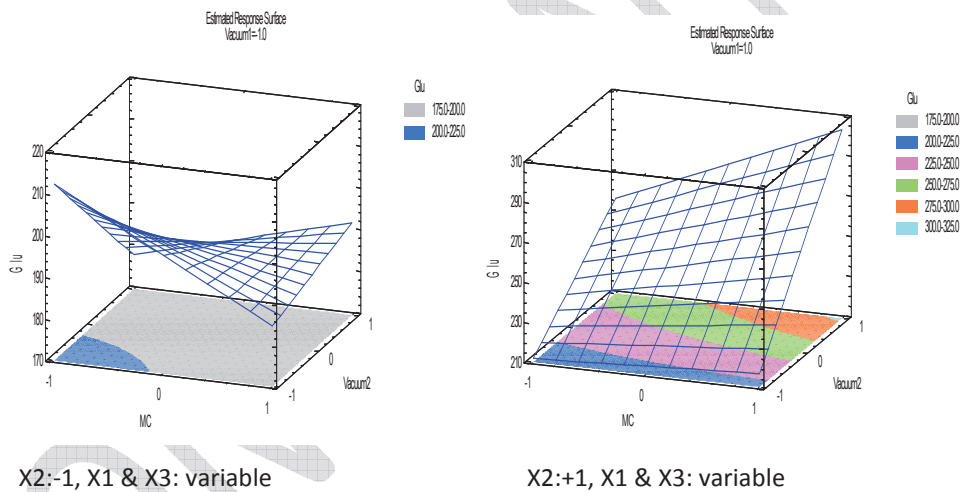


Figure III-18: Response surface model for first vacuum (X2) at low (-1) and high (+1) level

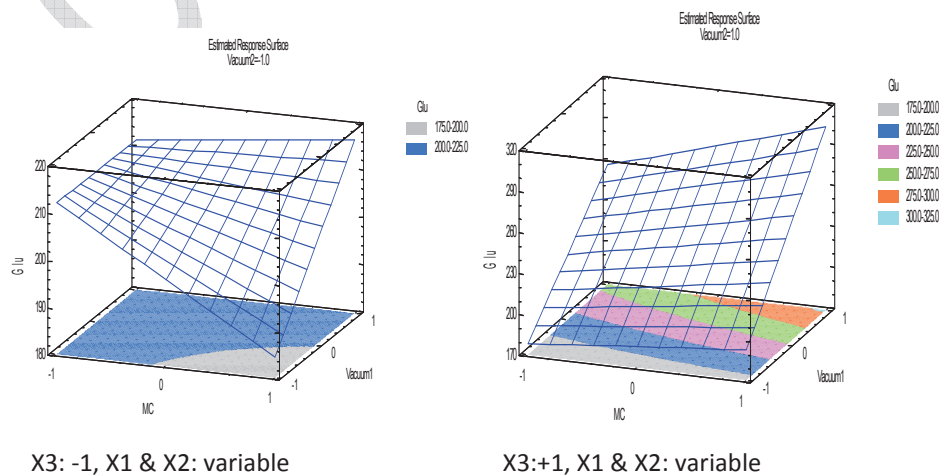


Figure III-19: Response surface model for second vacuum (X3) at low (-1) and high (+1) level

Based on response surface model, low factor level for all three factors was found to contribute low glucose yield. High factor level was found to increase the yield of glucose. For all vacuum cycle at high level was found to be associated with an increase in glucose yield as explained in the interaction factor study in Table III-13, Figure III-13 and Figure III-14. This indicator was very crucial for the selection of DIC process (i.e. X2:+1 and X3:+1 configuration) together with level of moisture content (X1) in the next optimization trials. The combination of moisture and both vacuum cycle was amalgamated as a single factor with moisture at 150% and both vacuum cycle will be used for the next optimization works.

We also have demonstrated that high glucose syrup can be obtained with 30% solid loading (i.e. 3 gram DIC treated material extracted 10 ml hot water), about 5 ml crude glucose syrup contains approximately 230 mg/ml glucose (equivalent to about 38% of total polysaccharides content) can be produced. This crude glucose was nearly an equivalent to 98 dextrose equivalent scale (98 DE) in sugar industry standard, considering small portion of starch still not fully hydrolyzed into glucose. In comparison, glucose processing plant from starch materials uses low solid : liquid ratio between 2 to 5% during liquefaction followed by hydrolysis. The dilute syrup will be concentrated with vacuum followed by drying into crystalline glucose.

The processes that presently studied and were proposed was following different processing route in comparison to the existing glucose processing from starch. This process utilizes crude starch in the form of SPW waste feed material. This process was done according to (i) depolymerized at high solid, followed by (ii) extraction by means of high solid: liquid loading as compared to existing starch to glucose processing as described above.

III.1.9. Conclusion

The autohydrolysis of crude starch in SPW during DIC treatment was part of the strategic way to obtain high glucose concentrate syrup. Application of vacuum in thermal treatment helps to increase the accessibility of steam towards hydrolysis surface during autohydrolysis of polysaccharides into glucose. This suggests the reason of sequencing of vacuum stages, and its interaction effects were found to be statistically significant for improving the yield of glucose during DIC pretreatment stage. This finding was a good basis to decide the importance of the vacuum cycle in the thermal treatment, especially for treatment that produced products that can be easily degraded upon extended exposure to high temperature.

Nearly 50% of starch was hydrolyzed into glucose within less than 4 minutes DIC treatment. The remaining 50% starch can further hydrolyzed at the second stage dilute acid hydrolysis together with certain portion of cellulose. This process further shows that DIC pretreatment can be a good starting point to process solid waste material, which contains high starch that cannot be economically extracted in a sago processing plant. DIC process, in particular, the utilization of second vacuum cycle, was found able to control the degree of glucose degradation due to rapid cooling of the treated materials.

Result from moisture factor level study also was able to differentiate the minimum moisture level required for the conversion of polysaccharide into glucose. Based on above results, X1: 150% was selected for use in the next parameter optimization study of SPW polysaccharides

into glucose. This selection was done to ensure highly intact polysaccharides are still remained in DIC treated material for representative statistical analysis.

As the main conclusion of this Chapter, moisture and both vacuum cycles was combined together as a single factor with moisture at 150% and both vacuum cycles, and will be used for the next optimization works. This has enabled the utilization of much better experimental design for the development and optimization of the process, as well as to study the non-linear effect of factors on glucose yield.

CONFIDENTIAL

PART III. CHAP 2.
OPTIMIZATION WITH RESPONSE SURFACE METHODOLOGY (RSM)
MODEL AND KINETIC MODEL

Paper 3: (i) Optimization of DIC process at Low DIC severity condition for the conversion of polysaccharides/crude starch to LMW oligosaccharide fraction and glucose by RSM (ii) Development of kinetic model of polysaccharides/crude starch conversion under Low DIC severity process.

Abstract

Central composite design (CCD) was used to study the effect of DIC autohydrolysis of polysaccharides into low molecular weight (LMW) oligosaccharide and glucose using a low DIC severity combination with 22 experimental points. Polynomial equation obtained from CCD was used to generate response surface model and new set of kinetic data. RSM shows that with low DIC severity, autohydrolysis process was linear in terms of temperature, acid concentration and treatment time. Consecutive first order kinetic model were developed using data generated from RSM polynomial equation. F Statistics was used to check data and kinetic models in terms of its statistical significance. From kinetic model, A_0 values were found to be very closely related to the severity of treatment, whereby A_0 values will indicate DIC treatment severity towards SPW. Rate constant for hydrolysis (k_1) and degradation (k_2) was calculated together with kinetic model. Finding shows that, at low acid concentration and low temperature, conversion of polysaccharides into glucose was due to hydrolytic conversion reaction, and both factors; consequently become a factor for glucose degradation.

III.2.1.Objective

Objective of this work was to optimize DIC treatment for the conversion of polysaccharide's hydrolysis into LMW oligosaccharides and glucose through RSM. The nature and magnitude of various factors which influence the formation of glucose were also evaluated. Kinetic model based on empirical data from RSM polynomial equation also was developed in order to find important kinetic data at low DIC severity.

III.2.2.Introduction

In the present work, an enhanced experimental design, i.e. central composite design (CCD) was used after successfully eliminated the non continuous factor during the exploratory and screening stage. Both vacuum stages were combined into single treatment as DIC cycle only. Another three DIC derivatives was eliminated and will not be included in study. Final form of work throughout this thesis will be based on DIC treatment with two vacuum stages: X2:+1 and X3:+1. Details of DIC technology, application and its treatment sequences were presented in various publications related to this technology [4, 5, 115, 117].

Experimental design that was used in present work was CCD with center points. Similar five level of CCD was previously used to describe an effect of DIC treatment factors towards the

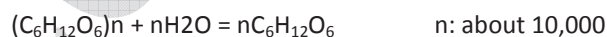
application response such as for isolation of essential oils [5, 121], studies on the porosity and expansion of various materials [3, 4, 120, 161], and improvement in drying operations after DIC pretreatment [115, 162]. For the present work and after elimination of another three DIC derivative operations together with fixing of initial moisture content (X1) to 150%, there are still three factors that need to be optimized: treatment time (X4), acid concentration (X5), and treatment pressure/ temperature (X6). Acid concentration in previous work during vacuum cycle studies were set at maximum 0.2 molar while during extreme parameter study was at maximum of 1.25 molar. This was done in order to obtain a good representation of total polysaccharides autohydrolysis for both starch and cellulose. However, it was very clear that only starch was undergoing autohydrolysis reaction into glucose in vacuum cycle studies, while both starch and cellulose were converted into glucose in an extreme parameter combination studies.

We found that at much lower DIC severity treatment combination, starch will be converted into low DP oligosaccharides. This prompt to another potential application for DIC technology, i.e. to produce low DP oligosaccharide's that can be use as feed material for enzymatic hydrolysis and as functional short chain oligosaccharides (SCO). SCO is gaining acceptance as functional food ingredients, i.e. as prebiotics [163, 164]. On the other hand, during extreme parameter study, glucose degradation was very great during a prolonged treatment time. In order to understand the mechanism of both polysaccharides hydrolysis and glucose degradation, the following study was done for this Chapter 2:

- Paper 3: Full experimental design with CCD at lower severity DIC combination with low acid concentration and shorter treatment time; and
- Paper 4: Full CCD with higher severity DIC combination with high acid concentration and longer treatment time.

Both response surface models will be used to extract autohydrolysis kinetic data and calculate the kinetic rate constant for respective treatment severities.

Starch hydrolysis with acid can be represented as in the following expressions, where ***n mole*** of water was required for the hydrolysis of ***n mole*** of starch into ***n mole*** glucose [165]. Based on this information, it can be concluded that water was an important element for the process to starts. On top of this information, moisture content effect was studied in the previous trial in Chapter 1, and initial moisture content level of 150% was selected for the remaining of optimization studies.



Result from Exploratory Trial 2 (Chapter 1: Paper 2 in page 84) shows that moisture content behaves as a limiting factor in the DIC treatment. Initial moisture content for DIC treatment was decided to be at 150% on solid basis; this was upon understanding at higher moisture, there was a high potential for glucose degradation if initial moisture content of material was increased further. In order to explore the possibility for oligosaccharide production and understanding the behavior of this crude starch materials (or SPW) hydrolysis, the following experimental design based on CCD was developed followed by respective consecutive first order kinetic model development.

Consecutive first order kinetic reactions for both glucose generation (also referred as polysaccharide autohydrolysis) and glucose degradation based on general kinetic reaction was described much earlier in literature review for kinetic process and will be used to describe kinetic factors in this Chapter.

III.2.3. Material and Method

Material (SPW) was prepared according to Table III-16 and Table III-17. DIC pretreatment was done based on the experimental design described in the Table III-17. Detail procedure and calculation for moisture content and acid concentration adjustment was presented in Part 2 of this thesis.

Information on total polysaccharides composition of material used in this study was described in previous Chapter 1: Paper 1 in Figure III-2, page 75.

Glucose in hot water extract was analyzed and quantified with HPLC system as described earlier. Experimental data points were further analyzed with response surface methodology. Details of hot water extraction procedure, hydrolysate preparation and HPLC system used in this study were described earlier in Part 2 of this thesis.

III.2.3.1. Experimental Design

This study was designed to find quantitative estimates for total polysaccharides (starch hemicelluloses and cellulose) conversion to glucose upon exposed to high temperature for certain treatment time. The availability of dilute acid in the composition will help to hydrolyzed starch followed by cellulose into glucose. An extended hydrolysis, however, will degrade glucose into several chemicals such as furfural, levulinic acid, formic acid and acetic acid. Glucose will be measured to fit a quadratic type polynomial regression equation which is related to the actual composition of potential glucose in SPW. Other degradation products as described above, however, will be qualitatively identified to estimate its availability.

The central composite design (in Table III-16) was based upon a response from its central composition level (as 0) in combination with controlled variation from its $+\alpha$ and $-\alpha$ level together with +1 and -1 level. Space calculation for $\pm\alpha$ and ± 1 was reviews in Part 1 of the thesis and further summarized below. A complete representation of experimental run is presented in Table III-17 for both coded and actual parameter's level for DIC run. Actual experimental run was done in random orders to minimize any potential effect of unexplained external factors of selected response.

Design in Table III-16 and Table III-17 was based on the 2^k factorial design and $2k$ axial points, with k is number of factor ($k=3$), so full factorial 2^3 was 8 factorial points together with 6 ($2*3$) axial points also known as star points. Locations of star points were calculated with $\pm\alpha$ as ± 1.682 for design with 3 factors. Eight central points were added into the design to calculate the overall statistics that represent statistic of the design, i.e. to diagnose variation on the glucose response for overall trial. Three factors of interest in this study were X4: treatment pressure (MPa) or temperature ($^{\circ}\text{C}$), preferably X4 will later be referred only as temperature (in $^{\circ}\text{C}$) using steam table conversion; X5: acid concentration in molar, and X6: treatment time in minute. Single response of interest was glucose yield, in mg/ g.

Polynomial second degree quadratic equation for the model was represented by the following equation:

$$Y_{Glu} = b_{k0} + \sum_{i=1}^3 b_{ki} X_i + \sum_{i=1}^3 b_{ii} X_i^2 + \sum_{i \neq j=1}^3 b_{kij} X_i X_j$$

Equation 25

With b_{k0} as the value of fitted response of central points (0,0,0), b_{ki} , b_{ii} and b_{kij} , were the linear, quadratic and interaction regression terms respectively. Single polynomial equation obtained is product of regression analysis will be used later to estimate effect of hydrolysis kinetic of the process. Data obtained from experimental trials will be fitted into the equation by numerical technique as described in commercial statistical software Statgraphics (Centurion XV, version 15.2.11). Analysis of variance for the response was calculated and presented together with Pareto chart, correlation coefficient R^2 was targeted more than 90%. Statistic for F ratio and statistical probability (P) were calculated from experimental data with total degree of freedom of 21, which was high enough to achieve a good statistical model. Value of P less than 5% was required to decide whether factor or its interaction having significant difference or not against the model.

Response surface and contour plots for model based on polynomial equation were plotted as a function of any two variables at a time. A total three response surface and contour plots were available for this work.

Table III-16: Actual parameters and its coded form for independent variable of central composite design

Factors	Pressure, bar	[acid], M	Time, min	As
represented by:	X4	X5	X6	Coded form
Point max (+ α)	7.00	0.05	3.00	1.682
Point min (- α)	4.00	0.01	0.50	-1.682
Point central (0)	5.50	0.03	1.75	0
Point (-1):	4.61	0.02	1.01	-1
Point (+1):	6.39	0.04	2.49	+1

III.2.4. Result and Discussion

The amount of glucose formed as shown in Table III-17 was found to be very small (i.e. less than 1% of potential glucose available) if compared to previous result obtained during exploratory trials. This was expected as the lower severity combinations were used in this study.

Statistical analysis for central points shows that standard deviation was within 6.2%, which represent an overall statistic for this set of experimental data. Less than 1% glucose from total polysaccharides of 800 mg/g was converted into glucose for overall treatment. However, there was a high amount of oligosaccharides were present in hot water extract. This observation may suggest that the amount of glucose obtain exhibited a linear correlation to reaction factors, i.e. temperature, time and acid concentration for lower DIC severity treatment.

Calculated central points and average central points were 2.25 and 2.26 respectively; while the median for star and axis points was 2.21 and 2.40 respectively, i.e. very close the value of average value of calculated and experimental central points. This observation was presented in Figure III-20 below.

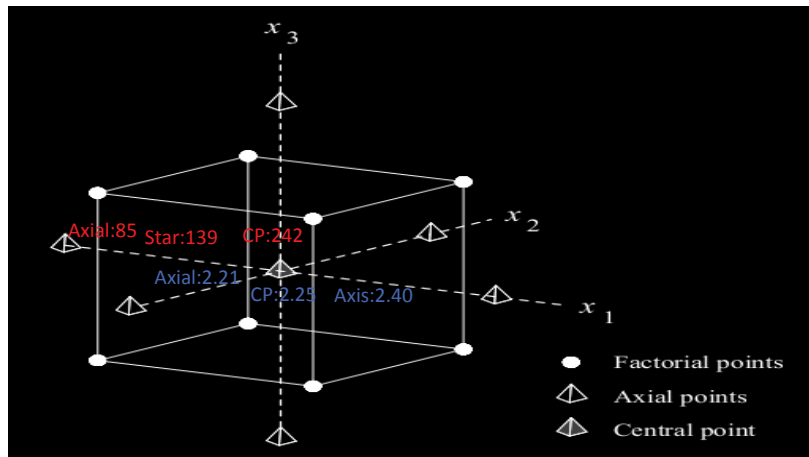


Figure III-20: Central composite design with 2^k factorial + $2k$ axial ($k: 3$). There are two level and three factors in this design. Simulation of two set of data at location of central point (CP), median star point (Star) and median axial point (axial) on axis x_1 to show data location due to affect of thermal treatment. Data set with **red color** for high DIC severity and **blue color** for low DIC severity.

In order to increase the rate of glucose generation, internal kinetic evaluations need to be conducted using available data of this experimental design. Optimization for kinetic hydrolysis can be done upon information based on this experimental design data. However, prior to that, several criteria were needed to be established to ensure that data and its model obtained from this trial can be use to generate kinetic data within the range of experimental design.

Table III-17: CCD experimental design in its coded and actual level (not in random order) with its respective glucose response and percentage of total polysaccharide.

No	Coded form			Actual level			Glucose mg/ g SPW	Glucose (%potential Glu)
	X4	X5	X6	X4	X5	X6		
1	0	0	0	5.50	0.03	1.75	2.400	0.30%
2	0	0	0	5.50	0.03	1.75	2.046	0.26%
3	0	0	0	5.50	0.03	1.75	2.093	0.26%
4	0	0	0	5.50	0.03	1.75	2.244	0.28%
5	0	0	0	5.50	0.03	1.75	2.393	0.30%
6	0	0	0	5.50	0.03	1.75	2.409	0.30%
7	0	0	0	5.50	0.03	1.75	2.226	0.28%
8	0	0	0	5.50	0.03	1.75	2.239	0.28%
9	-1	-1	-1	4.61	0.02	1.01	2.534	0.32%
10	1	-1	-1	6.39	0.02	1.01	2.126	0.27%
11	-1	1	-1	4.61	0.04	1.01	1.544	0.19%
12	1	1	-1	6.39	0.04	1.01	1.812	0.23%
13	-1	-1	1	4.61	0.02	2.49	2.253	0.28%
14	1	-1	1	6.39	0.02	2.49	3.460	0.43%
15	-1	1	1	4.61	0.04	2.49	2.165	0.27%
16	1	1	1	6.39	0.04	2.49	3.872	0.48%
17	-1.682	0	0	4.00	0.03	1.75	1.660	0.21%
18	1.682	0	0	7.00	0.03	1.75	2.891	0.36%
19	0	-1.682	0	5.50	0.01	1.75	3.307	0.41%
20	0	1.682	0	5.50	0.05	1.75	2.619	0.33%
21	0	0	-1.682	5.50	0.03	0.50	1.711	0.21%
22	0	0	1.682	5.50	0.03	3.00	2.189	0.27%

Summary of statistic for central points with unit of mg/ g glucose yield:

Total	18.05	Min (all)	1.54
Average	2.26	Max (all)	3.87
Std dev	0.14	Median star	2.21
Min	2.046	Median axis	2.40
Max	2.41		

ANOVA for the fitted model (Table III-18) was with very high correlation with R^2 of more than 90% for model and experimental data, suggesting that experimental data was significant to the model. This suggested that equation from this model can be used to estimate other responses required for internal analysis of the process itself such as to calculate constant of rate of polysaccharide's hydrolysis (k_1) and rate of degradation of glucose (k_2) which crucial for optimization of the process and to understand its underlying principle.

Table III-18: Analysis of variance for glucose fitted model

Source	Sum of Squares	Df	Mean Square	F-Ratio	P-Value
X4:Pressure	1.71834	1	1.71834	39.24	0.0000
X5:Acid	0.334417	1	0.334417	7.64	0.0172
X6:Time	1.50785	1	1.50785	34.43	0.0001
X4X4	0.00655616	1	0.00655616	0.15	0.7056
X4X5	0.172872	1	0.172872	3.95	0.0703
X4X6	1.16586	1	1.16586	26.62	0.0002
X5X5	1.07678	1	1.07678	24.59	0.0003
X5X6	0.331298	1	0.331298	7.57	0.0176
X6X6	0.138376	1	0.138376	3.16	0.1008
Total error	0.525511	12	0.0437926		
Total (corr.)	7.00074	21			

R-squared = 92.49 percent

R-squared (adjusted for d.f.) = 86.86 percent

Standard Error of Est. = 0.209

The coefficient for variables and its quadratic polynomial equation of the experimental design are presented in Table III-19 and Equation 25-1.

Table III-19: Regression coefficients for glucose yield

Coefficient	Estimate
constant	2.25465
X4:Pressure	0.354715
X5:Acid	-0.156484
X6:Time	0.33228
X4X4	0.0205718
X4X5	0.147
X4X6	0.38175
X5X5	0.263641
X5X6	0.2035
X6X6	-0.0945102

Model fit polynomial equation:

$$Glu = 2.25465 + 0.354715X_4 - 0.156484X_5 + 0.33228X_6 + 0.0205718X_4X_4 + 0.147X_4X_5 + 0.38175X_4X_6 + 0.263641X_5X_5 + 0.2035X_5X_6 - 0.0945102X_6X_6$$

Equation 25-1

Result from equation of fitted model together with actual result was presented in the following table. All observed values were fall within 95% confidence level of lower and upper limit of the mean response. Values obtained from this fitted model were used to develop further the response surface model in order to evaluate general correlation between glucose yield and factors level.

Table III-20: Estimation Results for Glucose

Row	Observed Value	Fitted Value	Lower 95.0% CL for Mean	Upper 95.0% CL for Mean
1	2.4	2.25465	2.09356	2.41573
2	2.046	2.25465	2.09356	2.41573
3	2.093	2.25465	2.09356	2.41573
4	2.244	2.25465	2.09356	2.41573
5	2.393	2.25465	2.09356	2.41573
6	2.409	2.25465	2.09356	2.41573
7	2.226	2.25465	2.09356	2.41573
8	2.239	2.25465	2.09356	2.41573
9	2.534	2.64609	2.27295	3.01923
10	2.126	2.29802	1.92488	2.67116
11	1.544	1.63212	1.25898	2.00527
12	1.812	1.87205	1.49891	2.2452
13	2.253	2.14015	1.76701	2.51329
14	3.46	3.31908	2.94594	3.69222
15	2.165	1.94018	1.56704	2.31333
16	3.872	3.70711	3.33397	4.08026
17	1.66	1.71628	1.36097	2.07159
18	2.891	2.90939	2.55408	3.2647
19	3.307	3.26351	2.9082	3.61882
20	2.619	2.73716	2.38185	3.09247
21	1.711	1.42851	1.0732	1.78382
22	2.189	2.54616	2.19085	2.90147

The statistic for central points was also very good, with 2.256 ± 0.139 together with its maximum and minimum values was fallen within 6.2% of average value as described earlier.

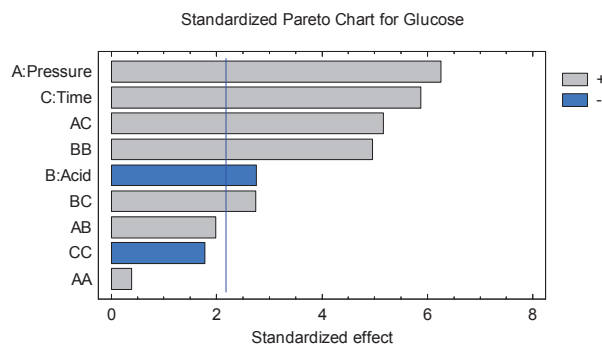


Figure III-21: Pareto chart for effect of treatment factor towards glucose response.

Based on ANOVA and Pareto chart in Figure III-21, there are 3 main factors and 3 interaction factors that were statistically significant that contribute to the glucose autohydrolysis. Temperature (as represented by pressure) was the highest effect, followed by treatment time and acid concentration for main factors. Both temperature and treatment time gives positive effect while an increase in acid concentration will reduce yield of glucose, the magnitude of the increments in yield of glucose for respective main factors is presented in

Figure III-22(a). For interaction effects, combination for temperature-time (X4X6), acid-acid (X5X5) and acid-time (X5X6) give a positive yield glucose increase with an increase in factor combination. Magnitude of increment for X4X6 is presented in Figure III-22(b).

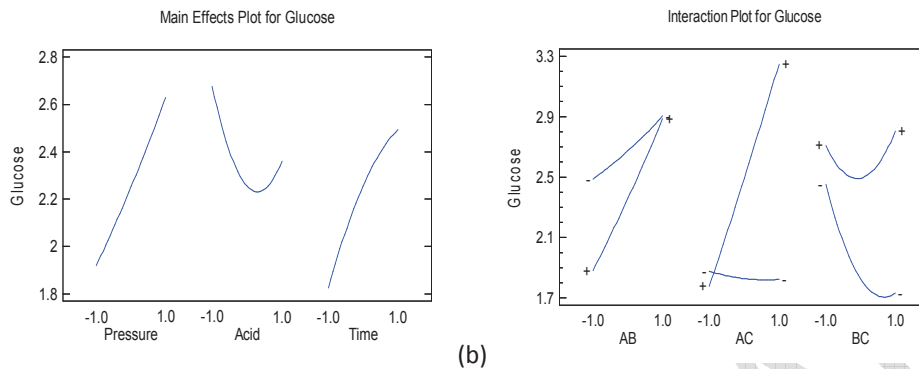


Figure III-22: Main effect and Interaction plots of factor towards glucose response

Response plot obtained from the trial were divided into 3 response surface plots where 2 of parameters were changeable while the 3rd parameters was fixed were presented below. Each plot will be evaluated to understand the effect of treatment combinations towards glucose yield.

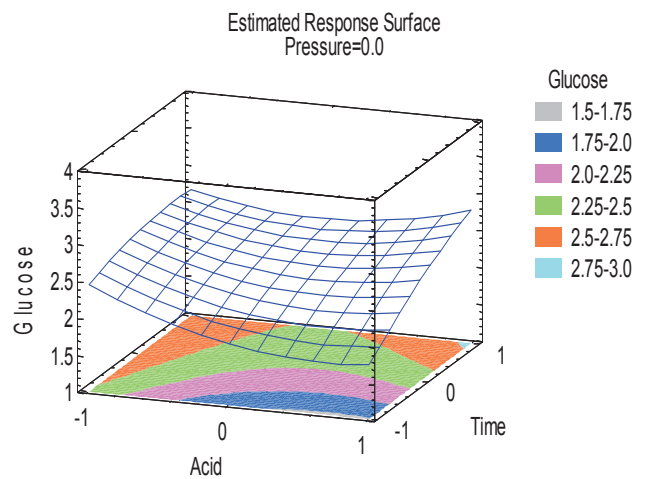


Figure III-23: Estimated response surface, with fix pressure

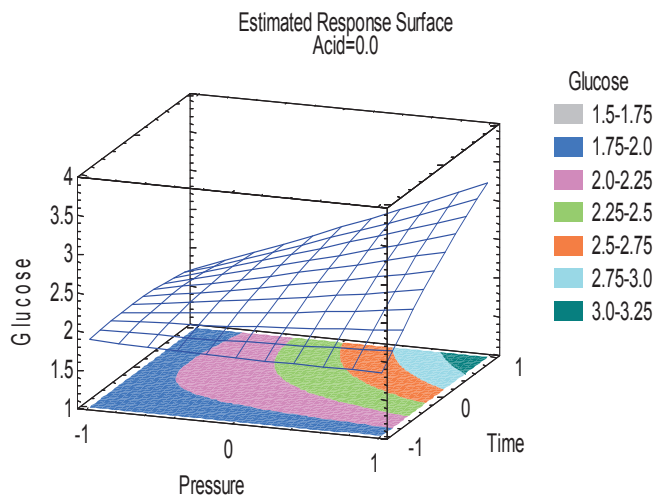


Figure III-24: Estimated response surface, with fix acid

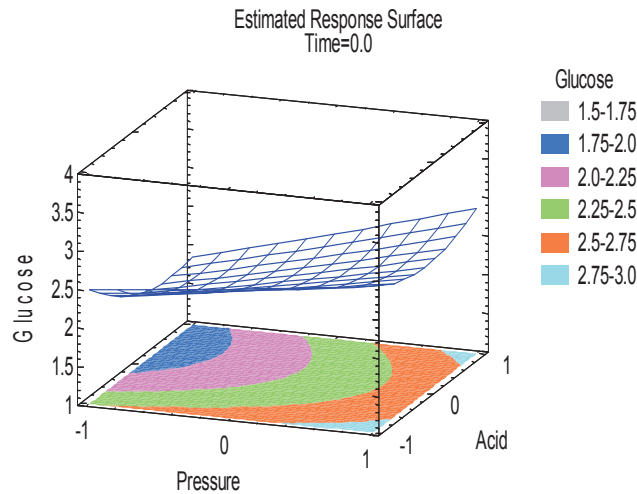


Figure III-25: Estimated response surface, with fix time

Based on Figure III-23, Figure III-24 and Figure III-25, an increase in treatment time (X6) together with an increase in acid concentration (X5) and pressure/ temperature (X4) will increase the yield of glucose. This estimated response was expected due to an increase in atohydrolysis reaction that simultaneously results to an increase in glucose. Glucose yields were in increasing trends for all factors studied due to the limitation of treatment time (X6). Increases in X6 were expected to increase the yield of glucose. To understand this, X6 were use as an estimate factor in the following kinetic study with glucose as a response.

III.2.4.1. Study of Kinetic for Glucose Yield

In order to estimate the kinetic rate of the process for different temperature and different acid concentration, equation of the fitted model was used to generate data corresponding to coded parameters as represented in Table III-15 above. Five acid concentrations of 0.01, 0.02, 0.03, 0.04 and 0.05 molar corresponding to code -1.68, -1, 0, 1 and 1.68 were used to extract kinetic's data and presented in Table III-21 – Table III-25 below.

Model for estimation of glucose from polynomial equation was proposed to follow the consecutive first order reactions as described in I.3.6 Modeling of Glucose Hydrolysis Kinetic in page 42. This was summarized into the following equations:



Final form of consecutive first order kinetic expression to calculate each species with respect to total polysaccharides $[A]_0$, $[A]_t$, $[B]_t$ and $[C]_t$ together with rate constant k_1 and k_2 can be represented as in the following three equations:

$$[A]_t = [A]_0 e^{-k_1 t} \quad \text{Equation 7}$$

$$[B]_t = [A]_0 \frac{k_1}{k_2 - k_1} [e^{-k_1 t} - e^{-k_2 t}] \quad \text{Equation 12}$$

$$[C]_t = [A]_0 \left[1 - \frac{k_1}{k_2 - k_1} e^{-k_1 t} + \frac{k_1}{k_2 - k_1} e^{-k_2 t} \right] \quad \text{Equation 15}$$

As expected, the information on initial material composition or the glucose potential was very important for development of the model. Content of total potential glucose was found to be 800 mg/ g SPW and will be used as A0 through out the calculation of rate constant of the hydrolysis and degradation of glucose. The following data in Table III-21 – Table III-25 were obtained with Equation 25-1 of response surface model based on fix acid concentration.

Table III-21: Data kinetic with acid concentration fix at 0.01 molar

T _{actual} (°C)	143.6	148.8	155.45	161.3	164.95
P _{actual} (bar)	4	4.61	5.5	6.39	6.39
P _{coded}	-1.68	-1	0	1	1.68
Acid _{coded}	-1.68	-1.68	-1.68	-1.68	-1.68
0	0	0	0	0	0
0.50	3.97	3.57	3.01	2.50	2.17
1.01	3.70	3.47	3.18	2.92	2.77
1.75	3.14	3.17	3.26	3.39	3.50
2.49	2.39	2.69	3.16	3.67	4.04
3.00	1.78	2.25	2.98	3.75	4.30

Table III-22: Data kinetic with acid concentration fix at 0.02 molar

T _{actual} (°C)	143.6	148.8	155.45	161.3	164.95
P _{actual} (bar)	4	4.61	5.5	6.39	6.39
P _{coded}	-1.68	-1	0	1	1.68
Acid _{coded}	-1	-1	-1	-1	-1
0	0	0	0	0	0
0.50	2.98	2.65	2.19	1.78	1.52
1.01	2.80	2.65	2.45	2.30	2.22
1.75	2.38	2.49	2.67	2.90	3.08
2.49	1.78	2.14	2.71	3.32	3.76
3.00	1.26	1.80	2.62	3.49	4.11

Table III-23: Data kinetic with acid concentration fix at 0.03 molar.

T _{actual} (°C)	143.6	148.8	155.45	161.3	164.95
P _{actual} (bar)	4	4.61	5.5	6.39	6.39
P _{coded}	-1.68	-1	0	1	1.68
Acid _{coded}	0	0	0	0	0
0	0	0	0	0	0
0.50	1.97	1.74	1.43	1.16	1.01
1.01	1.93	1.88	1.83	1.82	1.84
1.75	1.72	1.92	2.25	2.63	2.91
2.49	1.31	1.78	2.49	3.25	3.79
3.00	0.93	1.57	2.55	3.56	4.28

Table III-24: Data kinetic with acid concentration fix at 0.04 molar

T _{actual} (°C)	143.6	148.8	155.45	161.3	164.95
P _{actual} (bar)	4	4.61	5.5	6.39	6.39
P _{coded}	-1.68	-1	0	1	1.68
Acid _{coded}	1	1	1	1	1
0	0	0	0	0	0
0.50	1.49	1.36	1.19	1.08	1.02
1.01	1.59	1.63	1.73	1.87	1.99
1.75	1.58	1.88	2.36	2.88	3.26
2.49	1.38	1.94	2.80	3.71	4.35
3.00	1.13	1.87	3.00	4.16	4.97

Table III-25: Data kinetic with acid concentration fix at 0.05 molar

T_{actual} ($^{\circ}\text{C}$)	143.6	148.8	155.45	161.3	164.95
P_{actual} (bar)	4	4.61	5.5	6.39	6.39
P_{coded}	-1.68	-1	0	1	1.68
$\text{Acid}_{\text{coded}}$	1.68	1.68	1.68	1.68	1.68
0	0	0	0	0	0
0.50	1.46	1.40	1.34	1.32	1.33
1.01	1.66	1.77	1.97	2.21	2.39
1.75	1.78	2.15	2.74	3.36	3.80
2.49	1.72	2.35	3.32	4.32	5.03
3.00	1.57	2.38	3.60	4.87	5.75

Data obtained from Table III-21 – Table III-25 above were plotted as kinetic expressions to calculate k_1 and k_2 of each system using A_0 of 20 mg/g. Lower value of A_0 was used as a very small amount of glucose were produced, this decision was taken due to the fact that no glucose degradation was occurred in this treatment after inspection of HPLC chromatogram obtained from the experiment.

The only 'degradation' at this level of DIC severity that could occur was the transformation of starch into oligosaccharides. This could prompt for a development of a different model against present starch to glucose hydrolysis that was currently discussed. A specific method such as the study of intrinsic viscosity of starch solution obtained from treatment may be able to dictate the level of transformation of starch into the lower degree of molar of polymer or oligosaccharides. This information is further explained in future work, i.e. the development of a kinetic model based on change in DP of starch.

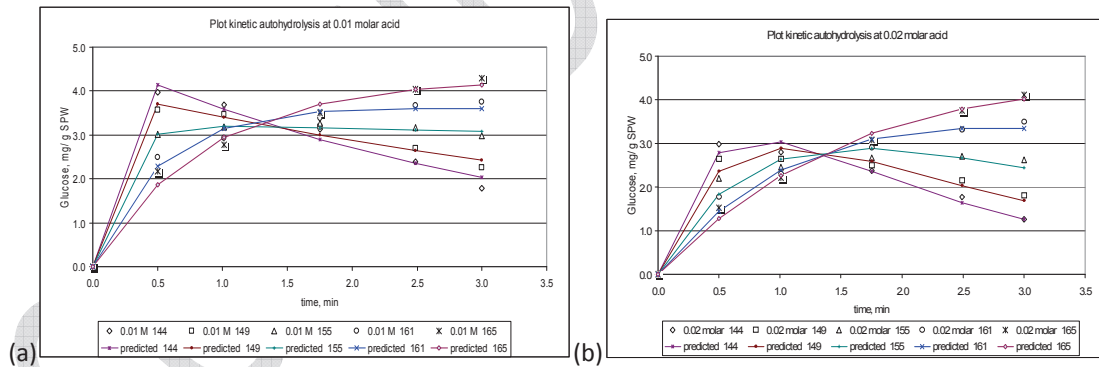


Figure III-26: Plot kinetic autohydrolysis for (a) 0.01 and (b) 0.02 molar acid

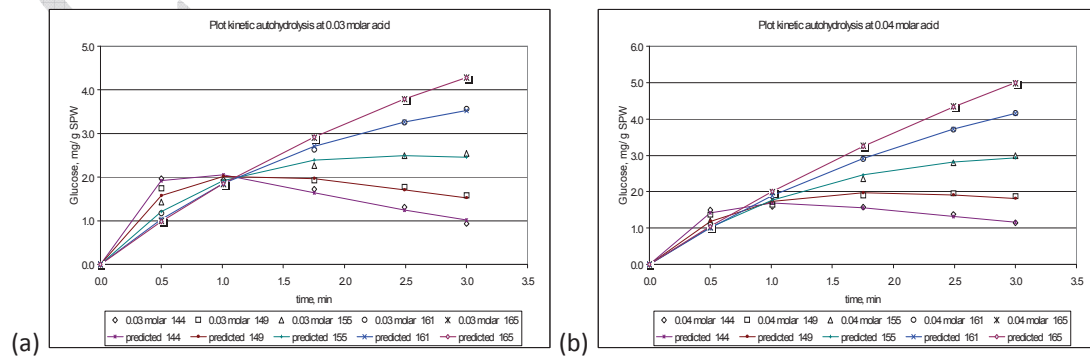


Figure III-27: Plot kinetic autohydrolysis for 0.03 and 0.04 molar acid

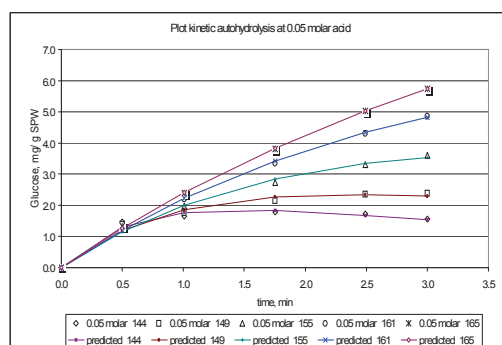


Figure III-28: Plot kinetic autohydrolysis for 0.05 molar acids

With this we can summarize that, sufficient information was needed, i.e. information on treatment severity from glucose degradation through inspection on HPLC chromatogram before fitting of the experimental data and their respective kinetic model can be developed. Based on that information, value of A_0 that was decided was very low compared to the actual total polysaccharides that were available in SPW.

Plot of Figure III-26 to Figure III-28 obtained from calculated data using fitted polynomial equation were fitted into their respective predicted points obtained using a kinetic model. Values of respective rate constant based on acid concentration of 0.01, 0.02, 0.03, 0.04 and 0.05 molar were presented in the following table. Data fit of a kinetic predicted model were based on minimization of sum of square difference between data in table 6 to table 10 against data generated from equation for respective treatment. Excel tools "Solver" was used to minimize the sum of square with change in k_1 and k_2 . With this method, both rate constant for starch hydrolysis (k_1) and glucose degradation (k_2) were obtained simultaneously.

Data fit for kinetic models at different acid concentration was found to have a good fit between polynomial equation data and kinetic equations.

III.2.4.2. Rate Constant and Activation Energy for the Model

Table III-26: Rate constant for glucose generation (k_1) and glucose degradation (k_2) at temperature 149, 155, 161 and 165°C for acid concentration 0.01, 0.02, 0.03, 0.04 and 0.05 molar.

Temperature	143.6	148.8	155.45	161.3	164.95
A_0	20	20	20	20	20
0.01 molar					
k_1	638.706×10^{-3}	513.9456×10^{-3}	365.3570×10^{-3}	259.6382×10^{-3}	209.907×10^{-3}
k_2	1745.868×10^{-3}	1552.548×10^{-3}	1193.2669×10^{-3}	809.1016×10^{-3}	570.417×10^{-3}
0.02 molar					
k_1	539.955×10^{-3}	402.952×10^{-3}	259.9526×10^{-3}	177.64765×10^{-3}	145.719×10^{-3}
k_2	2225.864×10^{-3}	1812.386×10^{-3}	1171.2809×10^{-3}	648.2344×10^{-3}	387.335×10^{-3}
0.03 molar					
k_1	400.268×10^{-3}	257.1541×10^{-3}	154.0241×10^{-3}	115.1248×10^{-3}	104.092×10^{-3}
k_2	2780.417×10^{-3}	1807.4753×10^{-3}	846.0320×10^{-3}	348.2599×10^{-3}	149.096×10^{-3}
0.04 molar					
k_1	257.209×10^{-3}	166.8399×10^{-3}	120.3707×10^{-3}	108.71267×10^{-3}	108.37×10^{-3}
k_2	2306.342×10^{-3}	1.2402599×10^{-3}	519.1193×10^{-3}	195.9299×10^{-3}	68.812×10^{-3}
0.05 molar					
k_1	204.418×10^{-3}	154.0483×10^{-3}	130.6144×10^{-3}	128.7959×10^{-3}	133.04×10^{-3}
k_2	1633.205×10^{-3}	914.1084×10^{-3}	422.2999×10^{-3}	185.8306×10^{-3}	88.273×10^{-3}

An assessment of the rate constant k_1 in Table III-26 shows for all acid concentrations it was observed that its values were decreased with an increase in temperature (eg. for 0.01 molar, value decreased from 0.638 min^{-1} at 144°C to 0.209 min^{-1} at 165°C). At the same time, for an increase in acid concentration, corresponding k_1 values were decreased in similar pattern (eg. for 144°C , value decreased from 0.638 min^{-1} at 0.01 molar to value decreased from 0.204 min^{-1} at 0.05 molar). This indicates that a rates of reaction decrease with an increase in temperature and acid for that particular acid concentration. This was also led to negative activation energy for the process respective process, which shows the probability for reaction to occur was barrier-less.

Table III-27: Activation energy, E_a (kJ/ mole) for different acid concentration.

Acid concentration	0.01 molar	0.02 molar	0.03 molar	0.04 molar	0.05 molar
$E_a \text{ Glu}_{\text{generation}}$	-79.70	-94.68	-97.29	-60.60	-29.48
R^2	0.9945	0.9989	0.9792	0.8909	0.7623
$E_a \text{ Glu}_{\text{degradation}}$	-78.03	-122.52	-203.31	-240.36	-202.24
R^2	0.9413	0.9536	0.9674	0.9715	0.9859

Activation energy has been defined as the energy that has to be overcome (also known as the potential barrier) in order for any chemical reaction to occur. Positive activation energy means that reactions were kept from occurring until that amount of energy was obtained from surrounding or environments. Lowering of activation energy usually need an addition of catalyst or reaction at a higher temperature. In this case, a negative activation energy concept cannot be used to explain the phenomenon, due to 'activation' cannot be negative. However, if we look into overall trends of Table III-27, there was an increase in activation energy i.e. -97.29 kJ/mole (at 0.03 molar acids) to -29.48 kJ/mole (at 0.05 molar acids). This means that there was about 67 kJ/mole increase in energy for reaction to occur between those two points.

In a similar way, for rate constant k_2 , at 0.03 molar and 0.01 molar, there was a difference of 125 kJ/ mole between both conditions. This means that there is huge degradation at much lower acid concentration than at higher acid concentration due to a limited amount of glucose was produced at lower acid concentration, but its degradation was bigger than glucose production. However, in actual determination, the degradation of glucose was not being able to be observed in the chromatogram due to very small concentration was produced. This situation was believed due to a majority of changes that was occurred during DIC pretreatment was involved with gelatinization and due to shorter treatment time, autohydrolysis into glucose and glucose degradation products was not able to proceed.

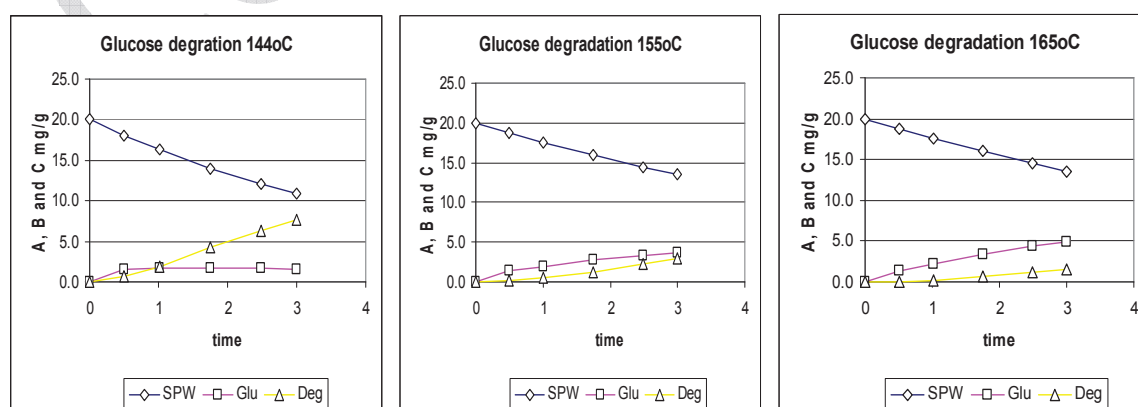


Figure III-29: Glucose degradation model for different temperatures at 144°C , 155°C and 165°C . At lower temperature, glucose degradation was bigger than at higher temperature.

The above explanations can be associated to the following model plots at 144°C, 155°C and 165°C for degradation of glucose across temperature range (Figure III-29). The following model plot was the degradation of glucose at various acid concentrations namely at 0.01 molar, 0.03 molar and 0.05 molar at 165°C (Figure III-30). Data point was extracted from experimental design model using polynomial equation described earlier. Note on the behavior of degradation points in each plot across the increase in temperature (in Figure III-29) and across the increase in acid concentration (in Figure III-30). The amount of glucose and degradation products was small and adjustment was done during HPLC determination with higher volume injection.

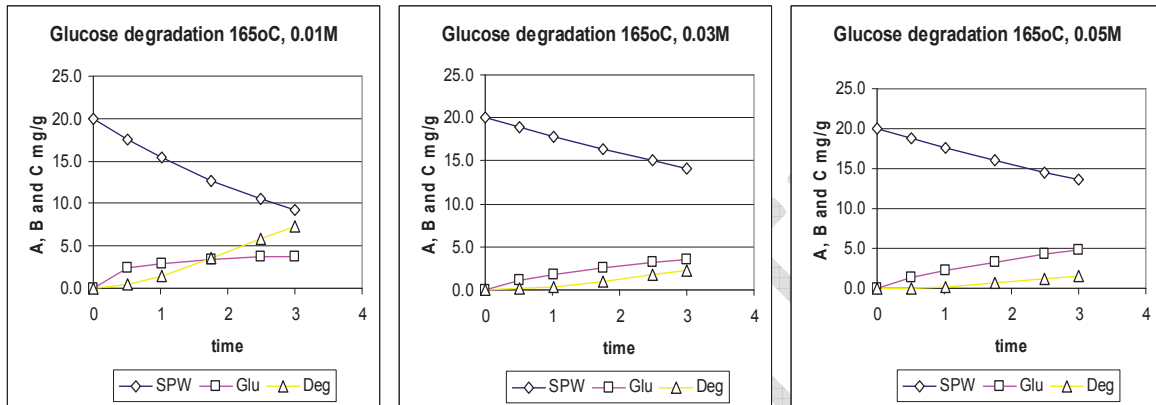


Figure III-30: Glucose degradation model for different acid concentration 0.01 molar, 0.03 molar and 0.05 molar at 165°C. At lower acid concentration, glucose degradation was bigger than at higher acid concentration.

From Figure III-29, the effects of temperature at a fix acid concentration on the degradation of glucose; it was observed that at a relative low temperature at 144°C, the degradation was higher than at a high temperature seems to indicate that rapid increase of glucose degradation products in function of time. Quantitatively more degradation products also generated at a low temperature. This may suggest that acid concentration is the limiting factor rather than the temperature for low DIC severity conditions. With the change in temperature at fix acid concentration, it will not affect the degradation. However, since data of this kinetic model was obtained from RSM models, further analyses with actual experiments were needed to establish the actual experimental data.

Figure III-30, was about the increase in acid concentration at fix temperature 165°C to study the glucose degradation product formation and the conversion of polysaccharides into glucose. It was observed that glucose degradation was acid dependent and glucose generation was stable; this shows that process was an acid dependent for degradation but temperature was more dominating factors in the case for the short treatment time with DIC.

Model kinetics for each temperature were verified using the F Distribution Statistic at P 0.05 and was found to be significant and can be accepted as in the following table.

Table III-28: Statistical data for model based on temperature

Group	No of points	No of param.	SS diff	SS total	R ²	F _{calc}	10F _{table}	F _{calc} >> 10F _{table}
144	30	5	0.51	411.30	0.99875	667.61	27	Yes
149	30	5	0.68	6,006.57	0.99989	7,318.45	27	Yes
155	30	5	0.84	514.29	0.99836	507.28	27	Yes
161	30	5	0.65	608.00	0.99836	777.17	27	Yes
165	30	5	0.41	688.31	0.99940	1,384.25	27	Yes

III.2.5. Conclusion

The study of polysaccharide's conversion with DIC treatment with low DIC severity shows that LMW oligosaccharides can be obtained together with small fraction of glucose. The result obtained in this work shows that hydrolysis of starch into glucose in DIC pretreatment was following the first order kinetic reactions. This will associate the dependent of substrate concentration for a high reaction rate and at the same time suggest that high degradation will be contributed by a prolonged reaction time.

Present DIC autohydrolysis produce a very small amount of glucose (i.e. less than 1%) and need further improvement. Very low hydrolysis process of starch into glucose was observed, the most severe treatment only able to generate about 6 mg/g SPW only. Kinetic model was developed and provided kinetic data input to understand the underlying principles of autohydrolysis during DIC treatment.

Response surface and contour plot for glucose yield suggest that with an increase in time at fix steam pressure (temperature) in Figure III-23 and fix acid concentration in Figure III-24 the yield of glucose will increase. Acid was found to be a limiting reaction factor for both an increase in steam pressure (temperature) and during an increase in treatment time, i.e. similar to finding of the kinetic model. An increase in temperature, acid concentration and treatment time is expected to increase the constant rate, k_1 . In present work rate constant of the hydrolysis of starch only involve only the alpha bond and an increase in DIC severity will include cellulose (beta bond) hydrolysis.

Kinetic models used in this study were able to fit data obtained from the quadratic polynomial model obtained from experimental design. However, due to the limitation of maximum temperature for DIC system used, only treatment time and acid concentration will be studied further in the next experimental design studies.

Paper 4: (i) Optimization of DIC process at High DIC severity condition for the conversion of polysaccharides/crude starch to glucose by RSM (ii) Development of kinetic model of polysaccharides/crude starch conversion under High DIC severity process.

Abstract

Central composite design (CCD) was used to study the effect of hydrolysis using higher acid concentration and longer treatment time with 22 experimental points. Polynomial equation obtained from CCD was used to generate response surface model and new set of consecutive first order kinetic data similar to lower DIC severity studies. Data obtained was used to calculate the rate constant for glucose generation and its degradation. F statistic result shows only two models were statistically fit to data obtained from polynomial equation. Both models were at near the optimum factors' level. Higher A_0 values were used for development of the hydrolysis kinetic model for detailing both glucose generation and degradation. Highest glucose amount generated in this study was 400 mg/g, about 67% of available starch or about 50% of available total polysaccharides. At much higher severity of DIC treatment combinations, both starch and cellulose were converted into glucose with some fraction of glucose degradation. This information shows that glucose degradation can be minimized with short treatment time. Rate constant for polysaccharide's autohydrolysis to glucose (k_1) and glucose degradation (k_2) was obtained using kinetic models developed from data of response surface.

III.2.6.Objective

This work continues the previous optimization of total polysaccharide's conversion into glucose at High DIC severity through RSM by an increase the level of treatment factors, i.e. treatment time, temperature and acid concentration. The nature and magnitude of treatment factors that influence the formation of glucose were evaluated. Kinetic model based on empirical data from RSM polynomial equation also was developed in order to find important kinetic data at high DIC severity combinations.

III.2.7.Introduction

Present work was run in a similar way as in low DIC severity pretreatment, except two factors were increased its level in order to obtain the maximum glucose yield from SPW. An enhanced central composite design (CCD) similar to earlier low DIC severity work was used, except two factors were increased into higher level for acid and treatment time as suggested in low DIC severity ANOVA result. All three main factors in low DIC severity CCD study was found to have positive effect on glucose yield if the level for each factor were increased as presented in Figure III 20 except for acid concentration. In the exploratory study also, a similar conclusion was found. However, due to the limitation of the system, only two factors, i.e. treatment time and acid concentration will be increased its level. Pressure/ temperature of treatment will be based on the existing maximum level permitted by the DIC system. For present work, initial moisture content (X1) was fixed at 150% for all treatments. Three other factors: treatment time (X4), acid concentration (X5), and treatment pressure/ temperature (X6) were established according to Table III-29.

III.2.8. Material and Method

III.2.8.1. Material Preparation

Material (SPW) was prepared according to Table III-29 and Table III-30. DIC pretreatment was done based on the experimental design described in Table III-30. Detail procedure and calculation for moisture content and acid concentration adjustment was presented in Part 2 of this thesis.

Glucose in hot water extract was analyzed and quantified with HPLC system as described earlier. Experimental data points were further analyzed with response surface methodology. Details of hot water extraction procedure, hydrolysate preparation and HPLC system used in this study were described earlier in Part 2 of this thesis.

III.2.8.2. Experimental Design

Similar experimental design as described in low DIC severity pretreatment was used in this study with factors and its level as presented in Table III-29 and Table III-30. Data obtained from experimental will be fitted into polynomial equation using numerical technique as described by commercial statistical software Statgraphics. Analysis of variance for response is calculated and presented as Pareto chart, with R^2 is targeted more than 90%.

Polynomial second degree quadratic equation for the model was represented by the following equation:

$$Y_{Glu} = b_{k0} + \sum_{i=1}^3 b_{ki} X_i + \sum_{i=1}^3 b_{ii} X_i^2 + \sum_{i \neq j=1}^3 b_{kij} X_i X_j \quad \text{Equation 25}$$

With b_{k0} as the value of fitted response of central points (0,0,0), b_{ki} , b_{ii} and b_{kij} , were the linear, quadratic and interaction regression terms respectively. Single polynomial equation obtained is product of regression analysis will be used later to estimate effect of hydrolysis kinetic of the process. Response surface and contour plots for model based on polynomial equation were plotted as a function of any two variables at a time. A total three response surface and contour plots were available for this work.

Table III-29: Actual parameters and its coded form for independent variable of central composite design

Factors	Pressure, bar	[acid], M	Time, min	As
represented by:	X4	X5	X6	Coded form
Point max (+ α)	7.00	0.20	10.00	1.682
Point min (- α)	4.00	0.05	3.00	-1.682
Point central (0)	5.50	0.13	6.50	0
Point (-1):	0.89	0.04	2.08	-1
Point (+1):	4.61	0.08	4.42	+1

III.2.9. Result and Discussion

As shown in Table III-30, the formation of glucose follows a similar trend as in the exploratory study, whereby about 30% of the total polysaccharides was converted into glucose at its central point's combination. Glucose yield obtained was much higher than with low DIC severity combinations.

Table III-30: CCD experimental design in its coded and actual level (not in random order) with its respective glucose response and percentage of total polysaccharide.

No	Coded form			Actual level			Glucose mg/ g SPW	Glucose (%potential Glu)
	X4	X5	X6	X4	X5	X6		
1	0	0	0	5.50	0.13	6.50	215.296	26.91%
2	0	0	0	5.50	0.13	6.50	254.236	31.78%
3	0	0	0	5.50	0.13	6.50	257.882	32.24%
4	0	0	0	5.50	0.13	6.50	200.169	25.02%
5	0	0	0	5.50	0.13	6.50	280.743	35.09%
6	0	0	0	5.50	0.13	6.50	244.758	30.59%
7	0	0	0	5.50	0.13	6.50	229.715	28.71%
8	0	0	0	5.50	0.13	6.50	268.499	33.56%
9	-1	-1	-1	4.61	0.08	4.42	24.284	3.04%
10	1	-1	-1	6.39	0.08	4.42	59.079	7.38%
11	-1	1	-1	4.61	0.17	4.42	220.389	27.55%
12	1	1	-1	6.39	0.17	4.42	292.442	36.56%
13	-1	-1	1	4.61	0.08	8.58	44.114	5.51%
14	1	-1	1	6.39	0.08	8.58	55.953	6.99%
15	-1	1	1	4.61	0.17	8.58	381.732	47.72%
16	1	1	1	6.39	0.17	8.58	220.111	27.51%
17	-1.682	0	0	4.00	0.13	6.50	39.378	4.92%
18	1.682	0	0	7.00	0.13	6.50	196.880	24.61%
19	0	-1.682	0	5.50	0.05	6.50	17.634	2.20%
20	0	1.682	0	5.50	0.20	6.50	357.293	44.66%
21	0	0	-1.682	5.50	0.13	3.00	38.988	4.87%
22	0	0	1.682	5.50	0.13	10.00	132.296	16.54%

Summary of statistic for central points with unit of mg/ g glucose yield:

Total	1,951.30	Min (all)	17.63
Average	243.91	Max (all)	381.73
Std dev	27.25	Median star/ factorial	139.59
Min	200.17	Median axis	85.84
Max	280.74		

The statistical analysis for central points shows that standard deviation was within 11.2%, which shows an overall representative for this set of experimental data. On the average about 30.5% of total polysaccharides were converted into glucose at the central point combination. The result may suggest that glucose formed may exhibit a non linear relationship with respect to temperature, time and acid concentration levels. Calculated central points and average central points were 242.97 and 243.91 respectively, while the median for star and axis was 139.54 and 85.84 respectively, i.e. very far and towards the lower end of average value of calculated and experimental central points. This observation may suggest that glucose yield were skewed towards the lower value due to several factors such as degradation of glucose itself (refer to Figure III-20, which summarize the overall result). This was somehow in contrast to lower treatment severity; whereby the central points were located in between median of star and axis points. This response surface model will not be able to fulfill three constraint set-out for the kinetic model data mining as it was skewed towards one end point for several experimental group. Only selected kinetic model that fulfills all three constraints will be presented.

Internal kinetic evaluations need to be conducted using available data of this experimental design to understand its hydrolysis kinetic and for optimization of glucose yield. Similarly, several criteria were needed to be established to ensure that data, and its model obtained from this trial can be use to generate kinetic data within the range of experimental design.

Analysis of variance for the fitted model (Table III-31) was found with very high correlation with R^2 of more than 90% for model and experimental data, suggesting that experimental data is very significant to the model obtained. This suggested that equation obtained from this model can be used to estimate other responses required for internal analysis of the process itself such as to calculate constant of rate of hydrolysis (k_1) and rate of degradation of glucose (k_2) which is crucial for the optimization of the process and to understand the underlying principle of hydrolysis and degradation.

Table III-31: Analysis of Variance for Glucose for fitted model, cell with grey color was with significant value.

Source	Sum of Squares	Df	Mean Square	F-Ratio	P-Value
X4:Pressure	3607.16	1	3607.16	1.66	0.2217
X5:Acid	165298.	1	165298.	76.13	0.0000
X6:Time	5050.95	1	5050.95	2.33	0.1531
X4X4	20529.9	1	20529.9	9.45	0.0096
X4X5	2318.87	1	2318.87	1.07	0.3218
X4X6	8232.37	1	8232.37	3.79	0.0753
X5X5	2190.07	1	2190.07	1.01	0.3351
X5X6	653.556	1	653.556	0.30	0.5933
X6X6	35528.9	1	35528.9	16.36	0.0016
Total error	26056.6	12	2171.38		
Total (corr.)	266957.	21			

R-squared = 90.24 percent

R-squared (adjusted for d.f.) = 82.92 percent

Standard Error of Est. = 46.59

The coefficient for variables and its quadratic polynomial equation of the experimental design are presented in Table III-32 and its fitted Equation 25-2.

Table III-32: Regression coefficients for glucose yield.

Coefficient	Estimate
constant	242.974
X4:Pressure	16.252
X5:Acid	110.017
X6:Time	19.2314
X4X4	-36.4034
X4X5	-17.0253
X4X6	-32.0787
X5X5	-11.8899
X5X6	9.0385
X6X6	-47.8893

Model fit polynomial equation:

$$Glu = 242.974 + 16.252X_4 + 110.017X_5 + 19.2314X_6 - 36.4034X_4^2 - 17.0253X_4X_5 - 32.0787X_4X_6 - 11.8899X_5^2 + 9.0385X_5X_6 - 47.8893X_6^2$$

Equation 25-2

Results from equation of fitted model together with its actual result are presented in Table III-33. All observed values were fall within 95% confidence level of lower and upper limit of

the mean response. Values obtained from this fitted model were used to develop further the response surface model to evaluate general correlation between glucose yield and factors level.

Table III-33: Estimation Results for Glucose

Row	Observed Value	Fitted Value	Lower 95.0% CL for Mean	Upper 95.0% CL for Mean
1	215.296	242.974	207.104	278.843
2	254.236	242.974	207.104	278.843
3	257.882	242.974	207.104	278.843
4	200.169	242.974	207.104	278.843
5	280.743	242.974	207.104	278.843
6	244.758	242.974	207.104	278.843
7	229.715	242.974	207.104	278.843
8	268.499	242.974	207.104	278.843
9	24.284	-38.7745	-121.863	44.3144
10	59.079	91.9375	8.84859	175.027
11	220.389	197.232	114.143	280.321
12	292.442	259.843	176.754	342.932
13	44.114	45.7688	-37.3201	128.858
14	55.953	48.1659	-34.9231	131.255
15	381.732	317.93	234.841	401.019
16	220.111	252.226	169.137	335.315
17	39.378	112.677	33.5594	191.795
18	196.88	167.342	88.2244	246.46
19	17.634	24.3193	-54.7984	103.437
20	357.293	394.369	315.251	473.487
21	38.988	75.1794	-3.93829	154.297
22	132.296	139.866	60.7482	218.984

The statistic for central points was also good, with 243.912 ± 27.249 together with its maximum and minimum values was fallen within 11.2% of average value as described earlier.

Based on results in ANOVA Table III-31 and Pareto chart in Figure III-31, only 1 main factor and 2 interaction factors were statistically significant that contribute to the polysaccharides autohydrolysis to glucose. Acid concentration was with the highest effect that gave positive effect to the yield of glucose; the magnitude of the increments in yield of glucose for respective main factors is presented in Figure III-32(a). For interaction effects, combination for time-time (X6X6) and temperature-temperature (X4X4) was found to give negative yield glucose with an increase in factor combination. Magnitudes of effect for interactions were presented in Figure III-32(b).

Mechanisms of autohydrolysis of polysaccharides into glucose as explained before have suggested that all main factors such as acid concentration, treatment time and treatment temperature plays very significant roles to the glucose yield. The effect of acid concentration at higher severity of treatment as observed in this study is in contrast to the previous study at lower severity treatment. At lower severity, it was found that increase in acid concentration will decrease glucose yield; while at higher severity, an increase in acid was found to increase glucose yield, which was similar to finding in OFAT study earlier.

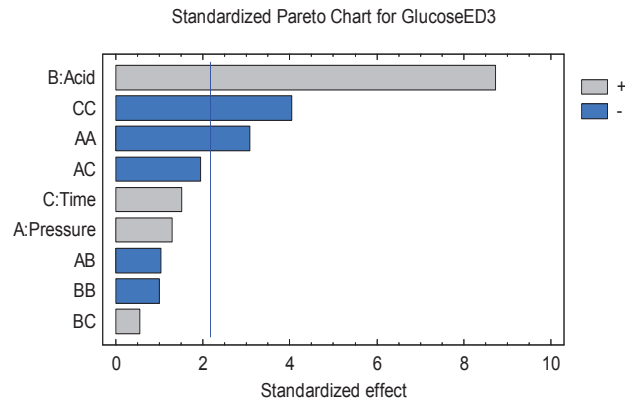


Figure III-31: Pareto chart for effect of treatment factor towards glucose response.

The mechanism of starch conversion to glucose was suggested involves two steps conversion before glucose as a final product could be obtained [166, 167]. Since two steps conversion means a longer time would be required, results for lower treatment severity may suggest that increase in treatment time will increase glucose yield, and subsequently, both acid and treatment time becomes correlated to each other. This combination was utilized during higher treatment severity to improve further yield of glucose as suggested in Figure III-32(b) which shows BC (i.e. acid-time) may increase the yield of glucose at both high and low factors level.

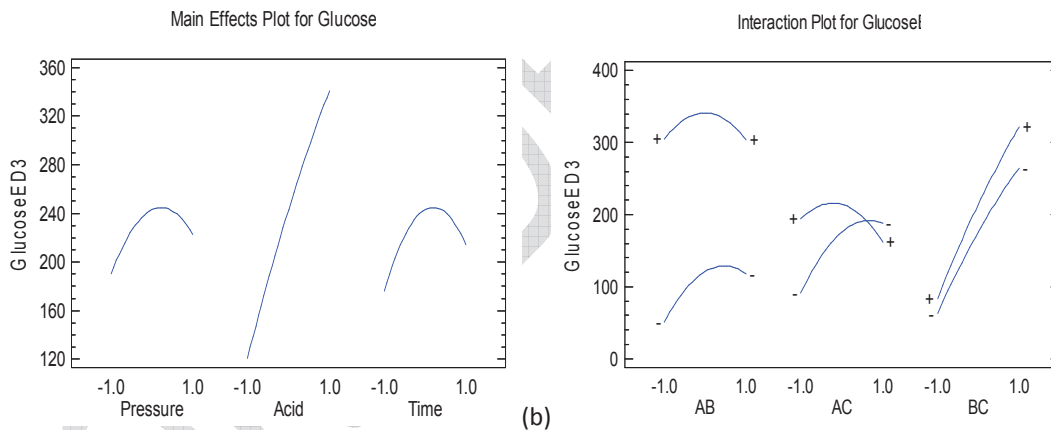


Figure III-32: Main effect and Interaction plots of factor towards glucose response

At higher treatment severity studied in this chapter, certain treatment condition such acid concentration was high enough to influence the two steps conversion. Together with longer treatment time we can expect the higher yield of glucose can be produced. It was reported earlier that the enzymic conversions of starch into lower DP were also affected by the composition of starch (amylose: amylopectin ratio) [167].

In the case of crude sago starch, we also observed the existence of some granular starch that remains intact after high severity DIC treatment combination as presented in Figure III-33. This may suggest the starch granules may behave like resistant starch; a type of starch needed in a human diet. This may indicate the existence of resistant starch in native sago starch. Further works such as isolation of this type of starch were required.

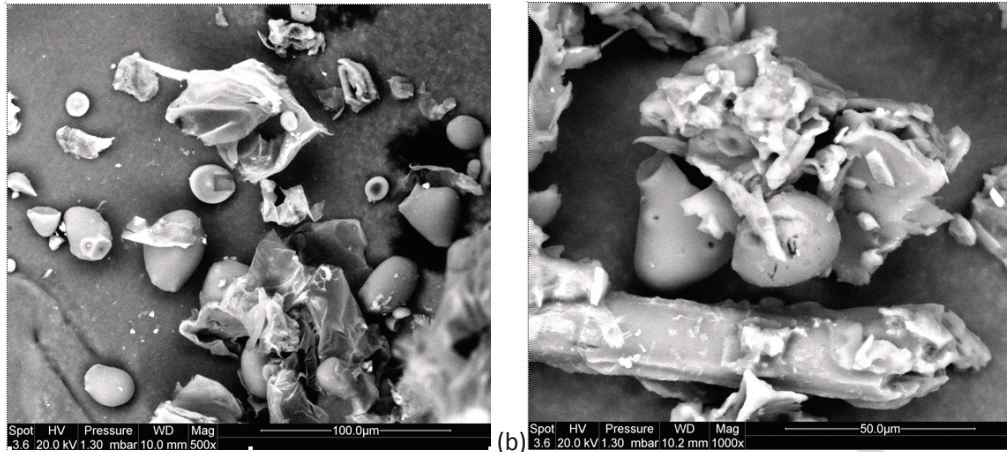


Figure III-33: ESEM of (a) crude starch and (b) DIC treated at high severity combination center point combination with X1:150%. Note in (b) for the modification of starch granules surface due to hydrolysis of granules surface with acid in combination with high temperature treatment.

Response plot obtained from the trial were divided into 3 response surface plots where 2 of parameters were changeable while the 3rd parameters was fixed as presented below. Each plot will be evaluated to understand the effect of treatment combinations towards glucose yield.

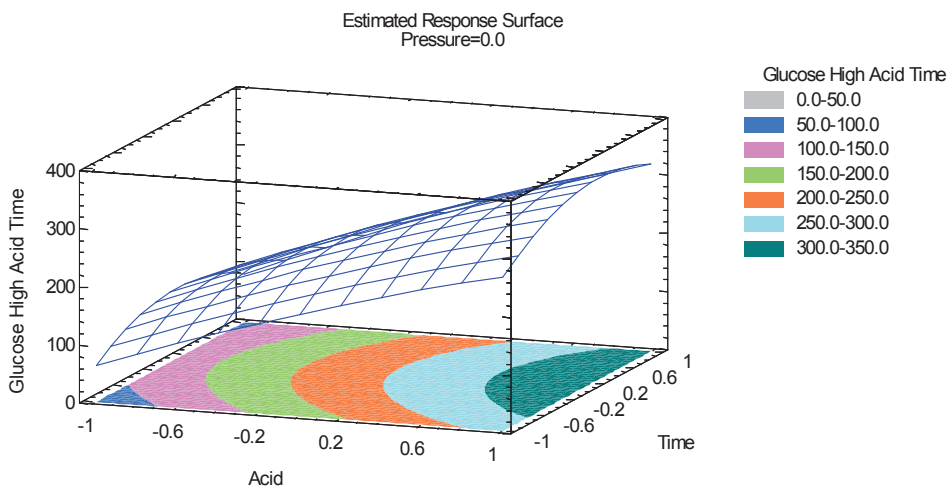


Figure III-34: Estimated response surface, with fix pressure

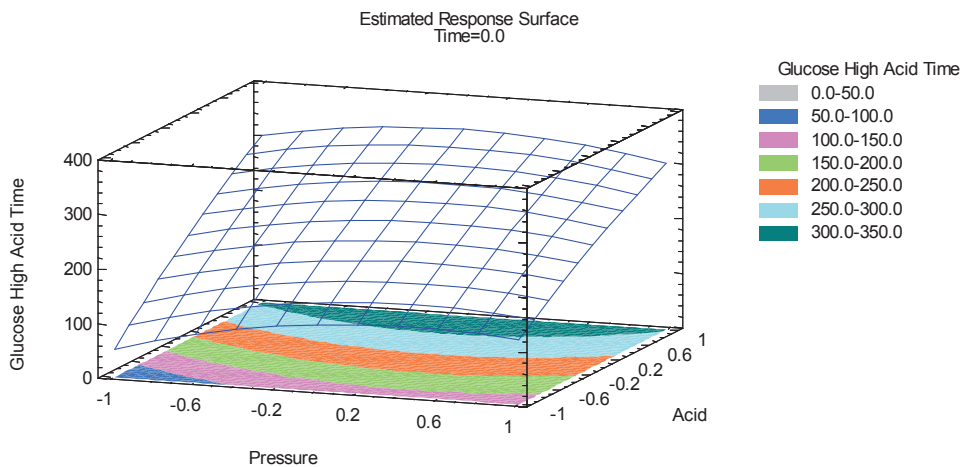


Figure III-35: Estimated response surface, with fix time

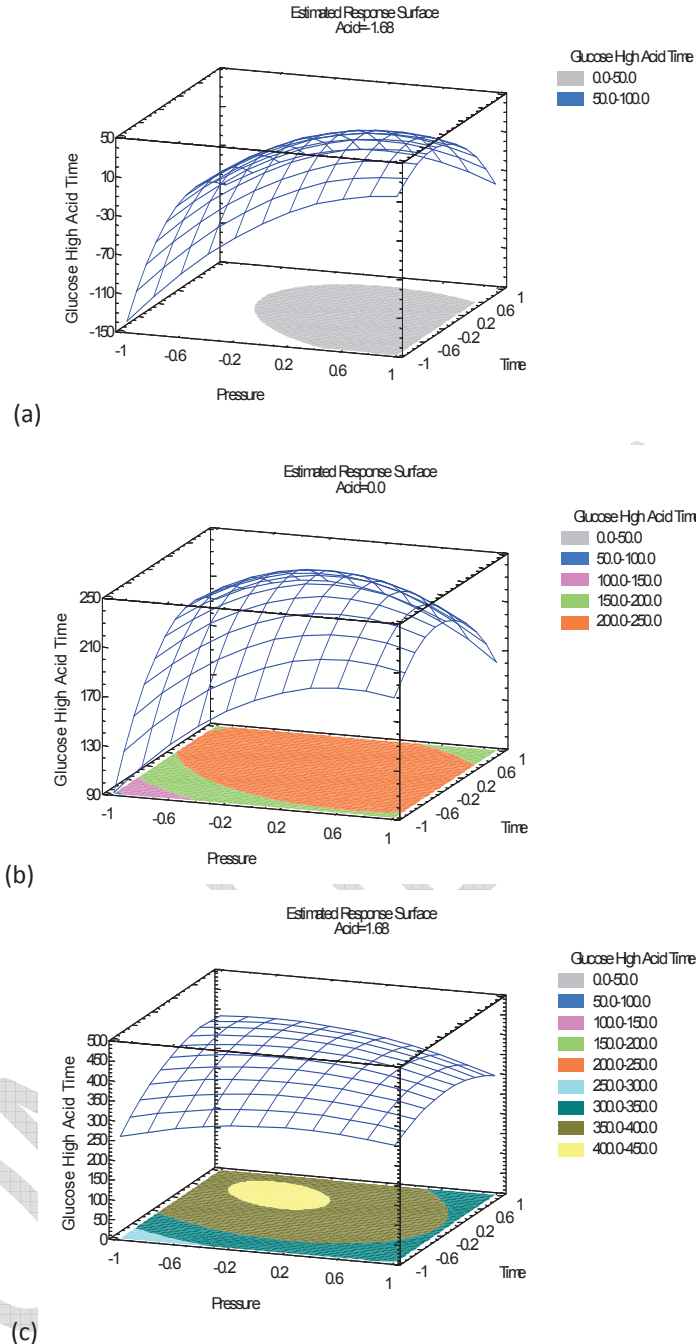


Figure III-36: Estimated response surface, with fix acid at (a) $-\alpha$, (b) central point and (c) $+\alpha$. Acid concentration was the single main effect that significant in this study.

Based on Figure III-34, Figure III-35 and Figure III-36; with an increase in treatment time (X6) together with an increase in acid concentration (X5) and pressure/temperature (X4) will increase the yield of glucose. This estimated response was expected due to enhancement of autohydrolysis reaction resulting in an increase in glucose formation. Glucose yields were exhibited an increasing trend for all factors studied due to the limitation of treatment time (X6). Increases in X6 were expected to increase the yield of glucose. To understand this, X6 were use as an estimate factor in the following kinetic study with glucose as a response.

III.2.9.1. Study of Kinetic for Glucose Yield

In order to estimate kinetic rate of the process for different temperature and different acid concentration, equation of the fitted model was used to generate data corresponding to coded parameters as represented in Table III-30 above. Four acid concentrations of 0.01, 0.02, 0.03, 0.04 and 0.05 molar corresponding to code -1.68, -1, 0, 1 and 1.68 were used to extract kinetics data and presented in Table III-34 to Table III-38 below.

Model for estimation of glucose from polynomial equation was proposed to follow the consecutive first order reactions as described in I.3.6 Modeling of Glucose Hydrolysis Kinetic in page 42. This was summarized into the following equations:



Final form of consecutive first order kinetic expression to calculate each species with respect to total polysaccharides $[A]_0$, $[A]_t$, $[B]_t$ and $[C]_t$ together with rate constant k_1 and k_2 can be represented as in the following three equations:

$$[A]_t = [A]_0 e^{-k_1 t} \quad \text{Equation 7}$$

$$[B]_t = [A]_0 \frac{k_1}{k_2 - k_1} [e^{-k_1 t} - e^{-k_2 t}] \quad \text{Equation 12}$$

$$[C]_t = [A]_0 \left[1 - \frac{k_1}{k_2 - k_1} e^{-k_1 t} + \frac{k_1}{k_2 - k_1} e^{-k_2 t} \right] \quad \text{Equation 15}$$

The following data in Table III-34 to Table III-38 were obtained with Equation 25-2 of response surface model based on fix acid concentration.

Table III-34: Data kinetic with acid concentration fix at 0.05 molar

T _{actual} (°C)	143.6	148.8	155.45	161.3	164.95
P _{actual} (bar)	4	4.61	5.5	6.39	6.39
P _{coded}	-1.68	-1	0	1	1.68
Acid _{coded}	-1.68	-1.68	-1.68	-1.68	-1.68
0	0	0	0	0	0
3.00	-386.01	-252.52	-117.37	-55.03	-54.22
4.42	-259.34	-140.69	-27.35	13.18	-0.85
6.50	-153.51	-56.67	24.59	33.04	-2.80
8.58	-143.46	-68.43	-19.26	-42.88	-100.54
10.00	-191.34	-131.14	-103.78	-149.22	-221.71

Table III-35: Data kinetic with acid concentration fix at 0.08 molar

T _{actual} (°C)	143.6	148.8	155.45	161.3	164.95
P _{actual} (bar)	4	4.61	5.5	6.39	6.39
P _{coded}	-1.68	-1	0	1	1.68
Acid _{coded}	-1	-1	-1	-1	-1
0	0	0	0	0	0
3.00	-280.41	-154.79	-31.22	19.55	12.48
4.42	-149.56	-38.77	62.98	91.94	70.04
6.50	-37.58	51.39	121.07	117.94	74.23
8.58	-21.39	45.77	83.37	48.17	-17.36
10.00	-65.08	-12.76	3.03	-53.99	-134.35

Table III-36: Data kinetic with acid concentration fix at 0.13 molar

T _{actual} (°C)	143.6	148.8	155.45	161.3	164.95
P _{actual} (bar)	4	4.61	5.5	6.39	6.39
P _{coded}	-1.68	-1	0	1	1.68
Acid _{coded}	0	0	0	0	0
0	0	0	0	0	0
3.00	-145.08	-31.05	75.50	109.24	90.60
4.42	-8.09	91.12	175.85	187.78	154.30
6.50	112.93	190.32	242.97	222.82	167.53
8.58	138.16	193.74	214.32	162.09	84.98
10.00	100.61	141.36	140.12	66.08	-25.86

Table III-37: Data kinetic with acid concentration fix at 0.17 molar

T _{actual} (°C)	143.6	148.8	155.45	161.3	164.95
P _{actual} (bar)	4	4.61	5.5	6.39	6.39
P _{coded}	-1.68	-1	0	1	1.68
Acid _{coded}	1	1	1	1	1
0	0	0	0	0	0
3.00	-33.54	68.92	158.44	175.16	144.94
4.42	109.60	197.23	264.94	259.84	214.79
6.50	239.66	305.47	341.10	303.92	237.06
8.58	273.93	317.93	321.48	252.23	163.55
10.00	242.52	271.69	253.43	162.36	58.85

Table III-38: Data kinetic with acid concentration fix at 0.20 molar

T _{actual} (°C)	143.6	148.8	155.45	161.3	164.95
P _{actual} (bar)	4	4.61	5.5	6.39	6.39
P _{coded}	-1.68	-1	0	1	1.68
Acid _{coded}	1.68	1.68	1.68	1.68	1.68
0	0	0	0	0	0
3.00	28.73	123.32	201.26	206.40	168.31
4.42	176.05	255.81	311.94	295.26	242.34
6.50	312.25	370.19	394.24	345.49	270.75
8.58	352.67	388.80	380.77	299.94	203.39
10.00	325.44	346.74	316.90	214.25	102.87

Data in Table III-34 to Table III-38 above were inspected for its value to check whether constraint for data mining from the polynomial model was satisfied or not. It was found that data from Table III-34 to Table III-37 was having negative glucose value corresponding to acid concentration fix at 0.05, 0.08, 0.13 and 0.17 molar. The Statistic of F distribution that was tested also show only group with acid concentration fix at 0.17 and 0.20 molar satisfy the constraints. With this constraint, only data from 0.17 and 0.20 molar sulfuric acids were accepted for the kinetic study.

Data in Table III-37 and Table III-38 were plotted as kinetic expressions to calculate k_1 and k_2 of both systems using A_0 of 800 mg/ g. Higher value of A_0 was used due to a high amount of glucose were produced, that indicate the process severity was high in term of conversion of polysaccharides into glucose, together high potential for glucose degradation to occur in this treatment regime.

Plot obtained from calculated data using fitted polynomial equation were fitted into kinetics models and checked for the statistical significant according to F statistical distribution. Significant models were presented in Figure III-37. Only two models that were significant

according to F statistic were presented in Table III-41, i.e. for acid concentration of 0.17 and 0.20 molar. Excel tools "Solver" was used to calculate the rate constant of k_1 and k_2 of respective condition and presented in Table III-39.

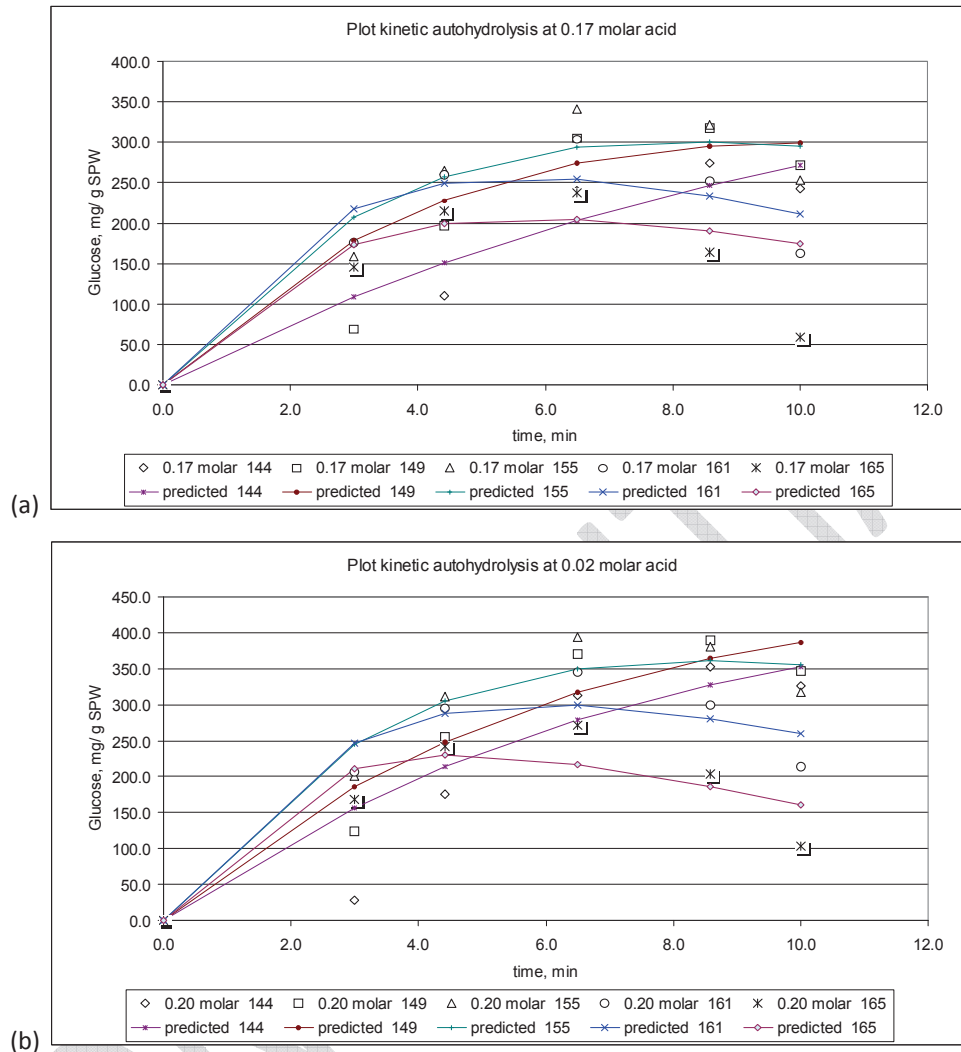


Figure III-37: Plot kinetic autohydrolysis for 0.17 and 0.20 molar acid (with statistical significant F distribution)

III.2.9.2. Rate Constant and Activation Energy for the Model

Only two acid concentrations (0.17 and 0.20 molar acid sulfuric) could fulfill all three constraints for data mining operation for kinetic study from the response surface model, i.e. (i) no negative glucose value, (ii) good correlation between model and data, and (iii) central points show linearity in the range of data being studied. In Table III-39, rate constant for 0.17 molar acids shows there was an increase in k_1 with an increase in temperature from 144 to 161, and decrease at 165°C, but k_2 was increasing at this range, shows that potential of high degradation for treatment with DIC at temperature 165°C. Relative rate constant k_1/k_2 was found to be less than 1 except at a lower temperature.

Data for 0.20 molar acid sulfuric shows that rate constant k_1 and k_2 was increased trends with highest k_1/k_2 value was at temperature 149°C ($k_1=2.3k_2$), 144°C ($k_1=2.1k_2$) and 155°C ($k_1=1.6k_2$). Value k_1/k_2 for 161 and 165°C was less than 1 that shows degradation was higher than glucose generation.

Table III-39: Rate constant for hydrolysis (k_1) and degradation of glucose (k_2) at temperature 144, 149, 155, 161 and 165°C for acid concentration 0.05, 0.08, 0.13, 0.17 and 0.20 molar.

Temperature	143.6	148.8	155.45	161.3	164.95
A_0	800	800	800	800	800
0.17 molar					
k_1	51.53×10^{-3}	99.5896×10^{-3}	123.8826×10^{-3}	154.3490×10^{-3}	121.77×10^{-3}
k_2	32.727×10^{-3}	96.2737×10^{-3}	118.2866×10^{-3}	200.0275×10^{-3}	231.834×10^{-3}
0.20 molar					
k_1	77.637×10^{-3}	95.0019×10^{-3}	146.4811×10^{-3}	168.1695×10^{-3}	167.787×10^{-3}
k_2	37.035×10^{-3}	42.4052×10^{-3}	94.3127×10^{-3}	161.3579×10^{-3}	264.644×10^{-3}

Table III-40: Activation energy E_a , (kJ/ mole) for respective acid concentration range

Acid concentration	0.05 molar	0.08 molar	0.13 molar	0.17 molar	0.20 molar
E_a Glu _{generation}	n/a	n/a	n/a	61.78	59.44
R^2	n/a	n/a	n/a	0.9549	0.9691
E_a Glu _{degradation}	n/a	n/a	n/a	128.28	144.12
R^2	n/a	n/a	n/a	0.9549	0.9844

n/a – not applicable due to the presence of negative k_1 or k_2 value in range.

Correlation coefficients (R^2) in activation energy 0.17 molar and 0.20 molar acid sulfuric in Table III-40 was higher than 0.95 to show that it was quite good estimation based on the model presented above. Comparison of activation energy obtained from the response model was found that glucose generation requires less energy than glucose degradation, which was an important observation for this study. At 0.17 and 0.20 molar activation energy for glucose generation was less than half of activation energy required for the degradation to proceed.

Activation energy for degradation of glucose, a similar trend was observed in lower acid-shorter time in previous article, i.e. an increase in activation energy with an increase in acid concentration. Difference for E_a at 0.03 molar and 0.01 molar was about 125 kJ/ mole, while at acid concentration of 0.17 molar, the value was 128.28 kJ/ mole.

Model kinetics for each temperature were verified using F statistic for its statistic at P 0.05 and was found to be significant and can be accepted as presented in Table III-41.

Table III-41: Statistical data for model based on temperature

Temp °C	No of points	No of param	SS diff	SS total	R^2	F_{calc}	$10F_{table}$	$F_{calc} \gg 10F_{table}$
144	30	5	163,896.2	1,631,560.3	0.89955	7.46	27	No
149	30	5	46,340.01	776,509.80	0.94032	13.13	27	No
155	30	5	24,685.25	776,509.80	0.96821	25.38	27	No
161	30	5	8,809.20	836,765.45	0.98947	78.32	27	Yes
165	30	5	7,829.50	649,880.14	0.98795	68.34	27	Yes

This shows that model at 161 and 165°C were statistically significant at 95% level of confidence to explain the result for kinetic data obtained from the response surface. The other three models were not significant. In the same way, it was found that high acid was provided good correlation with this result.

This study shows that it was possible to use data from the response surface model to generate data for hydrolysis kinetic provided that constraint that explained earlier was fulfilled. This is due to the limitation of the polynomial equation was limited to a second order only, making response surface model based on quadratic polynomial equation does not allow to study kinetic at condition far from optimized condition.

III.2.10. Conclusion

Present DIC autohydrolysis produce a considerable amount of glucose (30% to 35% of available polysaccharides, higher if compared to low severity). Kinetic model was developed to understand the underlying principles of autohydrolysis during DIC treatment. Response surface and contour plots for pressure against time at fix acid, and for pressure against acid at fix time suggest in global view that to maximize glucose yield need to increase time and acid concentration. Autohydrolysis reaction in DIC pretreatment was following first order kinetic reactions as expected.

For the operation in the data mining operation for response surface models comparison, it was observed in the first part of this study that data mining to establish the kinetic model was quite good and was significant according to the F distribution. In this second part of work, a much higher severity treatment was done for optimization of DIC assisted hydrolytic conversion of polysaccharides into glucose. Data mining using quadratic model response surface is not enough to explain the detail of the operation for kinetic study. A much higher polynomial equation was needed to ensure all data point can be accurately presented on the surface of the response model. Operation for data mining was good at a point very near to the optimum points as presented in statistic in Table III-41 and Figure III-37. Data point at non-optimum condition was not able to be properly described by response surface model for data mining operation. Much higher polynomial or data fitting models were required such as Runge-kutta 4th order for data fitting in the form of response surface. The problem with existing response surface with quadratic polynomial equation was that it only gives good data fit for data that was near the optimum level [151, 168]. A prior information and understanding of the process were required if a much critical data such as to extract kinetic data was not sufficient for existing response surface model.

Based on both DIC severity trials, the optimization of SPW or crude starch into glucose was found to be able to be converted nearly 35% at the central point. Both combinations will be used in the evaluation of dilute acid hydrolysis kinetic. Several conclusions were developed from this study as follows:

- At higher acid concentration, treatment time and temperature the process could overcome the limitation of two steps conversion as observed in low DIC severity. Amount of glucose was increased in tandem with the increase in DIC severity factors.
- Crude sago starch containing resistant starch that good for another application related to food industry.
- Only two combinations were possible to be used for hydrolysis kinetic study. This was due to at higher operating condition; polynomial equation for response surface model does not allow data mining operation to be fit into exponential type reaction such as the first order kinetic study.
- At central point combination, only starch (alpha bond) was undergoing hydrolysis. Cellulose (beta bond) hydrolysis, need higher treatment severity combination; however, a precaution for degradation of glucose into several other products needs to look into.

PART III. CHAP 3.

DILUTE ACID HYDROLYSIS AND GLUCOSE DEGRADATION STUDY

Paper 5: Dilute Acid Hydrolysis of Post DIC Treated Crude Starch (i) Hydrolysis Kinetic Study and its Model (ii) RSM Study on Interaction of Reaction Factors on the Formation of Glucose.

Abstract

This work, study the two stages process conversion of SPW into glucose; the first stage was thermal pretreatment with DIC followed by second stage of dilute acid hydrolysis process with DIC treated materials. Second stage dilute acid hydrolysis were studied and modeled after consecutive first-order reaction kinetic to obtain reaction constant of the process; followed by analyzing it for optimum two-stage process combinations. SPW was subjected to a low severity and high severity DIC pretreatment, followed by the dilute acid hydrolysis experimental study to obtain the required data for respective DIC treated materials. Kinetic hydrolysis was studied on three process temperatures (110, 130 and 150°C) in combination of three acid concentration (0.01, 0.04 and 0.08 molar) during hydrolysis time of 5, 15, 30, 60, 90, 120 and 240 minutes. Optimum kinetic condition with the highest rate constant was found at the combination of high temperature (150°C) at all three acid concentrations. In order to optimize glucose yield, kinetic model was developed to obtain rate constant for glucose degradation. Data was further transformed into a response surface model with two levels factorial designs. Response surface model was developed to investigate the overall factors (acid concentration, temperature and time, as well as its interactions) level on glucose yield. F statistic result shows response surface models were statistically fit to data obtained from kinetic experiment. Higher A_0 values were used in the kinetic model to obtain rate constant of polysaccharide's autohydrolysis (k_1) and its corresponding glucose degradation (k_2). At high DIC severity, both starch and cellulose were converted into glucose with some level of glucose degradation. The level of glucose degradation can be minimized for the optimum conversion required, upon understanding that at low acid and temperature, high glucose degradation was high due to conditions favors the glucose degradation than the conversion of polysaccharides into glucose. Dilute acid hydrolysis within 20 to 30 minutes on high DIC severity materials produced about 700 to 800 mg/g glucose.

III.3.1.Objectives

Objectives of this work (i) to obtain an optimum glucose amount during second stage dilute acid hydrolysis (ii) to obtain kinetic data of the process (iii) to study the interaction effect of reaction factors on glucose formation, and (iv) to investigate whether DIC treatment alone is sufficient to convert SPW into glucose.

III.3.2.Introduction

This work was done to evaluate an affect of DIC severity pretreatment on yield of glucose during second stage dilute acid hydrolysis process. This was an important step to maximize the production of glucose in two production stage. Previously, it was shown that with low DIC severity, less than 1% of glucose were produced during DIC pretreatment. For treatment

with high DIC severity, nearly 50% of total polysaccharides can be converted into glucose with single step of DIC pretreatment. In an exploratory study at extreme pressure and acid, we have shown that nearly 80% of biomass can be converted into glucose within 3 to 4 minutes with DIC pretreatment.

In this work, kinetic study will be done on both low and high DIC treated materials in order to evaluate potential combination between DIC-DAH that will produce maximum glucose in two-stage process or will only concentrate on single DIC process for glucose production. Factors such as length of treatment, acid concentration, treatment temperature and degradation of glucose will be investigated to assist in the development of process-economic study.

During DIC treatment kinetic we have discovered that glucose was produced from SPW with some degradation occurs for high DIC severity and with almost no glucose degradation for low DIC severity process. In this work, glucose degradation and glucose formation will be studied simultaneously in order to decide the relevant process; i.e. whether to use DIC alone or DIC in combination with post DIC dilute acid hydrolysis process in order to maximize glucose production.

III.3.3. Materials and Methods

III.3.3.1. Sago Pith Waste (SPW)

SPW was obtained from a small sago processing plant in Batu Pahat, Johor; it was dried for 2 days under sun, characteristic of raw material was presented in Table II 1. Material was further dried for 12 hour in oven at temperature 40°C, followed by grinding with Retsch Grindomix at 4000 rpm for 30 seconds. Ground materials were sieved through several sieved sized and only materials that pass 600 nm sieves were used in this operation. Moisture content of material was 7.0 to 10.0% on dry basis.

III.3.3.2. Chemicals

All chemicals used in this study were of analytical grades and was use as it is. Sulphuric acid 98%, glucose, levulinic acid, acetic acid and formic acid was obtained from Sigma Aldrich. Mobile phase and water used in this study were prepared in our laboratory using deionized water system and pure water system [Purelab Option-Q, ELGA] as described earlier.

III.3.3.3. Material Characterization

Moisture content was determined with Sartorius MA 30 moisture analyzer at 105°C for 5 minutes using 500 mg to 1000 mg representative samples as described in Part 2 of thesis.

Compositional analysis was done using total polysaccharides method as described earlier to estimate A_0 values for respective DIC pretreatment severity for modeling of hydrolysis kinetic.

III.3.3.4. Determination of TGA Profile

TGA analysis was done on samples to estimate total polysaccharides content of materials and to study profile of SPW due to thermal pretreatment with DIC. Profile of DIC treated TGA was done according to method previously described.

III.3.3.5. Glucose Determination with HPLC

Glucose was determined using hydrolysate obtained from each hydrolysis. Hydrolysate was filtered into HPLC glass tube to separate SPW fibers, followed by dilution with mobile phase to ensure glucose concentration was within standard curve concentration. Diluted solution was filtered through 0.20 μm nylon filter into respective HPLC vials and injected into chromatography system as described in Part 2 for Instrumental Analysis.

III.3.3.6. ESEM and EDX Determination

Environmental scanning electron microscopy (ESEM) method was done as describe in detail before. ESEM detection was done using configuration under low vacuum of 1.30 mbar with two detectors SED (for solid state or morphology detector) and BSED (for chemical/elemental composition) with maximum resolution of 2.5nm at 20kV.

III.3.3.7. Experimental Procedures

III.3.3.7.1. Pretreatment with DIC

DIC pretreatment was done with DIC system that was described earlier. Briefly, system consists of treatment reactor with connection to steam and vacuum. Treatment was done by placing material in a perforated top aluminum foil container into DIC reactor, followed by closing the system, putting it under vacuum followed by steam injection. Variation treatment during DIC pretreatment was done using steam pressure and treatment time. Once treatment time is achieved, steam supply was closed and reactor was exposed to vacuum. Instant change from high pressure to vacuum affected reactor system and treated material will be immediately cool treatment reactor and treated materials.

Prior to DIC treatment, SPW materials were adjusted its moisture and acid level by adding acid solution of different concentration into known SPW weight and moisture content. Combinations of acid and moisture level of SPW were presented in Table III-42. Addition of acid solution in order to adjust both acid and moisture level simultaneously was done according to procedure set out in procedure II.2.1.3 in page 67.

About 10 grams materials were prepared in triplicate for each DIC treatment combination. Two DIC treatment combinations (low DIC severity and high DIC severity) were done to prepare material for this kinetic study. Treatment combinations used were from center points of previous DIC response surface studies at low severity and high severity conditions.

Table III-42: DIC treatment combinations for dilute acid hydrolysis studies, initial moisture content X_1 : 150%, together with vacuum cycles, X_2 :+1 and X_3 :+1 at 100 mbar.

No	Coded form			Actual level			HWE
	pressure	acid	time	pressure	acid	time	Glucose
Code	X4	X5	X6	X4	X5	X6	mg/ g (average)
1	L ₀	L ₀	L ₀	5.50	0.03	1.75	2.40
2	H ₀	H ₀	H ₀	5.50	0.13	6.50	215.30

Utilization of a perforated top aluminum container was very important to ensure all treated material can be recovered after DIC treatment. Immediately, after DIC pretreatment, materials were dried at room temperature for 12 hour and further dried in an oven at 50°C for another 12 hour. Dried materials were kept in a polyethylene bag with zip lock at room

temperature until used. Immediately, before kinetic experiment, both DIC treated SPW were determined its moisture content in order to estimate actual solid material. Hot water extractions were done to estimate glucose concentration due to DIC autohydrolysis. Results obtained from HPLC analysis was presented in Table III-42.

III.3.3.7.2. Dilute Acid Hydrolysis Kinetic Experiments

Hydrolysis kinetic was done using identical small pressure reactors made of stainless steel 316 with screw cap and fitted with Teflon insert. Total volume of reactor was 20 ml, while volume use for experiment was 10 ml to have good headspace for any volume expansion. Each reactor was determined its individual weight right before putting into oil bath and after taken out of oil bath. Any reactors with a change in weigh of more than 1% will be rejected, and experiment will be repeated for that particular point. Prior to these experiments, each pressure reactor was fully cleaned to ensure no error due to residues inside of reactor.

Hydrolysis was done with 5% solid: liquid ratio. 500 mg solid (low or high DIC severity materials) were added into respective reactor, followed by adding 10 ml acid solution (0.01, 0.04 or 0.08 molar sulfuric acid). Heating was done in an oil bath preset at required temperature until treatment time was achieved. Pressure reactor will be immediately cooled by dipping it into a cool ice bath. Profile of heating and cooling was done to estimate a non-isothermal effect during the process, with a detail result presented in the following Chapter 4, Paper 7.

Glucose concentration was obtained through HPLC analysis using a procedure as described earlier in Chapter II.1.5.2, page 62.

III.3.3.7.3. Response Surface Methodology

Data obtained from kinetic operation was fitted into factorial design and its response surface analyze with Statgraphics utilizing the following equation:

$$Y_{Glu} = a_o + \sum a_i x_i + \sum a_{ii} x_i^2 + \sum a_{ij} x_i x_j \quad \text{- Equation 24}$$

With $x_i = X1, X2$ or $X3$, $x_j = X1, X2$ or $X3$ and $x_i \neq x_j$

Y_{Glu} is the predicted response, a_o is the intercept at 0, a_i is the linear term, a_{ii} is quadratic term and a_{ij} is the interaction term.

The treatment factors (treatment time, temperature and acid concentration) are represented in Table III-42. Statistical analysis for design to study interaction effect for treatment factors were obtained from analysis of variance. Significance of factors was determined by their probability in the ANOVA analyses. It was considered significant if the p-value was lower than 0.05, meaning that the probability of noise causing the correlation between a factor and the response is lower than 0.05.

III.3.4. Result and Discussion

III.3.4.1. TGA Analysis

Two TGA/TGD profile in Figure III-38 shows (a) profile for raw SPW and (b) profile for DIC treated SPW at lower DIC severity central point combination. For raw SPW, there are three

phases for weight losses of materials: (1) between 30 to 140°C, losses of weight were attributed to the evaporation of water from composition, with a gap of constant weight between 140 to 200°C, (2) between 200 to 400°C, losses of weight were attributed to the decomposition of polysaccharides (hemicellulose, starch and cellulose) and (3) beyond 420°C, losses of weight were attributed to the decomposition of lignin, which remain as residues together with ashes and silica that present in composition [52, 169, 170]. In earlier TGA study for degradation of cellulose and starch, peak temperature for component degradation was 360°C and 320°C respectively [171, 172]. Based on DTA result, peak temperature for sago waste was 326°C, i.e. quite close to TGA peak temperature of starch degradation.

TGA profile for low DIC severity SPW, however, shows a contrast result against raw SPW, with almost no gap for phase in-between derivative TGA plot. There are seven distinctive phases: (1) 30-110°C for vaporization of water, (2) two small peaks belong to monosaccharide, 110-120°C and 120-140°C, (3) two peaks belong to higher oligosaccharides, 140-160°C and 160-240°C, (4) peak belong to cellulose 240-310°C, (5) peak belong to lignin 310-500°C, and (6) for 500°C and above belongs to residues and ashes. Percentage of each composition is presented in Table III-43.

In other research work related to the degradation of crystalline α -D glucose, TGD plot gave two degradation peak, with the first stage degradation was found at 235°C (508K) [173], i.e. in almost a similar spot for DIC SPW with respect to oligosaccharides degradation, it was followed by second peak at 330°C (603K) related to decomposition of glucose. Four TGD peak was found in low DIC severity SPW materials as detailed in Table III-43. With as high as 400 mg glucose/g found in low DIC severity SPW, we can expect high contribution of glucose and lower DP oligosaccharides towards those TGD peak parallel to above finding. Nearly identical TGA/TGD plot profile was observed with other DIC SPW materials at different DIC severities.

Mechanisms for starch and cellulose degradation during pyrolysis were reported [174-176], was related to the existence of monosaccharide during pyrolysis of cellulose and starch materials. Non-thermal treated biomass was found to have a similar profile as presented in Figure III-38(a) for material with high polysaccharides content [29, 177] and with some characteristic similar to Figure III-38(b)[171] upon treatments. It was observed that there was a change in percentage of lignin and residue after DIC treatment as summarized in Table III-43. This was expected due to the changes in material composition as well as due to generation of pseudo-lignin (i.e. combination of lignin and polysaccharides) during DIC treatment. Earlier investigation was shown that with changes in composition of material containing formulated starch-cellulose-lignin, its final residues will also be affected [172].

There were some differences in total polysaccharide's and residue of analysis with TGA if compared to total polysaccharides with Klason method. This was expected due to TGA analysis was done on a fraction of about 2% or lesser against total polysaccharides analysis, and a small change in the representative of sample used normally will affect the overall composition. Profile and results obtained from TGA however was good for overall representative of composition of other oligosaccharide components that cannot be obtained through total polysaccharide's method.

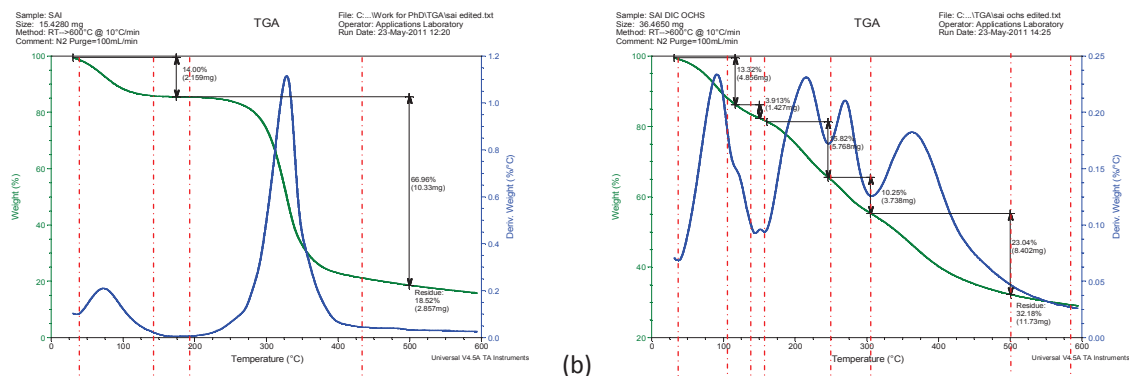


Figure III-38: TGA and derivative weight (TGD) plot of (a) raw SPW and (b) DIC SPW. Plot (a) show total polysaccharides were about 80% and ash content about 20%. Plot (b) shows that polysaccharides were undergoing changes into different molecular weight materials. Total polysaccharides were between 85 to 90% while ash content was about 15 to 10% of dry weight.

The existence of lower degree of polymerization polysaccharides in DIC treated SPW were confirmed by TGA analysis. Several mechanisms for the conversion of polysaccharides already explained in details in several thermal analysis publications, and will be explained further to support finding of this work. This is observation was something very significant for DIC pretreatment, as TGA result was able to show the existence of several oligosaccharides groups in treated material.

This information will enable a systematic processing step to capitalize different groups of oligosaccharides either through hot-water extraction or dilute acid hydrolysis.

Table III-43: Summary of TGA result for raw SPW and low DIC severity

Treatment	Composition	Temperature range (°C)	Percent (wb)
Raw SPW	Moisture	30-150	14%
	Total polysaccharide	200-420	67% (78% db)
	Residue	420 and above	19% (sum different)
DIC treated SPW	Moisture	30-110	13%
	Total polysaccharide (sum: 1+2+3)	110 - 420	55.6% (64% db)
	1. Lower DP polysaccharides (mainly mono & di-saccharides components)	110-140 140-160	4% 2.5%
	2. Oligosaccharide	160-240 240-310	15.8% 10.3%
	3. Cellulose	310-500	23%
	Residue	500 and above	31.4% (sum different)

These TGA results also confirm earlier suggestion, that DIC treatment can be a new potential process for pretreatment of this kind of crude starch waste into various degrees of polymerization (DP) of materials. Moreover, the capability of DIC process to capitalize high moisture content of the present waste without the need to reduce its moisture level was something very practical to overcome the present problem to utilize SPW. Further work on this area with respect to a different degree of polymerization can be expected to establish some linkage with the DIC treatment severity.

III.3.4.2. Kinetic of Dilute Acid Hydrolysis

This work will concentrate on the dilute acid hydrolysis at second processing stage. Kinetic study and response surface will be used to explain the experimental results together with its

respective models. Fifty four points of experimental data were obtained from each kinetic study of glucose degradation and hydrolysis of DIC treated materials for two DIC treatments. Plots for hydrolysis kinetic for experimental data and its data obtained from model fit according to consecutive first-order kinetics were presented in Figure III-39.

Rate of hydrolysis for each model point were calculated using A_0 of 900 mg/g. An average value of 880 mg/g was obtained and generalized further to 900 mg/g SPW for all modeling points. The same A_0 value was used for both lower severity and high severity of DIC treatments for data modeling purpose. Samples obtained from DIC treatments were used as it is, i.e. not undergoing hot water extract prior to hydrolysis. The same level of total polysaccharides was assumed for all experimental sources for experimental data model purpose.

Both DIC treated material at low and high severity will be evaluated its respective kinetic expressions with experimental data model to understand mechanism underlying the process. Conclusion obtained from this exercise can also be adopted for hot-water extraction kinetic exercise for its similarity, especially for the extraction at lower temperature and acid regime.

Profiles for substrate, product and degradation product were discussed based on models from dilute acid hydrolysis at 150°C at 0.01, 0.04 and 0.08 molar acid sulfuric concentration for both DIC treatment severities.

Plot of glucose yield as experimental data obtained from dilute acid hydrolysis for low and high severity DIC treatments were presented together with their respective model fit according to consecutive first order kinetic model. Rate constants obtained from model fit were presented in Table III-44.

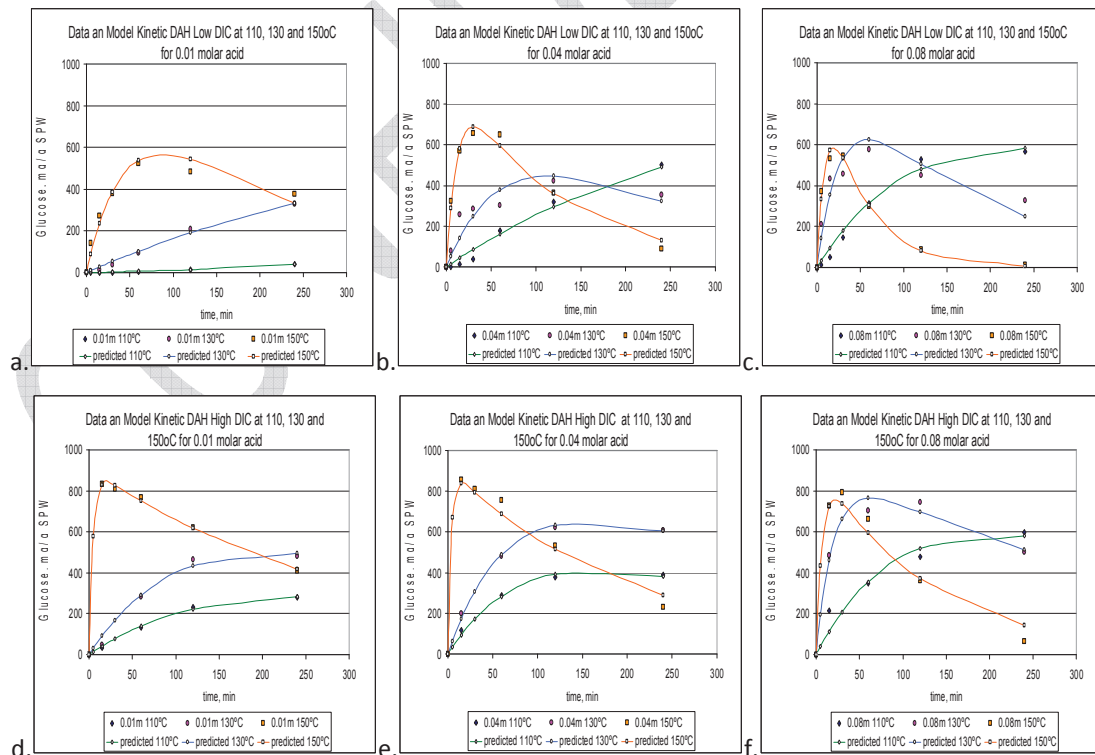


Figure III-39: Profile of glucose obtained from hydrolysis of DIC treatment in SPW with Low DIC severity (for a, b and c) and High DIC severity (for d, e and f) treatments. Hydrolysis was done with 0.01, 0.04 and 0.08 molar sulfuric acid respectively.

Table III-44: Kinetic data (rate constant k_1 and k_2) for dilute acid hydrolysis kinetic for two type of DIC treated materials: low severity and high severity DIC treatments.

Materials	DIC Low severity			DIC High severity		
	110°C	130°C	150°C	110°C	130°C	150°C
Ao	900	900	900	900	900	900
0.01 molar						
k_1	0.0839×10^{-3}	2.0268×10^{-3}	21.0225×10^{-3}	3.2475×10^{-3}	7.2497×10^{-3}	208.7208×10^{-3}
k_2	-6.2108×10^{-3}	0.3016×10^{-3}	5.2375×10^{-3}	4.3845×10^{-3}	2.7662×10^{-3}	3.2634×10^{-3}
k_1/k_2	n/a	6.72	4.01	0.74	2.62	63.96
0.04 molar						
k_1	3.3003×10^{-3}	11.9488×10^{-3}	79.3910×10^{-3}	7.5886×10^{-3}	14.489×10^{-3}	282.553×10^{-3}
k_2	0.0245×10^{-3}	0.6018×10^{-3}	8.5597×10^{-3}	4.7445×10^{-3}	2.0963×10^{-3}	4.7873×10^{-3}
k_1/k_2	134.52	1.99	9.27	1.60	6.91	59.02
0.08 molar						
k_1	7.70052×10^{-3}	35.6444×10^{-3}	100.6090×10^{-3}	9.0869×10^{-3}	49.4539×10^{-3}	135.4927×10^{-3}
k_2	1.74022×10^{-3}	6.1324×10^{-3}	22.1879×10^{-3}	2.0317×10^{-3}	2.5666×10^{-3}	7.8867×10^{-3}
k_1/k_2	4.43	5.81	4.53	4.47	19.27	17.18

Profiles of substrate, product and degradation product during dilute acid hydrolysis at 0.01, 0.04 and 0.08 molar acid with their respective rate constant ratio (k_1/k_2) for low severity DIC treatment and high severity DIC treatment were presented in the following Figure III-40, these models was developed from experimental data.

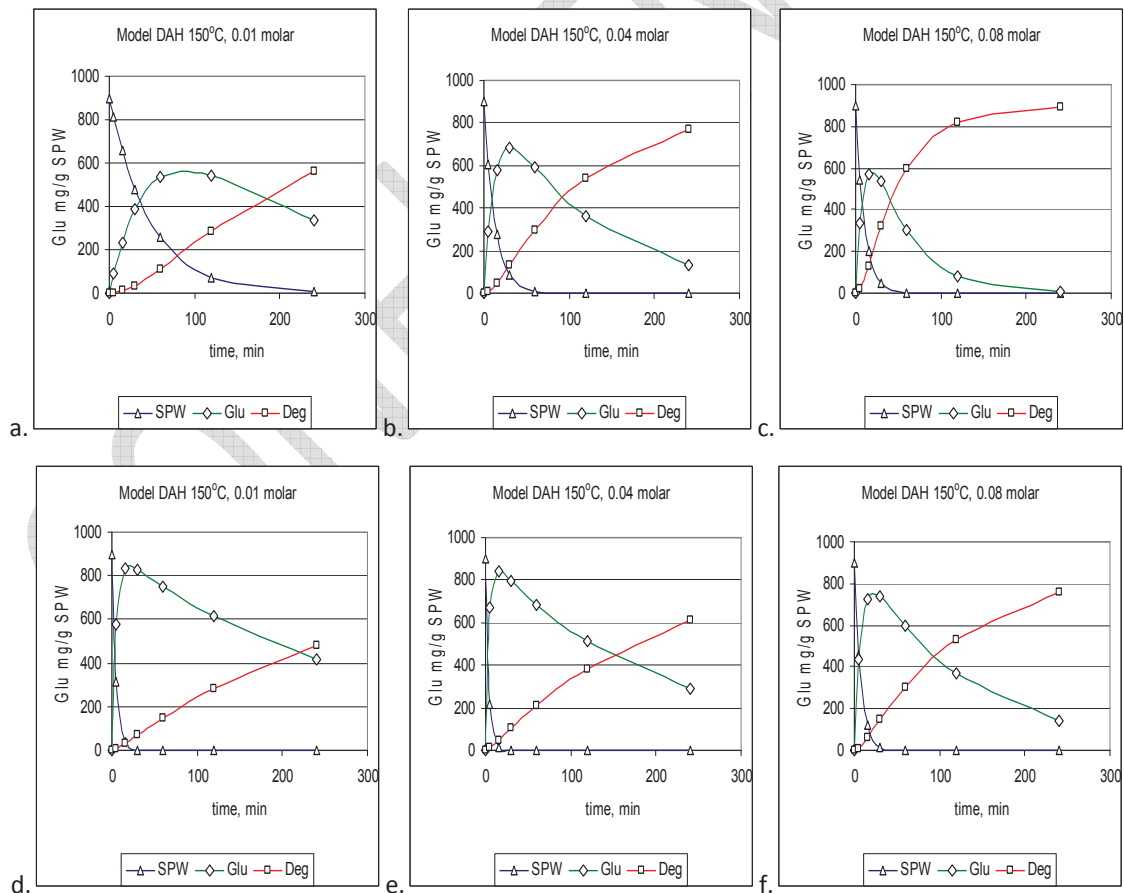


Figure III-40: a) Low DIC, k_1/k_2 : 4.01, $t_{Glu_{max}}$: 88.04 min; b) Low DIC, k_1/k_2 : 9.27, $t_{Glu_{max}}$: 31.45 min; c) Low DIC, k_1/k_2 : 4.53, $t_{Glu_{max}}$: 19.28 min; d) High DIC, k_1/k_2 : 63.96, $t_{Glu_{max}}$: 20.24 min; e) High DIC, k_1/k_2 : 59.02, $t_{Glu_{max}}$: 14.68 min; f) High DIC, k_1/k_2 : 17.18, $t_{Glu_{max}}$: 22.29 min.

III.3.5. Dilute Acid Hydrolysis (DAH)

There are two types of materials that were studied in this dilute acid hydrolysis: low severity and high severity DIC treatment on SPW. Plots for respective glucose yield were presented in Figure III-39: (a) to (c) for low severity; and (d) to (f) for high severity. Model plots for substrate, product and product degradation were presented in Figure III-40: (a) to (c) for low DIC severity; and Figure III-40: (d) to (f) for high DIC severity.

In general, there are several important characteristics that were observed in all kinetic plots of product in Figure III-39:

1. All product plots show an increase of glucose yield against an increase in treatment time, acid concentration and treatment temperature; which was a general characteristic for most of kinetic processes.
2. SPW treated at High DIC severity was found to give high yield of glucose if compared to Low DIC severity treatment. Maximum amount of glucose was 830 and 855 mg/g during hydrolysis with 0.01 molar and 0.04 molar respectively at 15 minute and treatment temperature of 150°C. Maximum amount for Low DIC severity treatment was 655 mg/g with 0.04 molar acid during 30 minute treatment at 150°C.
3. At high temperature (150°C) favor high rate of glucose but after reach certain treatment time, degradation will occur depending on acid concentration; high acid concentration was found to almost degrade all glucose within 150 minute (Figure III-39:(c)).
4. At high acid concentration (0.08 molar), favor high rate of glucose generation but also increase the rate of glucose degradation at high temperature (150°C) and medium temperature (130°C) use in this study (Figure III-39:(c) and (f)). No degradation observed for temperature 110°C.
5. DIC treatment with high severity was found to contribute to higher rate of glucose generation if compared with lower DIC severity. Treatment with high DIC severity at 150°C for all acid concentrations was found to achieve maximum glucose during 14 to 22 minutes treatment compared to DIC treated at lower DIC severity was 20 to 88 minutes treatment (data in Figure III-40).

Further to analysis of Table III-44 and Figure III-40, three criteria for optimization of dilute acid hydrolysis were made and summarized as follows:

1. Higher value k_1/k_2 is favorable to the process; which is related to the rate of glucose generation compared to glucose degradation. A higher value means glucose generation is bigger than its degradation. Rate constant k_1 for treatment of High DIC severity materials with 0.01 molar and 0.04 molar acids at 150°C were the highest at 0.20872 min^{-1} and 0.28255 min^{-1} respectively. This was corresponding to condition for the highest amount of glucose yield obtained for the process at 830 and 855 mg/g respectively.
2. Lower t_{Glumax} is favorable to the process in particular for obtaining glucose with very minimum degradation products in hot water extract.
3. High value of A_0 ; which shows the amount of available total polysaccharides in materials.

Table III-45: Activation energy (kJ/mole) for dilute acid hydrolysis for two DIC treatment severities at 0.01, 0.04 and 0.08 molar acid sulfuric

Treatment type	Low severity DIC treatment			High severity DIC treatment		
Acid concentration	0.01 molar	0.04 molar	0.08 molar	0.01 molar	0.04 molar	0.08 molar
Ea Glu _{generation}	186.31	106.67	86.74	138.65	120.41	91.30
R ²	0.9982	0.9904	0.9966	0.9325	0.9272	0.9932
Ea Glu _{degradation}	n/a	199.86	85.63	-10.28	-0.61	45.14
R ²	n/a	0.9042	0.9994	0.6547	0.1912	0.9247

Note: n/a – not available

Activation energy for each process was determined and presented in Table III-45. In general by increasing the acid concentration activation energy of the system will decrease similar to observation in the study of DIC kinetic for High DIC severity treatment. In this dilute acid hydrolysis study, dilute acid hydrolysis at Lower severity DIC treatment for medium and high acid concentration was having lower activation energy if compared to High severity DIC treatment. Combination at Low DIC severity with acid concentration of 0.04 molar was found to have been favorable for dilute acid hydrolysis due to low activation energy for glucose generation but high activation energy to favor the glucose degradation. We can expect that glucose degradation will require high energy to start occurring for process using Low DIC treated material at 0.04 molar in the region of temperature 110 to 150°C compared to other treatment combinations.

Data from activation energy, even though suggest the most favorable condition for dilute acid hydrolysis process was with materials from Low DIC treatment severity with treatment at 0.04 molar acid and treatment range 110 to 150°C however its have rate constant k_1 value was in range of 0.00330 to 0.07939 min⁻¹ only. This was smaller than rate constant for High DIC severity treatment for the highest amount as described previously, thus not satisfy the requirement for optimization of the this two stage process.

This information, however, was useful as starting base for process improvement if end product of the process was oligosaccharides materials as described in TGA result and as found in chromatographic analysis.

III.3.6.RSM Model Study

Further investigation for optimizing the process and to study the main effect and interaction effect of treatment parameters towards yield of glucose, data obtained from experiment was done by transformed experimental data into a multilevel factorial design with three parameters. Data was analyzed for selected treatment range until 120 minutes to avoid a higher effect of glucose degradation. RSM model was analyzed with 35 error degree of freedom (df) in one design block. Statistical analysis on glucose yield, including ANOVA are presented in Table III-46 and Table III-47 and corresponding Pareto chart in Figure III-41(a) and Figure III-41(b) for High DIC severity and Low DIC severity respectively.

Based on ANOVA analysis, all three main factors are common factors that affect the yield of glucose. An increase in all main factors will increase the yield of glucose as well. Common interaction factor that significantly affects the yield of glucose for both DIC treatments was CC (time-time). For High DIC severity, another two factors AC (temperature-time) and AB (temperature-acid) when at high level will reduce the yield of glucose. Based on kinetic analysis also, it was established that high temperature together with lower acid (0.01 molar)

the glucose yield was the highest. Correlation coefficient was found to be highly related to glucose degradation. At full range analysis, R^2 value was less than 80% and less than 60% for High DIC severity and Low DIC severity respectively. In order to correlate an effect of treatment parameters effectively, high correlation coefficients were required. Factors that affects high correlation were due to very high degradation such as observed in Figure III-40(c) and (f).

Table III-46: Analysis of Variance for Glucose yield from High DIC severity

Source	Sum of Squares	Df	Mean Square	F-Ratio	P-Value
A:Temp	1.04411E6	1	1.04411E6	60.70	0.0000
B:Acid	98019.3	1	98019.3	5.70	0.0225
C:time	265615.	1	265615.	15.44	0.0004
AA	34179.6	1	34179.6	1.99	0.1675
AB	111435.	1	111435.	6.48	0.0155
AC	267591.	1	267591.	15.56	0.0004
BB	3214.36	1	3214.36	0.19	0.6682
BC	1592.95	1	1592.95	0.09	0.7627
CC	138238.	1	138238.	8.04	0.0076
Total error	602036.	35	17201.0		
Total (corr.)	3.25517E6	44			

R-squared = 81.5052 percent

Table III-47: Analysis of Variance for Glucose Low DIC severity

Source	Sum of Squares	Df	Mean Square	F-Ratio	P-Value
A:Temp	427059.	1	427059.	21.80	0.0000
B:Acid	235439.	1	235439.	12.02	0.0014
C:time	155368.	1	155368.	7.93	0.0079
AA	1292.77	1	1292.77	0.07	0.7988
AB	62194.5	1	62194.5	3.17	0.0835
AC	65608.9	1	65608.9	3.35	0.0758
BB	35488.2	1	35488.2	1.81	0.1870
BC	4397.44	1	4397.44	0.22	0.6386
CC	122280.	1	122280.	6.24	0.0173
Total error	685671.	35	19590.6		
Total (corr.)	2.07454E6	44			

R-squared = 66.9482 percent

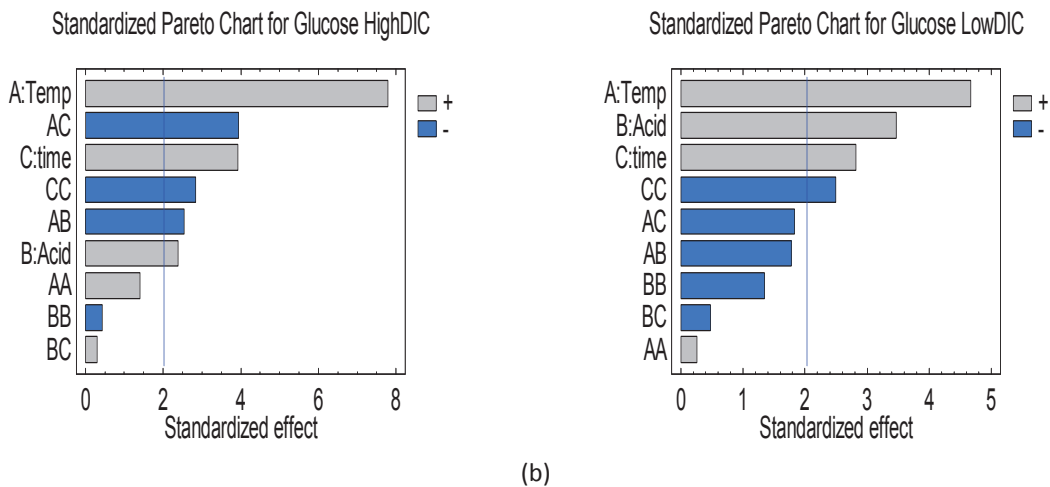
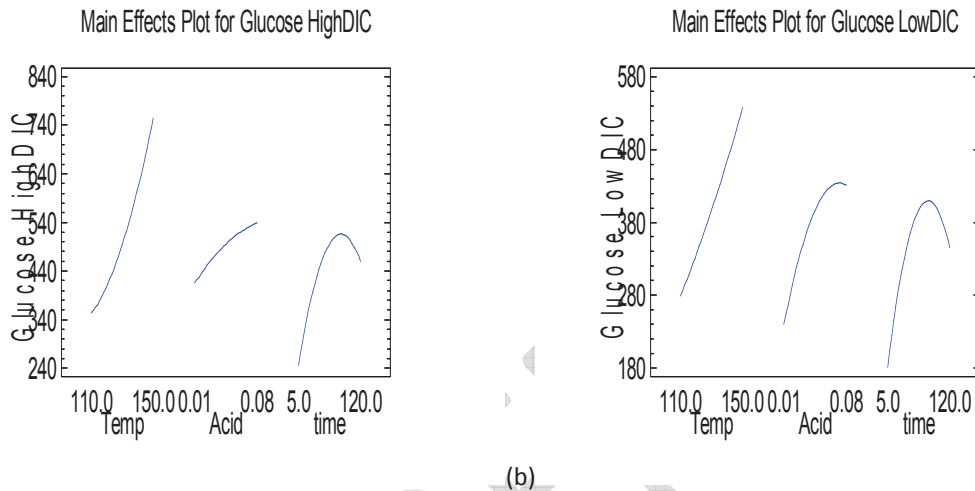


Figure III-41: Pareto chart for standardized effect of glucose at High DIC and Low DIC severities.

Magnitude of main effect for glucose yield for both treatments was found to have a similar pattern towards glucose yield (Figure III-42(a) and (b)). With respect to treatment time, a short treatment time (20 to 60 minutes) will increase about 300 and 200 mg/g glucose for respective DIC treatment severity. Longer treatment time will decrease glucose yield due to degradation. Dilute acid hydrolysis for both DIC treatment severities were highly affected by an increase in treatment temperature from 110°C to 150°C by nearly 400 mg/g and 270 mg/g in respective Figure III-42(a) and (b). Low DIC severity treated materials was found to required high level of acid to increase its glucose yield.



(a) (b)
Figure III-42: Main effect plots of glucose yield at High and Low DIC severity

All above combination effect will further explained in response surface model, and to construct both models; two polynomial equations were developed for both DIC severity treatments respectively as follows:

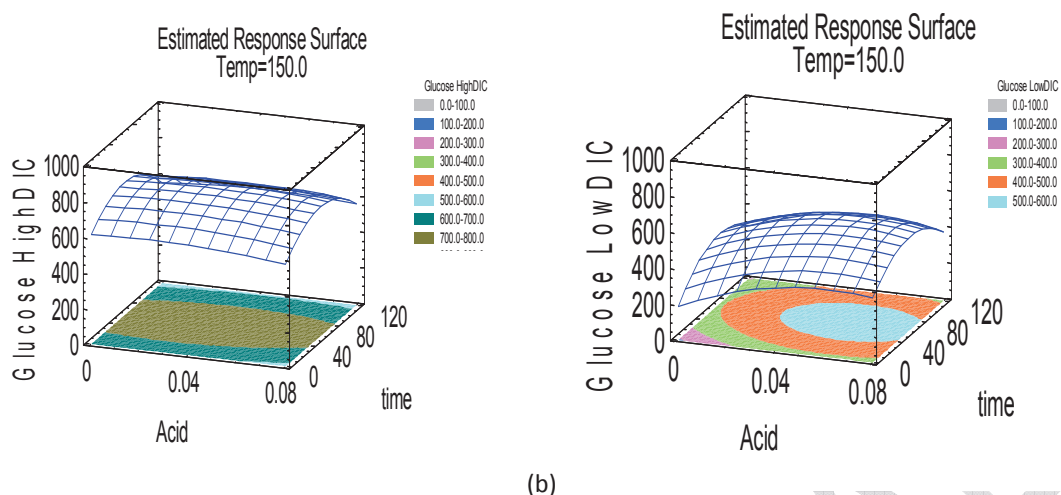
$$\begin{aligned} \text{Glucose HighDIC} = & -270.338 - 16.034*\text{Temp} + 16608.8*\text{Acid} + 21.8501*\text{time} + \\ & 0.146158*\text{Temp}^2 - 106.274*\text{Temp}*\text{Acid} - 0.114062*\text{Temp}*\text{time} - \\ & 14991.3*\text{Acid}^2 + 5.01181*\text{Acid}*\text{time} - 0.043058*\text{time}^2 \end{aligned} \quad \text{Equation 25-3}$$

$$\begin{aligned} \text{Glucose LowDIC} = & -1376.19 + 6.14346*\text{Temp} + 18048.3*\text{Acid} + 14.2057*\text{time} + 0.028425*\text{Temp}^2 - \\ & 79.3946*\text{Temp}*\text{Acid} - 0.0564788*\text{Temp}*\text{time} - 49811.9*\text{Acid}^2 - \\ & 8.3271*\text{Acid}*\text{time} - 0.0404966*\text{time}^2 \end{aligned} \quad \text{Equation 25-4}$$

The anticipated outcome from this polynomial model was that the maximum glucose optimum condition based on both consecutive first orders kinetic model and further supported by input from main and interaction effect as suggested in ANOVA analysis.

Based on the response surface model developed from both polynomial equations in Figure III-43(a); maximum amount glucose yield from High DIC severity can be obtained using acid concentration from 0.01 molar to 0.08 molar and within wide treatment time of about 20 minutes to 80 minutes. Glucose yields from these combinations were expected to be within 700 to 800 mg/ g material.

For Low DIC severity as presented in Figure III-43(b), highest glucose yield was expected to be within 500 to 600 mg/g material. Process will require medium to high acid concentration (0.04 to 0.08 molar) with treatment time of wide treatment range of 30 to 90 minutes.



(a) (b)
 Figure III-43: Response surface model and its contour for dilute acid hydrolysis of DIC treated SPW at (a) High severity and (b) Low severity at temperature 150°C. Acid concentration and treatment time were varied within treatment limit.

III.3.7. Conclusion

Both response surface model and kinetic models developed from experimental data in this study was found to be very useful to assist optimization for both process stages. Experimental data was found to have good fit with kinetic model developed using consecutive first order reaction. For response surface model, experimental data with high glucose degradation was removed to increase experimental data and model correlation in order to get a highly representative response model. Both models was successfully used to explain related phenomenon associated to first DIC stage and second dilute acid hydrolysis stage.

The extended levels of treatment parameters towards glucose degradation were studied in this work to optimize dilute acid hydrolysis. It was observed that glucose degradation affects the correlation coefficient for response surface model as well as reduce the final product yield. It was observed that there are interaction effects that contribute significantly towards the glucose yield such as interaction effect of AC (temperature-time), AB (temperature-acid) and CC (time-time) which will reduce the yield of glucose at respective high level.

It was found that low treatment time is favorable to the process, such as at high temperature, only short treatment time was required to achieve a maximum amount of glucose. With such information, reduction in treatment time was expected to reduce other contributing factors as well; such as the coefficient of AC and CC that (related to time) will be reduced further if short treatment time is used. It was also found that materials treated with DIC at high severity favor a short treatment time and high temperature.

Information on the combinations of reaction factors and its associated level assist the study of the **“Optimization of DIC Assisted Hydrolytic Conversion of Polysaccharides (Starch and Cellulose)”** with a conclusion that for this combined two stage thermal process (DIC treatment followed by dilute acid hydrolysis), on materials containing high crude starch, we will require first stage DIC treatment with High severity combination followed by second stage dilute acid hydrolysis with dilute acid hydrolysis in low and medium acid concentration (0.01 molar and 0.04 molar) at 150°C with short hydrolysis time within 20 minutes. About

830 to 850 mg/g glucose was produced using above combination. With this treatment combination, degraded glucose as calculated from the kinetic models were estimated to be 43 mg/g and 68 mg/g for respective treatment combination.

In a similar way estimated maximum glucose yield for DIC Low severity with acid concentration 0.04 molar at 110, 130 and 150°C were 491 mg/g, 450 mg/g and 687 mg/g respectively. Glucose degradation products for respective condition were 2 mg/g, 130 mg/g and 130 mg/g at respective treatment time 240 min, 120 min and 30 min.

Based on results obtained from the study in this Chapter 3 and previous Chapter 1 and Chapter 2, we can conclude that:

1. It was possible to use only DIC as treatment to convert SPW into glucose, with some degradation of glucose into formic acid and levulinic acid in hot water extract.
2. Further study needs to be conducted on actual DIC kinetic involving level of reaction factors to obtain and compare the experimental result and model as presented in Chapter 2.
3. Second stage dilute acid hydrolysis also may assist the total conversion of DIC treated material into glucose, in particular, for the low DIC severity treated material.

The following Paper 6 and Paper 7 in Chapter 4 describe the study on glucose degradation and non-isothermal rate constant for heating in order to explore the details of the process respectively.

Paper 6: Glucose degradation kinetic study

Abstract

Glucose degradation kinetic was studied using similar reaction factors and condition during dilute acid hydrolysis; with three process temperatures (110, 130 and 150°C), three acid concentration (0.01, 0.04 and 0.08 molar) during hydrolysis time of 5, 15, 30, 60, 90, 120 and 240 minutes. Kinetic models were developed to calculate total degradation that could occur during the process. Data was further transformed into a response surface model with two levels factorial designs. Response surface model was developed to investigate the overall factors (acid concentration, temperature and time, as well as its interactions) level on glucose yield. Rate constant for glucose degradation (k_2) was calculated using first order kinetic models. Glucose degradation for dilute acid hydrolysis was contributed by external factors generated during DIC autohydrolysis such as acid soluble lignin and acetic acid, and need to be isolated through a hot water extraction step.

III.3.8.Objectives

Objectives for this work were to obtain glucose degradation level and its kinetic data that affect dilute acid hydrolysis of DIC treated materials. Experiment was done using similar treatment factor and level as in dilute acid hydrolysis in order to isolate and associate glucose degradation in this study with dilute acid hydrolysis on DIC treated SPW.

III.3.9.Introduction

This work was done to obtain important information of glucose degradation during dilute acid hydrolysis on DIC treated materials. This was an important step to understand the factors level that affected glucose degradation and mechanism that were suitable to avoid glucose degradation. Previously, it was shown that degradation of glucose was prevalent in the range beyond 160°C [138]. Also, we have shown that biomass hydrolysis research has progressed to the point where hydrolysis process and optimization require generalized kinetic correlation, mechanism of glucose generation and glucose degradation only [138, 139].

To study the degradation kinetic of glucose, Equation $[A]_t = [A]_0 e^{-k_2 t}$ will be used to describe the kinetic operation. This first order kinetic model equation will be solved with actual $[A]$ from experiment ($[A]_{act}$) fitted against $[A]$ calculated ($[A]_{cal}$) and k with the lowest sum of $([A]_{act} - [A]_{cal})^2$ will be obtained (using solver in Excel).

III.3.10. Materials and Methods

III.3.10.1. Chemicals

All chemicals used in this study were of analytical grades and was use as it is. Sulfuric acid 98%, glucose, levulinic acid, acetic acid and formic acid was obtained from Sigma Aldrich.

Mobile phase and water used in this study were prepared in our laboratory using deionized water system and pure water system [Purelab Option-Q, ELGA] as described earlier.

III.3.10.2. Experimental procedures

III.3.10.2.1. Glucose Degradation Kinetic and Glucose Residue Determination with HPLC

Glucose degradation kinetic was studied to determine the condition and rate of glucose degradation under condition used in dilute acid hydrolysis, i.e. acid concentration, temperature and stainless steel tube reactor used in dilute acid hydrolysis process for SPW treated with DIC.

Accurately, 10 ml 0.2 molar glucose solutions was prepared using three acid concentrations, 0.01, 0.04 and 0.08 molar sulfuric acids respectively and put into a stainless steel tube reactor. All stainless steel tubes were tightly capped and transferred into a hot oil bath previously set at 110, 130 or 150°C. Stainless steel tube will be taken out of oil bath and immediately cools under running water at a specific time of 5, 15, 30, 60, 120 and 240 minutes after taking into consideration non-isothermal time. 2 ml acid hydrolysate was withdrawn with micropipette into a centrifuge vial, closed and centrifuged at 5000 rpm for 10 minutes. 1 ml of a clear supernatant was carefully transferred into HPLC glass vial and determined with HPLC system for glucose residue as specified earlier.

III.3.10.2.2. RSM and Factors Interaction in Glucose Degradation

Response surface model will be developed to explain factors level effects that contribute to the degradation of glucose. Glucose degradation kinetic data was subjected to factorial design study to find main and interaction effect for each factors involved; temperature, time, and acid concentration.

The treatment factors (treatment time, temperature and acid concentration) were presented in above procedure. Statistical analysis for design to study interaction effect for treatment factors were obtained from analysis of variance. Significance of factors was determined by their probability in the ANOVA analyses. It was considered significant if the p-value was lower than 0.05, meaning that the probability of noise causing the correlation between a factor and the response is lower than 0.05.

III.3.11. Result and Discussion

III.3.11.1. Kinetic of Glucose Degradation

In general, glucose degradation was affected by an increase in treatment time, temperature and acid concentration. Degradation kinetic for glucose in different acid concentration was found to follow first order kinetic reaction similar to result of other research groups [157]. Important kinetic parameter was calculated and presented in Table III-48. Activation energy, as an indicator for the minimum energy required for glucose degradation to start was calculated and presented in Table III-49.

Prolonged treatment time to 240 minutes for a glucose solution at 0.01, 0.04 and 0.08 molar acids, and an increase in temperature from 110 to 150°C was found to degrade nearly 20%,

35% and 50% glucose respectively from its initial concentration. This was further supported by rate constant for glucose degradation as in Table III-48 that shows an increase in rate constant k_2 towards an increase in temperature and acid concentrations. As a comparison, for treatment at temperature 110°C and 150°C, relative degradation rate was increased from 17 times faster at 0.01 molar to 25 times faster when glucose was exposed to sulfuric acid with concentration of 0.04 and 0.08 molar.

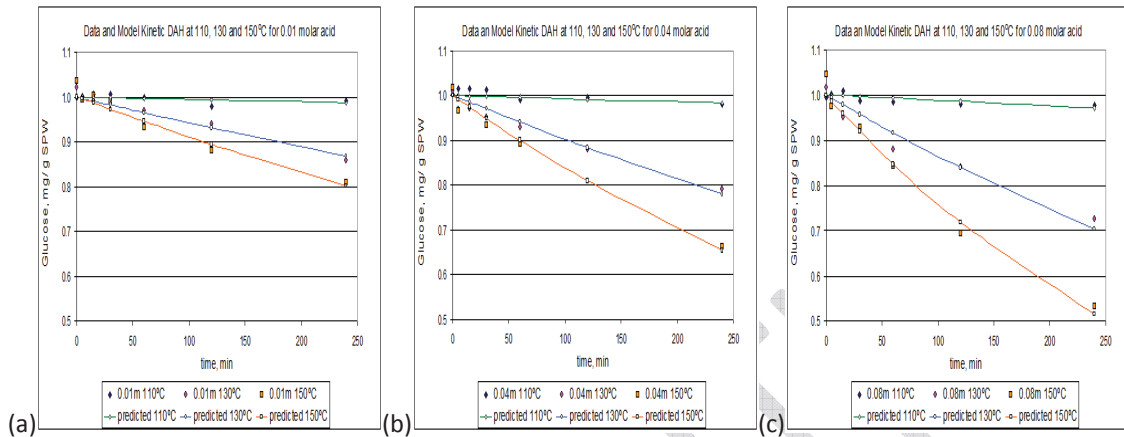


Figure III-44: Profile of glucose residue experimental point and respective kinetic model after hydrolysis kinetic for 0.2 molar glucose with (a) 0.01, (b) 0.04 and (c) 0.08 molar sulfuric acid respectively.

Table III-48: Kinetic data (rate constant k_2) for glucose degradation kinetic in dilute acid.

	Glucose degradation		
	110°C	130°C	150°C
T	110°C	130°C	150°C
Ao	100%	100%	100%
0.01 molar			
k_2	0.053583×10^{-3}	0.59161×10^{-3}	0.92129×10^{-3}
0.04 molar			
k_2	0.070866×10^{-3}	1.03385×10^{-3}	1.76955×10^{-3}
0.08 molar			
k_2	0.117438×10^{-3}	1.46167×10^{-3}	2.76225×10^{-3}

Table III-49: Activation energy (kJ/ mole) for degradation of glucose

Acid concentration	0.01 molar	0.04 molar	0.08 molar
Ea Glu _{degradation}	96.80	109.46	107.3
R ²	0.9395	0.9433	0.9544

Activation energy for several conditions during glucose degradation study using glass tube for temperature range in 90°C to 190°C with acid concentration of 4% to 20% was found to be in the range of 139.2 to 144.4 kJ/mole with an average of 141.6 kJ/mole [138]. Value that was obtained in this work in Table III-49 was lower than reported above. This may be due to different type of reactor materials used, i.e. stainless steel as compared to glass materials. Earlier it was reported that stainless steel reactor had caused higher degradation rate in comparison to the other materials with values obtained for glucose degradation was about 118 kJ/mole in 50 millimole sulfuric acid for a similar temperature range [157].

Finding in this work was important for the selection of type of materials for reactor design. In order to avoid interaction factor between reactor material and other treatment factor such as acid concentration and treatment temperature, similar study can be developed.

III.3.11.2. RSM Model of Glucose Degradation

RSM model to investigate main effect and interaction effect of treatment parameters towards glucose degradation was done by transformed experimental data into multilevel factorial design with three parameters. Data obtained from experiment including ANOVA, Pareto chart, main effect chart and interaction effect chart were presented below.

Table III-50: Analysis of Variance for glucose degradation

Source	Sum of Squares	Df	Mean Square	F-Ratio	P-Value
A:Temp	0.216409	1	0.216409	543.91	0.0000
B:Acid	0.0481232	1	0.0481232	120.95	0.0000
C:time	0.238515	1	0.238515	599.47	0.0000
AA	0.000675	1	0.000675	1.70	0.1995
AB	0.0159378	1	0.0159378	40.06	0.0000
AC	0.107313	1	0.107313	269.72	0.0000
BB	0.000287658	1	0.000287658	0.72	0.3998
BC	0.024778	1	0.024778	62.28	0.0000
CC	0.000382258	1	0.000382258	0.96	0.3324
Total error	0.0175064	44	0.000397873		
Total (corr.)	0.543067	53			

R-squared = 96.78 percent

R-squared (adjusted for d.f.) = 96.12 percent

Standard Error of Est. = 0.0199

In term of treatment factor; time treatment was giving highest effect in term of F-ratio, followed by temperature and acid concentration as shown in ANOVA in Table III-50, Pareto chart in Figure III-45 and main effect plot in Figure III-46.

Standardized Pareto Chart for Glu Deg

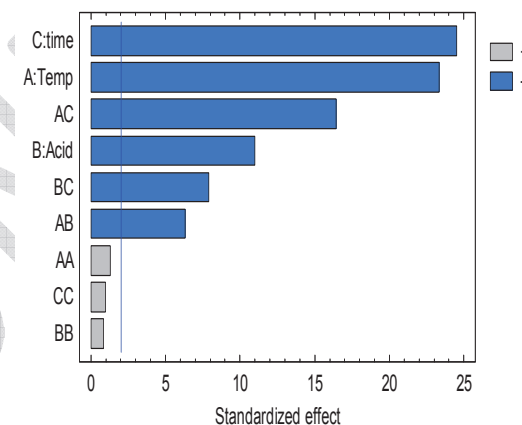


Figure III-45: Pareto chart for glucose degradation

Above result suggest that the longer the treatment will increase the amount of glucose degradations if compared to an increase in temperature and acid. This information was important for the establishment of an optimum treatment condition for the hydrolysis of polysaccharides in SPW.

Response surface model in Figure III-47 shows the residue after degradation of glucose for acid concentration of 0.01 molar and 0.08 molar. The minimum point with acid concentration 0.01 molar was within 0.6 to 0.8 ranges after treatment of 240 minutes. For model with acid concentration of 0.8 molar, as explained before, nearly half of glucose was converted into glucose a degradation product.

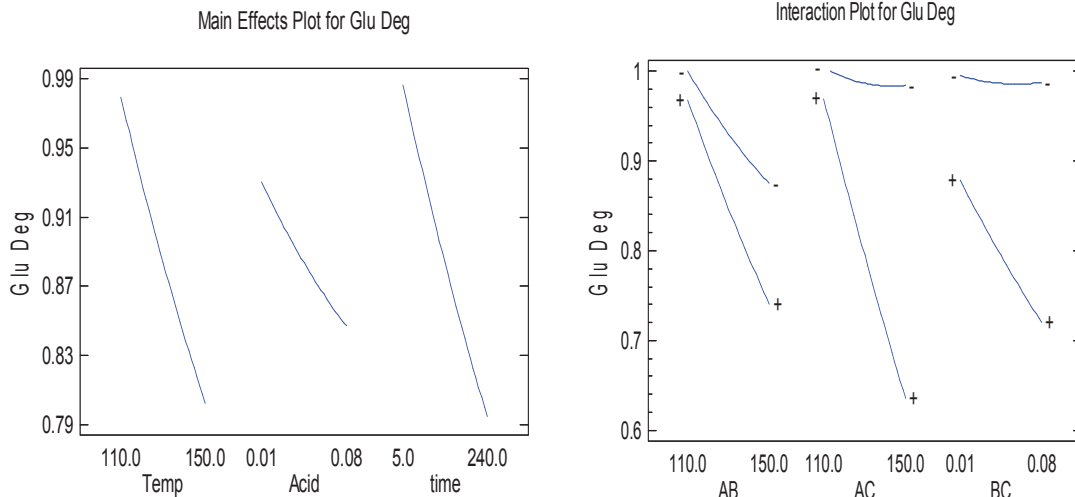


Figure III-46: Main effect and interaction effect for glucose degradation.

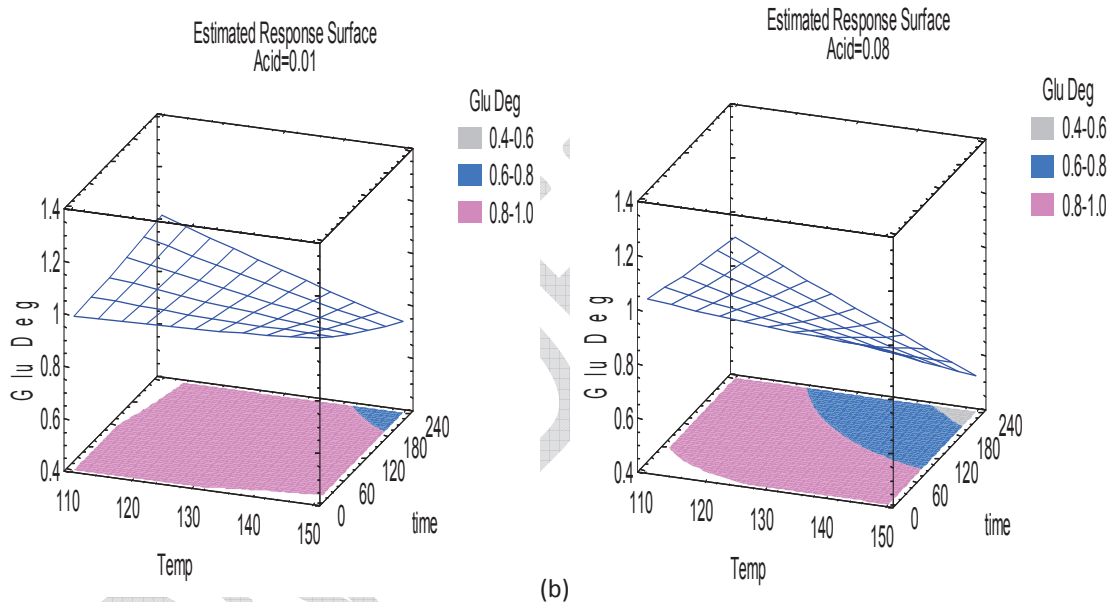


Figure III-47: Response surface model for glucose degradation at acid (a) 0.01 and (b) 0.08 molar.

Table III-51: Comparison of glucose degradation rate constant ($k_{2\text{SPW}}$) for DIC treated materials normalized against rate constant of pure glucose ($k_{2\text{deg}}$) of respective treatment condition.

Materials	Low DIC severity			High DIC severity		
	110°C	130°C	150°C	110°C	130°C	150°C
	0.01 molar					
$k_{2\text{SPW}}/k_{2\text{deg}}$	n/a	0.51	5.68	81.83	4.68	3.54
	0.04 molar					
$k_{2\text{SPW}}/k_{2\text{deg}}$	0.35	5.82	4.84	66.95	2.03	2.71
	0.08 molar					
$k_{2\text{SPW}}/k_{2\text{deg}}$	14.82	4.20	8.03	17.30	1.76	2.86

n/a: not available

In general, Table III-51 shows comparison of glucose degradation for SPW (value of k_2 from Table III-44) and pure glucose (value of k_2 from Table III-48). For example, for high DIC severity sample, at 110°C with acid concentration of 0.08 molar, degradation of glucose was

17.3 times relatively higher than pure glucose degradation. For low DIC severity SPW, there was no specific trend was found, however for high DIC severity materials it was found with an increase in temperature and acid concentration; the relative degradation of DIC materials against pure glucose will be decreased, which means glucose degradation is proceeds at almost the same rate whether it was originated from pure glucose or glucose from hydrolysis of the biomass. This was quite an important observation to decide the parameter of treatment during hydrolysis process.

The difference in magnitude of degradation for pure glucose and thermally treated material was due to different composition in an acid hydrolysate for both types. In DIC treated material, acid hydrolysate was exist in heterogeneous combinations with different type of materials, such as acetic acid, lignin and lignin soluble and various other components of degradation. High DIC severity was having higher capacity than low DIC treatment due to availability of various components during DIC autohydrolysis process, whereas for low DIC severity, the most possible component only oligosaccharides that have no potential to increase the degradation of glucose. In the case of low DIC severity treatment, contribution to glucose degradation was expected only coming from hydrolysis factors (acid, temperature and time), whereas for high DIC severity, other factors contribute to the degradation that not existed in low DIC severity treated materials, such as the contribution from acid soluble lignin from lignin [12, 178] and acetic acid from an acetyl group in hemicelluloses.

An example of other factors that possible to contribute to the increase in glucose degradation was the presence of acid soluble lignin as presented in Table III-52. Low severity DIC was shown to have very minimal acid soluble lignin while high DIC severity was shown to have a higher amount of acid soluble lignin. For sample that hot water extracted and dilute acid hydrolysis, its acid soluble content was lower than content in hot water extract, while for sample that was extracted with alkali was shown have a higher amount of acid soluble lignin, this was expected due to an exposure of lignin during extraction due to solubility of a certain cell wall of biomass. Acid hydrolysis on SPW treated with alkali (NaOH) also was shown to have an increase in its acid soluble lignin content due to exposure of certain lignin component during an extraction process.

Table III-52: *Content of acid soluble lignin in hydrolysate of several SPW based materials for reference. All DIC pretreatment was done at center points combination.*

	Acid soluble lignin, mg	Treatment
SPW	0.74	Hydrolysate of dilute acid hydrolysis
SPW Low DIC severity	0.48	Hot water extract
SPW High DIC severity	1.61	Hot water extract
SPW DIC, HWE & hydrolysis	1.29	Hydrolysate of dilute acid hydrolysis
SPW NaOH	3.27	5% NaOH extract, hydrolysate of dilute acid hydrolysis

Determination was done using acid soluble lignin method as described in Part 2, section II.1.3.4.1 in page 61. Content was determined using 10 ml hydrolysate of hot water extracts or dilute acid hydrolysis. Results presented here (Table III-52) was not to correlate the increase of glucose degradation with acid soluble lignin because no proper study plan was done, but only as a potential glucose degradation indicator for future study, with the first attempt to isolate potential contribution that help to increase the magnitude of relative degradation. The contribution of an external factor of material during treatment itself contributes to the increase in degradation rate constant and needs to be checked with a specific study objective.

III.3.12. Conclusion

Glucose degradation study of pure glucose was useful for understanding the mechanism related to another potential factor for glucose in actual biomass hydrolysis with dilute acid hydrolysis technology, i.e. the material in contact with a hydrolysate of hydrolysis process. This was important for the type of reactor materials selection, in particular material that was in contact with acidic solution. Selection of inert coating materials could be the solution for this type of reaction.

Comparison for rate constant k_2 of glucose degradation also shows that glucose degradation in a hydrolysate of biomass was higher than degradation for pure glucose. This information shows the potential step to decrease the degradation was including to prepare hot water extraction prior to dilute acid hydrolysis process, i.e. to remove existing soluble glucose and oligosaccharides and portion of potential contribution factors for glucose degradation such as acid soluble lignin and acetic acid.

CONFIDENTIAL

PART III. CHAP 4.
HYDROLYTIC BEHAVIOR OF NON-ISOTHERMAL STATE

Paper 7: The influence of non-isothermal state on the conversion of starch in both DIC and DAH processes.

Abstract

Non-isothermal condition during heating stage for DIC and dilute acid hydrolysis stage was studied to understand the mechanism of heating on materials for autohydrolysis reaction to starts. Rate constant for heating from heat source to the respective reaction mixture or material (min^{-1} or s^{-1}) was calculated and compared for both DIC and DAH systems. Data obtained from previous chapter was used to describe the usage of this study on a practical system.

III.4.1.Objective

This work was designed to describe the function of temperature kinetics during DIC operation upon realizing the importance of understanding the function of heat transfer during initial heating stages towards autohydrolysis on biomass. Rate constant for heating for both DIC and dilute acid hydrolysis system will be determined.

III.4.2.Introduction

DIC system and its function were clearly described by previous workers in this field. However, there exist an associated work that contributed towards understanding the heating and cooling mechanism and its contribution during heating cycle of DIC system. The closest work with the objective of this study was done by Mounir et al (2011) [122] within our research group, which described water condensation phenomenon in order to explain diffusivity of water during drying process after DIC treatment of agricultural products (such as onion and apple). Based on two drying stages, they conclude that, the DIC treatment on pre-dried material could help to expand the compact structure and remedying the shrinkage occurred during the first stage of hot air drying.

Time of the second stage of hot air drying (after DIC treatment) was found to greatly reduced to about 1 hour against conventional method of 6 h in the case of untreated apple dices. Important solution for their study was based on the mass transport of water within the onion or apple piece that based on ALLAF's presentation of Fick's type diffusion:

$$\frac{\rho_w}{\rho_d}(\vec{v}_w - \vec{v}_d) = -D_{eff} \vec{\nabla} \frac{\rho_w}{\rho_d}$$

Equation 26

At the final stage of drying, when the product was below their glass transition, drying was achieved without shrinkage and, thus, the second Fick's equation could be applied, with the Crank's solutions according to the geometry of the solid matrix [122]:

$\frac{W_{\infty} - W}{W_{\infty} - W_0} = \sum_1^{\infty} (A_i \exp(-q_i^2 t))$ which can be limited to its first term, to be expressed as:

$$\frac{W_{\infty} - W}{W_{\infty} - W_0} = A \exp\left(-\frac{\pi^2 D_{eff} t}{4d_p^2}\right)$$

Equation 27

Previously, in Part 1-1.3.7.1 in page 47 of the thesis, we have described the utilization of heat transfer equation and derived it into a final form of first-order kinetic equation (refer Equation 17 to Equation 22 in page 47) to relate the h_h (rate constant for heating from bath to reaction mixture, min^{-1} or s^{-1}) and h_c (rate constant for cooling from bath to reaction mixture, min^{-1} or s^{-1}). Only rate constant for heating, h_h was studied in this work.

The important final form of equation to study the heat-transfer coefficient during a non-isothermal state of a heating cycle for both DIC and dilute acid hydrolysis is described as follows:

$$T = T_{source} - (T_{source} - T_f) \exp^{-h_h t}$$

Equation 22

h_h – rate constant for heating from bath to reaction mixture, min^{-1} or s^{-1}

T_{source} – temperature of steam for DIC or oil bath for dilute acid hydrolysis, K or $^{\circ}\text{C}$

T_f – temperature of mixture, K or $^{\circ}\text{C}$

Notice the similar representation of the final form of both Equation 22 and Equation 27 was in the form of exponential equation. In Mounir et al (2011) work, several important process and products criteria such as moisture content (W), density (ρ), time (t), heat flow (\bar{q}) and dimensions (d) of products were required to calculate Fickian-type diffusivity, D_{eff} (i.e. effective diffusivity of water within the solid porous medium ($\text{m}^2 \text{s}^{-1}$)) from the Allaf's formula.

In this work, simple expression based on the change of temperature was developed, and Equation 22 was used to determine the value for h (unit min^{-1} or s^{-1}) at each temperature by fitting data obtained from experiment into equation to find T calculated. Similar first order kinetic model equation will be used by with actual T from experiment (T_{act}) is fitted against T calculated (T_{cal}) and h with the lowest sum of $(T_{act} - T_{cal})^2$ will be obtained (using solver in Excel). Further work in this area would be required to associate both factors.

III.4.3. Material and Method

III.4.3.1. DIC and Dilute Acid Hydrolysis System and Temperature Acquisition

The DIC system was described previously [3, 118, 121], the system composed of three main components; (1) DIC reactor (2) Vacuum system, with an initial vacuum level is maintained at 100 kPa in all trials, and (3) Pneumatic valve system that capable to open valve in less than 0.2 s to give an effect of abrupt pressure drop within a treatment vessel. Two thermocouple type J was attached to the internal thermocouple connector inside of reactor. One

thermocouple probe was placed inside of material (about 5 cm bed thickness) in treatment container, and the other one was exposed to reactor environments.

Temperature acquisition for dilute acid hydrolysis system was done with a stainless steel tube with cap and Teflon insert. Thermocouple probe Type J was attached to the screw cap, plug with Teflon from inside. High tension spring was attached to thermocouple probe from outside to ensure system was very tight. As a precaution, weight of reactor and thermocouple was recorded before and after each trial. About 10 ml 0.2 molar glucose solutions were added into tube and tightly capped and transferred into a hot oil bath previously set at 110, 130 or 150°C. End point of thermocouple was twisted several times to ensure it does not touch the reactor body. Another thermocouple probe end point was placed in the oil bath to record its temperature.

Data acquisition was done with four channels handheld data logger **Omega HH147U** and its data was downloaded into a computer through USB with software Temperature Monitor S2 (version 1.0.16; London, United Kingdom). Data acquisition rate was 10 data/second for DIC study and 1 data/second for dilute acid hydrolysis study. Accuracy of data was 0.1% for reading range between -100 to 1000°C according to manufacturer specifications. Data logger was calibrated according to manufacturer specification and equipped with thermocouple Type J, with four simultaneous data logging can be done at any time.

Further processing was done in Microsoft Excel (2003) fitting to Equation 22 according to similar way of data fitting procedure previously described.



Figure III-48: (a) Two thermocouple probe with one attached to the product and the other one exposed to reactor environment (b) Stainless steel reactor used for non-isothermal study.

III.4.4. Result and Discussion

Profile of non-isothermal plot of DIC treatment cycle at various pressures is presented in Figure III-49. Its corresponding numerical model was calculated and modeled after first kinetic reaction order using Equation 22 above. Rate constant for heating h_h was calculated for each steam pressure (in s^{-1} for DIC) condition, using initial condition at 28°C for all models. Similar treatment was done for dilute acid hydrolysis (h_h in min^{-1}).

Actual source data from several DIC treatments were presented in Figure III-49. Modeled data for both DIC and DAH processes were presented in Figure III-50.

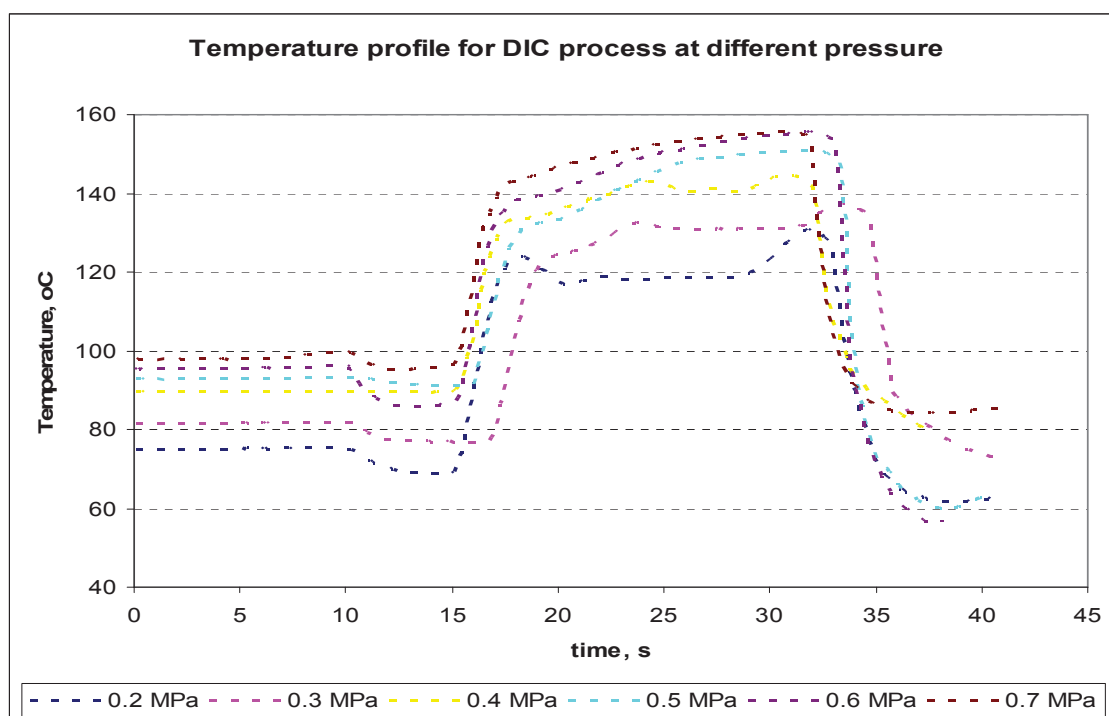


Figure III-49: Profile of the non-isothermal plot for product temperature during DIC cycles at several saturated steam pressure. Data acquisition was done at several starting temperature.

Value for h at each temperature was determined by fitting data obtained from experiment into equation to find T calculated. Actual T from experiment (T_{act}) is checked against T calculated (T_{cal}) and h with lowest sum of $(T_{act} - T_{cal})^2$ will be accepted (using solver in Excel). Plot for accepted T_{cal} and T_{act} is presented in the Figure III-50. Result for rate constant for heating for both DIC and dilute acid hydrolysis system were presented in Table III-53 and Table III-54 respectively.

Table III-53: DIC treatment rate constant for heating with unit in s^{-1} and min^{-1} .

P, MPa	T, °C	h, s^{-1}	h, min^{-1}
0.2	120.2	0.8050	48.300
0.3	133.5	0.7505	45.030
0.4	143.6	0.5505	33.030
0.5	151.8	0.5503	33.018
0.6	158.8	0.5504	33.022
0.7	164.9	0.5495	32.972

Table III-54: Dilute acid hydrolysis rate constant for heating with unit in s^{-1} and min^{-1} .

T, °C	T, °C	h, s^{-1}	h, min^{-1}
110	111	0.00780	0.4680
130	132	0.00942	0.5650
150	153	0.01208	0.7250

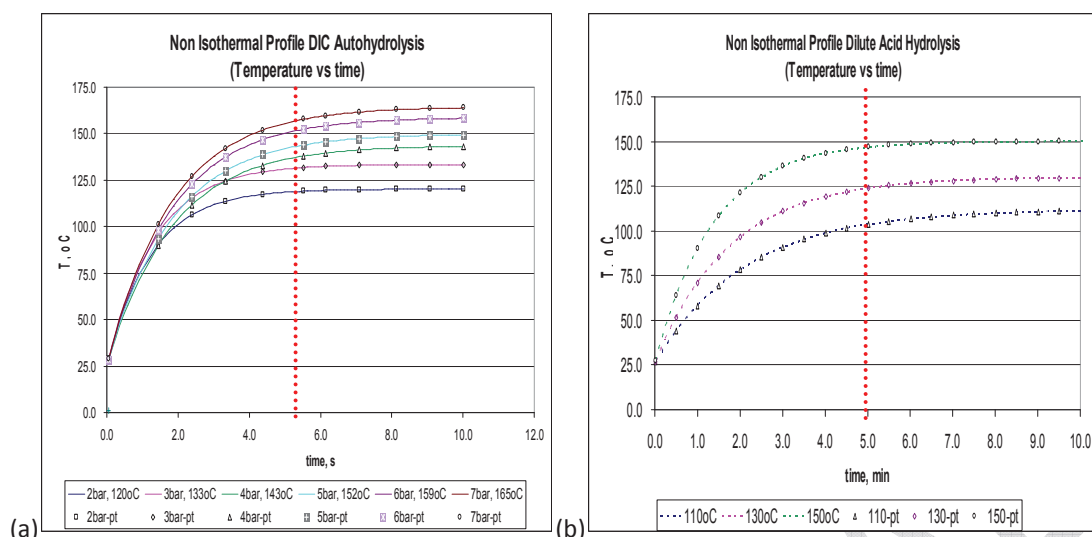


Figure III-50: Model plot of heating for (a) DIC and (b) dilute acid hydrolysis process, h value was obtained from experimental data fitting with calculated model data based on Equation 22. Red line indicated time required to pass the non-isothermal temperature.

Table III-55: Value of h , rate constant for heating at 110, 130 and 150°C as compared to the nearest temperature value.

Temperature, °C	Dilute acid hydrolysis, h , min ⁻¹	DIC heating, h , min ⁻¹	Relative rate of heating : $h_{DIC} / h_{\text{dilute acid hydrolysis}}$
110	0.468	n/a	n/a
130	0.565	45.030	79.7
150	0.725	33.018	45.5

Value of rate constant for heating in Table III-53 and Table III-54 was useful to describe the non-isothermal regime during start-up of the dilute acid hydrolysis kinetic. About 5 minutes was required to raise the product temperature towards oil bath temperature, while only about 5 second was required in DIC treatment. Calculated relative rate constant for heating for DIC and dilute acid hydrolysis as in Table III-55 was about 45 to 80 times higher in DIC system depending on final temperature of the system.

This information offers an insight into the difference in heat transfer of both systems, and it can be associated with the requirement of rate constant k_1 and k_2 (in which $k_1 \gg k_2$ was required for optimum hydrolysis of polysaccharides into glucose). Fast hydrolysis kinetic operation during conversion of polysaccharides into glucose with minimum glucose degradation was required in this study.

To compare the effect of approximate glucose obtained from existing process, the following Table III-56 is presented and its calculated data based on glucose generated at an initial isothermal time for respective system.

Table III-56: Value of glucose for DIC and dilute acid hydrolysis system at the end of non-isothermal time. Rate of glucose conversion was calculated to assist in comparison of both system at about 150°C

System	Time at end non-isothermal	Glucose	Glucose rate, mg/s	Data source
DIC	5 s	~30 mg/g	6.0	148°C, 0.2 molar for SPW treatment with DIC followed with hot water extraction.
DAH	6 min	371 mg/g	1.03	150°C, 0.08 molar for low DIC severity SPW treated material followed by DAH

Based on those data, DIC rate of conversion was calculated to relatively about 5.8 times much higher than using dilute acid hydrolysis process. Comparison for the DIC treatment

result was done with low DIC severity treated materials due to no data available for non treated SPW dilute acid hydrolysis.

Relative rate for the conversion based on glucose conversion in Table III-56 was found to less than the relative rate of heating in Table III-55, which was quite normal if we take into consideration for two steps conversion of polysaccharides into glucose. The consecutive reaction steps will normally require the concentration of substrate to achieve certain level before it started. So with some limitation on time and acid concentration the rate for that particular temperature will be affected. Moreover, DIC and dilute acid hydrolysis were involved with mass as compared to non-isothermal study only involved with temperature.

III.4.5. Conclusion

The study of non-isothermal region and determination of a rate constant for heating for both DIC and dilute acid hydrolysis was done to assist in understanding of the thermal process on products to be obtained. This was important for controlling the degradation that could occur during hydrolysis process. DIC system was shown to have a high-rate constant for heating of about 45 to 80 times higher than dilute acid hydrolysis process. Subsequently, the glucose rate generation was about 6 times higher in DIC if compared to dilute acid hydrolysis. During practical application of hydrolysis, its relative rate of conversion of polysaccharides into glucose was quite low if compared to the relative heat transfer of system due to involvement of mass and chemical reactions before glucose is obtained.

Significant of this work, including; (1) Estimation of heat loss for better system efficiency can be calculated (2) Control and efficiency of a thermal system can be pre-estimated using the heat-transfer coefficient for a very heat sensitive process or materials.

PART IV.
CONCLUSION AND FUTURE WORKS

CONFIDENTIAL

PART IV. CHAP 1.

CONCLUSION

Several important conclusions that could be derived from this work will be summarized according to the chronological order of appearance in the thesis.

Generally, there are three factors that correlated to each other in any chemical process industries: good input materials, output products and processing technology being used. Information of reaction factors will further enhance the study through understanding of a mechanism due to factor effect and interaction effect between them. Sago pith waste was selected for this work, mainly due to the availability of a high amount of polysaccharides, combined with high economic viability. The availability of high starch content and other polysaccharide's composition offer SPW's as a good starting material. High moisture content in SPW allows us to synergize the autohydrolysis reaction with unique DIC thermal pretreatment process. Both rapid autohydrolysis and rapid pressure drop was found to provide combined positive reactions to depolymerize crude starch into glucose and oligosaccharides. Rapid pressure drop during material being heated with steam has caused moisture evaporation and increased the potential to break the internal cell wall's cavities thus increase the surface area for hydrolysis reaction. Vacuum application in thermal treatment is the unique feature of DIC process not available in other thermal processes.

In terms of the process; we found that by controlling DIC treatment severity, crude starch can be transformed into either lower DP oligosaccharides or as glucose. This could offer the DIC process as a new novel and versatile process for the area of polysaccharide conversion studies. This work also shows that DIC treatment was having a high-heat transfer rate than dilute acid hydrolysis process. It was shown that with moderate DIC treatment combination, 67% starch was converted into glucose. Hot water extraction process of glucose also can be done at high solid loading compared to present processes, which uses excess water and low solid loading. Solid residue after hot water extracts still rich in cellulose and starch components constitute about 50 to 60% of solid residues can be further hydrolyzed either as feed material in second stage dilute acid hydrolysis or through another DIC treatment at much lower treatment severity. Dilute acid hydrolysis on DIC treated material (post-DIC) was shown to be able to convert nearly 80% of biomass into glucose and with very minimal degradation on glucose obtained.

Based on the study of both low DIC severity and high DIC severity, it can be concluded that starch undergo two steps process for the conversion of starch polymer into glucose. Crude starch will undergo conversion into oligosaccharides followed by the hydrolysis of alpha-bond of oligosaccharides into glucose. This was confirmed by the high availability of DP>2 products in HPLC chromatogram.

In hydrolysis kinetic studies, rate constant of the process was calculated in order to identify time for maximum glucose concentration, rate constant ratio for generation and degradation as well as to determine activation energy of the respective process. It was found that DIC treatment would require 3 to 4 minutes to fully hydrolyzed polysaccharides in SPW into glucose. On contrary, in dilute acid hydrolysis process, DIC treated material will require 20 to 30 minutes to be converted into glucose. Activation energy for glucose generation was

found to be lower than glucose degradation, which was the requirement for a good hydrolysis process and to avoid degradation from starts.

Response surface model and kinetic models were developed to assist fundamental understanding of the process. Response surface was developed to study main effect and interaction effect of factors while the kinetic model was developed to determine the rate constant of the process. Data obtained from both response surface and kinetic models were useful for the development and critical decision in the process. At high DIC severity, only low acid concentration at 0.01 and 0.05 molar sulfuric acid, with an initial moisture content of 150% were required to autohydrolysed nearly 800 mg/g polysaccharides into glucose. From RSM model, it was found that an increase in temperature and acid concentration will help to increase the autohydrolysis of glucose. However, with an increase in treatment time, initially it will increase the glucose yield and after certain treatment time (within 3-4 minute) it will decrease the glucose amount due to the degradation was taking place. Both models were found to complement to each other provided the constraints were satisfied.

Consecutive first order kinetic reaction model was used to explain results obtained from both DIC kinetic and dilute acid hydrolysis kinetic. It shows that an increase in glucose degradation was very closely associated with treatment time. Through the study of main effect and interaction effect using response surface, we can conclude that by lowering the treatment time, all other interaction effect for time also will be lowered. This was demonstrated in the treatment of less than 4 minutes with DIC for raw crude starch material and with about less than 30 minutes for dilutes acid hydrolysis process with material that was treated at high DIC severity. The lowering of treatment time for both process have lowered its interaction effect (factor time) thus contribute to the lowering of glucose degradation in the actual process.

Process that was developed in this work was closely related to the dilute acid hydrolysis reaction. From existing data of other workers, acid process at high concentration (1.5 molar sulfuric acids) was found to hydrolyze about 623 mg/g of SPW into glucose, while enzymatic process yield was much lower at about 560 mg/g. If compared to result in this work, for DIC at combination described above, about 800 mg/g glucose can be produced at much lower acid concentration of 0.2 molar within short treatment time. For two stage operation, a similar amount was recorded at lower concentration of 0.01 to .04 molar sulfuric acid compared to data of other workers. This shows that DIC treatment alone was possible for the total conversion of SPW into glucose. No comparison can be made presently for enzymatic process.

In comparison to another thermal biomass process, such as the steam explosion process; DIC process developed in this study was at lower saturated steam pressure of less than 1.0 MPa compare to steam explosion need a minimum 1.0 MPa steam pressure and in most cases operated at 1.5 MPa and above. The advantage for DIC is that, vacuum treatment will remove a thin layer of moisture from the surface of material being treated, and will increase the heat transfer operation for the autohydrolysis to starts. It was recorded that yield of steam exploded material was quite low due to losses of treated material's inside steam condensate generated during the process. In comparison, DIC system was found to produce very minimum amount of condensate.

From information gathered based on quantitative and statistical analysis during the (i) exploratory studies, (ii) study of kinetic models obtained from RSM of DIC process, as well as

from (iii) kinetic data based on experimental works during dilute acid hydrolysis study; we found that all data and models support the assumption that DIC treatment alone is sufficient for the total conversion of SPW into glucose.

From above observation, we conclude that the strategy to utilize both DIC and crude starch in the form of sago pith waste for conversion through thermo-mechanical route with DIC process and technology into glucose was practical and can be offered as a novel operation to solve present ineffective starch extraction in sago industry.

We also discover several potential areas for further development as summarized in the following chapter.

CONFIDENTIAL

PART IV. CHAP 2.

FUTURE WORKS

Through out the study, we have found several interesting potential future works associated with DIC treatment on sago pith waste as follows:

1. At a lower treatment severity, glucose was the degradation products with oligosaccharides as the product of interest. Methodology based on intrinsic viscosity studies can be used to study in detail this phenomenon, with output of the process will have direct application in prebiotic and food applications.
2. To study combination of DIC derivatives with no vacuum at second cycle; its rate of cooling was not as great as with vacuum, in the exploratory study, we found that at higher moisture content, and without second vacuum cycle, the yield of glucose was much higher than the other treatment. Study should combine the heat transfer at a non-isothermal range to adjust the rate of cooling due to relaxation towards vacuum and rate of cooling due to relaxation towards atmospheric pressure. This non-isothermal study will enable to understand into mechanism and calculate the rate constant of glucose generation and degradation in comparison to present study.
3. Current interest was to develop single DIC process for full conversion of polysaccharides into glucose. It was shown that at moderate DIC treatment 67% starch was converted into glucose and can be immediately extracted. The remaining polysaccharides will constitute about 50 to 60% of residues. It was shown that the materials have higher accessibility towards enzymatic activity, thus a second process utilizes celluclast for conversion of cellulose can be done after starch fully converted into glucose.
4. Degradation of glucose also was found to be associated with type of materials used as the reactor body during dilute acid hydrolysis. In this work, we use stainless steel as the reactor body with Teflon as insert to avoid losses of reaction mixture to the environment. It was found that activation energy for glucose degradation with glass reactor was higher than activation energy with reactor made of stainless steel by nearly 20% (i.e. 144 kJ/mol against 118 kJ/mol respectively). The lowering of activation energy for glucose degradation must be avoided to ensure the relative rate of k_1/k_2 to be as high as possible. Based on this, similar study could be done using different coating material on reactor surface to evaluate kinetic parameters. Similarly, main effect and interaction effect using response surface methodology could be developed. Input from this study could be used to decide reactor material or its surface contact coating to improve further glucose generation and minimize glucose degradation.
5. In the present work, we use single study response, i.e. glucose concentration; however, we realized that there are several other study responses was possible such as acid soluble lignin, degree of polymerization, crystallinity index, moisture content and heat of vaporization in order to associate effect of DIC treatment on biomass materials. There is a need to study further which one will give highest correlation with the actual objective. Eg. for acid soluble lignin was directly related to the solubilization of lignin in available in materials, which in turn maybe able to describe the deconstruction of lignin that exist in biomass and its effect towards glucose generation.

REFERENCE

1. Wyman, C.E., et al., *Coordinated development of leading biomass pretreatment technologies*. Bioresource Technology, 2005. **96**(18): p. 1959-1966.
2. Hendriks, A.T.W.M. and G. Zeeman, *Pretreatments to enhance the digestibility of lignocellulosic biomass*. Bioresource Technology, 2009. **100**(1): p. 10-18.
3. Louka, N. and K. Allaf, *Expansion ratio and color improvement of dried vegetables texturized by a new process "Controlled Sudden Decompression to the vacuum": Application to potatoes, carrots and onions*. Journal of Food Engineering, 2004. **65**(2): p. 233-243.
4. Kamal, I.M., et al., *Structure expansion of green coffee beans using instantaneous controlled pressure drop process*. Innovative Food Science & Emerging Technologies, 2008. **9**(4): p. 534-541.
5. Kristiawan, M., V. Sobolik, and K. Allaf, *Isolation of Indonesian cananga oil using multi-cycle pressure drop process*. Journal of Chromatography A, 2008. **1192**(2): p. 306-318.
6. Taherzadeh, M.J., et al., *Characterization and Fermentation of Dilute-Acid Hydrolyzates from Wood*. Industrial & Engineering Chemistry Research, 1997. **36**(11): p. 4659-4665.
7. Torget, R.W., J.S. Kim, and Y.Y. Lee, *Fundamental Aspects of Dilute Acid Hydrolysis/Fractionation Kinetics of Hardwood Carbohydrates. 1. Cellulose Hydrolysis*. Industrial & Engineering Chemistry Research, 2000. **39**(8): p. 2817-2825.
8. Heitz, M., et al., *Fractionation of Populus Tremuloides at the Pilot Plant scale: optimization of steam pretreatment conditions using the Stake II Technology*. Bioresource Technology, 1991. **35**: p. 23-32.
9. Cara, C., et al., *Conversion of olive tree biomass into fermentable sugars by dilute acid pretreatment and enzymatic saccharification*. Bioresource Technology, 2008. **99**(6): p. 1869-1876.
10. Kumoro, A.C., et al., *Conversion of Fibrous Sago (Metroxylon sagu) Waste into Fermentable Sugar via Acid and Enzymatic Hydrolysis*. Asian Journal of Scientific Research, 2008. **1**: p. 412-420.
11. Awg-Adeni, D.S., et al., *Bioconversion of sago residue into value added products* African Journal of Biotechnology, 2010. **9**(14): p. 2016-2021.
12. Sun, X.F., et al., *Characteristics of degraded cellulose obtained from steam-exploded wheat straw*. Carbohydrate Research, 2005. **340**(1): p. 97-106.
13. Xu, W., et al., *Modification of wool fiber using steam explosion*. European Polymer Journal, 2006. **42**(9): p. 2168-2173.
14. Palmqvist, E., et al., *Simultaneous detoxification and enzyme production of hemicellulose hydrolysates obtained after steam pretreatment*. Enzyme and Microbial Technology, 1997. **20**(4): p. 286-293.
15. Jeoh, T. and F.A. Agblevor, *Characterization and fermentation of steam exploded cotton gin waste*. Biomass and Bioenergy, 2001. **21**(2): p. 109-120.
16. Bell, A.T., B.C. Gates, and D. Ray, *Basic research needs: catalysis for energy - Report from the US Department of Energy Basic Energy Sciences Workshop, in US Department of Energy Basic Energy Sciences Workshop*. 2007, U.S. Department of Energy.

17. Huber, G.W. and J.A. Dumesic, *An overview of aqueous-phase catalytic processes for production of hydrogen and alkanes in a biorefinery*. *Catalysis Today*, 2006. **111**(1-2): p. 119-132.
18. Sarip, H., K. Allaf, and M.A.M. Noor, *Pure cellulose conversion to glucose with Instant Pressure Drop (DIC) Technology*. *International Journal of Engineering and Technology*, 2011. **8**(2).
19. John F. Kennedy, Charles J. Knill, and D.W. Taylor, *Conversion of Cellulosic Feedstocks into Useful Products*, in *Polysaccharides: structural diversity and functional versatility*, S. Dumitriu, Editor. 1998, Marcel Dekker. p. 1147
20. Leber, J., *Economics Improve for First Commercial Cellulosic Ethanol Plants*, in *New York Times*. 2010, New York Times: New York.
21. Wyman, C.E. and J.C. Cutler, *Ethanol Fuel*, in *Encyclopedia of Energy*. 2004, Elsevier: New York. p. 541-555.
22. Howard, R.L., et al., *Review - Lignocellulose biotechnology: issues of bioconversion and enzyme production*. *African Journal of Biotechnology* 2(12), 2003.
23. Mosier, N., et al., *Features of promising technologies for pretreatment of lignocellulosic biomass*. *Bioresource Technology*, 2005. **96**(6): p. 673-686.
24. Huber, G.W., S. Iborra, and A. Corma, *Synthesis of Transportation Fuels from Biomass: Chemistry, Catalysts, and Engineering*. *Chemical Reviews*, 2006. **106**(9): p. 4044-4098.
25. Choi, C.H. and A.P. Mathews, *Two-step acid hydrolysis process kinetics in the saccharification of low-grade biomass: 1. Experimental studies on the formation and degradation of sugars*. *Bioresource Technology*, 1996. **58**(2): p. 101-106.
26. Yang, B. and C.E. Wyman, *Characterization of the degree of polymerization of xylooligomers produced by flowthrough hydrolysis of pure xylan and corn stover with water*. *Bioresource Technology*, 2008. **99**(13): p. 5756-5762.
27. Sainz, M., *Commercial cellulosic ethanol: The role of plant-expressed enzymes*. *In Vitro Cellular & Developmental Biology - Plant*, 2009. **45**(3): p. 314-329.
28. Saeman, J.F., *Kinetics of Wood Saccharification - Hydrolysis of Cellulose and Decomposition of Sugars in Dilute Acid at High Temperature*. *Industrial & Engineering Chemistry*, 1945. **37**(1): p. 43-52.
29. Bouchard, J., et al., *Characterization of depolymerized cellulosic residues*. *Wood Science and Technology*, 1989. **23**(4): p. 343-355.
30. Overend, R.P., E. Chornet, and J.A. Gascoigne, *Fractionation of Lignocellulosics by Steam-Aqueous Pretreatments [and Discussion]*. *Philosophical Transactions of the Royal Society of London. Series A, Mathematical and Physical Sciences*, 1987. **321**(1561): p. 523-536.
31. Zhao, H., et al., *Metal Chlorides in Ionic Liquid Solvents Convert Sugars to 5-Hydroxymethylfurfural*. *SCIENCE*, 2007. **316**(5831): p. 1597-1600.
32. Téllez-Luis, S.J., J.A. Ramírez, and M. Vázquez, *Mathematical modelling of hemicellulosic sugar production from sorghum straw*. *Journal of Food Engineering*, 2002. **52**(3): p. 285-291.
33. Merino, S., J. Cherry, and L. Olsson, *Progress and Challenges in Enzyme Development for Biomass Utilization* *Adv Biochem Engin/Biotechnol*, 2007. **108**: p. 95-120.
34. Lichtenthaler, F.W., *Carbohydrates*, in *Ullmann's encyclopedia of industrial chemistry*, B. Elvers, S. Hawkins, and W. Russey, Editors. 2005, VCH.

35. Sjöström, E., *Wood chemistry: fundamentals and applications*. 2nd Ed. ed. 1993: Gulf Professional Publishing. 293.
36. Walker, J.C.F., *Primary wood processing: principles and practice*. 2006: Springer.
37. Hobbs, L., *Sweeteners from starch: production, properties and use*, in *Starch: chemistry and technology*, J.N. BeMiller and R.L. Whistler, Editors. 2009, Academic. p. 797.
38. (NREL), T.N.R.E.L. *What Is a Biorefinery?* 2009 [cited 25 October 2011]; Available from: <http://www.nrel.gov/biomass/biorefinery.html>.
39. Speight, J.G., et al., *The Biofuels Handbook*. 2011: Royal Society of Chemistry.
40. Crocker, M., *Thermochemical Conversion of Biomass to Liquid Fuels and Chemicals*: Royal Society of Chemistry.
41. Zaldivar, J., J. Nielsen, and L. Olsson, *Fuel ethanol production from lignocellulose: a challenge for metabolic engineering and process integration*. *Applied Microbiology and Biotechnology*, 2001. **56**(1): p. 17-34.
42. Pandey, A., et al., *Biofuels: Alternative Feedstocks and Conversion Processes*. 2011: Elsevier Science.
43. Ghosh, T.K. and M.A. Prelas, *Energy Resources and Systems: Renewable Resources*. 2011: Springer London, Limited.
44. Fengel, D. and G. Wegener, *Wood: chemistry, ultrastructure, reactions*. 1984: W. de Gruyter.
45. Dumitriu, S., *Polysaccharides: structural diversity and functional versatility* *Food science and technology*, ed. S. Dumitriu. 1998: Marcel Dekker. 1147
46. Zugenmaier, P., *Crystalline Cellulose and Derivatives: Characterization and Structures*. Springer Series in Wood Science. 2007: Springer. 285.
47. Wyman, C.E., et al., *Comparative sugar recovery data from laboratory scale application of leading pretreatment technologies to corn stover*. *Bioresource Technology*, 2005. **96**(18): p. 2026-2032.
48. Hatakeyama, T. and H. Hatakeyama, *Thermal properties of green polymers and biocomposites*. 2004: Kluwer Academic Publishers.
49. Shafizadeh, F. and P.P.S. Chin, *Thermal degradation of wood.*, in *Wood Technology: Chemical Aspects*, I.S. Goldstein, Editor. 1977, American Chemical Society Symposium Series: Washington, DC, . p. 57-81.
50. Krässig, H., et al., *Cellulose*, in *Ullmann's encyclopedia of industrial chemistry*, B. Elvers, S. Hawkins, and W. Russey, Editors. 2005, VCH.
51. Park, S., et al., *Changes in pore size distribution during the drying of cellulose fibers as measured by differential scanning calorimetry*. *Carbohydrate Polymers*, 2006. **66**(1): p. 97-103.
52. Nakamura, K., T. Hatakeyama, and H. Hatakeyama, *Studies on bound water of cellulose by differential scanning calorimetry*. *Textile Research Journal*, 1981: p. 607-613.
53. Sarkanen, K.V. and C.H. Ludwig, *Lignins: occurrence, formation, structure and reactions*. 1971: Wiley-Interscience.
54. BeMiller, J.N. and R.L. Whistler, *Starch: chemistry and technology*. 2009: Academic.
55. Soni, S.K., *Microbes: A Source of Energy for 21st Century*. 2007: New India Publishing Agency.

56. Gallagher, P.K., M.E. Brown, and R.B. Kemp, *Handbook of Thermal Analysis and Calorimetry: From macromolecules to man*. 1999: Elsevier.
57. Aseeva, R.M., B.D. Thanh, and B.B. Serkov, *Factor affecting heat release at the combustion of the different species of wood*, in *Chemical physics of pyrolysis, combustion, and oxidation*, A.A. Berlin, Editor. 2005, Nova Science Publishers. p. 45-53.
58. Nelson, R.A., *The determination of moisture transitions in cellulosic materials using differential scanning calorimetry*. *Journal of Applied Polymer Science*, 1977. **21**(3): p. 645-654.
59. Kouali, M. and J.M. Vergnaud, *Modeling the process of absorption and desorption of water above and below the fiber saturation point*. *Wood Science and Technology*, 1991. **25**(5): p. 327-339.
60. Leonard, Y.M. and P.A. Martin, *Chemical modification of hemp, sisal, jute, and kapok fibers by alkalization*. *Journal of Applied Polymer Science*, 2002. **84**(12): p. 2222-2234.
61. Szcześniak, L., A. Rachocki, and J. Tritt-Goc, *Glass transition temperature and thermal decomposition of cellulose powder*. *Cellulose*, 2008. **15**(3): p. 445-451.
62. John, R.P., *Biotechnological potential for cassava bagasse*, in *Biotechnology for Agro-Industrial Residues Utilisation: Utilisation of Agro-Residues*, P.S. Nigam and A. Pandey, Editors. 2009, Springer.
63. Milbrandt, A. and R.P. Overend, *Survey of Biomass Resource Assessments and Assessment Capabilities in APEC Economies*, in *APEC Energy Working Group*. 2008.
64. Nguyen Xuan Thuy, Nguyen Minh Thao, and colleagues. *Research on technology and equipment for waste treatment at cassava starch processing villages or clusters*. 2008 [cited 25 October 2011]; Available from: <http://cassava.vn.refer.org/spip.php?article93>.
65. Sriroth, K., B. Lamchaiyaphum, and K. Piyachomkwan. *Present situation and future potential of cassava in Thailand*. 2008 [cited 25 October 2011]; Available from: <http://cassava.vn.refer.org/spip.php?article87>.
66. Breuninger, W.F., K. Piyachomkwan, and K. Sriroth, *Tapoica/ cassava starch: production and use*, in *Starch: chemistry and technology*, J.N. BeMiller and R.L. Whistler, Editors. 2009, Academic. p. 797.
67. Mathur, P.N., et al. *Conservation and sustainable use of sago (Metroxylon sago) genetic resources in Proceedings of the Sixth International Sago Symposium*. 1998. Pekanbaru, Riau, Indonesia: Riau Univ. Training Centre.
68. Flach, M., *Sago palm. Metroxylon sago Rottb. Promoting the conservation and use of underutilized and neglected crops*. 13. 1997, Rome, Italy: Institute of Plant Genetics and Crop Plant Research, Gatersleben/International Plant Genetic Resources Institute.
69. Stanton, W.R., *Perspectives on, and future prospects for, the sago palm*. *Sago Palm*, 1993(1): p. 2-7.
70. Ruddle, K., et al., *Palm sago: a tropical starch from marginal lands*. 1978, Honolulu, Hawaii: Univ. Press of Hawaii.
71. Flach, M. and D.L. Schuiling, *Revival of an ancient starch crop: a review of the agronomy of sago palm*. *Agroforestry Syst*, 1989. **7**: p. 259-81.
72. Kraalingen van, D.W.G., *Starch contents of sago palm trunks in relation to morphological characters and ecological conditions*, in *The development of the sago palm and its products*. 1986, FAO/BPPT consultation, Jakarta, Indonesia, : FAO, Rome. p. 105-111.

73. Yamamoto, Y., et al. *Estimation of annual starch productivity per unit area in sago palm (Metroxylon sagu Rottb.) : a case study*. in *Ninth International Sago Symposium*. 2007. Tebing Tinggi Island, Riau, Indonesia.: The Philippines: Ormoc City.
74. Karim, A.A., et al., *Starch from the Sago (Metroxylon sagu) Palm Tree—Properties, Prospects, and Challenges as a New Industrial Source for Food and Other Uses*. *Comprehensive Reviews in Food Science and Food Safety*, 2008. **7**(3): p. 215-228.
75. Singhal, R.S., et al., *Industrial production, processing, and utilization of sago palm-derived products*. *Carbohydrate Polymers*, 2008. **72**(1): p. 1-20.
76. Eckhoff, S.R. and S.A. Watson, *Corn and sorghum starches: production*, in *Starch: chemistry and technology*, J.N. BeMiller and R.L. Whistler, Editors. 2009, Academic. p. 797.
77. Kunhi, A.A.M., et al., *Studies on Production of Alcohol from Saccharified Waste Residue from Cassava Starch Processing Industries*. *Starch - Stärke*, 1981. **33**(8): p. 275-279.
78. Srinorakutara, T., L. Kaewvimol, and L.-a. Saengow, *Approach of Cassava Waste Pretreatments for Fuel Ethanol Production in Thailand* *J. Sci. Res.Chula. Univ*, 2006. **31**(1).
79. Sun, R., et al., *Fractional isolation and partial characterization of non-starch polysaccharides and lignin from sago pith*. *Industrial Crops and Products*, 1999. **9**(3): p. 211-220.
80. Bernama, *Sarawak Expanding Sago Industry By Another 50,000 Hectares*, in *Bernama*. 2007, Bernama: Kuala Lumpur.
81. Bernama, *Unimas Sets Up First Centre For Sago Research In Region*, in *Bernama*. 2010: Kuala Lumpur.
82. Mohd, A.M.D., M.N. Islam, and B.M. Noor, *Enzymic Extraction of Native Starch from Sago (Metroxylon sagu) Waste Residue*. *Starch - Stärke*, 2001. **53**(12): p. 639-643.
83. Akmar, P.F. and J.F. Kennedy, *Carbohydrate composition of the water soluble materials of the oil palm trunk and sago waste*. *Carbohydrate Polymers*, 1997. **34**(4): p. 436-436.
84. A.C. Kumoro, et al., *Conversion of Fibrous Sago (Metroxylon sagu) Waste into Fermentable Sugar via Acid and Enzymatic Hydrolysis*. *Asian Journal of Scientific Research*, 2008. **1**: p. 412-420.
85. Sun, Y. and J. Cheng, *Hydrolysis of lignocellulosic materials for ethanol production: a review*. *Bioresource Technology*, 2002. **83**(1): p. 1-11.
86. Duff, S.J.B. and W.D. Murray, *Bioconversion of forest products industry waste cellulose to fuel ethanol: A review*. *Bioresource Technology*, 1996. **55**(1): p. 1-33.
87. Bonaventura Focher, Annamaria Marzetti, and V. Crescenzi, *Steam Explosion Techniques: Fundamentals and Industrial Applications: Proceedings of the International Workshop on Steam Explosion Techniques: Fundamentals and Industrial Applications, 20-21 October 1988*, ed. A.M. B. Focher, Vittorio Crescenzi. 1990, Milan, Italy: Taylor & Francis. 412.
88. Garrote, G., H. Domínguez, and J.C. Parajó, *Mild autohydrolysis: an environmentally friendly technology for xylooligosaccharide production from wood*. *Journal of Chemical Technology & Biotechnology*, 1999. **74**(11): p. 1101-1109.
89. Linde, M., M. Galbe, and G. Zacchi, *Simultaneous saccharification and fermentation of steam-pretreated barley straw at low enzyme loadings and low yeast concentration*. *Enzyme and Microbial Technology*, 2007. **40**(5): p. 1100-1107.
90. Oliva, J.M., et al., *Effects of acetic acid, furfural and catechol combinations on ethanol fermentation of Kluyveromyces marxianus*. *Process Biochemistry*, 2006. **41**(5): p. 1223-1228.

91. Cowling, E.B., *Physical and chemical constraints in the hydrolysis of cellulose and lignocellulosic materials*. Biotechnol. and Bioeng. Symp., 1975. **5**: p. 163-182.
92. Saeman Jerome, F., *Key Factors in the Hydrolysis of Cellulose*, in *Biomass as a Nonfossil Fuel Source*. 1981, American Chemical Society. p. 185-197.
93. Harris, J.F., et al., *Two-Stage, Dilute Sulfuric Acid Hydrolysis of Wood: An Investigation of Fundamentals*. 1985, U.S. Department of Agriculture, Forest Service, Forest Products Laboratory. p. 73 p.
94. Mok, W.S., M.J. Antal, and G. Varhegyi, *Productive and parasitic pathways in dilute acid-catalyzed hydrolysis of cellulose*. Industrial & Engineering Chemistry Research, 1992. **31**(1): p. 94-100.
95. Melvin P. Tucker, et al., *Effects of Temperature and Moisture on Dilute-Acid Steam Explosion Pretreatment of Corn Stover and Cellulase Enzyme Digestibility*. Applied Biochemistry and Biotechnology, 2003. **105**(1 - 3): p. 165 - 177.
96. Girisuta, B., *Levulinic Acid from Lignocellulosic Biomass* 2007.
97. Fang, Q. and M.A. Hanna, *Experimental studies for levulinic acid production from whole kernel grain sorghum*. Bioresource Technology, 2002. **81**(3): p. 187-192.
98. Nabarlantz, D., X. Farriol, and D. Montane, *Autohydrolysis of Almond Shells for the Production of Xylo-oligosaccharides: Product Characteristics and Reaction Kinetics*. Industrial & Engineering Chemistry Research, 2005. **44**(20): p. 7746-7755.
99. Larsson, S., et al., *The generation of fermentation inhibitors during dilute acid hydrolysis of softwood*. Enzyme and Microbial Technology, 1999. **24**(3-4): p. 151-159.
100. Sun, Y., et al., *Clean conversion of cellulose into fermentable glucose*. Biotechnology Advances. **27**(5): p. 625-632.
101. Cantarella, M., et al., *Comparison of different detoxification methods for steam-exploded poplar wood as a substrate for the bioproduction of ethanol in SHF and SSF*. Process Biochemistry, 2004. **39**(11): p. 1533-1542.
102. Cara, C., et al., *Production of fuel ethanol from steam-explosion pretreated olive tree pruning*. Fuel, 2008. **87**(6): p. 692-700.
103. Eggeman, T. and R.T. Elander, *Process and economic analysis of pretreatment technologies*. Bioresource Technology, 2005. **96**(18): p. 2019-2025.
104. Hiden, A., et al., *Wet disk milling pretreatment without sulfuric acid for enzymatic hydrolysis of rice straw*. Bioresource Technology, 2009. **100**(10): p. 2706-2711.
105. Taherzadeh, M.J. and K. Karimi, *Pretreatment of Lignocellulosic Wastes to Improve Ethanol and Biogas Production: A Review*. International journal of molecular sciences, 2008. **9**(9): p. 1621-51.
106. Montané D., et al., *Polysaccharides from biomass via thermomechanical process*, in *Polysaccharides: structural diversity and functional versatility* S. Dumitriu, Editor. 1998, Marcel Dekker. p. 1147
107. Morjanoff, P.J. and P.P. Gray, *Optimization of steam explosion as a method for increasing susceptibility of sugarcane bagasse to enzymatic saccharification*. Biotechnology and Bioengineering, 1987. **29**(6): p. 733-741.
108. Bouchard, J., et al., *Analytical methodology for biomass pretreatment - part 1: Solid residues*. Biomass, 1990. **23**(4): p. 243-261.

109. Nabarlatz, D., X. Farriol, and D. Montane, *Kinetic Modeling of the Autohydrolysis of Lignocellulosic Biomass for the Production of Hemicellulose-Derived Oligosaccharides*. Industrial & Engineering Chemistry Research, 2004. **43**(15): p. 4124-4131.
110. Zimbardi, F., et al., *Acid impregnation and steam explosion of corn stover in batch processes*. Industrial Crops and Products, 2007. **26**(2): p. 195-206.
111. Jin, S. and H. Chen, *Fractionation of fibrous fraction from steam-exploded rice straw*. Process Biochemistry, 2007. **42**(2): p. 188-192.
112. Sun, X.F., et al., *Characteristics of degraded hemicellulosic polymers obtained from steam exploded wheat straw*. Carbohydrate Polymers, 2005. **60**(1): p. 15-26.
113. Wyman, C., ed. *Handbook on Bioethanol: Production and Utilization*. Applied Energy Technology Series. 1996, Taylor & Francis.
114. M. R. Rosa, G.J.M. Rocha, and A.A.S. Curvelo, *Organosolv delignification of steam exploded wheat straw*, in *Environmentally friendly technologies for the pulp and paper industry*, R.A. Young and M. Akhtar, Editors. 1998, John Wiley & Sons Inc., p. 49-55.
115. Louka, N., F. Juhel, and K. Allaf, *Quality studies on various types of partially dried vegetables texturized by Controlled Sudden Decompression: General patterns for the variation of the expansion ratio*. Journal of Food Engineering, 2004. **65**(2): p. 245-253.
116. Haddad, J. and K. Allaf, *A study of the impact of instantaneous controlled pressure drop on the trypsin inhibitors of soybean*. Journal of Food Engineering, 2007. **79**(1): p. 353-357.
117. Haddad, J., R. Greiner, and K. Allaf, *Effect of instantaneous controlled pressure drop on the phytate content of lupin*. LWT - Food Science and Technology, 2007. **40**(3): p. 448-453.
118. Amor, B.B., et al., *Effect of instant controlled pressure drop treatments on the oligosaccharides extractability and microstructure of Tephrosia purpurea seeds*. Journal of Chromatography A, 2008. **1213**(2): p. 118-124.
119. Hamid Mellouk, et al., *Total Valorisation of Red Cedar (Thuja Plicata) sawmills wastes. Isolation of extractives and production of activated carbon from the solid residue*. BioResources, 2008. **3**(4): p. 1156-1172.
120. Iguedjal, T., N. Louka, and K. Allaf, *Sorption isotherms of potato slices dried and texturized by controlled sudden decompression*. Journal of Food Engineering, 2008. **85**(2): p. 180-190.
121. Kristiawan, M., et al., *Effect of pressure-drop rate on the isolation of cananga oil using instantaneous controlled pressure-drop process*. Chemical Engineering and Processing: Process Intensification, 2008. **47**(1): p. 66-75.
122. Mounir, S., et al., *Study of instant controlled pressure drop DIC treatment in manufacturing snacking and expanded granule powder of apple and onion*. DRYING TECHNOLOGY, 2011. **29**(3): p. 331-341.
123. Liu, Y., et al., *Separation and characterization of underivatized oligosaccharides using liquid chromatography and liquid chromatography-electrospray ionization mass spectrometry*. Journal of Chromatography A, 2005. **1079**(1-2): p. 146-152.
124. Garrote, G., H. Domínguez, and J.C. Parajó, *Autohydrolysis of corncob: study of non-isothermal operation for xylooligosaccharide production*. Journal of Food Engineering, 2002. **52**(3): p. 211-218.
125. Girisuta, B., L.P.B.M. Janssen, and H.J. Heeres, *Kinetic Study on the Acid-Catalyzed Hydrolysis of Cellulose to Levulinic Acid*. Industrial & Engineering Chemistry Research, 2007. **46**(6): p. 1696-1708.

126. Balan, V., et al., *Lignocellulosic biomass pretreatment using AFEX*. Methods in molecular biology (Clifton, N.J.), 2009. **581**: p. 61-77.
127. Shevchenko, S.M., et al., *Optimization of monosaccharide recovery by post-hydrolysis of the water-soluble hemicellulose component after steam explosion of softwood chips*. Bioresource Technology, 2000. **72**(3): p. 207-211.
128. Zhao, H., et al., *Studying cellulose fiber structure by SEM, XRD, NMR and acid hydrolysis*. Carbohydrate Polymers, 2007. **68**(2): p. 235-241.
129. Taherzadeh, M.J., C. Niklasson, and G. Lidén, *Conversion of dilute-acid hydrolyzates of spruce and birch to ethanol by fed-batch fermentation*. Bioresource Technology, 1999. **69**(1): p. 59-66.
130. Soudham, V.P., B. Alriksson, and L.J. Jönsson, *Reducing agents improve enzymatic hydrolysis of cellulosic substrates in the presence of pretreatment liquid*. Journal of Biotechnology. **155**(2): p. 244-250.
131. Mussatto, S.I., et al., *Production, characterization and application of activated carbon from brewers spent grain lignin*. Bioresource Technology. **101**(7): p. 2450-2457.
132. Gurram, R.N., et al., *Removal of enzymatic and fermentation inhibitory compounds from biomass slurries for enhanced biorefinery process efficiencies*. Bioresource Technology, 2011. **102**(17): p. 7850-7859.
133. Walker, J.M., et al., *Enzymatic Saccharification of Cellulosic Materials*, in *Environmental Microbiology*, J.M. Walker, Editor. 2004, Humana Press. p. 219-233.
134. Zheng, Y., et al., *Enzymatic saccharification of dilute acid pretreated saline crops for fermentable sugar production*. Applied Energy, 2009. **86**(11): p. 2459-2465.
135. Walker, L.P. and D.B. Wilson, *Enzymatic hydrolysis of cellulose: An overview*. Bioresource Technology, 1991. **36**(1): p. 3-14.
136. Connors, K.A., *Chemical kinetics: the study of reaction rates in solution*. 1990: VCH.
137. Billo, E.J., *Excel for chemists: a comprehensive guide*. 2001: Wiley-VCH.
138. Bienkowski, P.R., et al., *Correlation of glucose (dextrose) degradation at 90 to 190°C in 0.4 to 20% acid*. Chemical Engineering Communications, 1987. **51**(1-6): p. 179-192.
139. Sun, Y., et al., *Clean conversion of cellulose into fermentable glucose*. Biotechnology Advances, 2009. **27**(5): p. 625-632.
140. Coker, A.K., *Modeling of Chemical Kinetics and Reactor Design*. 2001, Houston, Texas: Gulf Publishing Company.
141. Schwald, W., et al., *Comparison of HPLC and colorimetric methods for measuring cellulolytic activity*. Applied Microbiology and Biotechnology, 1988. **28**(4): p. 398-403.
142. Antal, M.J., G. Varhegyi, and E. Jakab, *Cellulose Pyrolysis Kinetics: Revisited*. Industrial & Engineering Chemistry Research, 1998. **37**(4): p. 1267-1275.
143. Anthony H. Conner, Kimball Libkie, and E.L. Springer, *Kinetic Modeling of Hardwood Prehydrolysis. Part II. Xylan Removal by Dilute Hydrochloric Acid Prehydrolysis*. Wood and Fiber Science, 1984. **17**(4): p. 540-548.
144. Box, G.E.P. and N.R. Draper, *Empirical model-building and response surfaces*. 1987: Wiley.
145. Phadke, M.S., *Quality engineering using robust design*. 1989: Prentice Hall.
146. Montgomery, D.C., *Design and analysis of experiments*. 2008: Wiley.

147. Lazić, Ž.R., *Design of Experiments in Chemical Engineering: A Practical Guide*. 2004: Wiley-VCH.
148. Oehlert, G.W., *A first course in design and analysis of experiments*. 2000: W.H. Freeman.
149. Statgraphic®, *STATGRAPHICS® Centurion XV User Manual* 2009.
150. Box, B.E.P. and W.G. Hunter, *On the experimental attainment of optimum conditions*. Journal of the Royal Statistical Society, 1951. **13**: p. 1-45.
151. Baş, D. and İ.H. Boyacı, *Modeling and optimization I: Usability of response surface methodology*. Journal of Food Engineering, 2007. **78**(3): p. 836-845.
152. CHOW, P.S. and S.M. LANDHÄUSSER, *A method for routine measurements of total sugar and starch content in woody plant tissues*. Tree Physiology, 2004. **24**: p. 1129-1136.
153. Sluiter, A., et al. *Determination of Structural Carbohydrates and Lignin in Biomass*. National Renewable Energy Laboratory of the USA (NREL), Laboratory Analytical Procedure (LAP) 2008 [cited 11 July 2011]; Available from: http://www.nrel.gov/biomass/analytical_procedures.html#lap-002.
154. ASTM D7481, *Standard Test Methods for Determining Loose and Tapped Bulk Densities of Powders using a Graduated Cylinder* ASTM International, West Conshohocken, PA, 2009.
155. Sarip, H., K. Allaf, and M.A.M. Noor. *Cellulosic materials conversion to glucose through instant pressure drop (DIC) technology*. in *World Engineering Congress 2010 Conference on Natural Resources and Green Technology*. 2010. Kuching, Sarawak.: Federation of Engineering Institutions of Islamic Countries.
156. Vikineswary, S., et al., *Possible microbial utilization of sago processing wastes*. Resources, Conservation and Recycling, 1994. **11**(1-4): p. 289-296.
157. Mosier, N.S., C.M. Ladisch, and M.R. Ladisch, *Characterization of acid catalytic domains for cellulose hydrolysis and glucose degradation*. Biotechnology and bioengineering, 2002. **79**(6): p. 610-618.
158. Girisuta, B., et al., *Experimental and kinetic modelling studies on the acid-catalysed hydrolysis of the water hyacinth plant to levulinic acid*. Bioresource Technology, 2008. **99**(17): p. 8367-8375.
159. Garrote, G., H. Domínguez, and J.C. Parajó, *Generation of xylose solutions from Eucalyptus globulus wood by autohydrolysis-posthydrolysis processes: posthydrolysis kinetics*. Bioresource Technology, 2001. **79**(2): p. 155-164.
160. Princi, E., et al., *Thermal characterisation of cellulose based materials*. Journal of Thermal Analysis and Calorimetry, 2005. **80**(2): p. 369-373.
161. Galal Abdulla, et al., *Sechage De Produits Granulaires Par Deshydratation Par Detentes Successives (DDS)*, in *IXème Colloque Inter universitaire Franco-Québécois sur la Thermique des Systèmes* 2009: Lille, France.
162. Rakotozafy, et al., *Drying of Baker's Yeast by a New Method: Dehydration by Successive Pressure Drops (DDS). Effect on Cell Survival and Enzymatic Activities*. Drying Technology, 2000. **18**(10): p. 2253-2272
163. Fuller, R., G. Gibson, and C. Editor-in-Chief:Â Â Benjamin, *PROBIOTICS AND PREBIOTICS | Definition and Role*, in *Encyclopedia of Human Nutrition (Second Edition)*. 1998, Elsevier: Oxford. p. 1633-1639.

164. Ziemer, C.J. and G.R. Gibson, *An Overview of Probiotics, Prebiotics and Synbiotics in the Functional Food Concept: Perspectives and Future Strategies*. International Dairy Journal, 1998. **8**(6): p. 473-479.
165. Elvers, B., S. Hawkins, and W. Russey, *Ullmann's encyclopedia of industrial chemistry*. Vol. Vols.1 to 39. 2005: VCH.
166. Jane, J.-I., *Structural Features of Starch Granules II* in *Starch: chemistry and technology*, J.N. BeMiller and R.L. Whistler, Editors. 2009, Academic. p. 193-236.
167. Vasanthan, T. and R. Hoover, *Barley Starch: Production, Properties, Modification and Uses*, in *Starch: chemistry and technology*, J.N. BeMiller and R.L. Whistler, Editors. 2009, Academic. p. 601-625.
168. Hong, F.-L., J. Peng, and W.-B. Lui, *Optimization of the process variables for the synthesis of starch-based biodegradable resin using response surface methodology*. Journal of Applied Polymer Science, 2010. **119**(3): p. 1797-1804.
169. Várhegyi, G., et al., *Kinetic modeling of biomass pyrolysis*. Journal of Analytical and Applied Pyrolysis, 1997. **42**(1): p. 73-87.
170. Aggarwal, P. and D. Dollimore, *The combustion of starch, cellulose and cationically modified products of these compounds investigated using thermal analysis*. Thermochimica Acta, 1997. **291**(1-2): p. 65-72.
171. Aggarwal, P. and D. Dollimore, *The effect of chemical modification on starch studied using thermal analysis*. Thermochimica Acta, 1998. **324**(1-2): p. 1-8.
172. Aggarwal, P., D. Dollimore, and K. Heon, *Comparative thermal analysis study of two biopolymers, starch and cellulose*. Journal of Thermal Analysis and Calorimetry, 1997. **50**(1): p. 7-17.
173. A. Magoń and M. Pyda, *Melting, glass transition, and apparent heat capacity of α -D-glucose by thermal analysis*. Carbohydrate Research, 2011.
174. Baker, R.R., et al., *Pyrolysis of saccharide tobacco ingredients: a TGA-FTIR investigation*. Journal of Analytical and Applied Pyrolysis, 2005. **74**(1-2): p. 171-180.
175. Scheirs, J., G. Camino, and W. Tumiatti, *Overview of water evolution during the thermal degradation of cellulose*. European Polymer Journal, 2001. **37**(5): p. 933-942.
176. Patwardhan, P.R., et al., *Product distribution from fast pyrolysis of glucose-based carbohydrates*. Journal of Analytical and Applied Pyrolysis, 2009. **86**(2): p. 323-330.
177. Pappa, A.A., et al., *Thermal analysis of Pinus halepensis pine-needles and their main components in the presence of $(\text{NH}_4)_2\text{HPO}_4$ and $(\text{NH}_4)_2\text{SO}_4$* . Thermochimica Acta, 1995. **261**: p. 165-173.
178. Xiang, Q., J. Kim, and Y. Lee, *A comprehensive kinetic model for dilute-acid hydrolysis of cellulose*. Applied Biochemistry and Biotechnology, 2003. **106**(1): p. 337-352.